Universitat Autònoma de Barcelona

Estudi de la relació estructura-funció de les metal·lotioneïnes en sistemes polimòrfics d'animals (eriçó de mar) i de plantes (soja i gira-sol)

Mireia Tomàs i Giner

Tesi Doctoral

Estudis de Doctorat en Química

Dirigida per Sílvia Atrian i Roger Bofill

Departament de Química
Facultat de Ciències

2014

Memòria presentada per aspirar al Grau de Doctor per Mireia Tomàs i Giner

Vist i plau

Sílvia Atrian i Ventura

Roger Bofill i Arasa

Bellaterra, a 25 de març de 2014

ABREVIACIONS

CXC:	Cisteïna-aminoàcid X-cisteïna
Da:	Dalton
DC:	Dicroisme circular
DEPC:	Pirocarbonat de dietil
ESI-MS:	Espectrometria de masses amb ionització per electroesprai
GSH:	Glutatió
GSSG:	Disulfur de glutatió
HSAB:	Principi dels àcids i bases durs i tous
ICP-AES:	Espectroscòpia d'emissió atòmica amb plasma d'inducció acoblat
KO:	Genoanul·lat
M:	Metall
MT:	Metal·lotioneïna
MRE:	Element de resposta a metalls
RMN:	Ressonància magnètica nuclear
UV-vis:	Ultraviolat-visible

ÍNDEX

1. RESUM/ABSTRACT

1. RESUM/ABSTRACT

Les metal·lotioneïnes (MT) constitueixen una superfamília de metal·loproteïnes de baix pes molecular que es caracteritzen pel seu elevat contingut en residus Cys, els quals els confereixen les seues propietats coordinants i reductores. És com a conseqüència d'aquestes propietats que se'ls atribueixen funcions d'homeòstasi i destoxicació de metalls, així com de regulació i protecció en processos redox. Les MT són ubíqües i les seues seqüències són molt diverses. En la present Tesi Doctoral hem tractat d'ampliar els coneixements actuals sobre aquestes metal·loproteïnes i aprofundir en la seua relació estructura-funció. Així, d'una banda s'han analitzat les preferències metàl·liques envers metalls mono- i divalents de les dues isoformes de MT presents en l'eriçó de mar (*Strongylocentrotus purpuratus*), SpMTA i SpMTB, les quals presenten patrons de Cys alineables. S'ha determinat que SpMTA mostra millors habilitats per a coordinar Zn(II) i Cd(II) que SpMTB i que, en canvi, SpMTB mostra millors propietats per a coordinar Cu(I) que SpMTA. Aquestes preferències metàl·liques s'han relacionat amb una diferenciació funcional en l'organisme. D'altra banda, s'han estudiat els sistemes MT de les plantes de soja (*Glycine max*) i gira-sol (*Helianthus annuus*), les quals s'ha vist que sintetitzen representants de les quatre subfamílies en què es divideix la família de les MT de planta, que presenten patrons de Cys no alineables. Així, s'ha determinat que les MT1 i MT2 de gira-sol estudiades (HaMT1 i HaMT2) presenten una major capacitat de coordinació de Cd(II) que les MT1 i MT2 de soja (GmMT1 i GmMT2), probablement a causa del seu major contingut en Cys. A més, s'ha vist que les His C-terminals que ambdues MT3 (GmMT3 i HaMT3) contenen i que es troben semiconservades en la subfamília participen en l'enllaç al Cd(II). MT4 de soja (GmMT4) presenta la mutació natural His54Tyr que trenca amb el patró de Cys i His conservat en la subfamília MT4, la qual s'ha demostrat que suposa una disminució en la capacitat de coordinació de Zn(II). En canvi, tant GmMT4 com MT4 de gira-sol (HaMT4), que presenta el patró típic de Cys i His, presenten capacitats de coordinació de Cd(II) anàlogues, donat que cap de les seues His no participa en l'enllaç al Cd(II). A més, l'estudi de capacitats antioxidants i/o de captadors de radicals lliures de les quatre MT de soja ha permés proposar que la llargària de l'espaiador (regió lliure de Cys) és determinant per a la protecció enfront de l'oxidació de les Cys provocada per l'exposició a peròxid d'hidrogen, així com que Zn-GmMT1 és el complex que ha mostrat les millors propietats per a protegir les cèl·lules davant l'atac de les espècies reactives d'oxigen.

1. RESUM/ABSTRACT

Metallothioneins (MT) constitute a low molecular weight metalloprotein superfamily characterised by their high Cys residue content, which confers them their coordinative and reducing properties. As a result of these properties, MTs are proposed to be involved in homeostasis and metal detoxification functions, as well as in regulation and protection during redox processes. MTs are ubiquitous and their sequences are extremely variable. In this PhD Thesis we have tried to expand the current knowledge about these metalloproteins and to deepen into their structure-function relationship. Thus, on the one hand, the metallic preferences towards mono- and divalent metal ions of the two MT isoforms present in sea urchin (*Strongylocentrotus purpuratus*), SpMTA and SpMTB, which display alignable Cys patterns, have been analysed. It has been determined that SpMTA shows better Zn(II)- and Cd(II)-binding abilities than SpMTB, and that, on the contrary, SpMTB shows better Cu(I)-binding abilitites than SpMTA. These metallic preferences have been related to a functional differentiation within the organism. On the other hand, the MT systems from the soybean (*Glycine max*) and sunflower (*Helianthus annuus*) plants have been studied, which have been proven to synthesise representatives of the four subfamilies in which the plant MT family is divided, and that show non-alignable Cys patterns. Thus, it has been shown that sunflower MT1 and MT2 (HaMT1 and HaMT2) display a greater Cd(II)-binding capacity than MT1 and MT2 from soybean (GmMT1 and GmMT2), probably due to their higher Cys content. In addition, it has been shown that the C-terminal His present in both MT3 (GmMT3 and HaMT3), which are semiconserved within this subfamily, are involved in Cd(II) coordination. Soybean MT4 (GmMT4) presents the natural His54Tyr mutation that breaks the highly conserved Cys and His pattern in MT4 subfamily, which has been shown to provoke a decrease in its Zn(II)-binding capacity. However, both GmMT4 and sunflower MT4 (HaMT4), which presents the typical MT4 Cys and His pattern, show analogous Cd(II) coordination capacities, since none of their His are involved in Cd(II) binding. In addition, the study of the antioxidant and/or free radicals scavenging capacities of the four soybean MTs has allowed to propose that the length of the spacer (Cys-free region) is crucial to protect Cys from the oxidation caused by hydrogen peroxide exposure, and that the Zn-GmMT1 complex has been the best suited to protect the cells against the attack by reactive oxygen species.

2. INTRODUCCIÓ

2. INTRODUCCIÓ

2.1. Característiques generals de les metal·lotioneïnes

Les metal·lotioneïnes (MT) són proteïnes caracteritzades per un baix pes molecular (<10 kDa) i un alt contingut en residus Cys (15-30% del total), els quals els confereixen una elevada capacitat per a enllaçar ions metàl·lics a través dels seus àtoms de sofre. La primera d'aquestes metal·loproteïnes fou descoberta el 1957 en renyó de cavall,[1] i des d'aleshores trobem més de 200 seqüències anotades en la base de dades de proteïnes UniProtKB que es distribueixen en més de 100 organismes diferents.[2] Si bé la informació de què es disposa sobre aquestes metal·loproteïnes ubiqües és molt extensa, particularment pel que fa a les MT de mamífer, en aquest apartat només se n'introduiran els trets més rellevants per emmarcar els resultats obtinguts en aquesta Tesi Doctoral i s'insistirà en les MT que han estat objecte d'estudi.

2.1.1. Classificació

2.1.1.1. Primera classificació

L'àmplia distribució d'aquestes proteïnes en la natura (en animals, plantes, fongs i alguns bacteris) i la gran diversitat de les seues seqüències fan necessària una classificació per a les MT (Taula 1).

Taula 1. Exemples de seqüències aminoacídiques de MT de diversos organismes. Els residus Cys apareixen destacats en gris. Els pèptids mostrats corresponen a les MT3 d'*Homo sapiens* (UniProtKB P25713), MT3 d'*Arabidopsis thaliana* (O22433), CMT de *Neurospora crassa* (P02807) i SmtA de *Synechococcus elongatus* (P30331).

Organisme	**Seqüència aminoacídica**
Animal (*H. sapiens*)	MDPETCPCPSGGSCTCADSCKCEGCKCTSCKKSCCSCCPAECEKCAKDCVCKGGEAAEAEAEKCSCCQ
Planta (*A. thaliana*)	MSSNCGSCDCADKTQCVKKGTSYTFDIVETQESYKEAMIMDVGAEENNANCKCKCGSSCSCVNCTCCPN
Fong (*N. crassa*)	MGDCGCSGASSCNCGSGCSCSNCGSK
Bacteri (*S. elongatus*)	MTSTTLVKCACEPCLCNVDPSKAIDRNGLYYCSEACADGHTGGSKGCGHTGCNCHG

[1] M. Margoshes, B.L. Vallee, J. Am. Chem. Soc. 79 (1957) 4813-1814.
[2] M. Capdevila, R. Bofill, O. Palacios, S. Atrian, Coord. Chem. Rev. 256 (2012) 46-62.

És per això que ja l'any 1985, durant el Segon Congrés Internacional de Metal·lotioneïnes, es proposà organitzar aquestes proteïnes en tres classes, en funció de la seua estructura primària:[3]

a) La *Classe I* la formarien aquelles MT que són homòlogues a MT1 de renyó de cavall, i que per tant presenten una seqüència peptídica al voltant de 60 aminoàcids, d'entre els quals 20 són Cys. Aquestes MT les trobem en la majoria de vertebrats i en alguns invertebrats.
b) La *Classe II* comprendria les MT amb seqüències aminoacídiques no alineables a les anteriors, i així inclouria un conjunt molt heterogeni de pèptids que trobem en plantes, fongs, invertebrats i alguns bacteris.
c) La *Classe III* agruparia pèptids sintetitzats enzimàticament que contenen unitats γ-Glu-Cys, com són fitoquelatines i cadistines, els quals quedarien així separats de la resta de proteïnes codificades genèticament. Aquests pèptids els trobem principalment en plantes i llevats.

2.1.1.2. Segona classificació

Aviat es féu evident que aquesta divisió era insuficient, i el 1999 Binz i Kägi proposaren un nou sistema d'ordenació en base a similituds de seqüència i relacions filogenètiques.[4] Així, el conjunt de MT constituirien una *superfamília* que es divideix en 15 *famílies* que, alhora, es subdivideixen en *subfamílies* i *subgrups*. Trobem així per exemple la família 1, la de les MT de vertebrats, o la família 15, la de les MT de planta, que més endavant veurem com es divideix en funció del nombre i distribució de les seues Cys (*cf*. apartat 2.3.). A més a més, es podrien definir també *clans* que reagruparien MT en funció d'alguna característica comuna que la divisió anterior no haguera considerat.

2.1.1.3. Tercera classificació

Més recentment, el grup d'investigació en què s'ha realitzat aquesta Tesi proposà un nou model de classificació de les MT en funció, bàsicament, de les

[3] J.H.R. Kägi, Y. Kojima, Experientia Supplementum Metallothionein II, vol. 52, Birkhäuser Verlag, Basel, 1987.
[4] http://www.bioc.unizh.ch/mtpage/classif.html, 2013 (accés 25.11.13)

preferències de cada MT per a enllaçar Zn(II) o Cu(I).[5] Es defineixen així dos grups extrems clarament diferenciats, les Zn-tioneïnes i les Cu-tioneïnes genuïnes, que es troben units per tota una sèrie gradada de nivells que permeten classificar les MT segons el seu major o menor caràcter de Zn- o de Cu-tioneïna.[6] Les Zn-tioneïnes genuïnes formen espècies Zn(II)-MT úniques i ben plegades, retenen ions Zn(II) de manera que donen lloc a espècies Zn,Cu-MT quan es biosintetitzen en medis rics en coure i a espècies Zn,Cd-MT quan es biosintetitzen en medis rics en cadmi, i les espècies Cu(I)-MT biosintetitzades en medis rics en coure s'obtenen fàcilment addicionant un petit nombre d'equivalents de Cu(I) (proporció Cu:Cys) sobre solucions que contenen les Zn(II)-MT. Les Cu-tioneïnes genuïnes, en canvi, formen espècies Cu(I)-MT úniques i homometàl·liques quan es biosintetitzen en medis rics en coure, contenen lligands S^{2-} en els seus complexos Cd(II)-MT i donen lloc a mescles d'espècies amb diferent càrrega d'ions Zn(II) quan s'obtenen per síntesi recombinant en medis rics en zinc. D'aquestes observacions sorgeix per tant que, a l'hora de classificar les MT, hi hauria quatre criteris a considerar:

a) La presència/absència de Zn(II) en els complexos metall-MT biosintetitzats en medis rics en coure,
b) el nombre d'equivalents de Cu(I) (fent referència a mols de Cu per mol de Cys) necessaris per a reproduir, mitjançant experiments de substitució Zn(II)/Cu(I), les espècies Cu(I)-MT biosintetitzades en medis rics en coure,
c) la presència/absència de lligands S^{2-} i/o Zn(II) en els complexos metall-MT biosintetitzats en medis rics en cadmi, i
d) la reticència a reemplaçar completament el Zn(II) pel Cd(II) en experiments en què s'addiciona un excés de Cd(II) sobre solucions que contenen espècies Zn(II)-MT.

Trobem aquí com a exemples de Zn- i Cu-tioneïnes genuïnes CeMT1 del nemàtode *Caenorhabditis elegans* i Cup1 del llevat *Saccharomyces cerevisiae*, respectivament.

[5] M. Valls, R. Bofill, R. González-Duarte, P. González-Duarte, M. Capdevila, S. Atrian, J. Biol. Chem. 276 (2001) 32835-32843.
[6] R. Bofill, M. Capdevila, S. Atrian, Metallomics 1 (2009) 229-234.

2.1.2. Estructura

2.1.2.1. Patrons de seqüència

D'entre la gran diversitat d'estructures primàries que presenten les MT, cal destacar les següents característiques que els són comunes:[7]

a) La presència de motius CXC i CXXC, on X≠Cys, així com la presència menys habitual de doblets CC i triplets CCC.
b) El predomini de residus aminoacídics petits, com són Gly i Ala, que permeten girs i, en definitiva, un plegament de la cadena polipeptídica que no seria possible amb una major presència de residus més voluminosos.
c) L'escassedat de residus hidrofòbics (Ile, Leu) i aromàtics (Tyr, Trp, Phe), amb les corresponents conseqüències en el plegament de les MT, donat que aquests residus generalment estabilitzen l'estructura proteica a través d'interaccions hidrofòbiques. En les MT, en canvi, aquesta estabilització ve donada principalment per la formació dels clústers metall-tiolat.

2.1.2.2. Estructura tridimensional

Actualment, es disposa en el Protein Data Bank (PDB) de 35 entrades corresponents a diverses estructures d'agregats metall-MT que es mostren en la Taula 2. D'entre aquestes, només Cd_5Zn_2-MT2 de rata (4MT2) i Cu_8-Cup1 de llevat (1RJU) han estat resoltes per difracció de raigs X, mentre que per a la resta s'han fet servir tècniques de RMN. A més, tot i que no és accessible a través del PDB, està resolta també per RMN l'estructura de Cd_7-MT10 del musclo *Mytilus galloprovincialis*.[8]

Taula 2. Complexos metall-MT amb l'estructura tridimensional disponible en el Protein Data Bank (PDB).

Organisme	**Complex metall-MT**	**Codi accés PDB**	**Any publicació**
Humà (*Homo sapiens*)	Cd_3-βMT2	2MHU	1990[9]
	Cd_4-αMT2	1MHU	
	Cd_4-αMT3	2FJ4, 2FJ5, 2F5H	2006

[7] C.A. Blindauer, O.I. Leszczyszyn, Nat. Prod. Rep. 27 (2010) 720-741.
[8] G. Digilio, C. Bracco, L. Vergani, M. Botta, D. Osella, A. Viarengo, J. Biol. Inorg. Chem. 14 (2009) 167-178.
[9] B.A. Messerle, A. Schäffer, M. Vašák, J.H. Kägi, K. Wüthrich, J. Mol. Biol. 214 (1990) 765-779.

Organisme	**Complex metall-MT**	**Codi accés PDB**	**Any publicació**
Ratolí	Cd_3-βMT1	1DFT	1999[10]
(*Mus musculus*)	Cd_4-αMT1	1DFS	
	Cd_4-αMT3	1JI9	2001[11]
Rata	Cd_5Zn_2-MT2	4MT2	1983-1992[12]
(*Rattus rattus*)	Cd_3-βMT2	2MRT	1988[13]
	Cd_4-αMT2	1MRT	
Conill	Cd_3-βMT2A	2MRB	1980-1988[14]
(*Oryctolagus cuniculus*)	Cd_4-αMT2A	1MRB	
Eriçó de mar	Cd_4-αMTA	1QJK	1999[15]
(*Strongylocentrotus purpuratus*)	Cd_3-βMTA	1QJL	
Peix de l'Antàrtida	Cd_3-βMT	1M0J	2003[16]
(*Notothenia coriiceps*)	Cd_4-αMT	1M0G	
Cranc blau	Cd_3-β_NMT1	1DME, 1DMF	1995[17]
(*Callinectes sapidus*)	Cd_3- β_CMT1	1DMC, 1DMD	
Llamàntol americà	Cd_3-β_NMT1	1J5M	2002[18]
(*Homarus americanus*)	Cd_3- β_CMT1	1J5L	
Llevat	Ag_7-Cup1	1AOO, 1AQQ	1996[19]
(*Saccharomyces cerevisiae*)	Cu_7-Cup1	1AQR, 1AQS, 1FMY	1996,[19] 2000[20]
	Cu_8-Cup1	1RJU	2005[21]
Bacteri (*Synechococcus elongatus*)	Zn_4-SmtA	1JJD	2001[22]
Fong (*Neurospora crassa*)	Cu_6-NcMT	1T2Y	2004[23]
Blat	Zn_4-β_E-Ec-1[24]	2KAK	2009-2013
(*Triticum aestivum*)	Zn_2-γEc-1[25]	2L62	
	Cd_2-γEc-1[25,26]	2L61, 2MFP	

[10] K. Zangger, G. Oz, J.D. Otvos, I.M. Armitage, Protein Sci. 8 (1999) 2630-2638.
[11] G. Oz, K. Zangger, I.M. Armitage, Biochemistry 40 (2001) 11433-11441.
[12] W. Braun, M. Vašák, A.H. Robbins, C.D. Stout, G. Wagner, J.H. Kägi, K. Wüthrich, Proc. Natl. Acad. Sci. USA 89 (1992) 10124-10128.
[13] P. Schultze, E. Wörgötter, W. Braun, G. Wagner, M. Vašák, J.H. Kägi, K. Wüthrich, J. Mol. Biol. 203 (1988) 251-268.
[14] A. Arseniev, P. Schultze, E. Wörgötter, W. Braun, G. Wagner, M. Vašák, J.H. Kägi, K. Wüthrich, J. Mol. Biol. 201 (1988) 637-657.
[15] R. Riek, B. Prêcheur, Y. Wang, E.A. Mackay, G. Wider, P. Güntert, A. Liu, J.H. Kägi, K. Wüthrich, J. Mol. Biol. 291 (1999) 417-428.
[16] C. Capasso, V. Carginale, O. Crescenzi, D. Di Maro, E. Parisi, R. Spadaccini, P.A. Temussi, Structure 11 (2003) 435-443.
[17] S.S. Narula, M. Brouwer, Y. Hua, I.M. Armitage, Biochemistry 34 (1995) 620-631.
[18] A. Muñoz, F.H. Försterling, C.F. Shaw 3rd, D.H. Petering, J. Biol. Inorg. Chem. 7 (2002) 713-724.
[19] C.W. Peterson, S.S. Narula, I.M. Armitage, FEBS Lett. 379 (1996) 85-93.
[20] I. Bertini, H.J. Hartmann, T. Klein, G. Liu, C. Luchinat, U. Weser, Eur. J. Biochem. 267 (2000) 1008-1018.
[21] V. Calderone, B. Dolderer, H.J. Hartmann, H. Echner, C. Luchinat, C. Del Bianco, S. Mangani, U. Weser, Proc. Natl. Acad. Sci. USA 102 (2005) 51-56.
[22] C.A. Blindauer, M.D. Harrison, J.A. Parkinson, A.K. Robinson, J.S. Cavet, N.J. Robinson, P.J. Sadler, Proc. Natl. Acad. Sci. USA 98 (2001) 9593-9598.
[23] P.A. Cobine, R.T. McKay, K. Zangger, C.T. Dameron, I.M. Armitage, Eur. J. Biochem. 271 (2004) 4213-4221.
[24] E.A. Peroza, R. Schmucki, P. Güntert, E. Freisinger, O. Zerbe, J. Mol. Biol. 387 (2009) 207-218.
[25] J. Loebus, E.A. Peroza, N. Blüthgen, T. Fox, W. Meyer-Klaucke, O. Zerbe, E. Freisinger, J. Biol. Inorg. Chem. 16 (2011) 683-694.

La majoria dels complexos M(II)-MT (on M(II) són els metalls divalents Zn(II) o Cd(II)) dels quals se'n coneix l'estructura presenten dos dominis, cadascun amb un clúster metall-tiolat. L'excepció és Zn_4-SmtA de bacteri, que presenta un sol domini. En canvi $M(I)_{7/8}$-Cup1 (on M(I) són metalls monovalents Ag(I) o Cu(I)) de llevat, i Cu_6-NcMT de fong són monodominials, ja que formen un únic clúster metàl·lic. Se sap també que les MT presenten una estructura desordenada quan no enllacen cap metall (apo-MT)[27] i que, en canvi, en presència de metalls formen els agregats polinuclears que defineixen la seua estructura terciària. S'esdevé així que el plegament de les MT ve principalment determinat pel nombre i la naturalesa dels metalls que enllacen i, donat que s'assumeix que la funció d'una proteïna depén de la seua estructura terciària, que aquests determinen les seues funcions biològiques.

Les MT de mamífer (humà, ratolí, rata i conill) han estat les més estudiades. D'aquestes es coneix que enllacen 7 metalls divalents a través de les seues vint Cys (Fig. 1A), formant dos clústers metall-tiolat del tipus $M(II)_3$-$(SCys)_9$ i $M(II)_4$-$(SCys)_{11}$ (Fig. 1B,C) en l'interior dels dominis anomenats β (N-terminal) i α (C-terminal), respectivament. Tots els ions metàl·lics presenten un entorn de coordinació tetraèdric.[9,10,11,12,13,14]

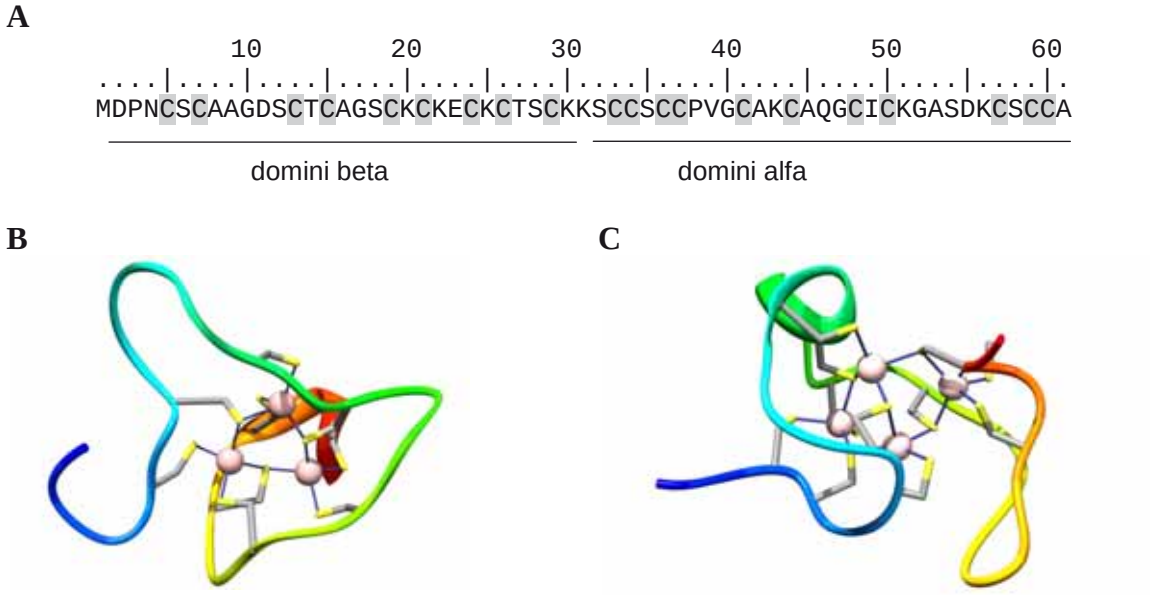

Figura 1. Estructura de les MT de mamífer: (**A**) seqüència aminoacídica de la MT2 humana (UniprotKB P02795); estructura 3D dels seus clústers (**B**) Cd_3-$(SCys)_9$ (PDB 2MHU) i (**C**) Cd_4-$(SCys)_{11}$ (1MHU), situats als dominis β i α, respectivament.

[26] K. Tarasava, S. Johannsen, E. Freisinger, Molecules 18 (2013) 14414-14429.
[27] M. Vašák, A. Galdes, H. Allen, O. Hill, J.H.R. Kägi, I. Bremner, B.W. Young, Biochemistry 19 (1980) 416-425.

Pel que fa a la coordinació de metalls monovalents (Cu(I)), en la Taula 2 es pot observar que no hi ha cap estructura resolta per a les MT de mamífer coordinant aquest ió metàl·lic. No obstant, es coneix que aquestes MT enllacen preferentment 6 ions Cu(I) en cadascun dels dominis, donant lloc així a espècies Cu_{12}-MT. Els ions Cu(I) s'enllacen a través de dos o tres lligands tiolat cisteínics amb una geometria lineal o trigonal plana, respectivament.[28,29]

Així, hom considera les estequiometries metall:Cys per a les ben conegudes MT de mamífer (1:2.8 per al clúster $M(II)_4(SCys)_{11}$ i 1:1.8 per al clúster $M(I)_6(SCys)_{11}$ al domini α; 1:3.0 per al clúster $M(II)_3(SCys)_9$ i 1:1.5 per al clúster $M(I)_6(SCys)_9$ al domini β) com a model quan s'estudia la coordinació d'ions metàl·lics en complexos metall-MT de què es desconeix l'estructura. Tanmateix, l'existència del clúster $M(II)_2(SCys)_6$ descrit recentment en el domini γ de Ec-1 de blat,[24,25,26] així com la possibilitat de participació de lligands diferents dels residus Cys s'han de tindre presents.

2.1.3. Lligands alternatius a les cisteïnes

2.1.3.1. Les histidines

Durant molt de temps, la creença que els residus Cys eren els únics que participaven en l'enllaç als ions metàl·lics en les MT no havia estat posada en dubte. Actualment, però, es coneix l'estructura 3D de dues MT que contenen residus His que coordinen metalls divalents: SmtA del bacteri *Synechococcus elongatus* i Ec-1 de la planta *Triticum aestivum* (Figura 2).

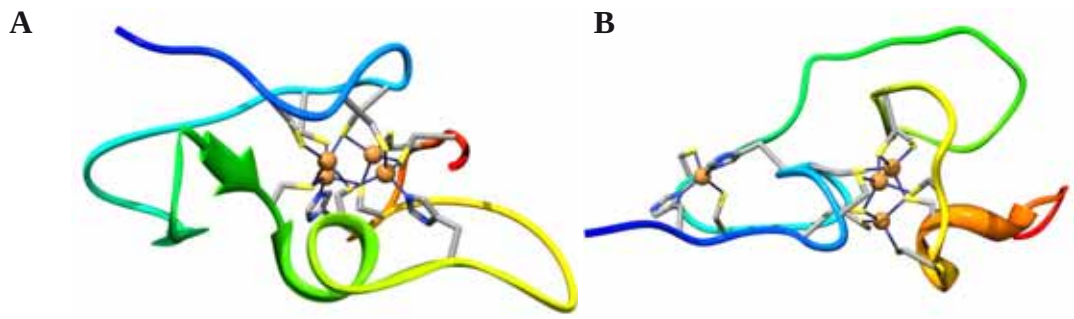

Figura 2. Estructura 3D de (**A**) Zn_4-SmtA de *S. elongatus* (PDB 1JJD) i (**B**) Zn_4-β_E-Ec-1 del domini β_E de Ec-1 de *T. aestivum* (2KAK).

[28] A. Presta, A.R. Green, A. Zelazowski, M.J. Stillman, Eur. J. Biochem. 227 (1995) 226-240.
[29] N. Romero-Isart, M. Vašák, J. Inorg. Biochem. 88 (2002) 388-396.

La primera en ser descrita fou SmtA, que forma un clúster $M(II)_4$-$(SCys)_9(NHis)_2$ quan enllaça Zn(II) o Cd(II) (Figura 2A).[22] Aquí destaca la similitud d'estructura entre aquest clúster i el ja conegut $M(II)_4$-$(SCys)_{11}$ del domini α de les MT paradigmàtiques, les de mamífer, en què l'única diferència radica en el bescanvi de dos lligands SCys per dos lligands NHis (Figura 3A). Aquest fet té conseqüències en les afinitats relatives d'enllaç a Zn(II) i Cd(II) donat que, a pH neutre, mentre que els llocs de coordinació Cys_4 enllacen Cd(II) amb major afinitat que Zn(II), els llocs de coordinació Cys_3His presents en SmtA tenen afinitats comparables per a ambdós cations.[30] Més recentment, es resolgué l'estructura del complex que forma la MT de blat (*Triticum aestivum*), Ec-1, amb el Zn(II),[24,25] que presenta el lloc de coordinació mononuclear Zn-$(SCys)_2(NHis)_2$ en l'anomenat domini β_E (Figura 2B). Aquí trobem de nou la similitud estructural amb les MT de mamífer donat que, de fet, el domini β_E (de l'anglés *beta expanded*) rep el seu nom perquè conté l'abans citat lloc de coordinació mononuclear, però també un clúster Zn_3-$(SCys)_9$ anàleg al present en el domini βMT de mamífer (Figura 3B). Una vegada més, cal destacar la major afinitat que aquest lloc de coordinació Zn-$(SCys)_2(NHis)_2$ introdueix per al Zn(II) comparat amb el Cd(II), coneixent que l'entorn Cys_2His_2 suposa una avidesa per al Zn(II) 350 vegades major que per al Cd(II).[30]

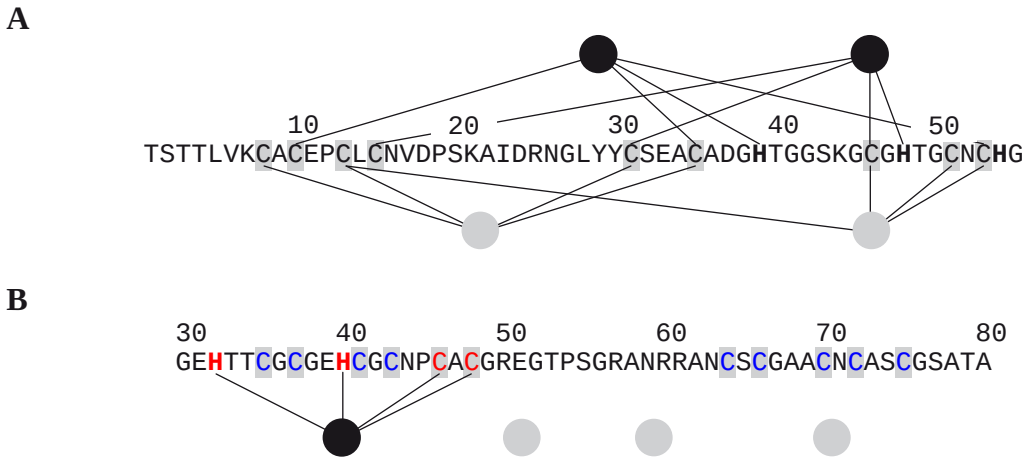

Figura 3. Seqüència aminoacídica i connectivitats metall-lligand per a (**A**) el clúster $M(II)_4$-$(SCys)_9(NHis)_2$ en SmtA de *S. elongatus* (adaptat de Blindauer *et al.*[22]) i (**B**) el lloc de coordinació Zn-$(SCys)_2(NHis)_2$ en el domini β_E de Ec-1 de blat. Es mostra la seqüència del domini β_E sencer (residus 30 a 80 de Ec-1, sense considerar la Met N-term), tot indicant la participació dels residus Cys i His en el lloc de coordinació mononuclear (roig) i en el clúster Zn_3-$(SCys)_9$ (blau), per al qual es desconeixen les connectivitats metall-lligand (adaptat de Peroza *et al.*[24] i Leszczyszyn *et al.*[31]). Les esferes negres representen els ions metàl·lics en entorns de coordinació Cys_3His o Cys_2His_2, mentre que les grises representen els metalls en llocs de coordinació Cys_4.

[30] C.A. Blindauer, J. Inorg. Biochem. 121 (2013) 145-155.
[31] O.I. Leszczyszyn, C.R. White, C.A. Blindauer, Mol. Biosyst. 6 (2010) 1592-1603.

La presència de residus His coordinants i les conseqüències pel que fa a la funció de les MT que això pot implicar ha generat un important tema de discussió científica.[30,32] En general, des d'un punt de vista termodinàmic se suggereix que les His augmenten l'afinitat relativa per al Zn(II) en comparació amb el Cd(II), d'acord amb el principi dels àcids i bases durs i tous (o HSAB, de l'anglés *Hard-Soft Acid-Base*). Des d'un punt de vist cinètic, sembla que aquestes suposen una disminució de la reactivitat.[33] Per exemple, estudis amb mutants puntuals His/Cys han demostrat que els lligands His suposen la reducció en la sensibilitat a l'oxidació i l'augment de l'especificitat per als ions Zn(II) en SmtA.[34] També, la presència de residus His coordinants en Ec-1 es relaciona amb una major selectivitat per al Zn(II) en detriment del Cd(II) que, alhora, es relaciona amb la seua funció com a reservori de zinc. De fet, s'ha demostrat que Ec-1 discrimina entre zinc i cadmi a causa del plegament alterat de la proteïna que suposa l'enllaç dels ions Cd(II).[31] Sembla que la distància i l'orientació entre Cys48 i His40 és determinant per al seu correcte plegament i que, quan Ec-1 s'exposa a Cd(II), la major afinitat d'aquest catió metàl·lic per a les Cys fa que probablement forme un clúster Cd_4-$(SCys)_{11}$ en lloc d'organitzar-se en Cd-$(SCys)_2(NHis)_2$ + Cd_3-$(SCys)_9$.[30] Així, la presuposició que els complexos d'una MT amb Zn(II) o Cd(II) són isoestructurals no és vàlida per a Ec-1. A més, cal destacar altres resultats que relacionen la presència d'His coordinants amb la selectivitat Zn/Cd. És el cas, per exemple, de les dues isoformes de MT del nemàtode *Caenorhabditis elegans*, CeMT-1 i CeMT-2, de les quals tot i que se'n desconeix l'estructura 3D sí que s'ha proposat la participació de les His que conté CeMT-1 en la coordinació metàl·lica.[35] Per a aquestes MT s'ha vist que els ions Cd(II) enllacen preferentment CeMT-2.[36,37] Novament, les His poden condicionar aquí la funció biològica. De fet, cal esperar que les conseqüències de la participació de residus His en aquestes metal·loproteïnes riques en Cys siguen importants. El fet que, per a la cèl·lula, el cost energètic de la síntesi d'His siga dels més alts d'entre tots els aminoàcids i major que el de les Cys no s'ha de menystenir.[38]

[32] O.I. Leszczyszyn, H.T. Imam, C.A. Blindauer, Metallomics 5 (2013) 1146-1169.
[33] C.A. Blindauer, J. Inorg. Biochem. 102 (2008) 507-521.
[34] C.A. Blindauer, M.T. Razi, D.J. Campopiano, P.J. Sadler, J. Biol. Inorg. Chem. 12 (2007) 393-405.
[35] R. Bofill, R. Orihuela, M. Romagosa, J. Domènech, S. Atrian, M. Capdevila, FEBS J. 276 (2009) 7040-7069.
[36] S. Zeitoun-Ghandour, J.M. Charnock, M.E. Hodson, O.I. Leszczyszyn, C.A. Blindauer, S.R. Stürzenbaum, FEBS J. 277 (2010) 2531-2542.
[37] O.I. Leszczyszyn, S. Zeitoun-Ghandour, S.R: Stürzenbaum, C.A: Blindauer, Chem. Commun. 47 (2011) 448-450.
[38] H. Akashi, T. Gojobori, Proc. Natl. Acad. Sci. USA 99 (2002) 3695-3700.

2.1.3.2. Els anions sulfur

La participació dels anions sulfur, juntament amb les Cys, en la coordinació d'ions metàl·lics es descrigué ja el 1983 en els pèptids sintetitzats enzimàticament de fòrmula general $(\gamma\text{-Glu-Cys})_n\text{Gly}$, les anomenades fitoquelatines (PC) que en la 'Primera classificació de les MT' s'incloïen en la *Classe III* (*cf.* subapartat 2.1.1.1.).[39] Les PC del llevat *Schizosaccharomyces pombe* foren les primeres en què es trobaren aquests lligands en complexos d'estequiometria $Cd_{5.4}S[(\gamma\text{-Glu-Cys})_3]Gly_4$. En aquestes molècules tan properes a les MT trobem microcristalls de sulfur de cadmi que queden envoltats pel polipèptid, i unides a aquest a través d'enllaços Cd-SCys (Figura 4). [40,41]

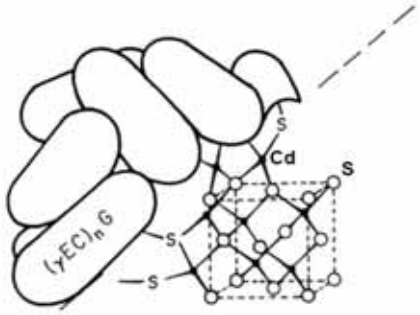

Figura 4. Representació de PC envoltant els microcristalls de sulfur de cadmi, els quals queden units a les PC a través d'enllaços Cd-SCys (extret de Winge *et al.*[41]).

Tanmateix, no fou fins l'any 2005 que el grup de recerca en què s'ha realitzat aquesta Tesi descrigué per primera vegada la presència d'aquests lligands en complexos metall-MT obtinguts per síntesi heteròloga en bacteris *Escherichia coli*.[42] La caracterització analítica de diversos complexos Zn(II)- i Cd(II)-MT donava lloc a alguns resultats que no es podien explicar d'acord amb una composició de les mostres on no existia res més que no fóra la MT i el metall, i en canvi l'evidència que en aquests complexos s'hi trobaven també lligands sulfur féu quadrar tots aquests resultats. És per això que ara determinem el contingut en sofre de les preparacions Zn/Cd-MT abans i després d'un tractament amb àcid donat que, en acidificar, aquests anions sulfur es desprenen en forma de sulfur d'hidrogen. Així, un dels indicis de la presència d'anions sulfur àcid-làbils en les mostres és que la quantitat de sofre determinada per

[39] A. Murasugui, C. Wada, Y.J. Hayashi, J. Biochem. 93 (1983) 661-664.
[40] C.T. Dameron, R.N. Reese, R.K. Mehra, A.R. Kortan, P.J. Carroll, M.L. Steigerwald, L.E. Brus, D.R. Winge, Nature 338 (1989) 596-597.
[41] D. Winge, C.T. Dameron, R.K. Mehra (1992), dins: J.H.R. Kägi, Y. Kojima (Eds.), Metallothionein II, 52 (1992) 257-270.
[42] M. Capdevila, J. Domènech, A. Pagani, L. Tío, L. Villarreal, S. Atrian, Angew. Chem. Int. Ed. 44 (2005) 4618-4622.

espectroscòpia d'emissió atòmica amb plasma d'inducció acoblat (ICP-AES) és, per a una mateixa preparació, major en la mostra original que quan ha sigut acidificada i posteriorment reneutralitzada. També, en les preparacions que contenen aquests lligands àcid-làbils generalment observem absorcions al voltant dels 280 nm en els espectres de dicroisme circular (DC) i d'absorció en l'ultraviolat (UV), les quals desapareixen en ser acidificades i seguidament reneutralitzades. En la Figura 5 es mostren alguns espectres de DC i UV que presenten aquestes absorcions característiques. A més, és possible detectar les espècies Cd_xS_y-MT per espectrometria de masses amb ionització per electroesprai.

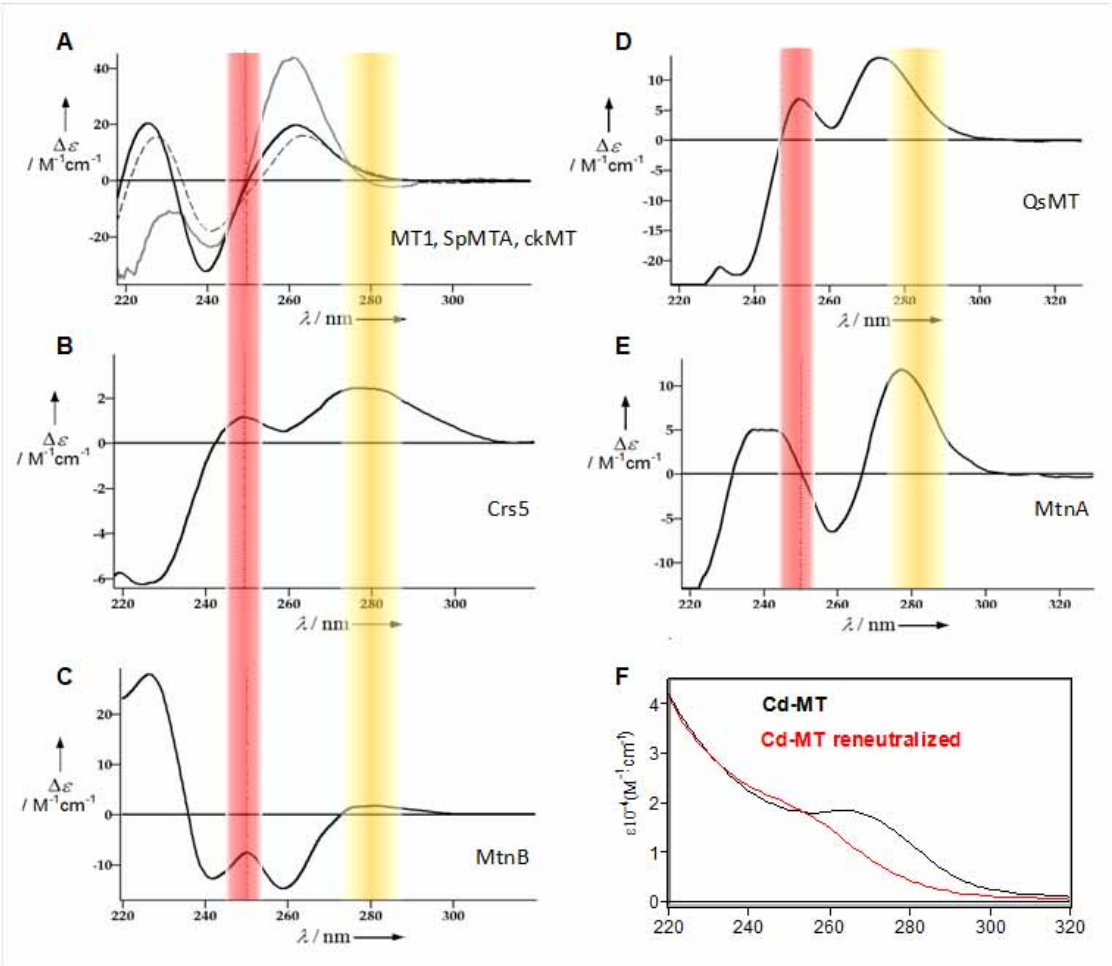

Figura 5. (**A-E**) Espectres de DC de diferents preparacions Cd-MT que mostren les absorcions característiques dels cromòfors Cd-$(SCys)_4$ a *ca.* 250 nm (roig) i les absorcions atribuïdes a la presència d'espècies $Cd_x(S^{2-})_y$-MT a *ca.* 280 nm (groc). (**F**) Espectre UV d'una preparació Cd-MT que conté lligands sulfur àcid-làbils obtinguda per síntesi heteròloga abans (línia negra) i després (línia roja) d'un cicle d'acidificació-reneutralització (extret de Palacios *et al.*[43])

La presència de lligands sulfur àcid-làbils s'ha descrit en complexos de les MT de diversos organismes amb Cd(II) i Zn(II), però mai amb Cu(I). Encara que es descrigueren inicialment en complexos metall-MT obtinguts per síntesi heteròloga en *E.*

[43] O. Palacios, S. Atrian, M. Capdevila, J. Biol. Inorg. Chem. 16 (2011) 991-1009.

coli, cal destacar l'existència d'aquests també en els complexos Cd-S-Cup1 natius aïllats del llevat *S. cerevisiae*, fet que demostra que els lligands sulfur no són tan sols un artefacte derivat de la síntesi de les MT recombinants en *E. coli*.[44]

2.1.4. Funcions

Des del seu descobriment, s'han proposat desenes de funcions per a les MT.[2,7] Per una banda, el fet que el polimorfisme siga un tret característic d'aquesta superfamília de proteïnes ja fa pensar en diferents funcions biològiques per a cadascuna de les isoformes que sintetitza un mateix organisme.[45] Així doncs, aquest fet, juntament amb l'heterogeneïtat de les seqüències aminoacídiques que presenten i la varietat de metalls que poden enllaçar, donant lloc a diverses estructures 3D per a un mateix pèptid, fa que la definició d'una funció única per al conjunt de MT no tinga gaire sentit.[2,7] A més, cal diferenciar entre allò que s'han anomenat les funcions moleculars de les anomenades funcions biològiques. Així, com a funcions moleculars cal destacar la seua capacitat d'enllaçar ions metàl·lics i el seu poder reductor, ambdues conseqüència de les propietats dels àtoms de sofre de les Cys que contenen, mentre que com a funcions biològiques cal esmentar principalment l'homeòstasi de metalls essencials i la destoxicació de metalls pesants tòxics, així com la protecció enfront d'agents oxidants i de radicals lliures.[2]

2.1.4.1. Homeòstasi i destoxicació de metalls

Com ja s'ha introduït abans, el manteniment dels nivells de metalls essencials (zinc i coure) en les cèl·lules és una de les funcions que es proposa per a les MT. Per la seua capacitat per a enllaçar metalls amb elevada estabilitat termodinàmica i baixa estabilitat cinètica, tant els processos d'incorporació de metalls com els d'intercanvi amb altres metal·loproteïnes estan afavorits.[29] És per aquestes raons que les MT poden actuar com a reservoris i/o transportadors de metalls. Com a exemple d'una MT amb aquestes funcions trobem Ec-1 en la llavor de blat, citada anteriorment. Sembla que aquesta MT emmagatzema ions Zn(II) fins que la llavor comença a germinar, moment en què allibera el metall que ara necessiten altres proteïnes/enzims per a la síntesi de noves estructures.[32]

[44] R. Orihuela, F. Monteiro, A. Pagani, M. Capdevila, S. Atrian, Chem. Eur. 16 (2010) 12363-12372.
[45] M. Capdevila, S. Atrian, J. Biol. Inorg. Chem. 16 (2011) 977-989.

D'altra banda, de la mateixa manera que es proposa la participació de les MT en l'homeòstasi dels metalls que són indispensables per a la vida, s'ha suggerit que aquests pèptids participen en el segrest i eliminació de metalls que són tòxics per als éssers vius, com el plom, el mercuri o el cadmi. De fet, les MT foren primerament descrites com a detoxificadores de Cd(II),1 i diversos estudis en models animals han demostrat que protegeixen enfront dels efectes tòxics d'aquest metall.[46]

2.1.4.2. Regulació i protecció envers oxidants i radicals lliures

El paper de les MT en processos d'estrés radicalari i/o oxidatiu ha estat també àmpliament estudiat, ja siga en la regulació d'aquests fenòmens o en la protecció envers els efectes perjudicials que aquest estrés pot causar a nivell cel·lular.

D'una banda, han estat demostrades la capacitat de les MT per a actuar com a captadors de radicals hidroxil i d'anions radicals superòxid, i de poder reaccionar amb el peròxid d'hidrogen,[47,48,49,50] així com la inducció de la síntesi d'aquests pèptids com a conseqüència de l'exposició a agents oxidants.[48,51] És per això que es relaciona les MT amb el manteniment de l'equilibri redox i, per tant, amb processos de senyalització cel·lular, regulació de l'expressió gènica o apoptosi, entre d'altres. En són exemples significatius diferents MT de planta, com les QsMT de l'alzina surera (*Quercus suber*) o OsMT2b de l'arròs (*Oryza sativa*), que a través de la seua participació en l'homeòstasi redox contribueixen al desenvolupament de la planta.[52,53] També, juntament amb aquesta funció reguladora, trobem en la bibliografia una gran quantitat de treballs que relacionen la reactivitat de les MT envers oxidants i radicals lliures amb la protecció enfront del dany sobre altres biomolècules que això comporta, com és el cas d'algunes MT de planta en situacions d'estrés (salinitat, sequera o baixes temperatures, per exemple).[54]

[46] C.D. Klaassen, J. Liu, S. Chouhuri, Annu. Rev. Pharmacol. Toxicol 39 (1999) 267-294.
[47] P.J. Thornalley, M. Vašák, Biochim. Biophys. Acta 827 (1985) 36-44.
[48] J. Abel, N. de Ruiter, Toxicol. Lett. 47 (1989) 191-196.
[49] A.R. Quesada, R.W. Byrnes, S.O. Krezoski, D.H. Petering, Arch. Biochem. Biophys. 334 (1996) 241-250.
[50] S. Zeitoun-Ghandour, O.I. Leszczyszyn, C.A. Blindauer, F.M. Geier, J.G. Bundy, S.R. Stürzenbaum, Mol. Biosyst. 7 (2011) 2397-2406.
[51] T. Dalton, R.D. Palmiter, G.K. Andrews, Nucleic Acids Res. 22 (1994) 5016-5023.
[52] G. Mir, J. Domènech, G. Huguet, G. Woei-Jiun, P. Goldsbrough, S. Atrian, M. Molinas, J. Exp. Bot. 55 (2004) 2483-2493.
[53] H.L. Wong, T. Sakamoto, T. Kawasaki, K. Umemura, K. Shimamoto, Plant Physiol. 135 (2004) 1447-1456.
[54] V.H. Hassinen, A.I. Tervahauta, H. Schat, S.O. Kärenlampi, Plant Biol. 13 (2011) 225-232.

D'altra banda, cal considerar també que l'homeòstasi de metalls com zinc o coure i l'homeòstasi redox es troben relacionades. Resulta evident l'efecte protector del segrest, per part de les MT, de metalls que intervenen en les reaccions de Fenton i Haber-Weiss (Cu(I)/Cu(II)), que acaben en la producció de radicals hidroxil. No obstant això, la regulació dels nivells d'un metall inactiu en reaccions d'oxidoreducció com el zinc està també lligada al metabolisme redox. Aquesta relació es dóna a través d'un cicle que enllaça l'alliberament/incorporació del Zn(II) per part de les MT amb l'estat redox de la cèl·lula,[55,56] tal i com es mostra en la Figura 6.

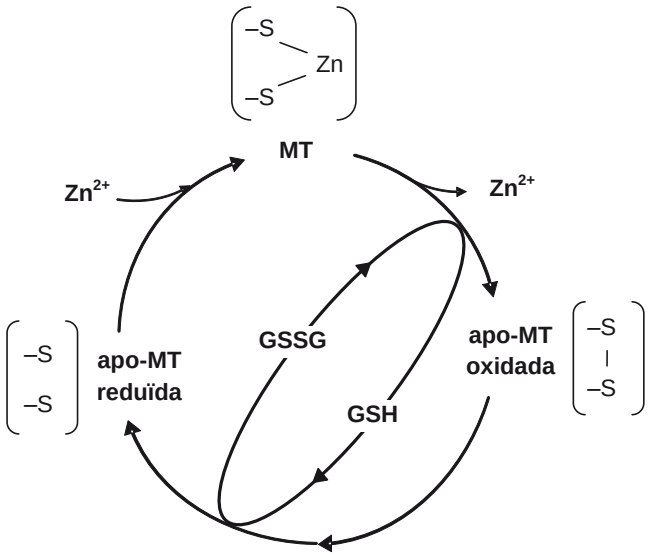

Figura 6. Esquema del cicle redox de les MT, que les relaciona amb l'estat redox cel·lular i l'homeòstasi del zinc (adaptat de Kang[55] i Maret[56]). GSH i GSSG són glutatió i disulfur de glutatió, respectivament.

És ben conegut que la disminució de la proporció glutatió (GSH):disulfur de glutatió (GSSG) a l'interior de la cèl·lula és un indicador d'estrés oxidatiu, açò és, que s'ha perdut l'equilibri entre la producció d'espècies oxidants i els mecanismes antioxidants. En aquest sentit, Maret i col·laboradors proposen que les MT participen en la recuperació dels nivells de GSH mitjançant l'oxidació dels tiols de les Cys, fet que comporta l'alliberament del metall, que queda així lliure per a altres accions.[57]

Per acabar amb les implicacions de les MT en funcions relacionades amb l'homeòstasi redox, cal afegir que s'ha posat de manifest la reactivitat de les MT amb espècies reductores, com àtoms d'hidrogen o electrons solvatats, la qual resulta en el dany

[55] Y.J. Kang, Exp. Biol. Med. 231 (2006) 1459-1467.
[56] W. Maret, J. Biol. Inorg. Chem. 16 (2011) 1079-1086.
[57] W. Maret, B.L. Vallee, Proc. Natl. Acad. Sci. USA 95 (1998) 3478-3482.

a fosfolípids de membrana en estudis *in vitro* amb models de membrana cel·lular.[58] Tot i que l'estudi de l'efecte dels radicals lliures en el medi biològic sovint ha estat centrat en l'estudi d'espècies oxidants, principalment el radical hidroxil, s'ha posat en evidència que algunes malalties humanes (malalties degeneratives, diabetis i cardiomiopaties) estan relacionades amb l'estrés reductor.[59,60,61] És en aquest context que cal considerar la possible participació de les MT en aquests processos i d'altres de relacionats en altres organismes, que fins ara han estat poc estudiats.

2.2. Les metal·lotioneïnes d'equinoderm

Els equinoderms (del grec *echinos* i *derma* que signifiquen eriçó i pell, respectivament) constitueixen un fílum d'animals invertebrats marins on s'inclouen els eriçons de mar, els quals s'usen en biologia com a organismes model. Les MT d'equinoderm constitueixen la família 4 de la classificació de Binz i Kägi.4

2.2.1. Estructura

En la base de dades de proteïnes UniProtKB trobem les set MT d'equinoderm que es mostren en la Figura 7.[62]

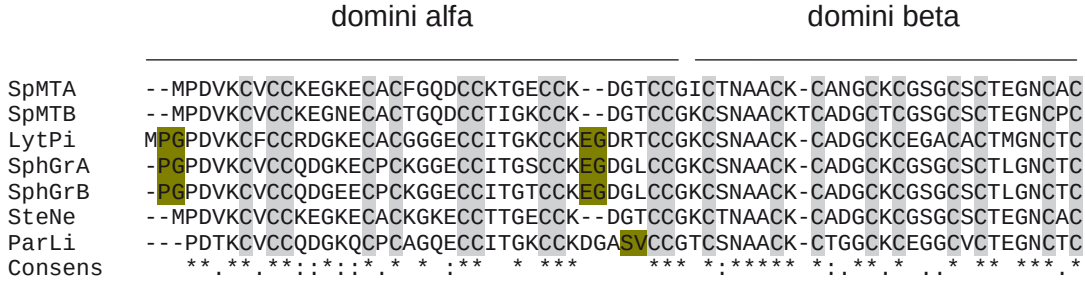

Figura 7. Alineament ClustalW de les seqüències aminoacídiques de SpMTA i SpMTB de *S. purpuratus* (UniprotKB P04734 i Q27287, respectivament), LytPi de *L. pictus* (O02033), SphGrA i SphGrB de *S. granularis* (Q26497 i Q26496), SteNe de *S. neumayeri* (P55953) i ParLi de *P. lividus* (P80367). L'asterisc (*) indica les posicions completament conservades, els dos punts (:) indiquen la presència de residus amb propietats molt semblants i el punt (.) indica la presència de residus amb propietats dispars. En verd s'indiquen les insercions de dipèptids presents en algunes de les seqüències de MT d'equinoderm que es comenten en el text.

[58] A. Torreggiani, C. Chatgilialoglu, C. Ferreri, M. Melchiorre, S. Atrian, M. Capdevila, J. Proteomics 92 (2013) 204-215.
[59] B. Lipinski, Br. J. Nutr. 87 (2002) 93-94.
[60] N.S. Rajasekaran, P. Connell, E.S. Christians, L.J. Yan, R.P. Taylor, et al., Cell 130 (2007) 427-439.
[61] X. Zhang, X. Min, C. Li, I.J. Benjamin, B. Qian, X. Zhang, et al., Hyperthension 55 (2010) 1412-1417.
[62] http://www.uniprot.org/, 2013 (accés 13-Gener-2014).

Les seqüències de les MT dels eriçons de mar difereixen de les de mamífer principalment a causa de la inversió de la localització dels dominis α i β: el domini α es troba ara en la part N-terminal del pèptid i el domini β en la C-terminal, contràriament a allò que ocorre en les MT de mamífer. Com s'observa en la Figura 7, els quatre doblets CC que en les MT de mamífer es troben en la part C-terminal (vegeu Fig. 1A) aquí apareixen en la N-terminal.[63] A més, el grau de similitud entre les MT de vertebrats és major que el de les MT dels eriçons de mar, on destaca la inserció dels dipèptids PG en el N-*terminus* i EG cinc posicions abans del doblet CC en l'extrem C-terminal del domini α per a les MT de *Lytechinus pictus* i *Sphaerechinus granularis*, així com del segment SV just abans del doblet CC en l'extrem C-terminal del domini α de la MT de *Paracentrotus lividus*.[64]

SpMTA de *Strongylocentrotus purpuratus* és la MT d'equinoderm millor caracteritzada. Per a aquesta se'n coneix l'estructura dels dos dominis que presenta el complex Cd_7-SpMTA (Figura 8),[15] amb formes semblants a les que presenta Cd_7-MT de mamífer. Tanmateix, a banda de la ja esmentada inversió de dominis, una altra diferència destacable és el plegament de la cadena polipeptídica en sentit antihorari en el domini β, al contrari del que passa en les MT de mamífer. Aquest és així l'únic cas de domini β plegat en sentit antihorari que es coneix.[63]

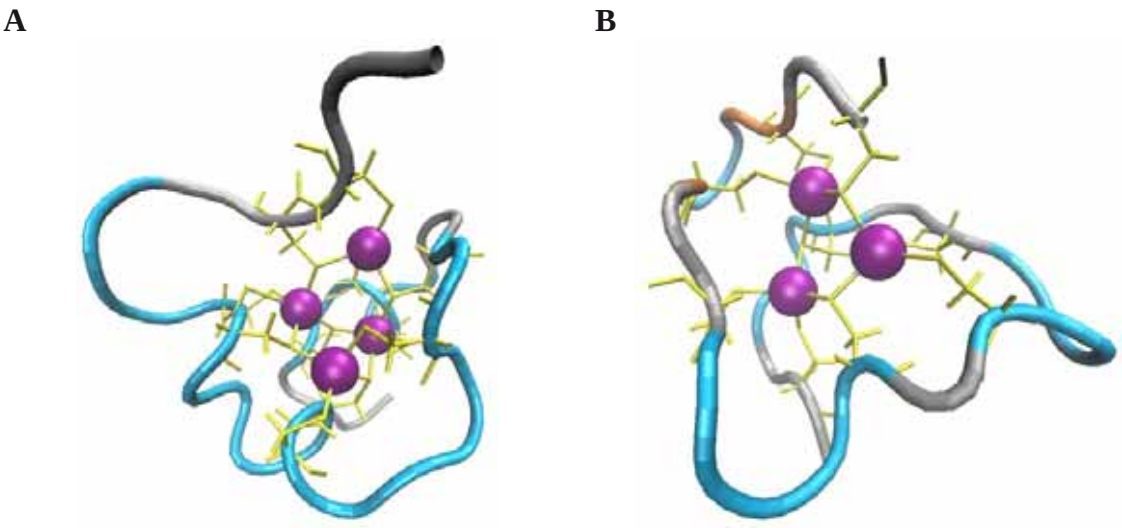

Figura 8. Estructura 3D de (**A**) Cd_4-αSpMTA (PDB 1QJK) i (**B**) Cd_3-βSpMTA (1QJL) de *S. purpuratus*.

[63] L. Vergani, Met. Ions Life Sci. 5 (2009) 199-237.
[64] R. Scudiero, C. Capasso, V. Carginale, M. Riggio, A. Capasso, M. Ciaramella, S. Filosa, E. Parisi, Cell. Mol. Life Sci. 53 (1997) 472-477.

2.2.2. Funcions

Cal destacar els resultats que indiquen que les MT dels eriçons de mar *S. granularis* i *S. neumayeri* tindrien la funció de dipòsit d'ions Zn(II), que serviria el metall per als processos metabòlics que el requereixen durant el seu desenvolupament,[64] de manera que recorda la funció esmentada abans per a Ec-1 en la planta de blat. És també interessant, en aquest sentit, el fet que els gens que codifiquen per a les dues isoformes de MT de *S. purpuratus* contenen múltiples elements de resposta a metalls (o MRE, de l'anglés *Metal Responsive Element*) que responen a Zn(II).[65] Es coneix també que tot i que ambdós gens s'expressen de manera constitutiva, *SpMTB* respon més que *SpMTA* a l'exposició de l'organisme a metalls.[66]

2.3. Les metal·lotioneïnes de planta

Les MT de planta són un cas particular dins el conjunt de les MT. Les característiques de les seues estructures primàries, amb un fragment lliure de Cys que comprén fins a uns 40 residus aminoacídics (anomenat espaiador), i la presència de residus aromàtics són els trets principals que les diferencien de la resta.[32] Si bé la primera MT es descobrí als anys 1950,1 no fou fins el 1983 que s'aïllà la primera MT de planta, Ec-1 de blat.[67] Des d'aleshores s'han descrit més de 1000 seqüències per a aquesta família de MT si tenim en compte tant bases de dades de proteïnes com de nucleòtids,[32] de les quals només 162 estan anotades en la base de dades de proteïnes UniprotKB.[62] De fet, la informació a nivell de proteïnes és escassa i se centra principalment en Ec-1 de blat, per a la qual ja s'ha vist que se'n coneixen tant la seua estructura 3D com la seua funció (vegeu Taula 2, i subapartats 2.1.3.1. i 2.1.4.1.). En aquest apartat introduïm els trets específics d'aquesta família de MT tan peculiar en què no s'ha aprofundit anteriorment.

2.3.1. Classificació: seqüències consens i variants

Les MT de planta es classifiquen dins la família 15 de les MT de la classificació de Binz i Kägi,4 la qual es divideix en quatre subfamílies en funció del

[65] G. Bai, E.W. Stuebing, H.R. Parker, P. Harlow, M. Nemer, Mol. Cell Biol. 13 (1993) 993-1001.
[66] D.G. Wilkinson, M. Nemer, Mol. Cell Biol. 7 (1987) 48-58.
[67] L. Hanley-Bowdoin, B.G. Lane, Eur. J. Biochem. 135 (1983) 9-15.

nombre i la distribució de les seues Cys.[68] Trobem així les subfamílies p1, p2 i p3 (d'ara endavant ens referirem a les MT que pertanyen a aquestes sufbamílies com a MT1, MT2 i MT3, respectivament), que comparteixen la característica de presentar dos dominis rics en Cys separats per un domini lliure d'aquestes (l'esmentat espaiador). A més, totes aquestes mostren sis Cys en el fragment C-terminal, i és en base al contingut en Cys al fragment N-terminal que les diferenciem en les tres subfamílies esmentades, amb sis, vuit i quatre residus Cys, respectivament. La subfamília p4 o pec (d'ara endavant MT4), però, presenta tres dominis rics en Cys que contenen seqüencialment sis, sis i cinc residus Cys, separats per tant per dos espaiadors (Figura 9).

```
          10        20        30        40        50        60        70        80
    ....|....|....|....|....|....|....|....|....|....|....|....|....|....|....|
    ---CXCGS-CXCG--CXC-------------------------------------CXCG--CXC-PCXC-
MT1 MSGCNCGSSCNCGDQCKCNKRSGLSYVEAGETTETVVLGVGPTKIHFEGAEMSVAAEDGGCKCGSSCTCDPCNCK

    -SCCGGXCGC---CXCG-GCGGC------------------GVAP-----------------CXC---CXC--CXC-
MT2 MSCCGGNCGCGTGCKCGSGCGGCKMFPDISSEKTTTETLIVGVAPQKTHFEGSEMGVGAENGCKCGSNCTCDPCNCK

    ---CXXCXCCDXXXC---------------------------------CKC---CXC--CXC--
MT3 MSTCGNCDCVDKSQCVKKGNSYGIDIVETEKSYVDEVIVAAEAAEHDGKCKCGAACACTDCKCGN

    --CXXXCGCXXPCXXXXXCRC-----------HXXCXCGXHCXCXPCXC---------------CXCXXXCXCXXC-----
MT4 MGCDDKCGCAVPCPGGTGCRCTSARSGAAAGEHTTCGCGEHCGCNPCACGREGTPSGRANRRANCSCGAACNCASCGSATA
```

Figura 9. Seqüències aminoacídiques representatives de les quatre subfamílies de MT de planta. Les seqüències corresponen a les MT1 de *C. arietinum* (UniprotKB Q39458), MT2 de *Q. suber* (Q93X22), MT3 de *M. acuminata* (Q40256) i MT4 de *T. aestivum* (P30569). S'han seleccionat aquestes perquè presenten els trets característics de cada subfamília i perquè se citen més endavant en el text. Dalt de cada pèptid es mostra la seqüència consens per a cada subfamília. Les Cys apareixen destacades en gris i els residus aromàtics en negreta.

Com s'observa, el polimorfisme en les MT de planta és especialment destacable. De fet, no és tan sols que en la majoria de plantes en què s'ha descrit la presència de MT s'han trobat representants de les quatre isoformes sinó que, també, l'existència de variants respecte de les seqüències consens per a cadascuna de les subfamílies és habitual. Així, les MT1 típiques contenen sis motius CXC distribuïts de tres en tres entre els dos fragments rics en Cys, que estan separats per un fragment lliure de Cys d'uns 40 residus aminoacídics. Addicionalment, hi ha tres Gly, una Ser i una Pro també conservades (Figura 9).[32,69,70] Tanmateix, d'una banda trobem variants on l'espaiador no conté més de 10 aminoàcids, com les MT1 d' *Arabidopsis lyrata* (GenBank XP_002892408), d'*A. thaliana* (UniProtKB P43392, Q38803 i Q38804), de *Brassica*

[68] C. Cobbett, P. Goldsbrough Annu. Rev. Plant Biol. 53 (2002) 159-182.
[69] E. Freisinger, Met. Ions Life Sci. 5 (2009) 107-153.
[70] N.H. Roosens, R. Leplae, C. Bernard, N. Verbruggen, Planta 222 (2005) 716-729.

juncea (UniProtKB A4URF6), de *B. napus* (GenBank ADP37975 i UniProtKB P43402), de *B. oleracea* (GenBank DK501359 i UniProtKB Q9M698) o de *Thlaspi caerulescens* (GenBank AY486003). A més, totes aquestes MT1 presenten un residu Cys extra al principi del domini ric en Cys C-terminal. D'altra banda, quan trobem variants amb residus Cys extra, majoritàriament n'és un de més que les MT1 típiques i es localitza en el domini N-terminal. En són exemples MT1 de *Betula platyphylla* (AAY16439), d'*Ephedra distachya* (JG721393), de *Grimmia pilifera* (GR307619), de *Huperzia serrata* (GO912370), de *Plantago major* (CAH59434), de *Pyrus pyrifolia* (UniProtKB Q9LUX2), de *Selaginella moellendorffii* (GenBank FE432113), de *S. lepidophylla* (BM402666), de *Syntrichia ruralis* (CN208803), de *Xerophyta humilis* (AAT45000) o de *Tamarix androssowii* (UniProtKB Q6IV93).

Pel que fa a la subfamília MT2, a banda de per les ja esmentades vuit Cys en el fragment N-terminal, identifiquem ràpidament una seqüència com a pertanyent a aquesta subfamília pel doblet CC amb què comença aquesta regió rica en Cys. Tal i com es mostra en la Figura 9, les MT2 típiques presenten aquí el motiu SCCGGXCGC que conté aquest doblet de Cys seguit dels motius CXCG i GCGGC. Aquestes contenen en el fragment C-terminal els tres motius CXC, i el tetrapèptid GVAP localitzat en l'espaiador està també conservat.[71] Les variants amb diferent contingut en residus Cys són també freqüents en la subfamília MT2, si bé la proporció de casos respecte del total de MT de la mateixa subfamília descrites fins ara és menor que per a les MT1. Trobem així, d'una banda, pèptids que contenen més Cys que les MT2 típiques en la regió C-terminal. Són els casos de les MT2 de *Fragaria ananassa* (UniProtKB P93134), de *Gingko biloba* (GenBank DR064960) o de *Solanum lycopersicum* (UniProtKB Q43515), amb una Cys extra; MT2 de *Colocasia esculenta* (UniProtKB Q19LA2), *d'Ipomoea batatas* (Q9SPE7) o de *Picea sinensis* (ABK21239), amb dues Cys de més; i MT2B i MT2C d'*Oryza sativa* (UniProtKB Q5JM82 i A3AZ88, respectivament), MT2 de *Welwitschia mirabilis* (GenBank DT598383) o MT2 de *Zea mays* (B6HS2, B6SPB8, B6SP45, B6T2H9, B6T303 i B6UC14), amb tres Cys extra. D'altra banda, trobem també MT2 amb un o dos residus Cys menys en la regió N-terminal. Són majoritàriament MT2 on una de les dues Cys del doblet CC ha estat mutada per una Gly o Ser, com són els casos de MT2 de *Grimmia pilifera* (GR307619), de *M. acuminata* (GenBank AAG44758 i UniProtKB O22319), de MT4B i MT4C d'*O. sativa* (Q2QNE8 i Q2QNC3, respectivament), de *Z. mays* (B6SP45,

[71] J. Guo, L. Xu, Y. Su, H. Wang, S. Gao, J. Xu, Y. Que, Biomed. Res. Int. (2013) doi: 0.1155/2013/904769

B6T2H9 i B6UC14), o la mateixa MT2 de *S. lycopersicum* (Q43515), que conté una Cys extra en la regió C-terminal. Tanmateix es donen també la mutació C10R en MT2 d'*Atropa belladonna* (Q94I87), la delecció del seté residu Cys en MT2 de *S. lycopersicum* o la delecció del vuité residu Cys en MT4A, MT4B i MT4C d'*Oryza sativa* (Q0IMG5, Q2QNE8 i Q2QNC3, respectivament), que no afecten el doblet CC.[32,69,71]

Les MT3 són les MT de planta que presenten les seqüències més curtes, amb un total de 60-65 residus aminoacídics. Les quatre Cys característiques del domini N-terminal apareixen amb una seqüència consens CXXCXCCDXXXC, separades dels tres motius CXC del domini C-terminal per una regió lliure de Cys d'uns 30-40 aminoàcids (Figura 9).[32,69] En aquesta subfamília trobem també algunes MT amb residus Cys extra, en aquest cas situats al final del segon fragment ric en Cys. Són per exemple MT3 de *Thlaspi caerulescens* (UniProtKB ACR46965), amb una Cys més; MT3 d'*Arabidopsis lyrata* (GenBank XP_002885083), d'*A. thaliana* (UniProtKB O22433), de *Brassica juncea* (BAB85601), de *B. napus* (AFP57435), d'*Eutrema halophilum* (AAM19713), d'*Olimarabidopsis pumila* (GenBank JZ152222) o de *Raphanus raphanistrum* (EY906858), amb dues Cys de més. A més, en aquesta subfamília hi ha una relativa conservació de les His, com veurem en el subapartat 2.4.3.1.

Les seqüències de les MT4 són molt diferents de les anteriors, amb dues regions lliures de Cys que contenen solament 10-15 aminoàcids i tres regions riques en Cys organitzades segons els motius conservats CXXXCGCXXPCXXXXXCRC (regió N-term), HXXCXCGXHCXCXPCXC (regió central) i XCXXXCXCXXC (regió C-term). Com s'observa en el fragment consens de la regió central, hi ha dues His en posicions molt conservades (Figura 9).[30,69] Pel que fa a les MT4 que difereixen de les típiques, trobem exemples de pèptids que contenen set, vuit i fins a nou residus Cys en la regió N-terminal en lloc de sis. Així, amb un residu Cys extra en aquesta localització tenim MT4 d'*Adiantum capillus-veneris* (GenBank DK953870), MT4a i MT4b de *Picea glauca* (GE478151 i EX413019), i MT4 de *Pseudotsuga menziesii* (CN637534), de *Pteridium aquilinum* (GW575141) o d'*Osmunda lancea* (FS994081). MT4 de *Chamaecyparis obtusa* (BW987215) o de *Cycas rumphii* (EX927452) presenten dues Cys extra en aquesta regió, i MT4 de *Marchantia polymorpha* (BJ852235) en presenta tres. MT4 de *Xerophyta humilis* (AAT45001) també conté una Cys més que les MT4 típiques, en aquest cas en l'extrem C-terminal de la regió rica en Cys C-terminal.[30] A més, es dóna també algun cas

en què manca la primera de les dues His conservades en la subfamília (*cf.* subapartat 2.4.3.1.).

2.3.2. Estructura tridimensional

2.3.2.1. Ec-1 de blat

Ja s'ha vist al llarg d'aquest text que Ec-1 de blat és la MT de planta per a la qual es disposa de més informació. Aquesta és l'única MT de planta de què s'ha resolt l'estructura. Es coneix així que aquesta enllaça 6 ions Zn(II), organitzant-se en dos dominis que s'anomenen γ i β_E (Figura 10A).

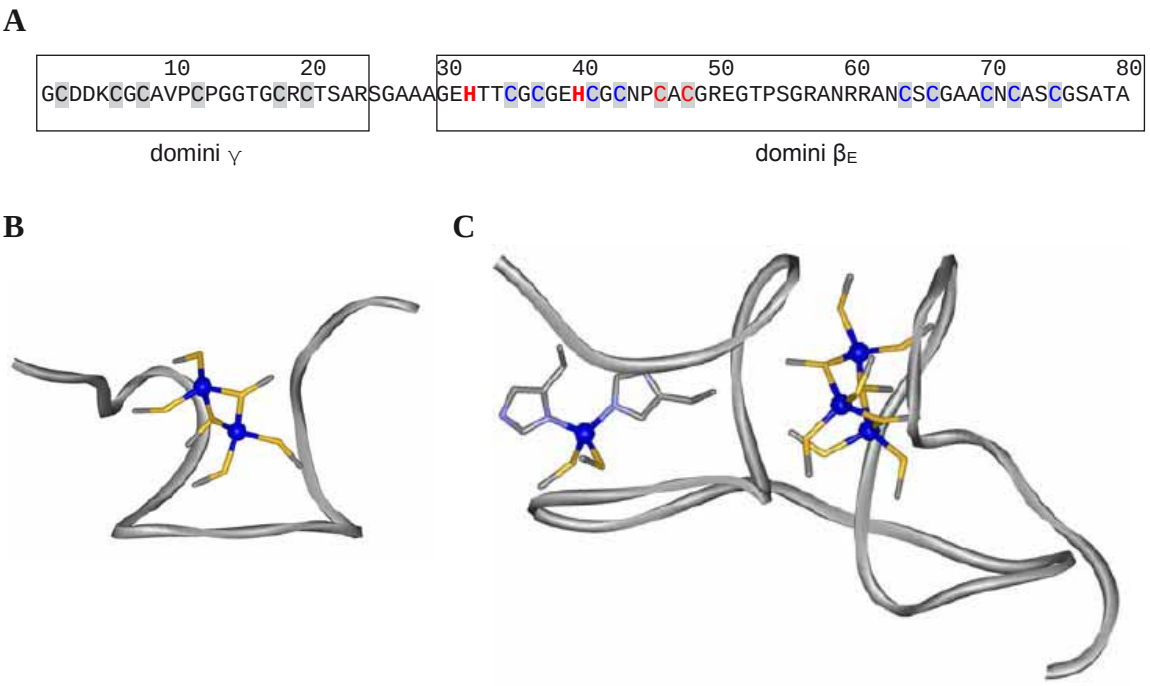

Figura 10. Estructura de Ec-1 de blat. (**A**) Seqüència aminoacídica (sense Met N-term) on els quadres tanquen els residus que pertanyen al domini γ (Gly1 a Arg24) i al domini β_E (Gly30 a Ala80). S'indica la participació dels residus Cys i His en el lloc de coordinació Zn-$(SCys)_2(NHis)_2$ (roig) i en el clúster Zn_3-$(SCys)_9$ (blau) situats en el domini β_E. Totes les Cys del domini γ participen en la coordinació metàl·lica (adaptat de Peroza *et al.*[24]). Estructura 3D del clúster (**B**) Zn_2-$(SCys)_6$ (PDB 2L62) situat en el domini γ, així com del (**C**) lloc de coordinació Zn-$(SCys)_2(NHis)_2$ i del clúster Zn_3-$(SCys)_9$ (PDB 2KAK), situats en el domini β_E (extret de Freisinger[72]).

Pel que fa al domini γ N-terminal, uns primers estudis servint-se de les espectroscòpies UV i DC, així com de digestió proteolítica seguida d'espectrometria de masses i anàlisi d'aminoàcids, ja demostraven l'existència del clúster Zn_2-$(SCys)_6$, fins

[72] E. Freisinger, J. Biol. Inorg. Chem. 16 (2011) 1035-1045.

aquell moment mai descrit en MT.[73] Més endavant se'n determinà l'estructura per RMN, que confirmava l'existència d'aquest clúster en què sis Cys, dues de pontals i quatre de terminals, enllaçaven 2 ions M(II) (Figura 10B).[25] Tanmateix, no es tenia la certesa de quins eren els residus Cys pontals, de manera que primerament es considerà la possibilitat que existira una estructura dinàmica on Cys8 era sempre pontal, però en canvi Cys2 i Cys20 s'intercanviaven com a lligands pontals o terminals. Si bé aquesta hipòtesi no ha estat descartada, la recent determinació de l'estructura de cyc-Cd_2-γEc-1, un homòleg cíclic de γEc, demostra que en aquest complex són Cys2 i Cys8 els residus que actuen com a lligands tiolat pontal.[32]

El domini β_E C-terminal forma el complex Zn_4-β_E-Ec-1, que conté el clúster Zn_3-$(SCys)_9$ i el lloc de coordinació Zn-$(SCys)_2(NHis)_2$ (Figura 10C). Per al lloc mononuclear es coneix que els residus Cys que participen en la coordinació d'aquest ió Zn(II) són els de les posicions 46 i 48 (Figura 10A). A més, ja s'ha vist anteriorment que els residus Cys48 i His40 són claus per al plegament del polipèptid i, per tant, per a la seua funció biològica (*cf.* subapartat 2.1.3.1). Pel que fa al clúster Zn_3-$(SCys)_9$, en canvi, no s'han pogut determinar experimentalment les connectivitats metall-lligand. El que sí que se sap a partir de les deu configuracions amb diferents coordinacions Zn-SCys que serien coherents amb les dades obtingudes per RMN és que els residus Cys38, Cys44 i Cys65 molt probablement actuen com a lligands terminals.[24]

2.3.2.2. Models estructurals proposats per a les MT de planta de tipus 1, 2 i 3

Pel que fa a les MT de planta menys estudiades, les de les subfamílies p1, p2 i p3, el llarg fragment lliure de Cys que els és característic pren importància degut a la seua possible implicació en el plegament i funcions d'aquests pèptids.[72] Així, tot i que encara no existeix cap estructura 3D resolta per als complexos metàl·lics d'aquestes MT, en la bibliografia s'han proposat dos models de plegament: d'una banda, un model anomenat en forma de pesa (Figura 11A), en què els dos dominis rics en Cys formarien dos clústers independents, i d'altra banda, un model anomenat en forma de pinça (Figura 11B), en què ambdós dominis interactuarien formant un únic clúster. A més, l'enllaç d'un ió metàl·lic

[73] E.A. Peroza, E. Freisinger, J. Biol. Inorg. Chem. 12 (2007) 377-391.

addicional a una MT que es plega en forma de pesa podria donar lloc a un plegament en forma de pinça, i ocorreria a l'inrevés si aquest s'alliberara (Figura 11).

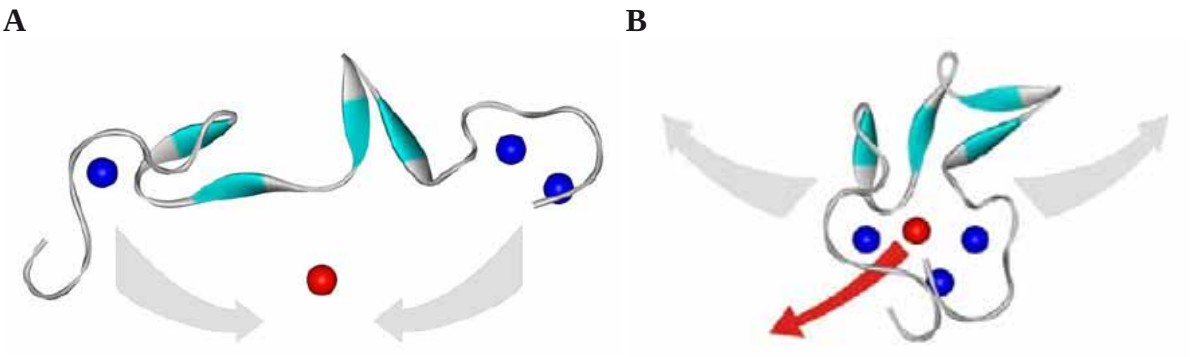

Figura 11. Models estructurals en forma (**A**) de pesa i (**B**) de pinça. Es mostra també la possible transformació pesa/pinça en incorporar/alliberar un metall addicional (extret de Freisinger[72]).

S'ha suggerit així l'estructura d'alguns d'aquests complexos metall-MT, com per exemple el que forma MT2 de cigró (*Cicer arietinum*) amb 5 metalls divalents. Per a aquesta MT, que conté catorze Cys, es proposa que en el complex $M(II)_5$-MT2 es dóna la interacció d'ambdós dominis i que adopta, per tant, l'anteriorment esmentada forma de pinça.[74] Per a la MT de tipus 2 de l'alzina surera (*Q. suber*) es proposa també aquest plegament, en aquest cas per als complexos que forma amb 4 ions Zn(II), d'una banda, i amb 8 ions Cu(I), de l'altra.[75] I trobem per últim els casos de les MT1 de *C. arietinum*[76] i MT3 de la banana (*Musa acuminata*),[77] per a les quals es proposa que es pleguen adoptant ambdós models. En concret, aquestes MT1 i MT3 enllacen 4 i 3 ions Zn(II), respectivament, quan s'obtenen per síntesi recombinant en medis rics en aquest metall, i s'especula que formen cadascuna dos agregats/llocs de coordinació separats ($Zn(II)_2$-$(SCys)_6$ + $Zn(II)_2$-$(SCys)_6$ per a MT1 i Zn(II)-$(SCys)_4$ + $Zn(II)_2$-$(SCys)_6$ per a MT3). En canvi, aquestes MT poden enllaçar 5 i 4 ions Cd(II) o Zn(II), respectivament, en condicions de major excés de metall, gràcies a la formació d'un únic clúster $M(II)_5$-$(SCys)_{12}$ per a MT1 i $M(II)_4$-$(SCys)_{10}$ o $M(II)_4$-$(SCys)_{10}(NHis)$ per a MT3.

[74] X. Wan, E. Freisinger, Metallomics 1 (2009) 489-500.
[75] J. Domènech, G. Mir, G. Huguet, M. Capdevila, M. Molinas, S. Atrian, Biochimie 88 (2006) 583-593.
[76] O. Schicht, E. Freisinger, Inorg. Chim. Acta 362 (2009) 714-724.
[77] E. Freisinger, Inorg. Chim. Acta 360 (2007) 369-380.

2.3.3. Els lligands His i S^{2-} en les MT de planta

2.3.3.1. Les histidines en cada subfamília

Una de les particularitats de les MT de la família 15, com és la presència de residus aromàtics, fa que la qüestió del possible paper de les His en la coordinació metàl·lica siga especialment rellevant en aquestes. De fet, en totes les subfamílies trobem residus His més o menys conservats (Figura 12).

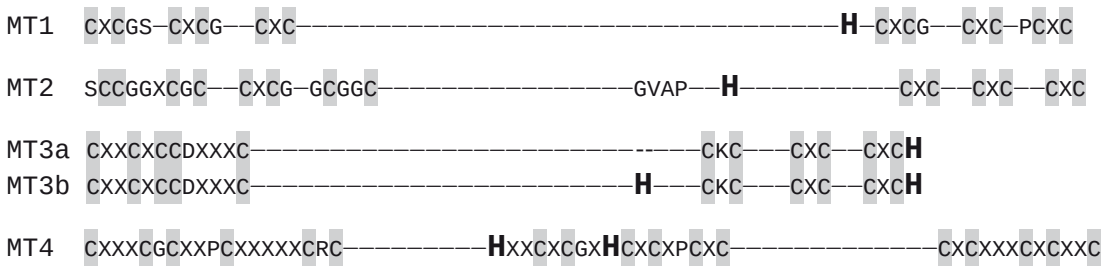

Figura 12. Representació esquemàtica dels patrons de seqüència típics de cada subfamília de MT de planta i la localització de les His.

Les MT1 o MT2 que contenen aquests residus potencialment coordinants en contenen només un. Així, en la subfamília MT1 trobem un residu His semiconservat que se situa dues posicions abans del motiu CXCG en l'extrem C-terminal del segon domini ric en Cys (Figura 12, MT1). Quasi tots els casos que presenten aquesta His ho fan en un motiu AHGCXCG. Trobem excepcions, però, en què hi ha dues His (les MT1 d'*O. sativa,* BAG87041, Q10N03, Q2QNC3, Q2QNE8) o, tot i haver-ne només una, aquesta se situa en l'extrem C-terminal del primer domini ric en Cys (MT1 de *Betula platyphylla*, Q508T1), en l'espaiador (MT1 de *C. arietinum*, Q39548; de *Festuca rubra*, O24528; de *Medicago sativa*, Q9SP23; o de *Vicia faba*, Q41669), o a continuació de la Cys C-terminal del segon domini ric en Cys (MT1 de *Grimmia pilifera*, GR307619; de *Pyrus pyrifolia*, Q9LUX2; de *Selaginella lepidophylla*, BM402666; de *S. moellendorffii*, FE432113; o de *Syntrichia ruralis*, CN208803). Algunes MT2 presenten un residu His que se situa també en aquesta regió propera al segment CXCG en l'extrem C-terminal del segon domini ric en Cys. No obstant, en la majoria dels casos es localitza entre una i sis posicions a continuació del motiu GVAP (Figura 12, MT2).[62] N'és un exemple QsMT de *Q. suber* (Q93X22), per a la qual es proposa que aquesta His contribueix a adoptar un plegament en forma de pinça en els complexos Zn_4-QsMT, tot i que sense participar en la coordinació

metàl·lica.[75] Tanmateix, s'ha proposat la participació d'aquesta mateixa His50 quan part de les Cys de QsMT s'han oxidat a causa de l'exposició a radicals lliures.[78]

Pel que fa a la subfamília MT3, és freqüent trobar un o dos residus His en aquests pèptids. Si n'hi ha un, allò més habitual és trobar-lo en la posició C-terminal (Figura 12, MT3a). Si n'hi ha dos, el segon el trobem majoritàriament en l'espaiador (Figura 12, MT3b), situant-se en el centre o a prop del domini ric en Cys C-terminal. Hi ha excepcions, però, que presenten un sol residu His que es localitza en l'espaiador, com són els casos de MT3 *d'Elaeis guineensis* (UniProtKB Q9STC4), de *Musa acuminata* (Q40256) o dues MT3 d'*Oryza sativa* (A2WLS0 i A3B0Y1). Trobem també els casos particulars de MT3 d'*Hordeum vulgare* (AFK12211), amb dues His en l'espaiador, i de MT3B d'*O. sativa* (A2Y1D7), que presenta una His en l'espaiador i una altra en la regió N-terminal. Si bé actualment trobem en les bases de dades de nucleòtids i de proteïnes gairebé tres desenes de MT3 que contenen residus His, només hi ha estudis que proposen la participació d'aquests en la coordinació metàl·lica per a MT3 de la banana (*M. acuminata*).[77]

El cas de les MT4 és més senzill i es coneixen millor les conseqüències de l'existència de les His que estan conservades en aquesta subfamília. Ja s'ha vist que les MT4 típiques contenen dues His molt conservades en el domini ric en Cys central (*cf.* subapartat 2.3.1.). També s'ha esmentat la importància d'aquestes per a permetre el correcte plegament del domini β_E en Ec-1 de blat, el qual condiciona la selectivitat Zn/Cd i per tant les funcions de la proteïna.[30,31] Tanmateix, existeixen MT4 en què falta un d'aquests dos residus His. Són MT4 de *Camellia japonica* (GenBank JK711196), on la primera de les His està substituïda per un residu Asp, i una de les MT de *Glycine max* amb què s'ha treballat en aquesta Tesi, que conté una Tyr en lloc de la segona de les His altament conservades en la subfamília.

2.3.3.2. Incorporació d'anions sulfur

Així com les His, els sulfurs àcid-làbils reben una especial atenció com a potencials lligands alternatius (o addicionals) a les Cys en les MT de planta. D'una banda, perquè primerament es van descriure en les PC, de les quals es pensà durant molt de temps

[78] A. Torreggiani, J. Domènech, A. Tinti, J. Raman Spectrosc. 40 (2009) 1687-1693.

que eren els pèptids que cobrien les funcions de les MT en les plantes, on es creia que no hi havia MT. D'altra banda, perquè fou en una MT2 de planta, QsMT de l'alzina surera (*Q. suber*), que es féu evident que existien els lligands sulfur en les MT.[52] A més, si bé el contingut en ions sulfur no suposa l'augment de la capacitat coordinant de les MT de mamífer[79] o de CRS5 de llevat,[80] per a algunes MT de planta s'ha trobat que sí. Tornem així al cas de QsMT, on es veié que la incorporació de 2-3 lligands sulfur permetia l'enllaç de 1-2 ions Cd(II) addicionals. En base a això, més recentment s'ha aprofundit en l'estudi de la incorporació d'anions sulfur als complexos Cd(II)-MT d'una altra MT de tipus 2 de planta, cicMT2 de *C. arietinum*.[81,82] Així, s'ha comprovat que la màxima capacitat coordinant d'aquesta MT que presenta catorze Cys és de 5 ions Cd(II) en absència de lligands sulfur, Cd_5-cicMT2, i de 9 ions Cd(II) quan ha incorporat 7 lligands S^{2-}, Cd_9S_7-cicMT2. A més, s'ha proposat que la raó per la qual hi ha un augment de la capacitat coordinant quan les MT de planta incorporen lligands sulfur, però no les de mamífer, és l'espaiador present en les primeres. Sembla raonable pensar en impediments estèrics per a les MT de mamífer, i en canvi en la possibilitat d'ajustar-se a la grandària del/s clúster/s metàl·lic/s per a les MT de planta, a través d'uns moviments que recorden als que hem vist per al pas des d'un plegament en forma de pesa a un plegament en forma de pinça (vegeu Figura 11).

2.3.4. Funcions

Les mateixes funcions d'homeòstasi i destoxicació de metalls, així com de protecció enfront l'estrés radicalari i/o oxidatiu que s'han proposat per a la superfamília de les MT (*cf.* subapartat 2.1.4.), en general, es proposen per al subconjunt que formen les MT de planta. Seguint amb la mateixa tendència, també si tractem d'identificar una relació estructura-funció en aquestes ens trobem que, com hem vist, la diversitat en el nombre i la localització dels residus coordinants fins i tot en una mateixa subfamília és tan gran que dificulta molt aquesta tasca. Com ja s'ha vist, Ec-1 de blat com a prototip i les MT4 per extensió, donada l'elevada conservació de les seqüències en aquesta subfamília, són les úniques MT de planta de què coneixem l'estructura i la funció, relacionades entre si. Tanmateix, els estudis d'expressió gènica han sigut majoritàriament les fonts a partir de

[79] L. Tío, L. Villarreal, S. Atrian, M. Capdevila, M. Exp. Biol. Med. 231 (2006) 1522-1527.
[80] A. Pagani, L. Villarreal, M. Capdevila, S. Atrian, Mol. Microbiol. 63 (2007) 256-269.
[81] X. Wan, E. Freisinger, Inorg. Chem. 52 (2013) 785-792.
[82] T. Huber, E. Freisinger, Dalton Trans. 42 (2013) 8878-8889.

què s'ha obtingut informació sobre les possibles funcions biològiques de les MT de planta, juntament amb estudis de complementació en llevat o amb plantes *knockout* en *MT*, entre d'altres.

2.3.4.1. Estudis d'expressió gènica

Se sap que les MT de planta corresponents a les subfamílies MT1, MT2 i MT3 s'expressen generalment en fulles, llavors i arrels, a diferència de MT4, que són específiques de llavor.[68] Aquestes dades, que ja *per se* permeten proposar funcions diferencials per a *MT* amb patrons d'expressió gènica diferencials, s'han complementat en molts casos amb l'anàlisi de la inducció/repressió de la transcripció d'un gen causada per agents externs (*e.g.* metalls, agents oxidants). En són exemples els resultats obtinguts amb els gens de *MT1*, *MT2* i *MT3* de *Brassica napus*, els nivells dels quals incrementen en plàntules exposades a peròxid d'hidrogen;[83] o també *FeMT3* de *Fagopyrum esculentum*, la transcripció del qual s'indueix en fulles com a conseqüència del tractament amb Cd(II) o Cu(II).[84]

2.3.4.2. Estudis de complementació en llevat

La capacitat de les MT per a conferir tolerància a un determinat agent estressant (*e.g.* metalls o agents oxidants, novament) a cèl·lules del llevat *S. cerevisiae* ha estat també analitzada amb l'objectiu de relacionar-la amb una possible funció biològica. Així, s'usen soques de llevat que careixen de les MT endògenes relacionades amb la tolerància a coure, CUP1 i CRS5,[85,86,87] i es determina si el creixement d'aquestes cèl·lules en unes condicions donades d'exposició a metalls o oxidants millora quan expressen una determinada MT. En aquest cas, n'és un exemple de nou FeMT3, que ha demostrat conferir tolerància a Cd(II) i Cu(II) en aquest tipus d'estudis, tot reforçant els resultats explicats en el subapartat anterior.[84] Cal esmentar també els resultats obtinguts amb QsMT de l'alzina surera, per a la qual s'ha proposat que la regió lliure de Cys present en aquesta

[83] Y.O. Ahn, S.H. Kim, J. Lee, H. Kim, H.S. Lee, S.S. Kwak, Mol. Biol. Rep. 39 (2012) 2059-2067.
[84] D.B. Nikolić, J.T. Samardžić, A.M. Bratić, I.P. Radin, S.P. Gavrilović, T. Rausch, V.R. Maksimović, J. Agric. Food Chem. 58 (2010) 3488-3494.
[85] A. Brenes-Pomales, G. Lindegren, C.C: Lindegren, Nature 176 (1955) 841-842.
[86] T.R: Butt, E.J. Sternberg, J.A. Gorman, P. Clark, D. Hamer, M. Rosenberg, S.T. Croke, Proc. Natl. Acad. Sci. USA 81 (1984) 3332-3336.
[87] V.C: Culotta, W.R. Howard, X.F. Liu, J. Biol. Chem. 269 (1994) 25295-25302.

MT2 participa en la funció destoxicadora de coure de la proteïna, donat que s'ha comprovat que un pèptid derivat de QsMT al qual se li ha tret l'espaiador disminueix la tolerància a aquest metall.[75]

2.3.4.3. Estudis en plantes *MT-knockout*

A través d'estudis en aquestes plantes incapaces d'expressar els gens que codifiquen per a una o diverses MT s'ha demostrat la capacitat de MT1A i MT2B d'*A. thaliana* per a complementar la funció de les fitoquelatines d'aquesta planta en la tolerància a coure i cadmi.[88] Així, els dobles mutants deficients en *MT1A* i *MT2B* no mostren una afectació en la tolerància als metalls, i en canvi els triples mutants que són també deficients en fitoquelatines són més sensibles a coure i cadmi que el mutant tan sols deficient en fitoquelatines.

[88] W.J. Guo, M. Meetam, P. Goldsbrough, Plant Physiol. 146 (2008) 1697-1706.

3. OBJECTIUS

3. OBJECTIUS

La finalitat del desenvolupament d'aquesta Tesi Doctoral ha estat ampliar els coneixements actuals sobre les MT i aprofundir en la seua relació estructura-funció. Hem centrat aquest objectiu general en tres sistemes MT polimòrfics diferents, a partir dels següents objectius específics:

1. Estudiar i comparar les habilitats coordinants envers Zn(II), Cd(II) i Cu(I) de les dues isoformes de MT que es coneixen per a l'equinoderm *Strongylocentrotus purpuratus*, i analitzar-ne el significat en relació a la seua possible funció.

2. Classificar les isoformes de MT que s'han identificat en les plantes de soja (*Glycine max*) i gira-sol (*Helianthus annuus*). Estudiar i comparar les habilitats coordinants envers Zn(II) i Cd(II) d'aquestes MT tant dins del mateix sistema com entre ambdós sistemes. S'ha pretés també considerar la variabilitat en el contingut de residus coordinants d'aquestes MT i analitzar-ne el significat en relació a la seua possible funció.

3. Estudiar comparativament les habilitats de les diferents isoformes de MT de soja com a antioxidants i/o captadors de radicals lliures.

4. RESULTATS

4. RESULTATS

Els resultats d'aquesta Tesi Doctoral es presenten en forma de 5 capítols que responen seqüencialment als objectius proposats en aquest treball. Així, el **Capítol 1** presentat (*The sea urchin metallothionein system: comparative evaluation of the SpMTA and SpMTB metal-binding preferences*) respon a l'**Objectiu 1**, els **Capítols 2** (*The response of the different soybean metallothionein isoforms to cadmium intoxication*), **3** (*Zn(II)- and Cd(II)-binding abilities of plant MT1 and MT2 isoforms with extra Cys residues*) i **4** (*His-containing plant metallothioneins: comparative study of divalent metal-ion binding by plant MT3 and MT4 isoforms*) se centren en l'**Objectiu 2**, mentre que el **Capítol 5** (*Comparative analysis of the soybean metallothionein system under radical and oxidative stress*) es dedica a l'**Objectiu 3** proposat.

Capítol 1

The sea urchin metallothionein system: comparative evaluation of the SpMTA and SpMTB metal-binding preferences

CAPÍTOL 1

The sea urchin metallothionein system: comparative evaluation of the SpMTA and SpMTB metal-binding preferences

1. Introduction

Metallothioneins (MTs) are a superfamily of universal and ubiquitous low molecular weight proteins that bind essential and toxic metal ions through their abundant Cys residues, forming multinuclear metal-thiolate clusters. They are involved in many crucial biological processes, such as metal homeostasis and detoxification, or oxidative stress protection, among others [1]. Although their protein sequences are dramatically heterogeneous and consequently their classification is not a trivial affair, their metal-binding behavior converges to either Zn-thioneins, which show a binding preference for divalent metal ions, or Cu-thioneins, with an optimized coordination of monovalent metal ions [2]. Beyond this simplistic dual model, the comprehensive consideration of the metal binding features of a huge number of MT peptides later led to the proposal of a continuous gradation between both extreme behaviors [3]. Unfortunately, the sequence determinants of the metal specificity of MTs are still unknown [4], although it should be considered a key element for a better understanding of the evolutive differentiation [5] and physiological function of these peculiar metalloproteins [6]. Polymorphism is one of the most significant features of MTs, since at least all the eukaryote organisms studied until now exhibit MT systems composed of almost similar paralog forms [5]. Ideally, each isoform would correspond to a definite physiological function, but it is plainly evident that in most cases ontogenic, tissular and/or functional differentiation has not been achieved, so that no clear correlation exists between multiple MT isoforms and their *in vivo* performance.

In this scenario, and with the aim of gathering data on the most prominent model organisms, we undertook the characterization of the metal-binding preferences of the purple sea urchin (*Strongylocentrotus purpuratus*, echinoderm) MT isoforms. Echinodermata constitute a very interesting phylum since, as the unique invertebrate deuterostomes, they are evolutively close to the Chordates, which are also deuterostomes (for a recent review on Echinodermata MTs, see [7]). At genomic level, 7 different

homologous MT genes have been reported in *S. purpuratus*, of which only three produce biologically relevant isoforms: *SpMTA* and the pair *SpMTB*$_1$-*SpMTB*$_2$, the latter encoding proteins with identical sequence [8,9,10]. Significantly, *SpMTA* and *SpMTB* exhibit different quantitative tissular and temporal expression patterns. Hence, *SpMTA* is transcribed in ectodermal tissues, while *SpMTB* is expressed in both the ectodermal and endodermal structures. Both genes are constitutively expressed, and under physiological conditions *SpMTA* mRNA levels reach up to 10 times those of *SpMTB*. However, under metal (zinc or cadmium) overload, *SpMTB* expression is further induced, so that SpMTB achieves protein levels similar to those of SpMTA [8,10].

SpMTA is a 64-amino acid peptide including 20 Cys, while the SpMTB sequence is two amino acids longer, with fully conserved Cys and only 10 residue substitutions (Fig. 1A), although some other changes have been detected in minor EST clones, attributable to natural polymorphism. Of both isoforms, only the study of SpMTA has attracted great interest, since the Cys-Cys motifs typical of the C-terminal moiety (or α domain) of the mammalian MTs are located here in the N-terminal moiety, and *vice versa* for the Cys-X-Cys motifs typical of the N-terminal half (or β domain) of the mammalian MTs (Fig. 1A). This inverted arrangement led to propose a specific evolutionary theory for the origin of different MT proteins, based on considering the number and position of the binding domains in different MTs [11]. Thereafter, several structural features of the Cd-SpMTA complexes were revealed by the work in the laboratory of Prof. Kägi on recombinant SpMTA [12,13,14], which culminated with the determination of the three-dimensional structure of reconstituted $^{113}Cd_7$-SpMTA, solved by NMR in 1999 (Fig. 1B) [15]. These results confirmed that the global structure of each Cd_7-SpMTA domain resembled that of the mammalian MTs, although a significantly different connectivity pattern of the Cd-S bonds and novel local polypeptide folds arose in SpMTA. Precisely, two globular domains separated by a flexible hinge and encompassing a $Cd_4(SCys)_{11}$ and a $Cd_3(SCys)_9$ cluster in an inverted order with respect to mammalian MTs were encountered. The $Cd_4(SCys)_{11}$ cluster (in the N-term protein α domain) consisted of the union of 2 six-membered rings sharing 2 Cd-S bonds, thus including 5 bridging and 6 terminal S atoms, whereas the $Cd_3(SCys)_9$ cluster (in the C-term protein β domain) consisted of 3 cadmium ions and 3 bridging Cys thiolates forming a six-membered ring, while the other six Cys acted as terminal ligands. Although it was not possible to determine the mutual orientation of the two domains, it was evident that both were twisted

to the left around the metal-thiolate cluster. This constrasts with the mammalian MT complexes, where the β domain is wrapped with right-handed chirality, thus representing the only known example of left-handed β domain.

A

```
                  10        20        30        40        50        60
          .. ..|....|....|....|....|....|....|....|....|....|....|....|...
SpMTA    (GS)MPDVKCVCCKEGKECACFGQDCCKTGECCKDGTCC-GICTNAACK-CANGCKCGSGCSCTEGNCAC
SpMTB    (GS)MPDVKCVCCKEGNECACKGQDCCTTGECCKGGTCCTGKCSNAACKTCADGCKCGSGCSCTEGNCPC
          ____________________________________ ____________________________________
                        alpha domain                      beta domain
```

B

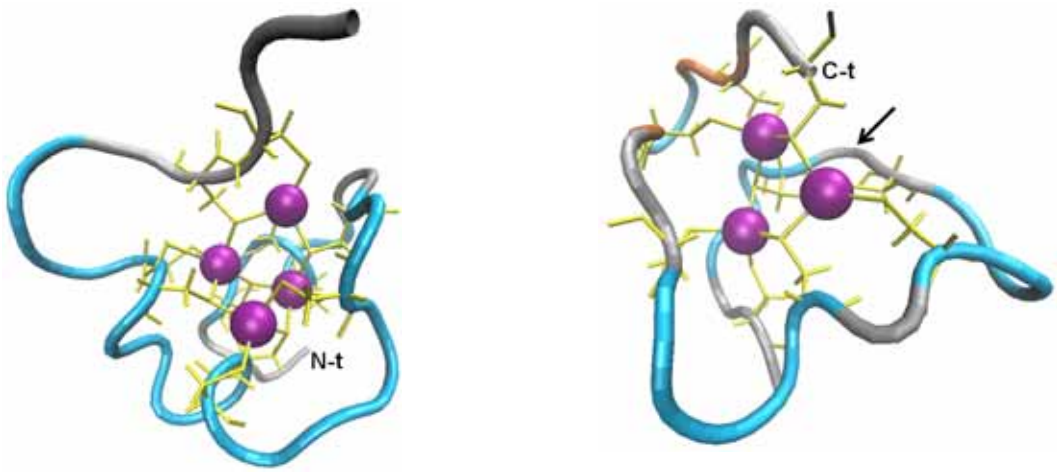

Figure 1. (**A**) Amino acid sequence alignment of recombinant SpMTA and SpMTB. Note that the N-term Gly-Ser residues derive from the GST-fusion system used for recombinant synthesis and purification. (**B**) 3D structures of Cd_4-αSpMTA (top) and Cd_3-βSpMTA (bottom) generated from PDB files 1QJK and 1QJL, respectively, with VMD software (http://www.ks.uiuc.edu/Research/vmd/) [Humphrey, W., Dalke, A. and Schulten, K., "VMD - Visual Molecular Dynamics", J. Molec. Graphics, 1996, vol. 14, pp. 33-38]. Color code: random coil, silver; turn, cyan; extended beta, orange; Cd(II) ions, purple; Cys residue backbone and Cys-Cd connectivities, yellow. N-term and C-term ends of SpMTA sequence are indicated, and an arrow marks the position of the insertion of a Thr residue in SpMTB.

This exhaustive information on the complexes yielded by SpMTA upon divalent metal ion coordination contrasts with the null information about its copper binding abilities nor about metal ion handling by SpMTB. Therefore, in order to gain an insight into the evolutive significance of the two different MT isoforms in sea urchin, we aimed at performing a comparative study of their metal ion coordination features. To this end, this work describes the Zn(II), Cd(II) and Cu(I)-binding abilities of recombinant SpMTA and SpMTB, as well as of their separate domains, in order to determine their metal binding behavior and preferences. The consideration of all the obtained results is consistent with a higher Zn/Cd-thionein character for SpMTA, and a better performance of

SpMTB when binding copper, and they confirm that a slight but consistent difference between the physiological functions of both isoforms may be envisaged.

2. Materials and Methods

2.1. Cloning of MT cDNA constructs

All the metal–MT complexes investigated in the present study were recombinantly synthesized in *E. coli* through cloning of their coding sequences into the pGEX-4T1 plasmid (GE Healthcare, Little Chalfont, UK) to yield primary glutathione S-transferase (GST)-MT fusions from which the corresponding metal–MT complexes were subsequently purified [16,17]. The SpMTA cDNA was kindly provided by Prof. J.H.R. Kägi and subsequently cloned into the pGEX-4T1 *Bam*HI/*Sal*I restriction sites added by PCR amplification, using 5'-CCCGGATCCATGCCTGATGTCAAG-3' as upstream primer and 5'-GCGCCCGTCGACCTAGCATGCACA-3' as downstream primer. According to the reported SpMTA domain boundaries [15], cDNAs encoding for its separate moieties were obtained by PCR reactions that added *Bam*HI/*Xho*I restriction sites with the following oligonucleotides: for the N-terminal fragment or α domain (encompassing residues 1–36 of the full polypeptide), 5'-CCCGGATCCATGCCTGATGTCAAG-3' (upstream) and 5'-AAACTCGAGTCATCCACAGCAGGTTCCATCCTTG -3' (downstream); and for the C-terminal fragment or β domain (residues 37-64 of the full polypeptide), 5'-ACACACGGATCCATATGCACAAACGCTGCATGC-3' (upstream) and 5'-AAACCCCTCGAGCTAGCATGCACAGTTCCCCTC-3' (downstream). The cDNA of the SpMTB isoform was obtained from the Sea Urchin Genome Project Library Collection, in the California Institute of Technology (Caltech), and corresponded to the EST clone PMC_62379562 (seq ID NCBI 214576). The corresponding ORF was amplified by a PCR reaction that added *BamH*I/*Xho*I restriction sites to the respective 5' and 3' ends of the coding sequence, using the purified cDNA of the EST clone as template and the following primers: 5'-CCCGGATCCATGCCTGATGTCAAGTGTGTCTGC-3' (upstream) and 5'-AAACCCCTCGAGCTAGCATGGACAGTTCCCCTC-3' (downstream). Based on the reported domain boundaries of SpMTA [15], cDNAs encoding for the separate SpMTB moieties were obtained by PCR reactions with the following oligonucleotides: for the N-terminal fragment or α domain (encompassing

residues 1–37 of the full polypeptide), 5'-CCCGGATCCATGCCTGATGTCAAGTGTGTCTGC-3' (upstream) and 5'-AAACTCGAGTCATCCAGTGCAGCAGGTTCCACC-3' (downstream); and for the C-terminal fragment or β domain (residues 38-66 of the full polypeptide), 5'-ACACACGGATCCAAATGCTCAAATGCGGCATGC-3' (upstream) and 5'-AAACCCCTCGAGCTAGCATGGACAGTTCCCCTC-3' (downstream). All the PCR reactions consisted of 35-cycle amplifications, performed with 1.25 U of GoTaq DNA polymerase (Promega, Madison, USA), 0.25 mM dNTPs and 0.24 μM of the required primers at 2 mM $MgCl_2$ (final concentration), in a final volume of 100 μL, under the following cycle conditions: 30 s at 94 ºC (denaturation), 30 s at 58 °C (hybridization) and 30 s at 72 °C (elongation). An initial denaturation step where samples were heated at 94°C for 2 minutes ensured that the target DNA was completely denatured, and elongation conditions were maintained for 7 min after the 35 cycles. The final products were analyzed by agarose gel electrophoresis/GelRed Nucleic Acid Gel Stain (Biotium, Hayward, CA, USA) staining; the band with the expected size was excised and subcloned into the pGEX-4T1 vector. Before recombinant protein synthesis, all coding sequences were confirmed by automated DNA sequencing. To this end, the pGEX-derived constructs were transformed into *E. coli* MATCH I cells, and sequenced using the ABI PRISM BigDye Terminator v3.1 Cycle Sequencing Kit (Applied Biosystems, Foster City, CA, USA) in an ABI PRISM 310 Automatic Sequencer (Applied Biosystems, Foster City, CA, USA). In all cases, the expected sequence was corroborated.

2.2. Recombinant synthesis and purification of metal-MT complexes

The SpMTA-GST and SpMTB-GST fusion polypeptides and their respective separate α and β domains were biosynthesized in 5 L cultures of transformed protease-deficient *E. coli* BL21 cells. Expression was induced with isopropyl β-D-thiogalactopyranoside (IPTG) and cultures were supplemented with 500 μM $CuSO_4$, 300 μM $ZnCl_2$ or 300 μM $CdCl_2$ (final concentrations) and were allowed to grow for a further 3 h. In the case of Cu(II)-enriched cultures, both normal and low aeration conditions (N.A. and L.A., respectively) were assayed according to the procedure described elsewhere [18]. A total protein extract was prepared from these cells as previously described [16]. Metal complexes were recovered from the MT-GST fusion constructs by thrombin cleavage and

batch-affinity chromatography using Glutathione-Sepharose 4B (General Electric HC). The metal complexes were finally purified through FPLC in a Superdex75 column (General Electric HC) equilibrated with 50 mM Tris-HCl, pH 7.0. Selected fractions were confirmed by 15 % SDS-PAGE and kept at -80 ºC until further use. All procedures were performed using Ar (pure grade 5.6) saturated buffers, and all syntheses were performed at least twice to ensure reproducibility. Further details on the purification procedure can be found in [16]. As a consequence of the cloning requirements, the dipeptide Gly-Ser was present at the N-terminus of all polypeptides; however, this had previously been shown not to alter the MT metal-binding capacities [17].

2.3. In vitro *Cd- and Cu-binding studies*

The titration of all Zn-MT complexes with Cd(II) or Cu(I) at pH 7 were carried out following the methodology previously described [19,20], using $CdCl_2$ or $[Cu(CH_3CN)_4]ClO_4$ solutions, respectively. The acidification/reneutralization experiments were also performed by adapting the procedure reported in [21]. Essentially, 10-20 μM preparations of the Cd-peptides were acidified from pH 7.0 to pH 1.0-2.0 with $1-10^{-3}$ M HCl. CD and UV–vis spectra were recorded at several pH values both immediately after acid addition and 10 min later, always with identical results. Finally, the samples were kept at pH 1.0-2.0 for 20 min and were then reneutralized with $1-10^{-3}$ M NaOH, and CD and UV–vis spectra were recorded at several pH values. In some cases, several molar equivalents of an aqueous solution of Na_2S were added to the reneutralized MT forms, with the aim of reproducing the original Cd-MT CD fingerprints. All results were corrected for dilution effects, and during all experiments strict oxygen-free conditions were kept by saturating all solutions with Ar.

2.4. Protein quantification and spectroscopic analyses

The S, Zn, Cd and Cu content of the Zn-, Cd- and Cu-MT preparations was analyzed by means of Inductively Coupled Plasma Atomic Emission Spectroscopy (ICP-AES) in a Polyscan 61E (Thermo Jarrell Ash) spectrometer, measuring S at 182.040 nm, Zn at 213.856 nm, Cd at 228.802 and Cu at 324.803 nm. Samples were treated as in [22], but were alternatively incubated in 1 M HCl at 65 °C for 5 min prior to measurements, in order to eliminate possible traces of labile sulfide ions, as otherwise described [23].

Protein concentrations were calculated from the acid ICP-AES sulfur measurement, assuming that all S atoms were contributed by the MT peptide. A Jasco spectropolarimeter (Model J-715) interfaced to a computer (J700 software) was used for CD measurements at a constant temperature of 25 ºC maintained by a Peltier PTC-351S apparatus. Electronic absorption measurements were performed on an HP-8453 Diode array UV-visible spectrophotometer. All spectra were recorded with 1 cm capped quartz cuvettes, corrected for the dilution effects and processed using the GRAMS 32 Software.

2.5. Mass spectrometry

MW determinations were performed by electrospray ionization time-of-flight mass spectrometry (ESI-TOF MS) on a Micro Tof-Q instrument (Bruker) interfaced with a Series 1100 HPLC Agilent pump, equipped with an autosampler, all of which were controlled by the Compass Software. Calibration was attained with 0.2 g NaI dissolved in 100 mL of a 1:1 H_2O:isopropanol mixture. Samples containing MT complexes with divalent metal ions were analyzed under the following conditions: 20 µL of protein solution injected through a PEEK (polyether heteroketone) column (1.5 m x 0.18 mm i.d.), at 40 $\mu L \cdot min^{-1}$; capillary counter-electrode voltage 5 kV; desolvation temperature 90-110ºC; dry gas 6 $L \cdot min^{-1}$; spectra collection range 800-2000 m/z. The carrier buffer was a 5:95 mixture of acetonitrile:ammonium acetate/ammonia (15 mM, pH 7.0). Alternatively, the Cu-MT samples were analyzed as follows: 20 µL of protein solution injected at 30 $\mu L \cdot min^{-1}$; capillary counter-electrode voltage 3.5 kV; lens counter-electrode voltage 4 kV; dry temperature 80ºC; dry gas 6 $L \cdot min^{-1}$. Here, the carrier was a 10:90 mixture of acetonitrile:ammonium acetate/ammonia (15 mM, pH 7.0). For analysis of all recombinant MT molecular masses, 20 µL of the corresponding Zn-MT samples were injected under the same conditions described before, but using a 5:95 mixture of acetonitrile:formic acid pH 2.5 as liquid carrier, which caused the complete demetalation of the peptides. The same conditions were then used to remove Zn(II) ions from mixed-metal Zn,Cu-MT species in order to quantify their total Cu content.

3. Results and Discussion

3.1. Integrity and identity of the recombinant polypeptides

The cDNAs coding for the SpMTA and SpMTB isoforms, as well as for their separate domains were cloned into the pGEX-4T1 plasmid for peptide synthesis. DNA sequencing confirmed that all these constructs included no artifactual nucleotide substitutions, and that the respective coding sequences were cloned in the correct frame after the GST encoding fragment. Recombinant syntheses yielded MT peptides of which the identity, purity and integrity was confirmed by ESI-MS of the respective apoforms, obtained by acidification at pH 2.5 of the corresponding Zn-MT complexes. Hence, in each synthesis a unique peak was detected, in which the MW was consistent with the calculated MW of the respective recombinant MT peptide, including N-terminal Gly-Ser residues derived from the GST-fusion construct (Table 1).

Table 1. List of theoretical and experimental molecular weights (MW) corresponding to the apoforms of the six recombinantly synthesized polypeptides.

MT	Theoretical MW	Experimental MW
SpMTA	6532.0	6534.9 ± 0.8
αSpMTA	3874.0	3873.9 ± 0.4
βSpMTA	2820.2	2819.6 ± 0.5
SpMTB	6700.7	6698.6 ± 0.4
αSpMTB	3913.5	3912.4 ± 0.1
βSpMTB	2949.3	2948.6 ± 0.4

3.2. SpMTA exhibits better Zn(II) and Cd(II) binding abilities than SpMTB

Both SpMTA and SpMTB yield a major Zn_7-MT species when recombinantly synthesized as Zn(II)-complexes (Table 2, Fig. 2A and D), although the occurrence of several minor undermetalated, partially oxidized species is markedly significant for SpMTB, where all the species ranging from Zn_6 to Zn_3 are produced (Fig. 2D). This result already suggests a lower Zn^{II}-binding ability for SpMTB compared to SpMTA. The CD fingerprints of both Zn-preparations are similar and characteristic of Zn-MT complexes (Fig. 3A), and the *ca.* 10 nm red-shift of Zn-SpMTB is attributable to the differences between the respective β domains, as analyzed below.

Table 2. Analytical characterization of recombinant SpMTA and SpMTB and their independent constitutive fragments synthesized in (**A**) Zn- and (**B**) Cd-enriched media.

	MT	Concentration & Metal/MT ratio[a]	ESI-MS[b]		
			Species (% abundance)	Theor. MW	Exp. MW
A	SpMTA	$3.2 \cdot 10^{-4}$ M 6.1 Zn	**Zn_7-SpMTA (100)**	6976.1	6978.8 ± 0.9
			Zn_7S_1-SpMTA (30)	7010.2	7016.5 ± 2.5
			Zn_4-SpMTA (20)	6786.0	6780.9 ± 0.2
			Zn_3-SpMTA (20)	6722.6	6715.9 ± 0.6
	αSpMTA	$0.9 \cdot 10^{-4}$ M 3.8 Zn	**Zn_4-αSpMTA**	4127.5	4127.2 ± 0.1
	βSpMTA	$0.7 \cdot 10^{-4}$ M 2.3 Zn	**Zn_3-βSpMTA (100)**	3010.3	3009.9 ± 0.1
			Zn_2-βSpMTA (30)	2947.0	2943.8 ± 1.5
			apo-βSpMTA (30)	2820.2	2811.0 ± 1.3
			Zn_1-βSpMTA (20)	2883.6	2877.0 ± 1.2
	SpMTB	$2.3 \cdot 10^{-4}$ M 5.2 Zn	**Zn_7-SpMTB (100)**	7144.4	7143.5 ± 0.5
			Zn_6-SpMTB (50)	7081.0	7076.9 ± 1.3
			Zn_5-SpMTB (50)	7017.6	7012.9 ± 1.1
			Zn_4-SpMTB (60)	6954.3	6944.0 ± 0.9
			Zn_3-SpMTB (20)	6890.9	6880.0 ± 1.4
	αSpMTB	$2.2 \cdot 10^{-4}$ M 3.8 Zn	**Zn_4-αSpMTB**	4167.0	4166.1 ± 0.1
	βSpMTB	$0.8 \cdot 10^{-4}$ M 3.1 Zn	**Zn_3-βSpMTB**	3139.5	3138.9 ± 0.1
B	SpMTA	$0.7 \cdot 10^{-4}$ M 7.7 Cd 0.0 Zn	**Cd_7-SpMTA (100)**	7305.3	7304.5 ± 0.5
			Cd_7S_1-SpMTA (20)	7339.4	7341.6 ± 1.8
	αSpMTA	$0.7 \cdot 10^{-4}$ M 3.9 Cd 0.0 Zn	**Cd_4-αSpMTA**	4315.6	4316.1 ± 0.1
	βSpMTA	$0.2 \cdot 10^{-4}$ M 2.8 Cd 0.4 Zn	**Cd_3-βSpMTA (100)**	3151.4	3151.8 ± 0.4
			Cd_3Zn_1-βSpMTA (30)	3214.8	3215.6 ± 0.6
	SpMTB	$0.8 \cdot 10^{-4}$ M 6.7 Cd 0.0 Zn	**Cd_8-SpMTB (100)**	7583.9	7584.1 ± 0.5
			Cd_7S_2-SpMTB (50)	7541.6	7534.4 ± 0.9
			Cd_7-SpMTB (40)	7473.5	7474.8 ± 0.4
	αSpMTB	$1.3 \cdot 10^{-4}$ M 4.0 Cd 0.0 Zn	**Cd_4-αSpMTB**	4355.1	4355.5 ± 0.4
	βSpMTB	$0.8 \cdot 10^{-4}$ M 2.9 Cd 0.0 Zn	**Cd_3S_2-βSpMTB (100)**	3348.7	3343.1 ± 0.5
			Cd_3-βSpMTB (40)	3280.5	3280.8 ± 0.3

[a] MT concentration and metal/MT ratio calculated from acid ICP-AES results.

[b] Experimental and theoretical molecular weights corresponding to the Zn- and Cd-peptides. Zn and Cd contents were calculated from the mass difference between holo- and apoproteins. Species shown in bold correspond to the major components of the preparations.

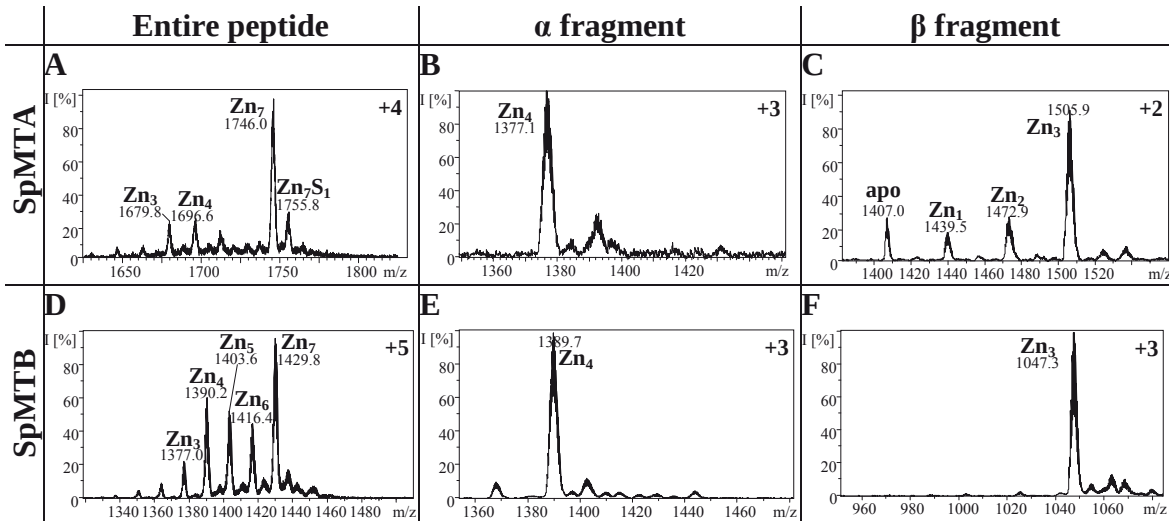

Figure 2. Representative charge states for the ESI-MS spectra recorded at pH 7.0 of recombinant Zn-SpMTA (**A**), Zn-αSpMTA (**B**), Zn-βSpMTA (**C**), Zn-SpMTB (**D**), Zn-αSpMTB (**E**) and Zn-βSpMTB (**F**). The observed species are collected in Table 2.

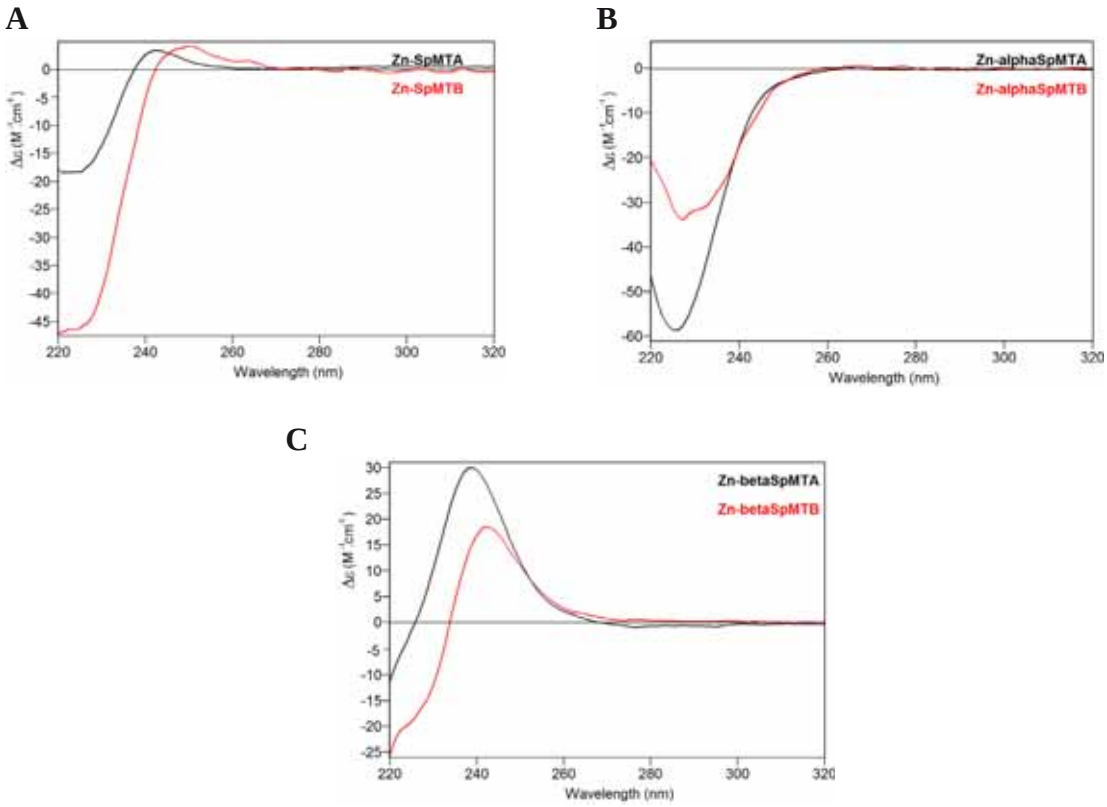

Figure 3. CD spectra corresponding to the entire MT (A) and the separate constitutive α (B) and β (C) domains of SpMTA (black) and SpMTB (red) recombinantly synthesized in Zn-supplemented media.

When synthesized in the presence of Cd(II), SpMTA yields a major Cd_7 species (Fig. 4A), whose CD fingerprint shows an intense exciton coupling centered at 250 nm (Fig. 5A) typical of type A Cd-MT complexes [23], and which is also very similar to the CD spectrum previously reported for recombinant Cd_7-SpMTA [12,13]. Even

though a very minor Cd_7S_1 species was identified in the Cd-SpMTA preparation (Table 2, Fig. 4A), its relative abundance is practically negligible if compared with the minor forms

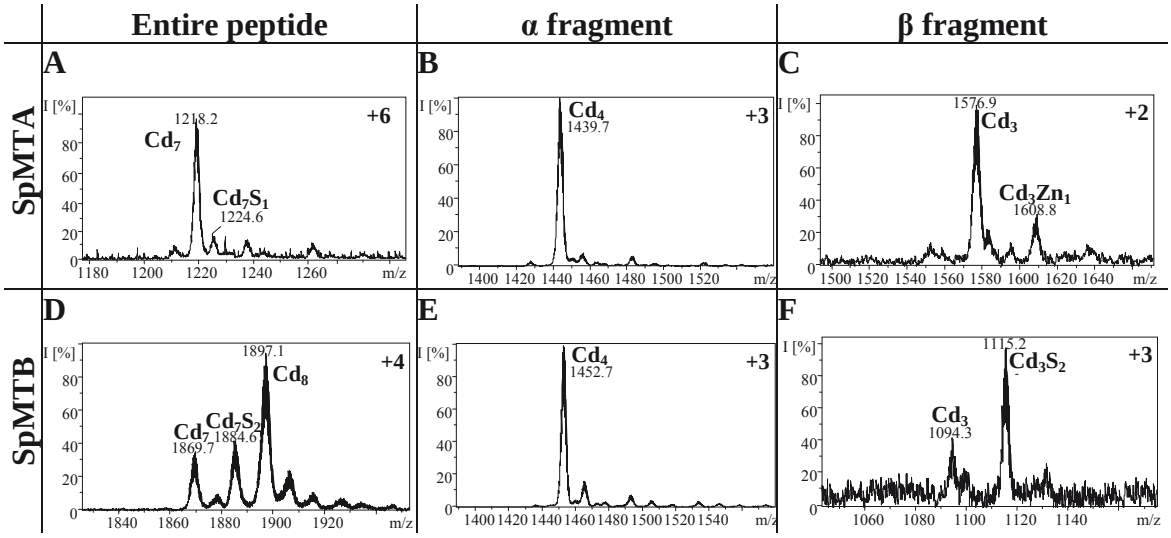

Figure 4. Representative charge states for the ESI-MS spectra recorded at pH 7.0 of recombinant Cd-SpMTA (**A**), Cd-αSpMTA (**B**), Cd-βSpMTA (**C**), Cd-SpMTB (**D**), Cd-αSpMTB (**E**) and Cd-βSpMTB (**F**). The observed species are collected in Table 2.

detected in Cd-SpMTB (Fig. 4D). In this case, an unexpected major Cd_8-SpMTB species was produced, together with several significantly abundant minor species, among which Cd_7- and Cd_7S_2-SpMTB are worth noting (Table 2, Fig. 4D). The CD fingerprint of this

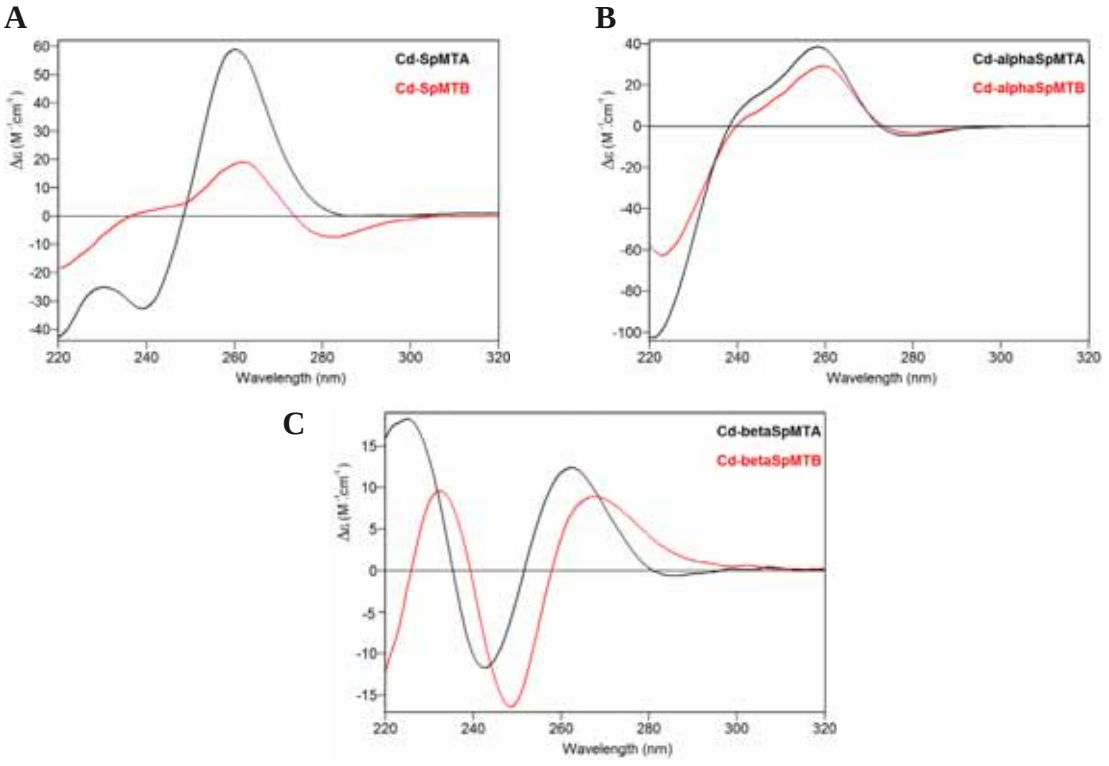

Figure 5. CD spectra corresponding to the entire MT (**A**) and the separate constitutive α (**B**) and β (**C**) domains of SpMTA (black) and SpMTB (red) recombinantly synthesized in Cd-supplemented media.

preparation differs from that of Cd-SpMTA, being significantly less intense and confirming the presence of sulfide ligands through the existence of the negative band at 280 nm (Fig. 5A). The occurrence of numerous species in the recombinant Cd-SpMTB preparation, some of which have a clear sulfide content, is again indicative of a low Cd^{II}-binding ability of SpMTB, as occurred for Zn(II) ions, according to the criteria reported by our group to differentiate MT peptides exhibiting either divalent or monovalent metal ion coordination preference [3].

The Zn(II) and Cd(II) binding abilities of the separate α domains appeared identical for both isoforms, generating almost single Zn_4 and Cd_4 species (Fig. 2B and E, and Fig. 4B and E, respectively, and Table 2), also with similar CD fingerprints (Fig. 3B and 5B). In the case of Cd_4-αSpMTA, the spectrum fully coincides with that previously reported after subtilisin digestion of the complete Cd_7-SpMTA complex [14]. Moreover, this spectrum can be also obtained by Zn/Cd replacement after the addition of 4 Cd(II) equivalents to Zn_4-αSpMTA at pH 7 (Fig. 6). In contrast to these results, the βSpMTA and

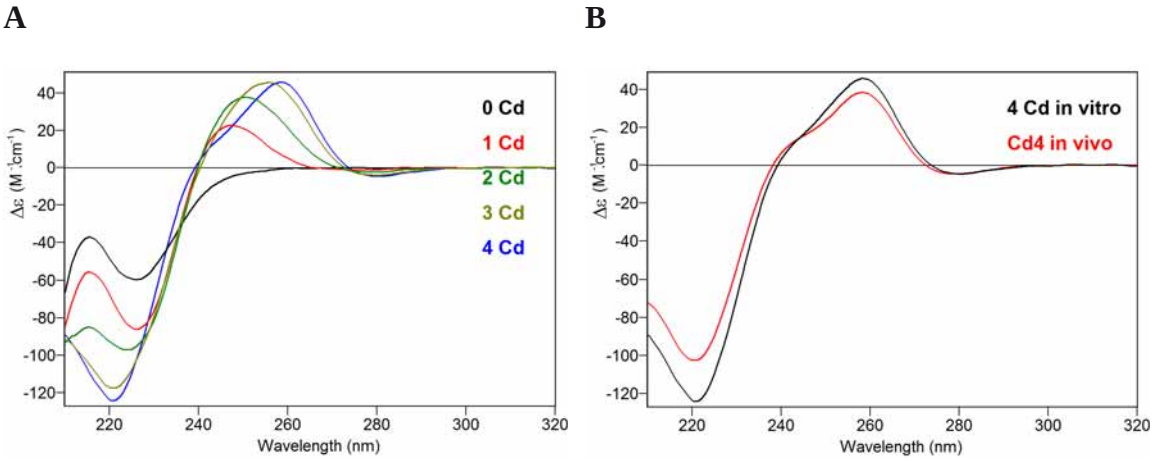

Figure 6. CD spectra recorded during the titration of Zn_4-αSpMTA with Cd(II) at pH 7 (**A**) and superimposition of CD spectra of Cd_4-αSpMTA obtained by Zn/Cd substitution over Zn_4-αSpMTA (*in vitro*; black) and by recombinant synthesis in Cd-enriched media (*in vivo*; red) (**B**).

βSpMTB domains yield patently different results when synthesized in Zn(II)- and Cd(II)-enriched media. Hence, both isoforms are recovered as major Zn_3 complexes, although the partially undermetalated species detectable for SpMTA do not appear for SpMTB (Table 2, Fig. 2C and F). Also, as determined from the difference between conventional and acid ICP-AES measurements (data not shown), the presence of inorganic sulfide in the recombinant Zn-βSpMTB preparations may account for the red-shift observed for Zn-βSpMTB CD spectrum in comparison to Zn-βSpMTA (Fig. 3C). Even more pronounced

differences arise for the Cd^{II}-binding capacity of the separate β domains, as βSpMTA yields a major, canonical Cd_3 species accompanied by minor Zn-containing complexes, while βSpMTB predominantly folds into Cd_3S_2-βSpMTB, thus with complete absence of Zn (Fig. 4C and F, respectively, and Table 2). Moreover, the Cd_3S_2-βSpMTB sulfide containing complex exhibits an acute red-shift in its CD spectrum when compared to Cd_3-βSpMTA (Fig. 5C).

At this point, it becomes evident that the Cd-binding abilities of SpMTB are poorer than those of SpMTA [3], and that this feature is most likely due to a patent lower M^{II}-binding ability of βSpMTB if compared to βSpMTA, as corroborated by the fact that the respective α domains exhibit no major differences. In order to better understand the peculiarities of the Cd-SpMTA and Cd-SpMTB complexes, and to support the higher M^{II}-binding preference of βSpMTA compared to βSpMTB, additional experimental results were considered. In the first place, it is worth noting that the CD spectra of the Zn/Cd replacement processes in both β domains evolved following a distinct pattern, especially after the 3rd Cd(II) equivalent added (Fig. 7A-D). But most interestingly, while the CD fingerprint of the recombinant Cd-βSpMTA preparation was reproduced after the 3rd Cd(II) equivalent added to Zn-βSpMTA (Fig. 7E), this was not the case for βSpMTB, even after the addition of 1-3 Na_2S equivalents, which provoked the conversion of the derivative-shaped band into a Gaussian band (Fig. 7F). For the Cd-βMTB isoform, the initial CD fingerprint can only be recovered after an acidification/reneutralization process followed by addition of 3 S^{2-} equivalents (Fig. 7G). Taken together, these data confirm that βSpMTB shows a diminished preference for divalent metal ion binding than βSpMTA, as highlighted by the need of S^{2-} ions in order to stabilize its M(II)-recombinant forms, and it is likely that the β moiety somehow confers its character to the entire SpMTB protein, which behaves as a less proficient Cd(II)-binding peptide. Since the analysis of the metal-binding behavior of a considerable number of MTs has revealed that the decrease of the divalent metal ion-preference (Zn(II) or Cd(II)) of an MT peptide entails the increase of its monovalent metal ion-preference (Cu(I)) and *vice versa* [3], it was plausible to hypothesize that SpMTB would exhibit a more accentuated Cu-thionein character than SpMTA. Thus, we thoroughly considered the results of recombinantly synthesizing both isoforms, and their independent domains, in copper-supplemented *E. coli* cells.

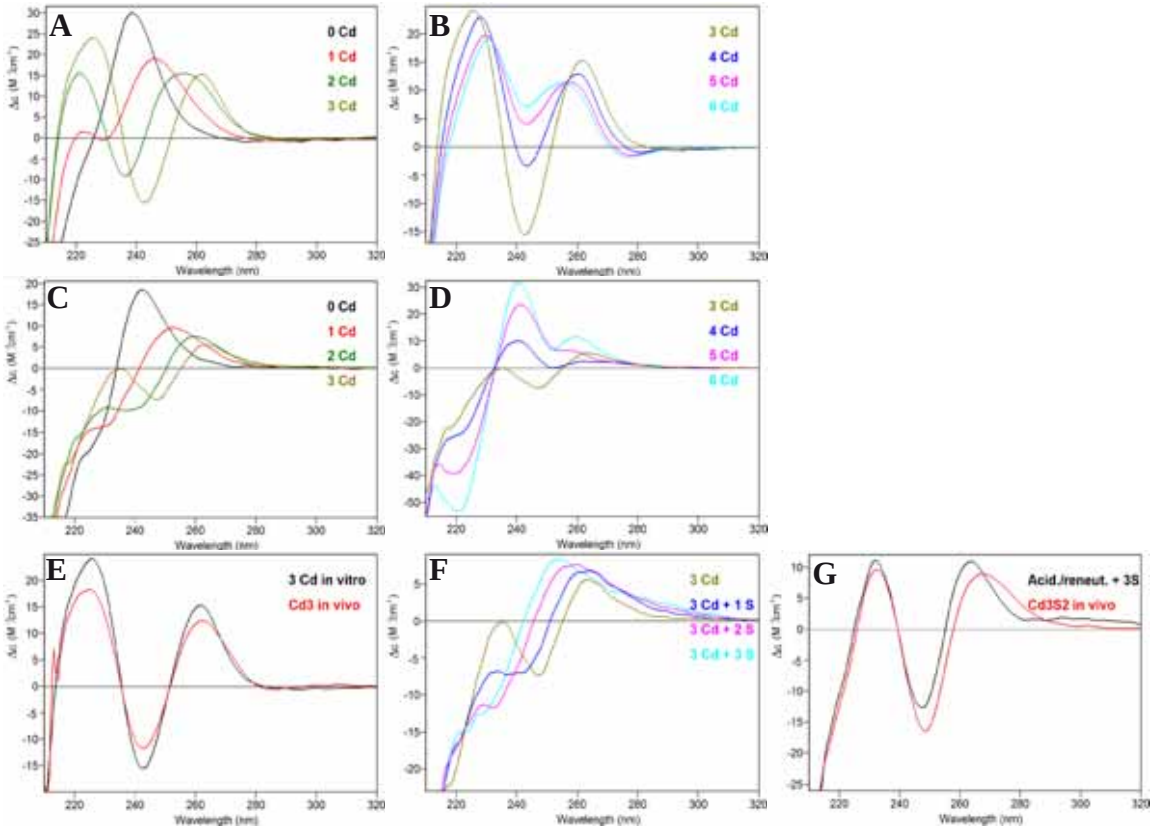

Figure 7. CD spectra recorded during the titrations of Zn-βSpMTA (**A**, **B**) and Zn-βSpMTB (**C**, **D**) with Cd(II) at pH 7. The effect of the addition of S^{2-} to βSpMTB is also shown (**F**), as well as the CD superimposition of *in vivo* (red) and *in vitro* (black) Cd-βSpMTA (**E**) and Cd-βSpMTB (**G**) species obtained after addition of 3 Cd(II) equivalents to Zn-βSpMTA or after an acidification/reneutralization process of Cd-βSpMTB plus addition of 3 S^{2-} equivalents.

3.3. Cu-binding abilities: SpMTB exhibits a stronger Cu-thionein character than SpMTA

Two different types of preparations were obtained for SpMTA when synthesized in Cu-supplemented *E. coli* cells, depending on the aeration conditions of the corresponding bacterial cultures (*cf.* Table 3). Although in both cases SpMTA was recovered as a mixture of Zn,Cu heteronuclear species, the average Zn content of the preparation was always higher in the normally aerated culture, with concomitant average lower Cu content (5.5 Cu: 3.0 Zn), and with the opposite results for the low aeration conditions (8.7 Cu: 1.7 Zn). In concordance with these ICP-AES results, in the former case the most abundant detected species by ESI-MS was M_4-SpMTA, followed by a collection of higher nuclearity complexes (M_5 to M_9, Fig. 8A), which should be mainly consisting of Cu_4Zn_x complexes ($1< x < 5$), since ESI-MS data at pH 2.5 identified a highly predominant Cu_4 cluster (Fig. 8B). Conversely, when SpMTA was synthesized

under low aeration, the most abundant species in solution switched to M_8 (M = Zn+Cu), readily followed by M_9 to M_{11} complexes (Fig. 8C), whose acid ESI-MS analyses revealed

Table 3. Analytical characterization of recombinant SpMTA and its independent constitutive fragments synthesized in Cu-enriched media under normal (N.A.) and low (L.A.) aeration conditions.

MT	Concentration & Metal/MT ratio[a]	ESI-MS[b]			
		Species (% abundance)		Theor. MW	Exp. MW
SpMTA (N.A.)	$0.5 \cdot 10^{-4}$ M 5.5 Cu 3.0 Zn	pH 7.0	**M_4-SpMTA (100)**	6782.7-6786.0	6771.0 ± 0.1
			M_8-SpMTA (80)	7032.8-7039.5	7029.7 ± 1.2
			M_5-SpMTA (40)	6845.2-6849.4	6838.0 ± 1.1
			M_9-SpMTA (40)	7095.3-7102.9	7092.5 ± 1.5
			M_6-SpMTA (30)	6907.7-6912.8	6899.8 ± 1.3
		pH 2.5	**Cu_4-SpMTA (100)**	6782.7	6773.5 ± 0.5
			Cu_8-SpMTA (20)	7032.8	7035.3 ± 2.2
			Apo-SpMTA (20)	6532.0	6522.5 ± 2.3
SpMTA (L.A.)	$0.5 \cdot 10^{-4}$ M 8.7 Cu 1.7 Zn	pH 7.0	**M_8-SpMTA (100)**	7032.8-7039.5	7030.6 ± 0.8
			M_{11}-SpMTA (60)	7220.4-7229.6	7224.6 ± 0.3
			M_9-SpMTA (60)	7095.3-7102.9	7096.8 ± 1.0
			M_{10}-SpMTA (40)	7157.9-7166.2	7161.4 ± 1.2
		pH 2.5	**Cu_8-SpMTA (100)**	7032.8	7029.1 ± 1.2
			Cu_9-SpMTA (40)	7095.3	7094.1 ± 1.8
αSpMTA (N.A.)	$0.3 \cdot 10^{-4}$ M 6.0 Cu 0.1 Zn	pH 7.0	oxidized dimeric species	----------	----------
		pH 2.5	N.D.	----------	----------
αSpMTA (L.A.)	$0.2 \cdot 10^{-4}$ M 4.2 Cu 0.2 Zn	pH 7.0	N.D.	----------	----------
		pH 2.5	oxidized dimeric species	----------	----------
βSpMTA (N.A.)	$0.7 \cdot 10^{-4}$ M 5.1 Cu 0.2 Zn	pH 7.0	**M_5-βSpMTA (100)**	3132.9-3137.1	3129.6 ± 0.1
			M_6-βSpMTA (30)	3195.5-3200.5	3195.6 ± 0.3
			M_4-βSpMTA (20)	3070.4-3073.7	3067.6 ± 2.1
			M_7-βSpMTA (20)	3258.0-3263.8	3255.4 ± 1.9
		pH 2.5	N.D.	----------	----------
βSpMTA (L.A.)	$0.05 \cdot 10^{-4}$ M 3.4 Cu 0.7 Zn	pH 7.0	**M_5-βSpMTA (100)**	3132.9-3137.1	3131.6 ± 1.6
			M_4-βSpMTA (40)	3070.4-3073.7	3066.8 ± 1.9
		pH 2.5	N.D.	----------	----------

[a] MT concentration and metal/MT ratio calculated from acid ICP-AES results.

[b] Experimental and theoretical molecular weights corresponding to the Cu-peptides. Species shown in bold correspond to the major components of the preparations. In the case of Zn,Cu mixed-metal species, the indicated theoretical molecular weights correspond to the homometallic Cu_x and Zn_x species ($MW_{Cu\text{-}MT}$-$MW_{Zn\text{-}MT}$), and the metal-to-protein stoichiometries deduced at pH 7.0 are indicated as M_x (M=Zn+Cu). Cu contents at pH 2.5 were calculated from the mass difference between holo- and apoproteins. N.D. Not detected.

to be built by Cu_8 and Cu_9 cores (Fig. 8D) plus some added Zn(II) ions. The homologous SpMTB was also synthesized under both culture conditions. Under normal aeration, this isoform yielded preparations similar to those of SpMTA when produced under low aeration, *i.e.* a predominant M_8 complex accompanied by M_9 and M_{10} species that acid

ESI-MS identified as predominant Cu_8Zn_y complexes (Table 4, Fig. 8E-F). With respect to the recombinant Cu-SpMTB synthesis at low aeration, ICP-AES results indicate the formation of homometallic Cu species (average metal content of 14.5 Cu/MT and absence of Zn(II) ions, Table 4). Unfortunately, due to the low concentration of the sample, possibly due to an intrinsic poor folding of these complexes (as pointed out by their CD spectra, Fig. 9), ESI-MS detection of the corresponding species was repeatedly unsuccessful. Since the less aerated an *E. coli* culture, the higher the Cu content of the grown cells, it is obvious that the capacity of SpMTB to exhibit, even under lower Cu assayed concentrations, the Cu(I)-binding behavior that SpMTA is only able to perform in the presence of higher copper amounts, argues in favor of the increased Cu-thionein character of the former. It is worth noting that the major stoichiometries reported here for both SpMT isoforms (*i.e.* Cu_4Zn_x and Cu_8Zn_y) have also been reported for mammalian MT1 [24,25] and MT3 [26], mussel Me-MT-10-IV [20], or nematode CeMT1 and CeMT2 [27], this indicating that this set of approximately 60-residue MTs commonly fold into clusters containing a multiple of 4 Cu(I) ions complemented with a variable number of Zn(II) ions.

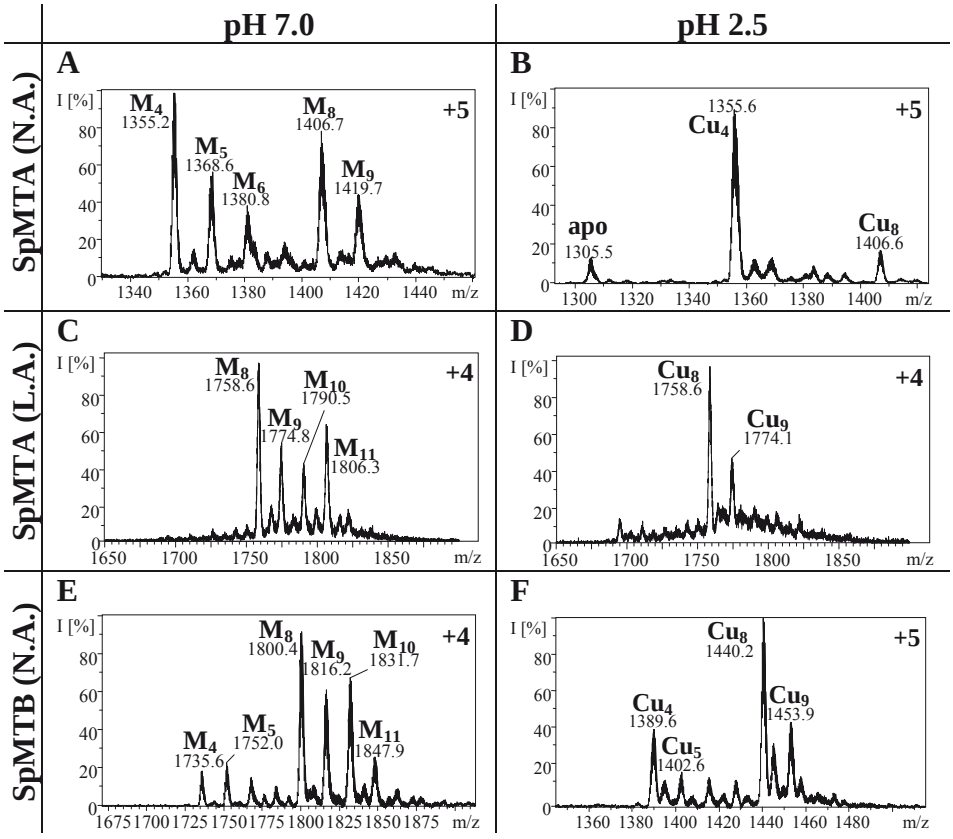

Figure 8. Representative charge states for the ESI-MS spectra recorded at pH 7.0 and pH 2.5 of recombinant SpMTA (**A**, **B**) and SpMTB (**E**, **F**) synthesized in Cu-supplemented *E. coli* media at normal aeration (N.A.) conditions, and SpMTA (**C**, **D**) obtained at low aeration (L.A.) conditions. The observed species are collected in Tables 3 and 4.

Table 4. Analytical characterization of recombinant SpMTB and its independent constitutive fragments synthesized in Cu-enriched media under normal (N.A.) and low (L.A.) aeration conditions.

MT	Concentration & Metal/MT ratio[a]	ESI-MS[b]			
		Species (% abundance)		Theor. MW	Exp. MW
SpMTB (N.A.)	$0.9 \cdot 10^{-4}$ M 5.5 Cu 1.9 Zn	pH 7.0	**M_8-SpMTB (100)**	7201.1-7207.8	7196.1 ± 0.6
			M_{10}-SpMTB (70)	7326.2-7334.6	7322.8 ± 1.0
			M_9-SpMTB (60)	7263.7-7271.2	7260.8 ± 0.9
			M_{11}-SpMTB (20)	7388.8-7398.0	7387.6 ± 0.7
			M_5-SpMTB (20)	7013.5-7017.7	7002.8 ± 1.1
		pH 2.5	**Cu_8-SpMTB (100)**	7201.1	7196.0 ± 0.1
			Cu_4-SpMTB (40)	6950.9	6944.6 ± 1.1
			Cu_9-SpMTB (40)	7263.7	7261.0 ± 1.2
			Cu_5-SpMTB (20)	7013.5	7008.0 ± 1.6
SpMTB (L.A.)	$0.2 \cdot 10^{-4}$ M 14.5 Cu 0.0 Zn	pH 7.0 & 2.5	N.D.	----------	----------
αSpMTB (N.A.)	$0.6 \cdot 10^{-4}$ M 5.5 Cu 0.5 Zn	pH 7.0	**M_5-αSpMTB (100)**	4226.2-4230.5	4223.0 ± 1.0
			M_4-αSpMTB (70)	4163.7-4167.1	4159.2 ± 1.1
			M_7-αSpMTB (60)	4351.3-4357.2	4350.0 ± 0.7
		pH 2.5	**Cu_4-αSpMTB (100)**	4163.7	4158.6 ± 0.6
			Cu_5-αSpMTB (80)	4226.2	4222.0 ± 0.9
			Cu_7-αSpMTB (40)	4351.3	4348.0 ± 1.2
αSpMTB (L.A.)	$0.3 \cdot 10^{-4}$ M 7.0 Cu 0.0 Zn	pH 7.0	N.D.	----------	----------
		pH 2.5	**Cu_4-αSpMTB (100)**	4163.7	4157.6 ± 0.5
			Cu_5-αSpMTB (90)	4226.2	4221.9 ± 0.9
			Apo-αSpMTB (90)	3913.5	3903.3 ± 0.1
βSpMTB (N.A.)	$0.3 \cdot 10^{-4}$ M 3.3 Cu 0.2 Zn	pH 7.0	**M_5-βSpMTB (100)**	3262.0-3266.3	3260.2 ± 0.4
			M_7-βSpMTB (80)	3387.1-3393.0	3386.6 ± 0.8
			M_8-βSpMTB (80)	3449.7-3456.4	3449.0 ± 0.5
			M_6-βSpMTB (40)	3324.6-3329.6	3322.6 ± 1.0
		pH 2.5	**Cu_8-βSpMTB (100)**	3449.7	3448.5 ± 0.1
			Apo-βSpMTB (100)	2949.3	2940.9 ± 1.2
			Cu_4-βSpMTB (60)	3199.5	3195.3 ± 0.6
			Cu_5-βSpMTB (60)	3262.0	3259.7 ± 1.0
			Cu_7-βSpMTB (60)	3387.1	3385.5 ± 0.1
βSpMTB (L.A.)	N.D.	pH 7.0 & 2.5	N.D.	----------	----------

[a] MT concentration and metal/MT ratio calculated from acid ICP-AES results.

[b] Experimental and theoretical molecular weights corresponding to the Cu-peptides. Species shown in bold correspond to the major components of the preparations. In the case of Zn,Cu mixed-metal species, the indicated theoretical molecular weights correspond to the homometallic Cu_x and Zn_x species ($MW_{Cu\text{-}MT}$-$MW_{Zn\text{-}MT}$), and the metal-to-protein stoichiometries deduced at pH 7.0 are indicated as M_x (M=Zn+Cu). Cu contents at pH 2.5 were calculated from the mass difference between holo- and apoproteins. N.D. Not detected.

Again, the characterization of the Cu(I) binding abilities of the separate domains of both SpMT isoforms proved to be a valuable tool to confirm and further analyze the higher Cu-thionein character of SpMTB regarding SpMTA. First unforeseen information was that both α moieties showed distinct Cu(I) binding behavior, contrarily to what was observed for divalent metal ions. Hence, αSpMTA yielded, under all assay

conditions, mixtures of Zn,Cu heterometallic complexes with highly oxidized and/or poorly metalated species, together with dimeric complexes (Table 3), which exhibit almost

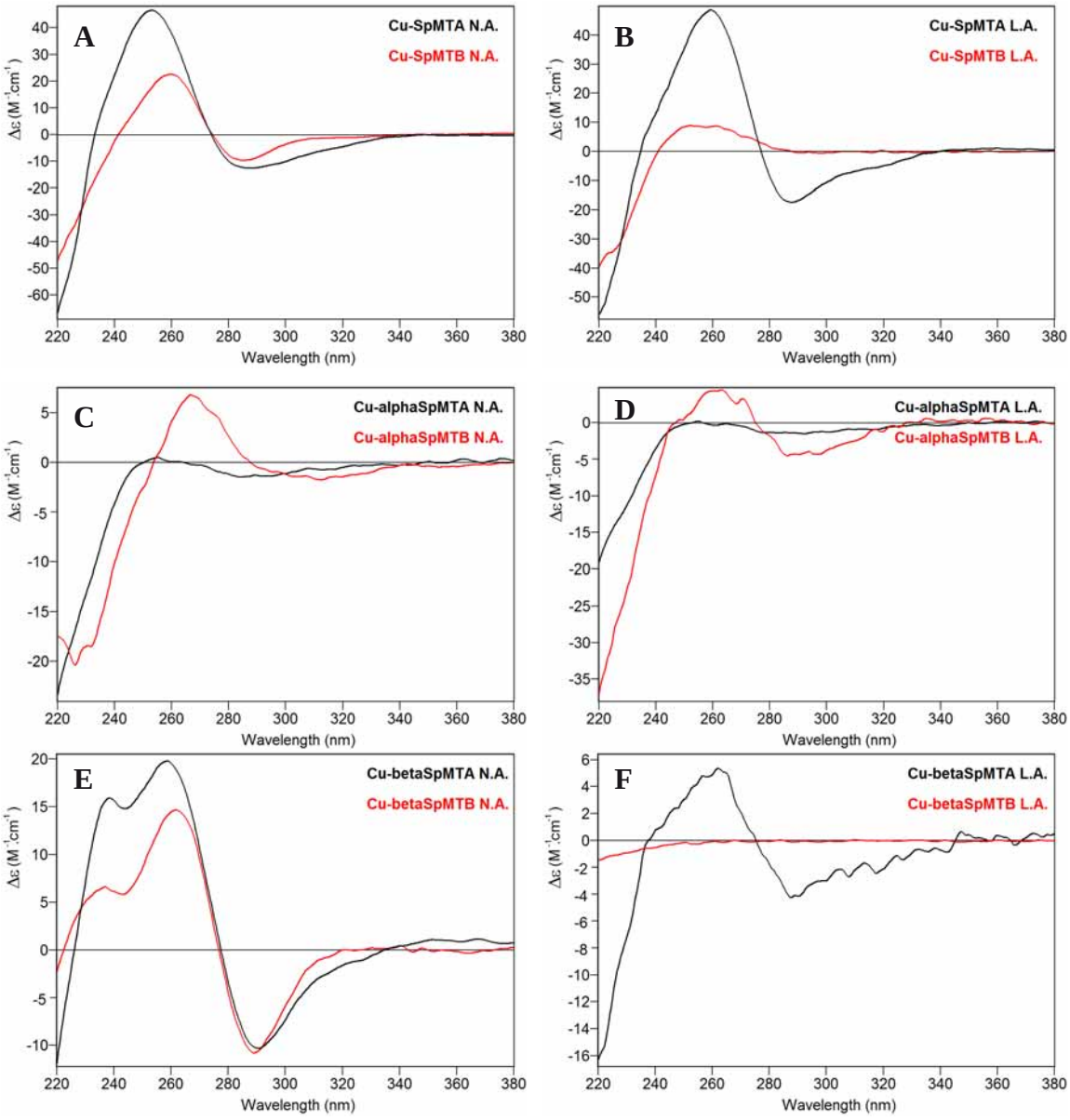

Figure 9. CD spectra corresponding to the entire MT (**A**, **B**) and the separate constitutive α (**C**, **D**) and β (**E**, **F**) domains of SpMTA (black) and SpMTB (red) recombinantly synthesized in Cu-supplemented media at normal aeration (N.A.) and low aeration (L.A.) conditions (left and right, respectively).

flat CD fingerprints (Fig. 9C-D). Contrarily, αSpMTB invariably yielded well defined results: at regular oxygenation Cu_5-, Cu_4Zn_1-, Cu_4- and Cu_7-αSpMTB were the predominant species (Fig. 10A and D, Table 4), and at low aeration conditions a mixture of homometallic Cu complexes with major Cu_4 and Cu_5 stoichiometries was detected (Fig. 10F, Table 4). These results were consistent with well-defined CD spectra, typical of Cu-MT chromophores, despite the fact that they exhibited rather low intensity (Fig. 9C-D). Contrarily to the α domains, no significant differences could be detected for the

recombinantly synthesized β peptides in copper-supplemented media. At normal aeration both isoforms yield a mixture of species with close average Zn/MT (0.2) and Cu/MT (3.3-5.1) ratios (Tables 3 and 4) and very similar CD spectra (Fig. 9E), where M_5 is the major species present (Fig. 10B-C). ESI-MS at pH 2.5 (Fig. 10E) confirmed the almost quasi homometallic nature of the Cu-βSpMTB preparations, and comparison with data at pH 7.0

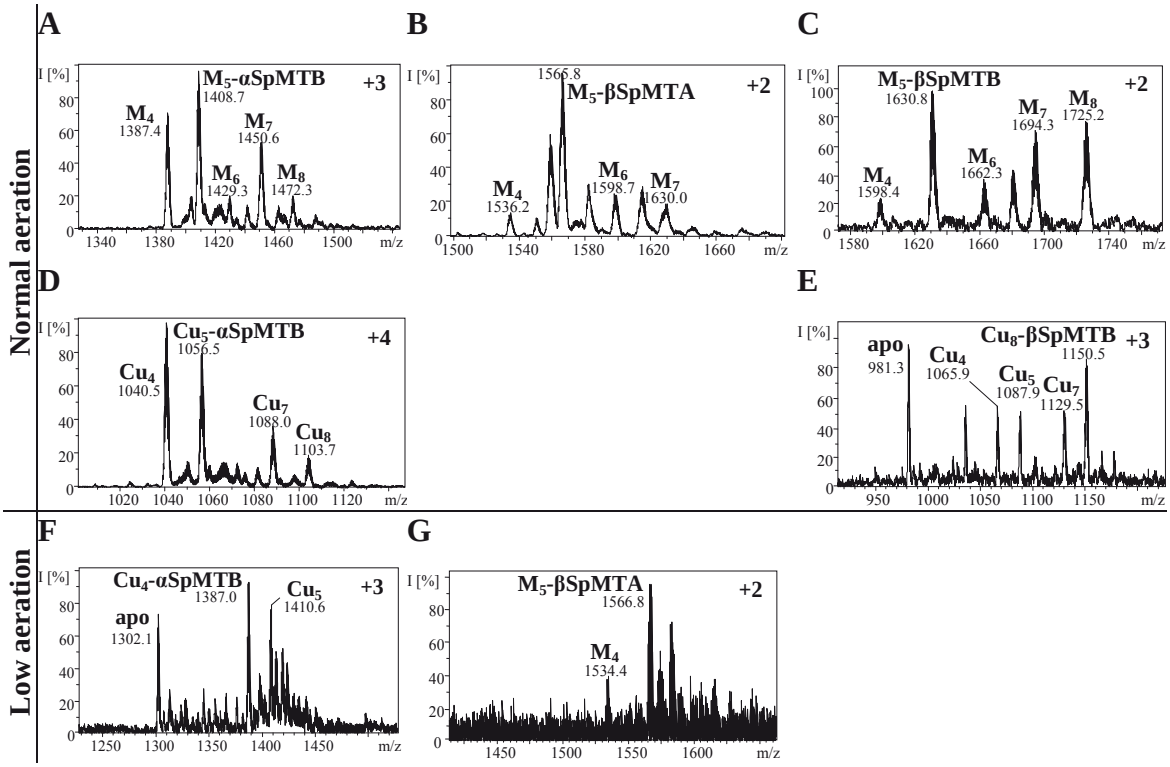

Figure 10. Representative charge states for the ESI-MS spectra of recombinant αSpMTB (**A**, **D**, **F**), βSpMTA (**B**, **G**) and βSpMTB (**C**, **E**) synthesized in Cu-supplemented *E. coli* media at normal and low aeration conditions. M-MT species where M=Zn+Cu are assigned in spectra recorded at pH 7.0 (**A**, **B**, **C**, **G**), while Cu-MT species are assigned when recorded at pH 2.5 (**D**, **E**, **F**). The observed species are collected in Tables 3 and 4.

allowed to deduce that the M_5 major species corresponds to a mixture of Cu_5 and Cu_4Zn_1 complexes. At low aeration, very diluted samples were obtained and consequently very weak CD spectra were recorded (Fig. 9F). However, βSpMTA ESI-MS analysis at pH 7.0 (Fig. 10G) shows a heterometallic species distribution similar to that observed at normal oxygenation, with a major M_5 form (Table 3). In view of the results obtained in the recombinant syntheses of the βSpMT fragments, and in order to have a more precise picture of their differential behavior when coordinating Cu(I), Zn/Cu titrations were performed and followed through their CD spectra evolution. In the case of βSpMTA, the maximum degree of folding was achieved for 3-4 Cu(I) equivalents added to the Zn(II)-βSpMTA preparation, with little further variation (Fig. 11A-C). Contrastingly, βSpMTB

reaches its maximum folding after 6 Cu(I) equivalents added (Fig. 11D-F), which is in concordance with a greater Cu(I) binding capacity. Finally, when comparing these results with those of the recombinant complexes, it becomes obvious that the CD spectrum of βSpMTA is fully reproduced after 4 Cu(I) equivalents added (Fig. 11G), whereas for βSpMTB, the highest CD spectra resemblance is attained after 7 Cu(I) equivalents added (Fig. 11H).

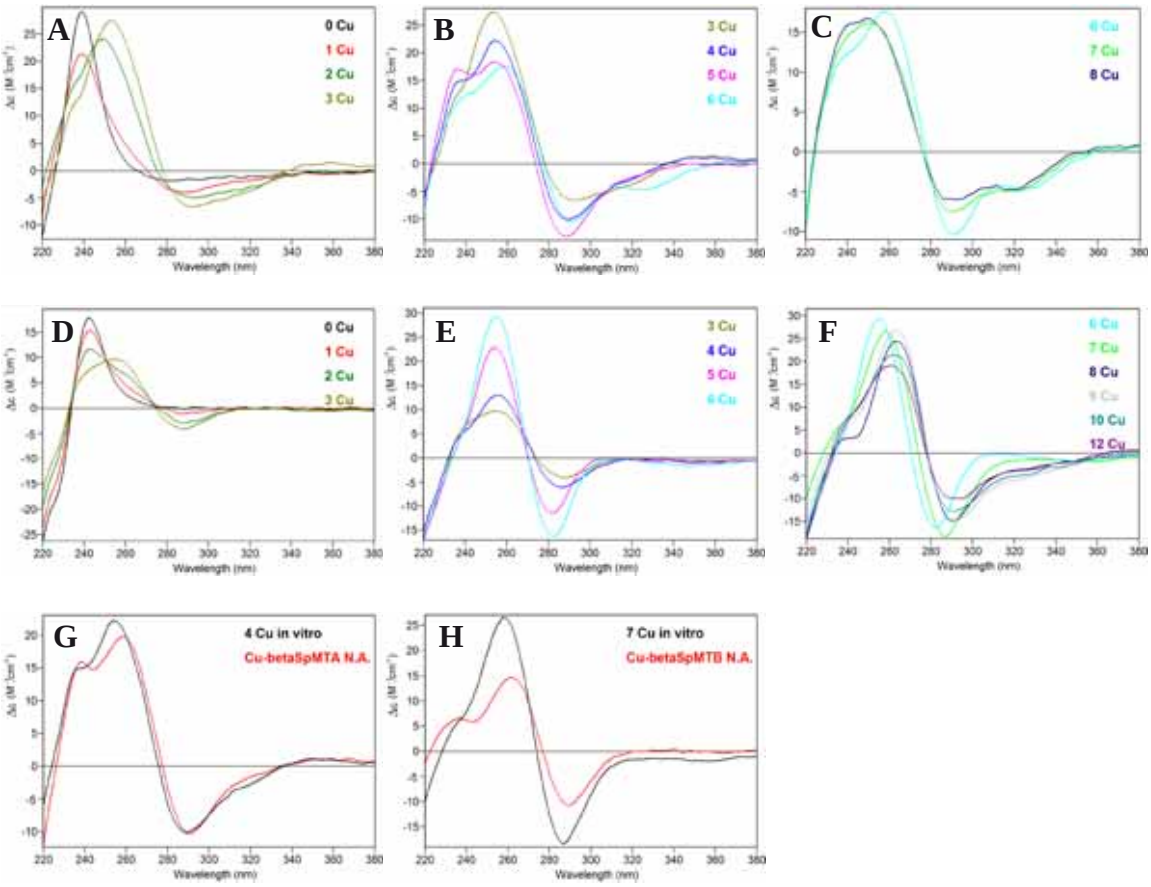

Figure 11. CD spectra recorded during the titration of Zn-βSpMTA (**A**-**C**) and Zn-βSpMTB (**D**-**F**) with Cu(I) at pH 7. Also, a comparison with the CD spectrum of the corresponding recombinant Cu-βMT samples obtained at normal aeration conditions (in red) is shown (**G**, **H**).

4. Conclusions

From the set of data reported in this work, a differential metal ion binding preference is envisaged for SpMTA and SpMTB, since different results attribute a more pronounced Cu-thionein character to SpMTB than to SpMTA, and *vice versa* for the Zn(II) and Cd(II)-thionein character. In summary, and according to the criteria proposed to evaluate the preference of a given MT peptide either for monovalent or divalent metal ion coordination [3], it is worth noting that (i) SpMTA is able to fold into almost unique and

sulfide-free Zn(II) or Cd(II)-complexes, while for these metal ions SpMTB yields preparations containing a large variety of species, and with a significant sulfide content; and (ii) SpMTB is able to yield, at standard bacterial cell copper concentrations (*i.e.* normal aeration of the *E. coli* cultures), Cu-complexes that SpMTA is only able to produce in higher-copper environments. Dissection of the metal-binding abilities of both isoforms into their domains suggests that while the β domain would be the only one responsible for the diminished divalent metal binding capacity of SpMTB, both domains would contribute to the enhanced capacity of SpMTB for Cu(I) binding.

The differential Zn/Cu binding performance of SpMTA and SpMTB suggests that both isoforms exert at least partially distinct complementary functions in the physiology of sea urchins. For divalent metal ions, SpMTA may be mostly responsible for housekeeping Zn homeostasis, while SpMTB would only come into play under Zn or Cd overload emergency situations. This hypothesis is supported by the fact that *SpMTA* is constitutively expressed at a higher rate than *SpMTB* at low Zn concentrations, while increased divalent metal ion concentrations induce *SpMTB* expression up to similar values than *SpMTA* [8], analogously to what has been described for the nematode CeMT1 and CeMT2 isoforms [27]. Interestingly, the existence of multiple MT isoforms involved in different physiological roles has been very recently confirmed in another sea urchin species, *P. lividus*, in which its 5 different MT isogenes respond disctinctively to Cd transcriptional activation, thus showing a certain degree of evolutive functional differentiation [28]. Unfortunately, no information is available for the copper physiology in sea urchin, or for copper requirements during its development stages, or for the response of both *SpMT* isogenes to copper overload. It would not be far-fetched to assume that SpMTB, given its higher Cu-thionein character, could better perform some function related to Cu metabolism in this group of organisms. Overall, and as for other taxa in which MT peptides have been previously characterized, more or less pronounced differential metal ion binding properties would underlie the observed polymorphism, even when the involved polypeptides share a 85% sequence identity, as is the case for *S. purpuratus* MTs.

5. References

[1] Capdevila, M., Bofill, R., Palacios, O. and Atrian, S. (2012) State-of-the-art of metallothioneins at the beginning of the 21st century. Coord. Chem. Rev. 256, 46-52.

[2] Valls, M., Bofill, R., Gonzàlez-Duarte, R., Gonzàlez-Duarte, P., Capdevila, M. and Atrian, S. (2001) A new insight into MT classification and evolution. The *in vivo* and *in vitro* metal binding features of *Homarus americanus* recombinant MT. J. Biol. Chem. 276, 32835-32843.

[3] Bofill, R., Capdevila, M. and Atrian, S. (2009) Independent metal-binding features of recombinant metallothioneins convergently draw a step gradation between Zn- and Cu-thioneins. Metallomics 1, 229-234.

[4] Palacios, O., Pagani, A., Pérez-Rafael, S., Egg, M., Höckner, M., Brandstätter, A., Capdevila, M., Atrian, S. and Dallinger, R. (2011) Shaping mechanisms of metal specificity in a family of metazoan metallothioneins: evolutionary differentiation of mollusc metallothioneins. BMC Biology 9, 4.

[5] Capdevila, M. and Atrian, S. (2011) Metallothionein protein evolution: a miniassay. J. Biol. Inorg. Chem. 16, 977-989.

[6] Palacios, O., Atrian, S. and Capdevila, M. (2011) Zn- and Cu-thioneins: a functional classification for metallothioneins? J. Biol. Inorg. Chem. 16, 991-1009.

[7] Vergani, L. (2009) Metallohioneins from echinoderms. In Metal ions in life sciences 5: metallothioneins and related chelators (Sigel, A., Sigel, H. and Sigel, R.K.O., eds), pp. 228-237. Royal Society of Chemistry, Cambridge.

[8] Wilkinson, D.G. and Nemer, M. (1987) Metallothionein genes MTa and MTb expressed under distinct quantitative and tissue-specific regulation in sea urchin embryos. Mol. Cell Biol. 7, 48-58.

[9] Harlow, P., Watkins, E., Thorton, R.D. and Nemer, M. (1989) Structure of an ectodermally sea urchin metallothionein gene and characterization of its metal-responsive region. Mol. Cell Biol. 9, 5445-5455.

[10] Nemer, M., Thornton, R.D., Stuebing, E.W. and Harlow, P. (1991) Structure, spatial and temporal expression of two sea urchin metallothionein genes, $SpMTB_1$ and $SpMTA^*$. J. Biol. Chem. 266, 6586-6593.

[11] Nemer, M., Wilkinson, D.G., Travaglini, E.C., Sternberg, E.J. and Butt, T.R. (1985) Sea urchin metallothionein sequence: key to an evolutionary diversity. Proc. Natl. Acad. Sci. USA 82, 4992-4994.

[12] Wang, Y., Mackay, E.A., Kurasaki, M. and Kägi, J.H.R. (1994) Purification and characterisation of recombinant sea urchin metallothionein expressed in Escherichia *coli*. Eur. J. Biochem. 225, 449-457.

[13] Wang, Y., Mackay, E.A., Zerbe, O., Hess, D., Hunziker, P.E., Vašák, M. and Kägi, J.H.R. (1995) Characterization and sequential localization of the metal clusters in sea urchin metallothionein. Biochemistry 34, 7460-7467.

[14] Wang, Y., Hess. D., Hunziker, P.E. and Kägi, J.H.R. (1996) Separation and characterization of the metal-thiolate-cluster domains of recombinant sea urchin metallothionein. Eur. J. Biochem. 241, 835-839.

[15] Riek, R., Prêcheur, B., Wang, Y., Mackay, E.A., Wider, G., Guntert, P., Liu, A., Kägi, J.H.R. and Wüthrich, K. (1999) NMR structure of the sea urchin (*Strongylocentrotus purpuratus*) metallothionein MTA. J. Mol. Biol. 291, 417-428.

[16] Capdevila, M., Cols, N., Romero-Isart, N., Gonzàlez-Duarte, R., Atrian, S. and Gonzàlez-Duarte, P. (1997) Recombinant synthesis of mouse Zn_3-beta and Zn_4-alpha metallothionein 1 domains and characterization of their cadmium(II) binding capacity. Cell. Mol. Life Sci. 53, 681-688.

[17] Cols, N., Romero-Isart, N., Capdevila, M., Oliva, B., Gonzàlez-Duarte, P., Gonzàlez-Duarte, R. and Atrian, S. (1997) Binding of excess cadmium(II) to Cd_7-metallothionein from recombinant mouse Zn_7-metallothionein 1. UV-VIS absorption and circular dichroism studies and theoretical location approach by surface accessibility analysis. J. Inorg. Biochem. 68, 157-166.

[18] Pagani, A., Villarreal, L., Capdevila, M. and Atrian, S. (2007) The *Saccharomyces cerevisiae* Crs5 Metallothionein metal-binding abilities and its role in the response to zinc overload. Mol. Microbiol. 63, 256-269.

[19] Bofill, R., Palacios, O., Capdevila, M., Cols, N., Gonzàlez-Duarte, R., Atrian, S. and Gonzàlez-Duarte, P. (1999) A new insight into the Ag^+ and Cu^+ binding sites in the metallothionein beta domain. J. Inorg. Biochem. 73, 57-64.

[20] Orihuela, R., Domènech, J., Bofill, R., You, C., Mackay, E.A., Kägi, J.H.R., Capdevila, M. and Atrian, S. (2008) The metal-binding features of the recombinant mussel *Mytilus edulis* MT-10-IV metallothionein. J. Biol. Inorg. Chem. 13, 801-812.

[21] Domènech, J., Orihuela, R., Mir, G., Molinas, M., Atrian, S. and Capdevila, M. (2007) The Cd(II)-binding abilities of recombinant *Quercus suber* metallothionein: bridging the gap between phytochelatins and metallothioneins. J. Biol. Inorg. Chem. 12, 867-882.

[22] Bongers, J., Walton, C.D., Richardson, D.E. and Bell, J.U. (1988) Micromolar protein concentrations and metalloprotein stoichiometries obtained by inductively coupled plasma atomic emission spectrometric determination of sulfur. Anal. Chem. 60, 2683-2686.

[23] Capdevila, M., Domènech, J., Pagani, A., Tío, L., Villarreal, L. and Atrian, S. (2005) Zn- and Cd-metallothionein recombinant species from the most diverse phyla may contain sulfide (S^{2-}) ligands. Angew. Chem. Int. Ed. Engl. 44, 4618-4622.

[24] Jensen, L.T., Peltier, J.M. and Winge, D.R. (1998) Identification of a four copper folding intermediate in mammalian copper metallothionein by electrospray ionization mass spectrometry. J. Biol. Inorg. Chem. 3, 627-631.

[25] Dolderer, B., Echner, H., Beck, A., Hartmann, H.J., Weser, U., Luchinat, C. and Del Bianco, C. (2007) Coordination of three and four Cu(I) to the alpha- and beta-domain of vertebrate Zn-metallothionein-1, respectively, induces significant structural changes. FEBS J. 274, 2349-2362.

[26] Bogumil, R., Faller, P., Pountney, D.L. and Vašák, M. (1996) Evidence for Cu(I) clusters and Zn(II) clusters in neuronal growth-inhibitory factor isolated from bovine brain. Eur. J. Biochem. 238, 698-705.

[27] Bofill, R., Orihuela, R., Romagosa, M., Domènech, J., Atrian, S. and Capdevila, M. (2009) *Caenorhabditis elegans* metallothionein isoform specificity: metal binding abilities and the role of histidine in CeMT1 and CeMT2. FEBS J. 276, 7040-7056.

[28] Ragusa, M.A., Costa, S., Gianguzza, M., Roccheri, M.C. and Gianguzza, F. (2012) Effects of cadmium exposure on sea urchin development assessed by SSH and RT-qPCR: metallothionein genes and their differential induction. Mol. Biol. Rep., DOI 10.1007/s11033-012-2275-7.

Capítol 2

The response of the different soybean metallothionein isoforms to cadmium intoxication

CAPÍTOL 2

Cadmium accumulation in soybean: contribution of the different metallothionein isoforms

1. Introduction

Of all the heavy metals, cadmium is considered to have one of the highest toxicities for humans and all other living organisms, without performing any known biological function [1]. Although its levels in the lithosphere are low, a major increase in the agricultural soil environment has been registered over the last 200 years, mainly associated to anthropogenic activities. The most widely known sources of Cd contamination are atmospheric deposition associated to mining, smelting industries and fossil fuel combustion, organic amendments derived from sewage sludge, manure and wastewater, and the application of phosphate fertilizers [2]. Phosphate fertilizers contain variable amounts of Cd, depending on the origin of the rocks from which they were obtained, those from the north of Africa being richer [3]. The presence of cadmium in agricultural soils is of major concern regarding the entry of the metal in the food chain. Cadmium compounds are more soluble than other heavy metals, so they are more available and readily absorbed by plants, which accumulate them in different edible parts. Although Cd-induced phytotoxicity is rarely of concern –because of the high basal tolerance of vegetables and the low contamination levels usually found in most agricultural soils- the amount of metal accumulated in plant tissues has to be considered a real threat for human health [4], considering that vegetables contribute to more than 70% of daily Cd intake [5]. The joint Food and Agriculture Organization (FAO) and World Health Organization (WHO) Committee on Food Additives and Contaminants proposes a limit of 0.1 mg/kg of Cd for cereals and grains [6], while the European Community has a limit of 0.2 mg/kg for wheat grain [7], and the FAO/WHO have proposed a maximum tolerable daily intake of 70 μg of Cd for humans [6], due to the risk associated with the long term consumption of Cd contaminated crops.

Different vegetable species vary widely in terms of Cd uptake and accumulation capacity. Some plants, including corn, pea and oat, accumulate low amounts of heavy metals, while leafy vegetables such as lettuce and spinach concentrate

metals in their leaves [8]. Soybean, the worldwide main source of oil and high protein feeds for the livestock sector [9], has a high Cd accumulation capacity in the grain [10]. Differences in the ability to accumulate Cd can also be found between cultivars of the same plant [11,12]. If the limits proposed by the FAO/WHO, European Community and the Codex Alimentrius are established, it will be of outmost importance to identify soybean genotypes that translocate low levels of Cd to the seed.

Therefore, the global characterization of the molecular mechanisms involved in cadmium accumulation in edible plants, such as soybean, is of major interest in agriculture and food exploitation. Plants produce different types of peptidic defences against heavy metals. On the one hand, phytochelatins are enzymatically-synthesized peptides that capture heavy metals by coordination and polinuclear cluster formation [for a recent review, see 13]. They were identified as the major agents in charge of the defence against Cd in plants [14], playing a role of direct chelators for metal immobilization, and nowadays they have been also characterized as transporters through the vegetal organisms to cope with cadmium root overload [15]. On the other hand, metallothioneins (MTs) remain the main gene-encoded peptides acting as a response to an inadequate type/dose of heavy metals, also operating by chelation and immobilization. MTs are small cysteine-rich proteins with the ability to coordinate heavy metal atoms through metal-thiolate bonds, which are widely distributed among the animal and plant kingdoms [cf. recent review in 16]. MTs are currently clustered in fifteen families following taxonomical criteria, since they show extremely heterogeneous amino acid sequences. Plant MTs, placed in Family 15, generally contain two small cysteine-rich domains (4 to 8 cysteine each) and a large spacer region (30-50 residues) devoid of this amino acid. As opposed to the large amount of knowledge of animal MTs, the structural and functional properties of plant MTs are little known (for recent plant MTs reviews *cf*. [17,18]). The distribution of cysteine residues, as well as the length of the spacer region, served to further classify plant MTs into four types [19,20]. Only a small number of plant MTs differ from the described canonical primary structure: type 4 MTs, characterized by three cysteine-rich regions, and the *Brassicaceae* subtype of Type 1 MTs, bearing a short spacer of less than 10 residues. In *Arabidopsis*, seven actively expressed MT genes have been identified that include representatives of the four types [19,21]. The further isolation of representatives of the four types in the distant model *Oryza sativa* (rice) [22] indicated that the multiplicity of MT forms precedes the

dicot/monocot split in Angiosperms, and suggests that it is a common feature among this entire group of plants. Single MT forms have been also isolated in Gimnosperms [23] and algae (*Fucus vesiculosus*) [24]. In general, plant MT genes respond to a wide variety of stresses (metal ions, abscisic acid, salt and oxidative stress, temperature, wounds and pathogen invasions), with a generally ubiquitous expression [25]. Specifically, it has been shown that Cd triggers plant MT gene response as a means of conferring protection against this metal [26,27,28]. Some trends in spatial distribution have been assigned to plant MT genes. Hence, there is an increased type 1 expression in subterranean tissues, while type 2 preferential synthesis seems to be located in aerial organs, type 3 MT mRNAs have been mainly purified from ripening fruits or leaves, and type 4 is practically restricted to seeds [21,25,29,30,31].

To undertake a full characterization of the response of soybean to cadmium overload, we started by determining the main features of the accumulation of this heavy metal in the plant, as well as defining the composition of its MT system and determining the behaviour of one member of each isoform subfamily under Cd stress. Overall, high soybean MT expression levels, particularly MT4 in seeds, and the cadmium binding capacity of all four isoforms studied, fully support the need to consider the MT system a main determinant of cadmium accumulation in soybean tissues.

2. Experimental

2.1. Plant culture conditions

Soybean seeds (*Glycine max* cv. Williams 82), surface sterilized by 2-min treatment with 10% (v/v) household bleach, were germinated for 3 days in Petri dishes in darkness and then 3 plants per biological replicate were transferred to individual 12-L pots with humus soil. Plants were grown in a greenhouse with 14 h light/10 h darkness until maturity. They were exposed to a background cadmium level of 0.04 ppm (control), or 1 ppm and 1.8 ppm of total cadmium (medium pollution), added as $CdCl_2$ in 0.1 μM solution, for the whole lifecycle (spanning 135 days for the used cultivar), after which the leaves, roots and seeds were separately collected, frozen in liquid nitrogen and stored at –80 °C (for qPCR experiments) or dried at 80 °C (for Cd content measurements). Short-time or acute cadmium exposure treatments were performed on 21 day-old plants,

grown on perlite with Hoagland nutrient solution, supplemented or not with 200 μM $CdCl_2$ for 16 h or 40 h, after which the leaves and roots were collected separately, frozen in liquid nitrogen and stored at –80 °C until use. All experiments were performed in triplicate.

2.2. Metal content determination in soil and vegetal tissues

Soil samples were dried in an oven at 80 °C for 48 h and then ground and 1-mm sieved. The amounts of available Cd were extracted with Mehlich 1 solution (0.05 mol/L HCl + 0.0125 mol/L H_2SO_4; pH 1.2) in a soil:solution ratio of 1:10, shaken for 1 h on a reciprocating shaker at 120 oscillations/min and left to stand overnight. After 16 h, cadmium in the extracts was determined by graphite furnace atomic absorption spectrophotometry (GFAAS) with a GBC 906AA system.

Harvested soybean leaves, roots and seeds were dried at 80 °C for 72 h until reaching constant weight. All leaves, roots and about 10 seeds were ground, and 0.5 g of each sample was completely digested at 100 °C in a dry bath, with 50% v/v HNO_3, at reflux. Determination of cadmium concentration was carried out by inductively coupled plasma atomic emission spectroscopy (ICP-AES) in a Polyscan 61E (Thermo Jarrell Ash) spectrometer, measuring Cd at 228.802 nm. To measure the Cd content of the commercial soybean seeds used to grow the plants of all the experiments, seeds were ground and then dried at 80 ºC for 48 h, and 0.1 g of the ground powder was completely digested at 80 ºC with 1 ml of HNO3. Determination of Cd was carried out by means of ICP-MS, using an Elan 6000 Perkin Elmer spectrometer. All samples were extracted in triplicate in three different biological samples, totaling nine replicates for determination.

2.3. In silico *identification of soybean MTs. Availability of cDNA clones.*

Sequences of the four metallothioneins under study here were obtained by searching with the NCBI Basic Local Alignment Search Tool (BLAST), specifically the nucleotide BLAST program using the blastn algorithm, in the ESTs library database, limiting the results to the *Glycine max* organism. *Arabidopsis thaliana* metallothionein mRNA sequences NM_100633.2 (MT1a), NM_111773.3 (MT2a), NM_112401.1 (MT3)

and NM_127888.1 (MT4a) were introduced as queries. Of the retrieved sequences, those showing a higher number of ESTs -indicative of a higher expression level- for each type of plant MTs, were selected. The ESTs clones BQ742738.1 (GmMT1), BQ629803.1 (GmMT2) and CA819971.1 (GmMT3) were acquired from Biogenetic Services (USA). Since there was no available EST clone for a GmMT4 isoform, the corresponding cDNA was synthesized as described in section 2.5. With the release of the complete soybean genome assembly 1.01 during the course of this work, the search for MT genes was performed with the Phytozome BLAT alignment tool using the four previously selected cDNA GmMT sequences as queries.

2.4. Quantitative real time PCR (qPCR)

Three biological replicates, consisting each sample of leaves, roots or seeds pooled from three plants, were analized. Total RNA was isolated with TRIZOL® Reagent (Invitrogen) following the manufacture's protocol and treated with DNase I (Fermentas). The cDNA was synthesized using an oligo(dT_{18}) primer from 1 µg of total RNA with the reverse transcriptase RevertAid™ (Fermentas) and RNaseOUT™ Recombinant RNase Inhibitor (Invitrogen). Quantitative real-time PCR reactions were performed in a 20-µl reaction volume with 0.5 µM gene-specific primers (listed in Table 1), 2 µl of 1/100 diluted cDNA as a template, and SYBR Green I (Invitrogen) as detection reagent. Soybean actin 11 (Glyma02g10170) was used as a reference gene. The amplicon lengths were 158 bp for GmMT1, 182 bp for GmMT2, 59 bp for GmMT3, 105 bp for GmMT4 and 94 bp for actin 11. The reactions were performed in an MX3000P QPCR System (Stratagene) in triplicate (technical replicates). PCR conditions were: 94 °C for 5 min, followed by 45 cycles of 94 °C for 15 s, 55 °C for 30 s and 72 °C for 15 s. After final annealing (72 °C, 5 min), a melt curve analysis was made by increasing the temperature from 65 °C to 95 °C at 0.5 °C intervals to check on the specificity of the assays, all real time PCR reactions passing this quality control. The SYBR® Green I fluorescent signal was determined for each cycle at the end of the extension step. The fold-change in gene expression was calculated using the comparative Ct method ($2^{-\Delta\Delta Ct}$) [32]. The correlation coefficient of amplification, determined from serial dilutions, was 0.996 for GmMT1, 0.998 for GmMT2, 0.995 for GmMT3 and 0.999 for GmMT4 and actin 11.

Table 1. Sequence of the oligonucleotides used for rtPCR assays (named GmMT) and for PCR synthesis of the cDNA for cloning into pGEX plasmids (named MT-*BamH*I and MT-*Xho*I). The introduced restriction sites are underlined.

Direct oligonucleotide

Name	Sequence
GmMT1 F	5′-TTTGACTTGAGTTACGTTGAGAAG
GmMT2 F	5′-TGTACCCAGACTTGAGCTACAC
GmMT3 F	5′-ACATCGAGACTGTTGTCATGGA
GmMT4 F	5′-TGGAGGAGATGCAGTGAGACC
GmACT F	5′- GCACCCAGCAGCATGAAGA
MT1-BamHI F	5′-ATCGGATCCATGTCTAGCTGTGG
MT2-BamHI F	5′-ATAGGATCCATGTCTTGCTGCGGTG
MT3-BamHI F	5′-AAAGGATCCATGTCGAACACATGC
MT4-BamHI F	5′-GAGGGATCCATGGCTGATACAAGTG

Reverse oligonucleotide

Name	Sequence
GmMT1 R	5′-CTTGCAGTTGCATGGGTCAC
GmMT2 R	5′-TCAGCGGGAACACCCATTTC
GmMT3 R	5′-CACACTTGCACTTCCCATCA
GmMT4 R	5′-TGTCATGCCGACACTTGTGC
GmACT R	5′- AGGTGCTAAGAGATGCCAAGA
MT1-XhoI R	5′-ATCCTCGAGTTACTTGCAGTTGC
MT2-XhoI R	5′-TCCCTCGAGAACACCTCACTTGC
MT3-XhoI R	5′-ACACTCGAGAACACATGGCAATTAC
MT4-XhoI R	5′-GGTCTCGAGTTAAGTGCGGCAAGAG

2.5. Recombinant synthesis of soybean MTs

Each of the four soybean MT cDNAs indicated in section 2.3. (GmMT1 to GmMT4) was amplified by PCR, using the primers shown in Table 1. The templates for GmMT1 to GmMT3 were the cDNAs recovered from the EST clones acquired. cDNA for GmMT4 was obtained from reverse transcription using total RNA from developing seeds, performed at the same conditions described in the preceding section. The 35-cycle PCR amplification was performed with the thermo resistant Taq DNA polymerase (Invitrogen) under the following conditions: 30 s at 94 ºC (denaturation), 30 s at 50 ºC (annealing) and 20 s at 72 ºC (elongation). This reaction added a 5' *BamH*I and a 3' *Xho*I restriction site to the GmMT coding regions, for cloning into the pGEX-4T1 (General

Electric HC) *E. coli* expression plasmid downstream from the glutathione-S-transferase (GST) open reading frame. The correct construction of the recombinant plasmids, pGEX-GmMT1 to pGEX-GmMT4, was confirmed by DNA sequencing (through Macrogen-Korea) and thereafter they were individually transferred into the protease defective strain *E. coli* BL21.

GmMT-GST fusion polypeptides were biosynthesized in 5L-cultures of transformed *E. coli* cells (BL21 strain). Expression was induced with isopropyl ß-D-thiogalactopyranoside (IPTG) and cultures were supplemented with final concentrations of 300 μM $ZnCl_2$ or 300 μM $CdCl_2$, and were allowed to grow for a further 3 h. Total protein extract was prepared from these cells as previously described in [33]. Metal complexes were recovered from the fusion constructs by thrombin cleavage and batch-affinity chromatography using Glutathione-Sepharose 4B (General Electric HC). After concentration using Centriprep Microcon 3 (Amicon), the metal complexes were finally purified through FPLC in a Superdex75 column (General Electric HC) equilibrated with 50 mM Tris-HCl, pH 7.0. Selected fractions were confirmed by 15 % SDS-PAGE and kept at -80 ºC until further use. All procedures were performed using Ar (pure grade 5.6) saturated buffers. Further details on the purification procedure specifically for a recombinant plant MT (*Quercus suber*) can be found in [34,35]. As a consequence of the cloning procedure, the dipeptide Gly-Ser is added to the N-terminus of the corresponding GmMT polypeptides, in relation to the sequences shown in Fig 2. This minor modification of the native form was previously shown not to alter any of the MT metal-binding capacities [36].

2.6. Characterization of the recombinant metal MT complexes

The S, Zn, Cd and Cu content of the Zn-, Cd- and Cu-GmMT preparations was analyzed by means of inductively coupled plasma atomic emission spectroscopy (ICP-AES) in a Polyscan 61E (Thermo Jarrell Ash) spectrometer, measuring S at 182.040 nm, Zn at 213.856 nm, Cd at 228.802 and Cu at 324.803 nm. Samples were treated as in [37], but were alternatively incubated in 1 M HCl at 65 °C for 15 min prior to measurement in order to eliminate possible traces of labile sulfide ions, as otherwise described in [38]. Protein concentrations were calculated from the acid ICP-AES sulfur measure, assuming that the GmMT peptides contributed to all S atoms.

Molecular weight determinations were performed by electrospray ionization time-of-flight mass spectrometry (ESI-TOF MS) on a Micro Tof-Q Bruker instrument interfaced with a Series 1200 HPLC Agilent pump, equipped with an autosampler, all of which were controlled by the Compass Software. Calibration was attained with 0.2 g NaI dissolved in 100 mL of a 1:1 H_2O:isopropanol mixture. Samples containing Zn- or Cd-GmMT complexes were analyzed under the following conditions: 20 μL of protein solution injected through a PEEK (polyether heteroketone) column (1.5 m x 0.18 mm i.d.), at 40 μL min^{-1}; capillary counter-electrode voltage 5 kV; desolvation temperature 90-110ºC; dry gas 6 L min^{-1}; spectra collection range 800-2000 m/z. The carrier buffer was a 5:95 mixture of acetonitrile:ammonium acetate/ammonia (15 mm, pH 7.0). Alternatively, for analysis of the GmMT apoforms, preparations at acidic pH of 20 μL of the corresponding sample were injected at 40 μL min^{-1}; capillary counter-electrode voltage 3.5 kV; lens counter-electrode voltage 4 kV; dry temperature 80ºC; dry gas 6 L min^{-1}. Here, the carrier was a 5:95 mixture of acetonitrile:formic acid at pH 2.4, which caused the complete demetalation of the Zn(II)- or Cd(II)-loaded peptides.

3. Results and discussion

3.1. Cadmium content in soil and vegetal tissues

Cadmium is extremely rare in the earth's crust with a mean concentration of 0.06 ppm but anthropogenic activities are raising its levels in the lithosphere [39]. The cadmium content of non-polluted soil is usually in the range of 0.1-2 ppm and mostly below 1 ppm [40]. The humus soil used in the experiment was naturally low in cadmium content. To simulate the conditions of medium contamination, $CdCl_2$ in solution was added up to a total level of 1 and 1.8 ppm of cadmium in the soil. After 1 month of stabilization, available Cd was extracted with Mehlich 1 solution and measured by GFAAS. Figure 1A shows that the amount of available cadmium is approximately 17% the quantity of added cadmium, confirming the fact that its compounds are more soluble than other heavy metals with much lower solubilities. The total cadmium concentration shown in Fig. 1A for the control soil has been estimated as 0.04 ppm –well below the considered hazardous concentrations for agricultural soils- taking into account the calculated Cd availability.

Although only a fraction of cadmium compounds are accessible to be taken up by soybean roots, in all three cadmium levels tested the concentration of the metal accumulated in all the vegetal tissues analyzed was higher than the available cadmium in the corresponding soil (Fig. 1B). For instance, the highest concentration index is observed for the roots in the control experiment where the accumulated cadmium is 150 times the amount of the available metal in the soil. In seeds, the commercially valuable and edible part of the plant, this concentration index ranges from 2 to 11. All these values point towards an active transport of the metal from the roots.

A **B**

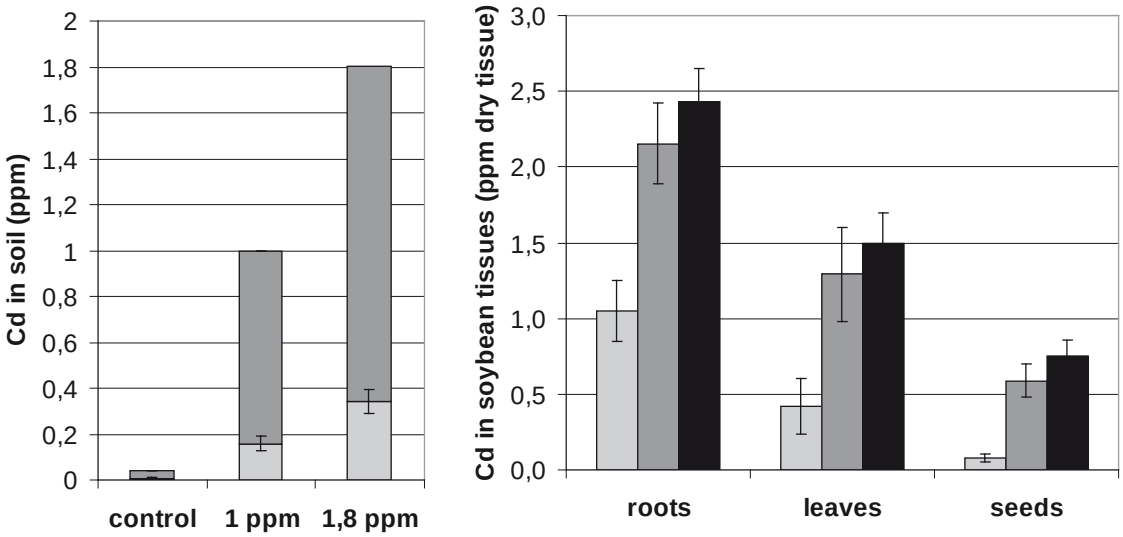

	Bioavailable Cd		Control soil	1 ppm Cd soil	1.8 ppm Cd soil
control soil	0.007 ± 0.005	roots	1.05 ± 0.20	2.15 ± 0.27	2.43 ± 0.22
1 ppm Cd soil	0.158 ± 0.032	leaves	0.42 ± 0.18	1.29 ± 0.31	1.50 ± 0.20
1.8 ppm Cd soil	0.343 ± 0.051	seeds	0.08 ± 0.03	0.59 ± 0.11	0.75 ± 0.11

Figure 1. Cadmium determinations in soils by GFAAS **(A)** and in soybean tissues by ICP-OES (**B**). In soils, light grey bars indicate the amount of Mehlich 1 extractable Cd (bioavailable), dark grey bars show the unextractable Cd, and the whole bar accounts for the total cadmium concentration. In soybean tissues, light grey bars represent the cadmium accumulated in plants from the control soil experiment whereas dark grey and black bars correspond to the cadmium concentration in plants from 1 and 1.8 ppm cadmium soils, respectively. For both graphs, tables with the measured values are provided to help follow some of the observations included in the text.

The mean Cd concentration of the commercial seeds from which the plants used in this study were grown was 0.0074 µg Cd ±0.0009 per g of dried seed). Therefore it has to be assumed that this content does interfere with none of results presented in this work. When comparing plants grown in moderately cadmium polluted soils to the

control situation, the metal content in the roots is doubled, tripled in the leaves, and increased more than seven times in the seeds. It seems that when the buffering capacity of the roots is exceeded, the aboveground tissues accumulate much higher amounts of cadmium. Nevertheless, more importantly, the seeds from metal treated plants had concentrations of cadmium 6-7 times above the 0.1 ppm limit proposed by the Codex Alimentarius Commission [6], in agreement with the results reported by other authors [41]. While the level of cadmium accumulated by the plants used in this study might be higher than the levels occurring under agricultural field conditions, these results reinforce the need to monitor the concentrations of cadmium in food crops and the maximum allowable amounts of cadmium in agricultural fields.

3.2. In silico *analysis of the soybean MT system*

As mentioned before, MT is the most important gene system devoted to metal defense in all types of organism. At the beginning of this study, no information was known for the soybean MT family members, either at protein or gene level, so we took advantage of the release of the soybean genome sequence to analyze the composition of the *G. max* MT system using *in silico* genomic screening. In total, nine genes, easily assignable to the four plant MT types, were identified. The corresponding translated protein sequences are shown in Fig. 2. For Type 1, characterized by two 6-Cys-containing domains separated by a commonly 40-amino acid long spacer, three genes were identified in chromosomes 03, 14 and 17. The three GmMT1 isoforms exhibit high sequence similarity, with only a few amino acid substitutions and a 2-residue deletion in Gm03 MT1. Two coordinating domains of 8 and 6 Cys, also separated by an approximately 40-residue long stretch, characterize type 2 MTs. In the soybean genome, we retrieved two genes for type 2 MTs, but only one (situated in chromosome 07) appeared as a functional copy, since the other (chromosome 18) is a truncated copy, lacking the full first exon (Fig. 2). Also, two genes were retrieved for the MT3 type, situated in chromosomes 06 and 12, containing the canonical 4- and 6 Cys-domains separated by a 38-spacer region. The most atypical MT4 type -also known as *pec* or Ec proteins- is constituted by peptides with two coordinating domains, but the second is, in turn, formed by two Cys-containing regions. Therefore, three Cys-rich boxes are found in Ec MTs, encompassing 6, 6 and 5 Cys residues. Two GmMT4

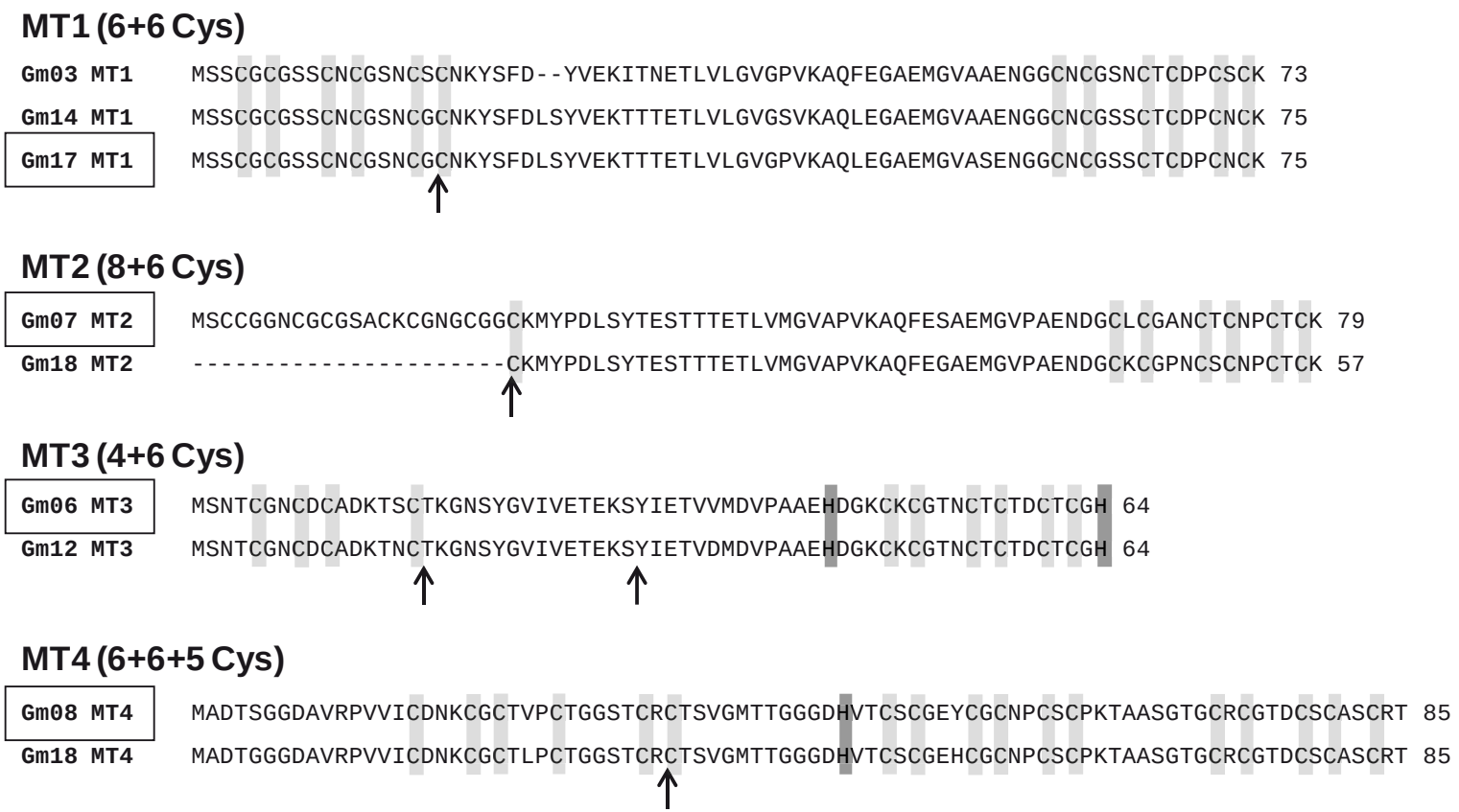

Figure 2. Sequences for all the members in the soybean metallothionein family. Each metallothionein is named with the chromosome number where it is encoded. Light grey and dark grey show the conserved cysteines and histidines, respectively, within each family type. Arrows indicate the exon-exon junctions. Boxes indicate the metallothioneins in this study.

soybean proteins, exhibiting this basic structure, are encoded by the respective genes identified in the 08 and 18 chromosomes. The two GmMT4 isoforms differ in three amino acid changes, two of which are conservative, and, strikingly, the third substitutes the second His in the polypeptide with a Tyr, which implies that Gm08 MT4 is the first member of this subfamily to lack its coordinating His, conversely including an aromatic residue in this sequence position. Supplementary Figure S1 shows the sequence alignment of all GmMTs against metallothioneins from the model plants *Arabidopsis thaliana* and *Oryza sativa,* as well as MTs from other plant species discussed in section 3.4, and Supplementary Tables S1-S4 present the sequence identity matrices for GmMTs compared to those MTs. As expected, a perfect conservation is observed for canonical cysteines; there is also a great conservation for some other residues within cysteine rich domains, and strikingly, some residues from the linker region of type 1, 2, and 3 MTs are almost fully conserved as well.

3.3. Basal and cadmium induced metallothionein expression

Expression of each *GmMT* gene was evaluated by quantitative real time PCR with SYBR Green I detection in roots, leaves and seeds of control and cadmium treated plants at harvest. In control plants, the expression patterns of all four MTs coincide with those described in the literature for each plant MT type [19]. *GmMT1, GmMT2* and *GmMT3* are expressed in all tissues studied, whereas *GmMT4* expression is restricted only to seeds (Fig. 3). *GmMT1* mRNA levels are the highest in roots, while the main isoforms in leaves are GmMT2 and GmMT3. Type 3 MTs are highly expressed in fleshy fruits, but in plants that do not produce them, such as soybean, they are instead expressed at high levels in leaves. In seeds, GmMT4 is by far the most expressed isoform. These results also confirm that *MT* genes are expressed at very high basal levels in plant tissues, at least in terms of transcript abundance.

A short-time, acute Cd exposure experiment was performed on 21-day old soybean plants treated with 200 μM $CdCl_2$ (aprox. 22.5 ppm Cd) for 16 h or 40 h and then harvested. Fig. 4 shows the expression level of all GmMTs present in roots and leaves of control and cadmium exposed plants, GmMT4 not being expressed either in roots or in leaves at any treatment condition. At 16 h treatment only *GmMT2* in leaves is

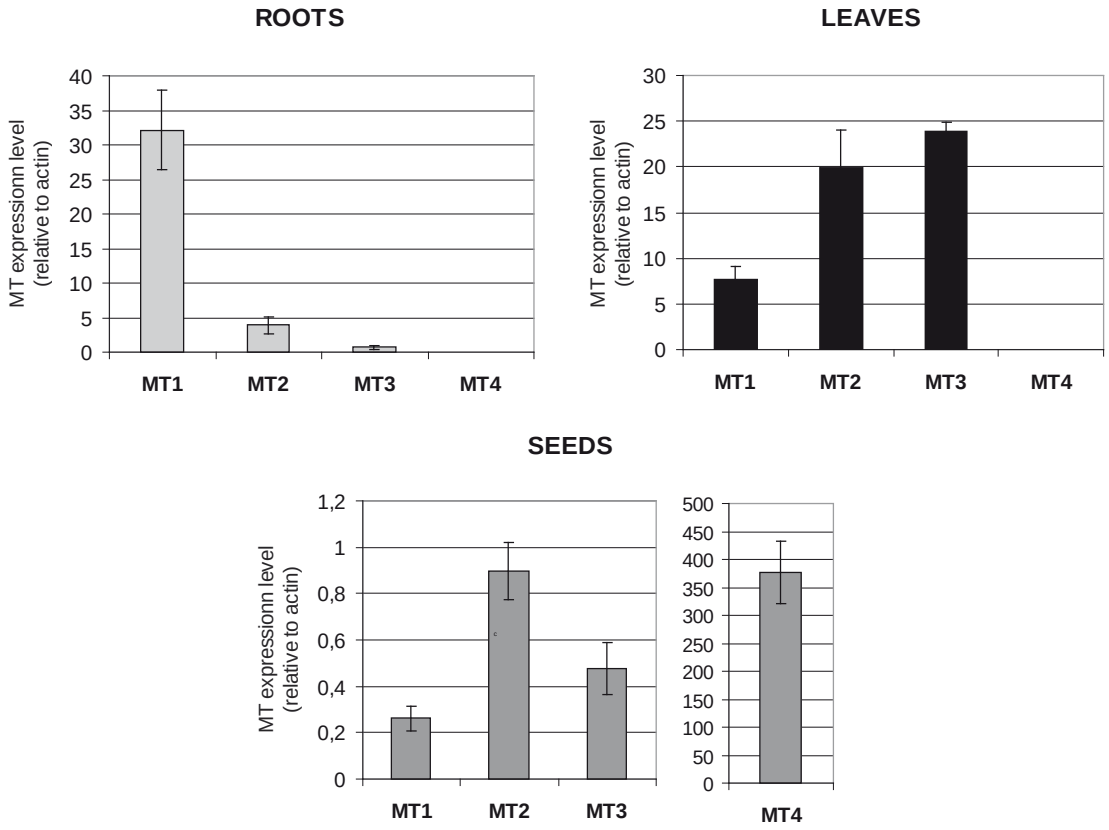

Figure 3. Real time PCR analysis of soybean metallothionein basal expression in roots (light grey), leaves (black) and seeds (dark grey) of mature plants. The means were generated from three independent measurements, and the bars indicate standard deviations.

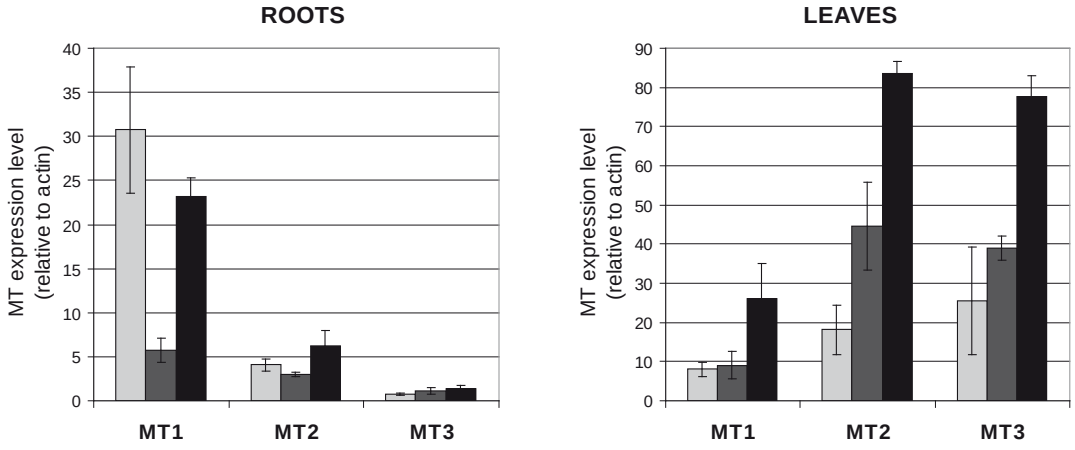

Figure 4. Real time PCR analysis of soybean metallothioneins expression in roots and leaves of plants treated with 200 μM $CdCl_2$ for 16 h (dark grey) and 40 h (black) *vs*. untreated plants (light grey). GmMT4 expression was measured in both tissues and both treatments and it was not detected (data not shown). The means were generated from three independent measurements, and the bars indicate standard deviations.

significantly induced but a clear induction of *GmMT1*, *GmMT2* and *GmMT3* can be observed in leaves at 40 h treatment, with an increase in the transcription level of 3.25, 4.59 and 3.03 for each gene respectively. On the contrary, we observed a strong repression of *GmMT1* in roots at 16 h treatment –almost recovering its expression level

at 40 h treatment-, but no significant changes in the expression level of *GmMT2* and *GmMT3* at 16 h or 40 h treatments. Concordant results have been observed before for other plant species; *MT3* is induced in the leaves of buckwheat at 5 and 24 h cadmium exposure [42] and in the leaves of *Prosopis juliflora* at 24, 48 and 72 h cadmium treatment [43], there is a strong correlation between foliar *MT2b* expression in hybrid aspen and Cd concentration [44], whereas *MT1* and *MT2* are inhibited in sugarcane roots, in this case at long time cadmium exposure [45]. While the inducibility of *GmMT1*, *GmMT2* and *GmMT3* indicates a role in cadmium defense/detoxification for these proteins, it is striking the inhibition of *GmMT1* in roots at 16 h treatment. We are currently performing a set of different stress experiments to see if the last is a common stress response or if it is specific for cadmium toxicity. It is our hypothesis that GmMT1 -the main isoform in roots- is repressed in this tissue –the site of first contact with the stressing agent-, to allow these cells to send signals in order to prevent or reduce the damage in other tissues. Systemic ROS signaling is one of those signals [46] and it is likely that activation of ROS scavengers, such as MTs, would diminish ROS accumulation being thus detrimental for the induction of the adaptative stress response, as it has been demonstrated for rice OsMT2b during biotic stress [47].

Quantitative real time PCR was also performed in order to determine the expression of all *GmMT* genes in roots, leaves and seeds of soybean plants grown in medium polluted soil (1 ppm and 1.8 ppm Cd) until maturity. No significant differences were observed in this case (data not shown), nevertheless it is important to mention that the high expression levels of all *GmMT* genes shown in Fig. 3 were maintained.

3.4. Metal binding capacities of the four soybean MT isoforms

Recombinant expression of the pGEX-GmMT constructs yielded GmMT polypeptides whose identity, purity and integrity was confirmed by ESI-MS of the respective apoforms obtained by acidification at pH 2.4 of the corresponding Zn-GmMT complexes. For the four cases, a single polypeptide of the expected molecular mass was detected: 7696.58 Da for GmMT1, 8085.20 Da for GmMT2, 6878.65 Da for GmMT3, and 8452.50 Da for GmMT4 (*cf*. sequences in Fig. 2). Commonly, the Zn- and Cd-GmMT complexes were recovered at a concentration range of about 1 x 10^{-4} M (*cf*. Table 2).

Exceptions were the synthesis of GmMT1, which invariably yielded a very low amount of protein both when synthesized in zinc- and cadmium-enriched cultures, and, notably, the production of the GmMT3 isoform as Cd-complex, which rendered a much lower yield than when produced as Zn-complex (Table 2).

When GmMT1 was synthesized as Zn-complex, the major species recovered was Zn_4-GmMT1 (Table 2, Fig. 5). Conversely, recombinant synthesis of GmMT1 yielded a major Cd_6S_1-GmMT1 species, together with minor Cd_5S_6-, Cd_7S_1- and Cd_5-GmMT1. (Table 2, Fig. 6). The presence of sulfide ligands in a subpopulation of the cadmium complexes was fully corroborated by the clear differences between the normal and acid ICP sulfur measurements [38]. For GmMT2, the results followed a similar trend but with lower sulfide content and a slight increase in the metal stoichiometries of the recovered Zn- and Cd-species, probably due to the two additional Cys residues of GmMT2 in relation to GmMT1. The globally diminished Zn(II)- and Cd(II) binding capacity of the GmMT3 isoform, rendering Zn_3-GmMT3 and Cd_4-GmMT3 respectively as major species, matches well with its lower Cys content (Table 2, Fig. 5 and 6). But significantly, for GmMT3, the major Cd-species were sulfide-devoid complexes rather than sulfide-containing species as for the previous cases. Finally, GmMT4 was the isoform that exhibited the highest Zn(II) and Cd(II) binding capacity, with Zn_6-GmMT4 and Zn_5-GmMT4 as major Zn(II) species and Cd_6-GmMT4 as the major product of synthesis in Cd(II) enriched media, accompanied by only very minor sulfide-containing (Cd_8S_1-GmMT4) complexes (Table 2, Fig. 5 and 6). It is worth noting that the Zn(II) and Cd(II) ion content here reported for the four GmMT isoforms are in good concordance with those for other plant MT isoforms found in the literature. Native metal-MT complexes have only been isolated and characterized for type 4 MTs, due to the purification impairments presented by 1, 2 and 3 plant MT types. Therefore, the few stoichiometry data available for these isoforms are from recombinant proteins synthesized in *E. coli*, usually as GST-fusion proteins, this ensuring their comparability beyond small differences due to protein sequence variability. Hence, the available divalent-metal-ion-to-protein ratios for type 1 MTs are 5.6 Zn(II) for *Pisum sativum* MT1 [48,49], 4-5 Zn(II) or Cd(II) for *Cicer arietinum* MT1 [50] and 4 Cd(II) for *Triticum durum* MT1 [51], which are in full concordance with the here reported major Zn_4-GmMT1, as well as the only identified S^{2-}-devoid Cd(II) species (Cd_5-GmMT1). Type 2 MTs of *Quercus suber* [35] and *Cicer*

arietinum [52] data are also fully coincident with those of Gm-MT2: 4 and 5 Zn(II), respectively (*cf.* major Zn_4- and minor Zn_5-GmMT2); and again Cd_5-MT2 as the only S^{2-}-

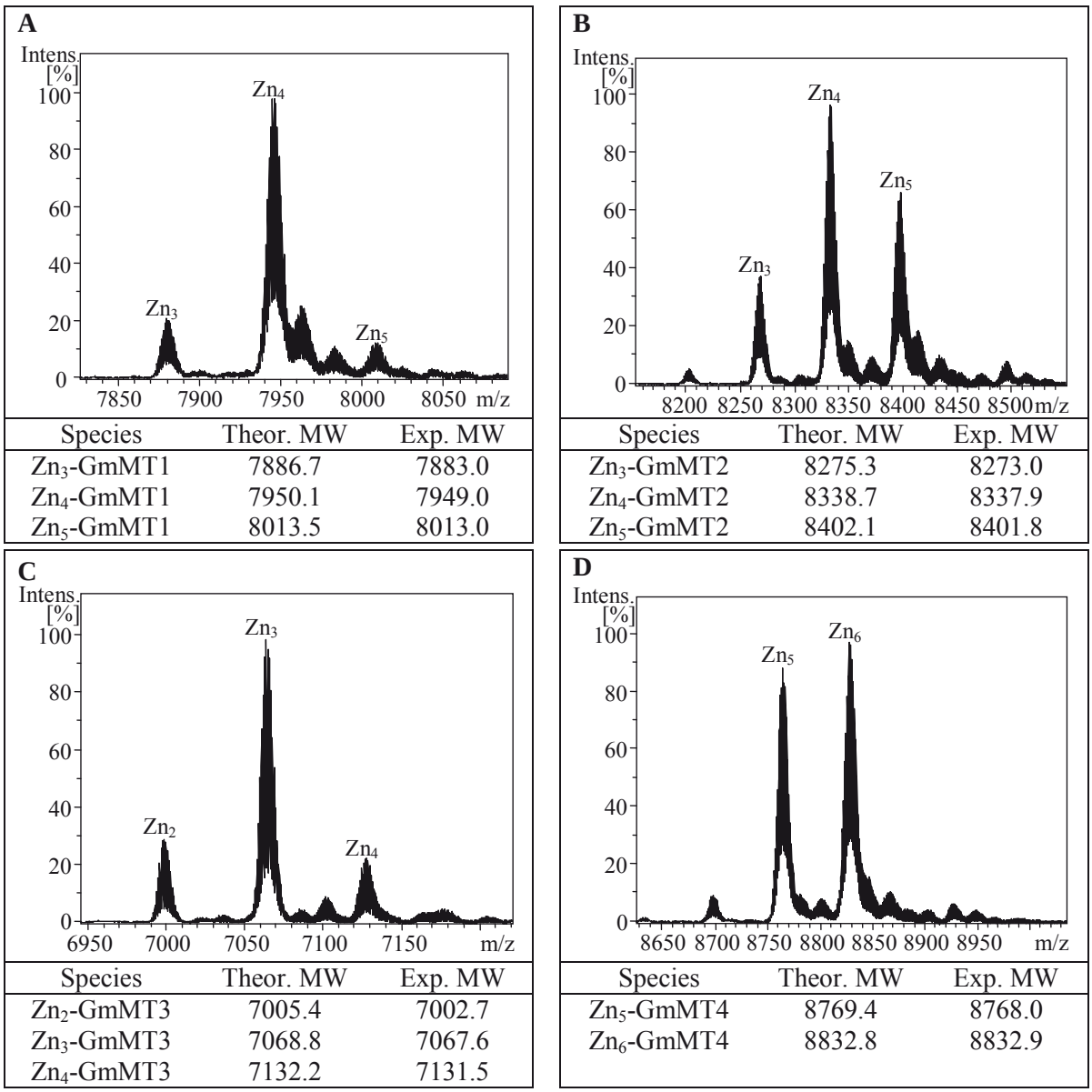

Species	Theor. MW	Exp. MW
Zn_3-GmMT1	7886.7	7883.0
Zn_4-GmMT1	7950.1	7949.0
Zn_5-GmMT1	8013.5	8013.0

Species	Theor. MW	Exp. MW
Zn_3-GmMT2	8275.3	8273.0
Zn_4-GmMT2	8338.7	8337.9
Zn_5-GmMT2	8402.1	8401.8

Species	Theor. MW	Exp. MW
Zn_2-GmMT3	7005.4	7002.7
Zn_3-GmMT3	7068.8	7067.6
Zn_4-GmMT3	7132.2	7131.5

Species	Theor. MW	Exp. MW
Zn_5-GmMT4	8769.4	8768.0
Zn_6-GmMT4	8832.8	8832.9

Figure 5. Deconvoluted ESI-MS spectra of the recombinant preparations obtained from Zn-supplemented *E. coli* cultures of **(A)** GmMT1, **(B)** GmMT2, **(C)** GmMT3, and **(D)** GmMT4, at pH 7.0. The error associated with the experimental MW values was always lower than 1 %, which allows a perfect correlation with the theoretical MW.

devoid Cd(II) species for the three cases, while for *Q. suber* MT2, Cd_6S_x-MT2 sulfide-containing complexes were the major constituent of the preparation, as for GmMT2 (Table 2). For GmMT3, the most comparable data, from a methodological point of view, were those of the banana *Musa acuminata* MT3, yielding Zn_3- and Cd_4-MT3 complexes [53], exactly as the soybean type 3 isoform. Finally, the similarity between the recombinant complexes rendered by Gm-MT4 and those for the wheat Ec-1 (type 4) protein are fully commented at the end of this section.

Table 2. Analytical characterization of the recombinant Zn- and Cd-complexes yielded by GmMT1, GmMT2, GmMT3 and GmMT4.

	Cys/His content	Protein concentration of Zn-complexes[a] (x 10^{-4} M)	Zn/GmMT content[b]	Zn-GmMT species[c]	Protein concentration of Cd-complexes[a] (x 10^{-4} M)	Cd/GmMT content[b]	Cd-GmMT species[c]
GmMT1	12 Cys 0 His	0.25/0.27	5.0/3.8	Zn_4>>Zn_3>Zn_5	0.13/0.06	3.9/8.1	Cd_6S_1 >Cd_5S_6> Cd_7S_1~ Cd_5
GmMT2	14 Cys 0 His	0.8/0.87	4.4/4.3	Zn_4>Zn_5>Zn_3	1.28/0.90	5.6/6.7	Cd_6S_1>Cd_7S_1~ Cd_5
GmMT3	10 Cys 2 His	1.10/1.00	3.2/3.2	Zn_3>>Zn_4 ~Zn_2	0.09/0.10	4.2/4.3	Cd_4>>Cd_3Zn_1
GmMT4	17 Cys 1 His	1.10/1.24	5.8/5.6	Zn_6~Zn_5>>>Zn_4	0.95/1.00	6.0/7.4	Cd_6>> Cd_8S_1

[a] Protein concentration calculated from the sulfur content calculated in normal/acid ICP-AES measurements, respectively.
[b] Metal per GmMT molar ratio calculated from the zinc or cadmium and sulfur content measured by normal or acid ICP-AES, respectively.
[c] Metal per GmMT molar ratio calculated from the difference between holo- and apoprotein molecular masses, obtained from ESI-MS.

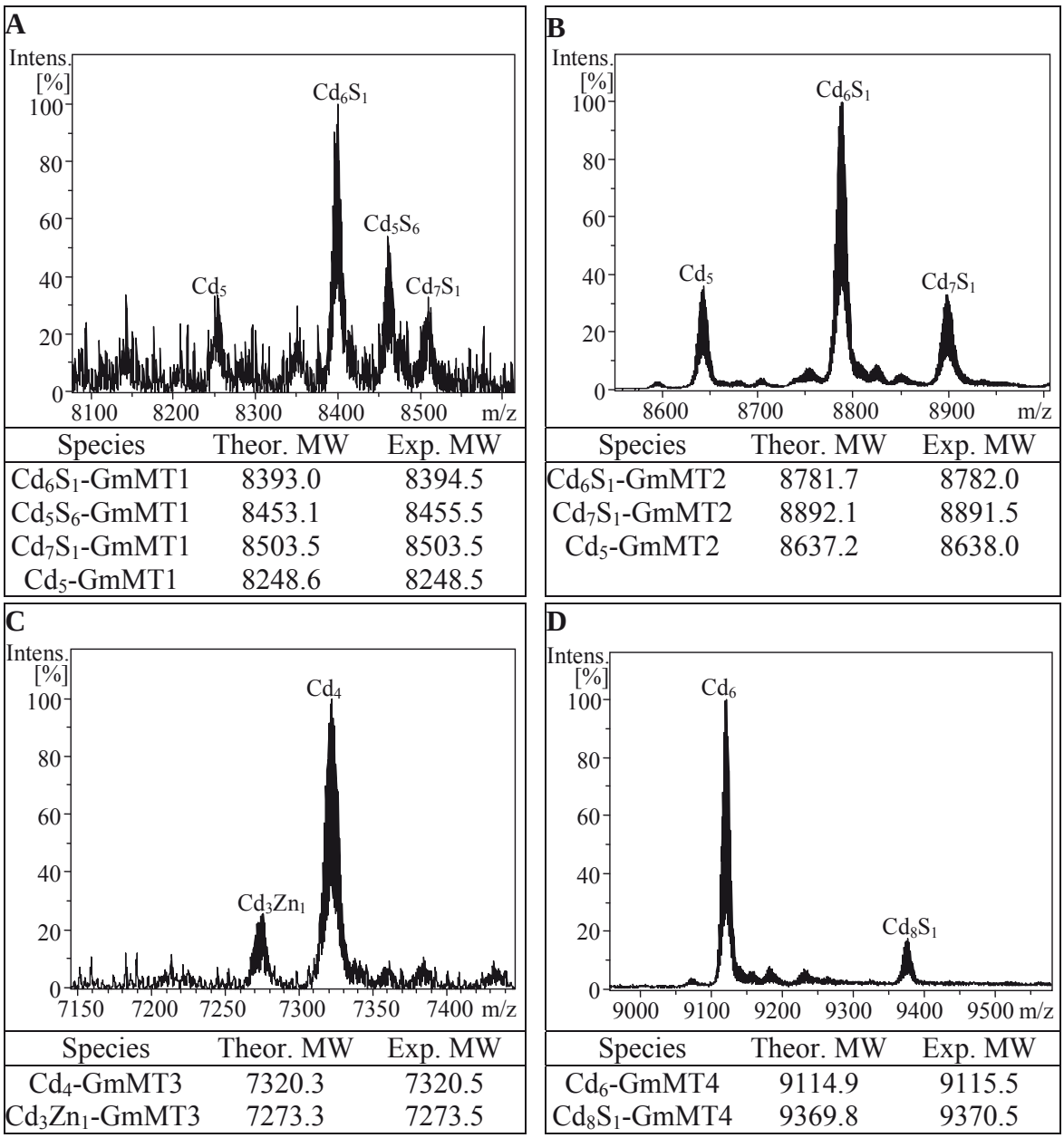

Species	Theor. MW	Exp. MW
Cd_6S_1-GmMT1	8393.0	8394.5
Cd_5S_6-GmMT1	8453.1	8455.5
Cd_7S_1-GmMT1	8503.5	8503.5
Cd_5-GmMT1	8248.6	8248.5

Species	Theor. MW	Exp. MW
Cd_6S_1-GmMT2	8781.7	8782.0
Cd_7S_1-GmMT2	8892.1	8891.5
Cd_5-GmMT2	8637.2	8638.0

Species	Theor. MW	Exp. MW
Cd_4-GmMT3	7320.3	7320.5
Cd_3Zn_1-GmMT3	7273.3	7273.5

Species	Theor. MW	Exp. MW
Cd_6-GmMT4	9114.9	9115.5
Cd_8S_1-GmMT4	9369.8	9370.5

Figure 6. Deconvoluted ESI-MS spectra of the recombinant preparations obtained from Cd-supplemented *E. coli* cultures of **(A)** GmMT1, **(B)** GmMT2, **(C)** GmMT3, and **(D)** GmMT4, at pH 7.0. The error associated with the experimental MW values was always lower than 1 %, which allows a perfect correlation with the theoretical MW.

A comprehensive consideration of these results leads us to conclude that the divalent metal ion binding capacities of the four GmMT isoforms would be on the basis of their differential role as putative cadmium detoxification/accumulation agents. A common trait observed for all cases is that the mean metal content of the cadmium preparations was always higher than that of the corresponding zinc-supplemented synthesis, so that cadmium stoichiometries invariably showed higher values than their cognate zinc-stoichiometries (Table 2). Globally, these stoichiometric values correlate well with the Cys content of the respective peptides. GmMT1 and GmMT2 share a similar Zn(II) and

Cd(II) binding behaviour, with sulfide-containing Cd-complexes prevalent over their sulfide-devoid counterparts (*cf*. Table 2, Fig. 5 and 6) This is the typical behaviour of Cu-thioneins, and is therefore indicative of a poor intrinsic ability to coordinate divalent metal ions [54,55]. The remarkable instability of the GmMT1 recombinant protein, which leads to a minimal recovery yield from the corresponding preparations, suggests native functions that are barely related with cell Zn(II) or Cd(II) handling. GmMT3 exhibits a metal binding behaviour compatible with a clear Zn-thionein character [54], although with a relatively low capacity due to the limited number of coordinating residues in its polypeptide sequence. In this scenario, it is clear that our results for GmMT4 reflect the best ability to act as a divalent metal ion chelator in soybean (Table 2, Fig. 5 and 6). It is worth remembering that the wheat Ec-1 metallothionein, the paradigm of plant MT4 isoforms, is natively isolated from seeds as Zn-complexes [56], so that it has been hypothesised as a Zn(II) reservoir for plant embryo development. Wheat Ec-1 coordinates 6 Zn(II) ions in two independent domains: two in the N-terminal (γ) domain, comprising 6 Cys, and four in the $ß_E$ C-terminal end, with 11 Cys and 2 His contributing to the typical Zn(II)-Cys2His2 cluster formation [57]. In our case, GmMT4 render major equimolar Zn_6- and Zn_5-GmMT4 species, but this decrease in metal binding capacity could be attributed to the lack of one His residue, precisely that included in the first Cys box of the $ß_E$ domain in wheat Ec-1 (Fig. 2). However, the major $M(II)_6$ stoichiometry is recovered in Cd(II)-complex syntheses, since they render an almost unique Cd_6-GmMT4 species. The fact that this major product lacks sulfide anions is in total agreement with a clear Zn-thionein character of GmMT4. It is worth considering how the behaviour of this soybean GmMT4 isoform, holding only one His residue, completely matches the results obtained for Zn(II) and Cd(II) coordination with the H40A site-directed-mutant of wheat Ec MT [58]. Thus, as in that case, the decrease in Zn(II) binding capacity and the increased stability of the Cd(II) complexes would be explained by the loss of the Cys2His2 site for optimal Zn(II) coordination and the preference of Cys binding for Cd(II). Further characterization of GmMTs metal binding features, and behaviour in relation to other stresses, is underway.

4. Conclusions

Analysis of the *Glycine max* (soybean) accumulation response to cadmium overload is essential for toxicological/nutritional purposes. Our results invariably show that, upon root uptake, the concentration of Cd(II) accumulated in all the analyzed soybean plant tissues was higher than the available cadmium in the corresponding soil. Precisely in seeds, the commercially valuable part of the plant, the concentration capacity ranges from a 2 to 11 factor, which means that in our experimental conditions, the seeds from metal treated plants accumulated Cd(II) levels clearly above the 0.1 ppm limit proposed by the Codex Alimentarius Commission. Since it was likely that MTs, the most relevant proteins devoted to metal defense in all types of organism, were responsible for at least part of the detected Cd(II) accumulation, we undertook the characterization of the unreported soybean MT system. The *G. max* genome includes nine MT genes, eight of which are identified as fully active by detection of the corresponding ESTs in databanks. The other corresponds to a truncated copy generated by the loss of an exon. The predicted GmMT polypeptides match well with the motives defining the four plant MT types, so that soybean representatives for each of them were identified. One *G. max* MT gene/protein of each type (GmMT1 to GmMT4) was selected for further studies. The described *GmMT* expression patterns were fully coincident with data on the literature for other Angiosperm plants, with *GmMT1, GmMT2* and *GmMT3* ubiquitously expressed, and GmMT4 synthesis restricted to seeds. GmMT1 is the main isoform in roots, while in leaves GmMT2 and GmMT3 are predominant. GmMT1, GmMT2 and GmMT3 were highly responsive to cadmium intoxication, which indicates their significant role in cadmium defence/detoxification mechanisms. The determination of the Zn(II) and Cd(II) binding abilities of the four GmMT peptides, recombinantly synthesized in metal supplemented *E. coli* cultures, suggested that GmMT3 and GmMT4 are the most optimal isoforms for divalent metal chelation, both exhibiting a significant Zn-thionein character. These results are fully consistent, on the one hand, with the high inducibility of *GmMT3* by cadmium, and on the other hand, with the previously reported isolation of type 4 plant MTs as zinc complexes from seeds. Overall, our data identify GmMT3 in leaves and GmMT4 in seeds as the main MT buffers for cadmium intoxication in soybean plants. Although neither Cd-MT complexes nor native MT protein have been isolated, and thus quantified, in this work, our data on increased MT mRNA synthesis on the one hand, and increased Cd accumulation on the other, fully

suggest the easy link between these two phenomena. In fact, the relation between cadmium binding by MTs and cadmium tolerance and accumulation has been directly stated before in other plants, such as *Arabidopsis thaliana* [27] and *Vicia faba* [28].

5. References

[1] G.J. Wagner, Adv. Agron. 51 (1993) 173-212.

[2] J. Weber, in: N.W. Lepp (Ed.), Effect of heavy metal pollution on plants: Metals in the environment, vol II, Applied Sci. Publ., London and New Jersey, 1981, pp. 159-184.

[3] J.J. Mortvedt, J.D. Beaton , in: H. Tiesen (Ed.), Phosphors in the global environment: transfer, cycles and management. Wiley, New York, 1995, pp. 93-106

[4] G.S. Dheri, M.S. Brar, S.S. Malhi, J. Plant Nutr. Sci. 170 (2007) 495-499.

[5] J.A. Ryan, H.R. Pahren, G.B. Lucas, Environ. Res. 18 (1982) 251-302.

[6] Codex Alimentrius Commission, Codex General Standard for Contaminants and Toxins in Foods. Report of the 34th Session of the Codex Committee on Food Additives and Contaminants, Rotterdam, The Netherlands, FAO/WHO, Rome, Italy, 2002, pp. 11-15.

[7] European Commission, Commission regulation EC No 466/2001. Setting maximum levels for certain contaminants in foodstuffs. Off. J. Eur. Commun. 77 (2001) 1-13.

[8] M. Puschenreiter, O. Horak, W. Friest, W. Hartl, Plant Soil Environ. 51 (2005) 1-11.

[9] World agriculture: towards 2030/2050. Interim report. Prospects for food, nutrition, agriculture and major commodity groups, Global Perspective Studies Unit, Food and Agriculture Organization of the United Nations, Rome, Italy, 2006, pp.52-58.

[10] K.A. Wolnik, F.L. Fricke, S.G. Capar, G.L. Braude, M. W. Meyer , R.D. Satzger, E. Bonnin, J. Agric. Food Chem. 31 (1983) 1240-1244.

[11] J. Liu, M. Qian, G. Cai, J. Yang, Q. Zhub, J. Hazard Mater. 143 (2007) 443-447.

[12] M.K. Jamali, T.G. Kazi, M.B. Arain, H.I. Afridi, N. Jalbani, G.A. Kandhro et al. J. Hazard Mater. 164 (2009) 1386-1391.

[13] A. Devez, E. Achterberg, M. Gledhill, in: A. Sigel, H. Sigel, R.K.O. Sigel (Eds.), Metallothioneins and Related Chelators, Metal Ions in Life Sciences vol. 5, Royal Society of Chemistry, Cambridge, U.K., 2009, pp. 441-481.

[14] E. Grill, E-L. Winnacker, M. ZenkInorg. Science 230 (1985) 674-676.

[15] J. Gong, D. Lee, J.I. Schroeder, Proc. Natl. Acad. Sci. USA 100 (2003) 10118-10123.

[16] M. Capdevila, R. Bofill, O. Palacios, S. Atrian, Coord. Chem. Rev. 256 (2012) 46-52, available at doi 10:1016/j.ccr.2011.07.006.

[17] E. Freisinger, in: A. Sigel, H. Sigel, R.K.O. Sigel (Eds.), Metallothioneins and Related Chelators, Metal Ions in Life Sciences vol. 5, Royal Society of Chemistry, Cambridge, U.K., 2009, pp. 107-154.

[18] E. Freisinger, J. Biol. Inorg. Chem. 16 (2011) 1035-1045.

[19] C. Cobbett, P.B. Goldsbrough, Annu. Rev. Plant Biol. 53 (2002) 159-82.

[20] N.J. Robinson, A.M. Tommey, C. Kuske, P.J. Jackson, Biochem. J. 295 (1993) 1-10.

[21] J. Zhou, P.B. Goldsbrough, Mol. Gen. Genet. 248 (1995) 318-28.

[22] G. Zhou, Y. Xu, J. Li, L. Yang, J.-Y. Liu, J. Biochem. Mol. Biol. 39 (2006) 595-606.

[23] M. Chatthai, K.H. Kaukinen, T.J. Tranbarger, P.K. Gupta, S. Misra, Plant Mol. Biol. 34 (1997) 243-54.

[24] C.A. Morris, B. Nicolaus, V. Sampson, J.L. Harwood, P. Kille, Biochem. J. 338 (1999) 553-60.

[25] W.J. Guo, W. Bundithya, P.B. Goldsbrough, New Phytologist 159 (2003) 369-381.

[26] H. Zhang, W. Zu, J. Guo, Z. He, M. Ma, Plant Sci. 169 (2005) 1059-1065.

[27] A.M. Zimeri, O.P. Dhankher, B. McCaig, R.B. Meagher, Plant Mol. Biol. 58 (2005) 839-855.

[28] J. Lee, D. Shim, W.Y. Song, I. Hwang, Y. Lee, Plant Mol. Biol. 54 (2004) 805-15.

[29] J. Zhou, P.B. Goldsbrough, Plant Cell 6 (1994) 875-884.

[30] H.M. Hsieh, W.K. Liu, P.C. Huang, Plant Mol. Biol. 28 (1995) 381-389.

[31] H.M. Hsieh, W.K. Liu, A. Chang, P.C. Huang, Plant Mol. Biol. 32 (1996) 525-529.

[32] K.J. Livak, T.D. Schmittgen TD, Methods 25 (2001) 402–408.

[33] M. Capdevila, N. Cols, N. Romero-Isart, R. González-Duarte, S. Atrian, P. González-Duarte, Cell. Mol. Life Sci. 53 (1997) 681-688.

[34] J. Domenech, G. Mir, G. Huguet, M. Molinas, M. Capdevila, S. Atrian, Biochimie 88 (2006) 583-593.

[35] J. Domènech, R. Orihuela, G. Mir, M. Molinas, S. Atrian, M. Capdevila, J. Biol. Inorg. Chem. 12 (2007) 867-882.

[36] N. Cols, N. Romero-Isart, M. Capdevila, B. Oliva, P. Gonzàlez-Duarte, R. Gonzàlez-Duarte, S. Atrian, J. Inorg. Biochem. 68 (1997) 157-166.

[37] J. Bongers, C.D. Walton, D.E. Richardson, J. U. Bell, Anal. Chem. 60 (1988) 2683-2686.

[38] M. Capdevila, J. Domenech, A. Pagani, L. Tio, L. Villarreal, S. Atrian, Angew. Chem. Int. Ed. (2005) 44, 4618-4622.

[39] Z.L. He, X.E. Yanga, P.J. Stofella, J. Trace Elem. Med. Biol. 19 (2005) 125-140.

[40] A. Kabata-Pendias, H. Pendias, Trace elements in soils and plants, third ed., CRC Press, Boca Raton, USA, 2001.

[41] T. Shute, S.M. Macfie, Sci. Total Environ. 371 (2006) 63-73.

[42] D.B. Nikolić, J.T. Samardzić, A.M. Bratić, I.P. Radin, S.P. Gavrilović, T. Rausch, V.R. Maksimović, J. Agric. Food Chem. 6 (2010) 3488-3494.

[43] B. Usha, G. Venkataraman, A. Parida, Mol. Genet. Genomics, 281 (2008) 99-108.

[44] Hassinen V, Vallinkoski M-V, Issakainen S, Trevahauta A, Karenlampi S, Servomaa K, Environ. Pollution, 157 (2009) 922-930.

[45] M.L. Sereno, R.S. Almeida, D.S. Nishimura, A. Figueira, J. Plant. Physiol. 164 (2007) 1499-1515.

[46] H.L. Wong and K. Shimamoto, Sci. Signal. 2 (2009) e60.

[47] H.L. Wong, T. Sakamoto, T. Kawasaki, K. Umemura, K. Shimamoto, Plant Physiol. 135 (2004) 1447-1456.

[48] A.M. Tommey, J. Shi, W.P. Lindsay, P.E Urwin, N.J. Robinson, FEBS Lett. 292 (1991) 48-52.

[49] P. Kille, D.R. Winge, J.L. Harwood, J. Kay, FEBS Lett. 295 (1991) 171-175.

[50] O. Schict, E. Freisinger, Inorg. Chim. Acta 362 (2009) 714-724.

[51] K. Bilecen, U.H. Ozturk, A.D. Duru, T. Sutlu, M.V. Petoukhov, D.I. Svergun, M.H. Koch, U.O. Sezerman, I. Cakmak, Z. Sayers, J. Biol. Chem. 280 (2005) 13701-11.

[52] X. Wan, E. Freisinger, Metallomics 1 (2009) 489-500.

[53] E. Freisinger, Inorg. Chim. Acta 360 (2007) 369-380.

[54] R. Bofill, M. Capdevila, S. Atrian, Metallomics 1 (2009) 229-234.

[55] R. Orihuela, F. Monteiro, A. Pagani, M. Capdevila, S. Atrian, Chem. A Eur. J. 16 (2010) 12363-12372.

[56] B.G. Lane, R. Kajiota, T.D. Kennedy, Biochem. Cell Biol. 65 (1987) 1001-1005.

[57] E.A. Peroza, E. Freisinger, J. Biol. Inorg. Chem. 12 (2007) 377-391.

[58] O.I. Leszczyszyn, C.R.J. White, C.A. Blindauer, Mol. Biosys. 6 (2010) 1592-1603.

Supplementary material

Figure S1. Multiple sequence alignment of different plant metallothionein types. Sequences were aligned using the ClustalW 2.0 Multiple alignment program. Dashes indicate gaps in the sequence to allow for maximal alignment. Back coloring is used to designate amino acids conserved at a given position with a threshold of 70%. Ca MT1 (*Cicer arietinum* CAA65008), Ps MT1 (*Pisum sativum* CAA80645), Td MT1 (*Triticum durum* AAT99563), At MT1A (*Arabidopsis thaliana* NP_172239), At MT1C (*Arabidopsis thaliana* NP_172240), Os MT-I-1a (*Oryza sativa* AAC49626), Os MT-I-1b (*Oryza sativa* BAG87041), Os MT-I-4a (*Oryza sativa* AK103445), Os MT-I-4b (*Oryza sativa* BE039194), Os MT-I-4c (*Oryza sativa* BE039221), Ca MT2 (*Cicer arietinum* CAA65009), Qs MT2 (*Quercus suber* CAC39481), At MT2A (*Arabidopsis thaliana* NP_187550), At MT2B (*Arabidopsis thaliana* NP_195858) MT-I-2a (*Oryza sativa* D15602), Os MT-I-2b (*Oryza sativa* BAA19661), Os MT-I-2c (*Oryza sativa* AAB18814), Ma MT3 (*Musa acuminata* AAB82615), At MT3 (*Arabidopsis thaliana* NP_566509), Os MT-I-3a (*Oryza sativa* AAB53811), Os MT-I-3b (*Oryza sativa* AAB65698), Ta Ec-1 (*Triticum aestivum* CAA48349), At MT4 1 (*Arabidopsis thaliana* NP_181731), At MT4 2 (*Arabidopsis thaliana* NP_179905), Os MT-II-1a (*Oryza sativa* BAG955542).

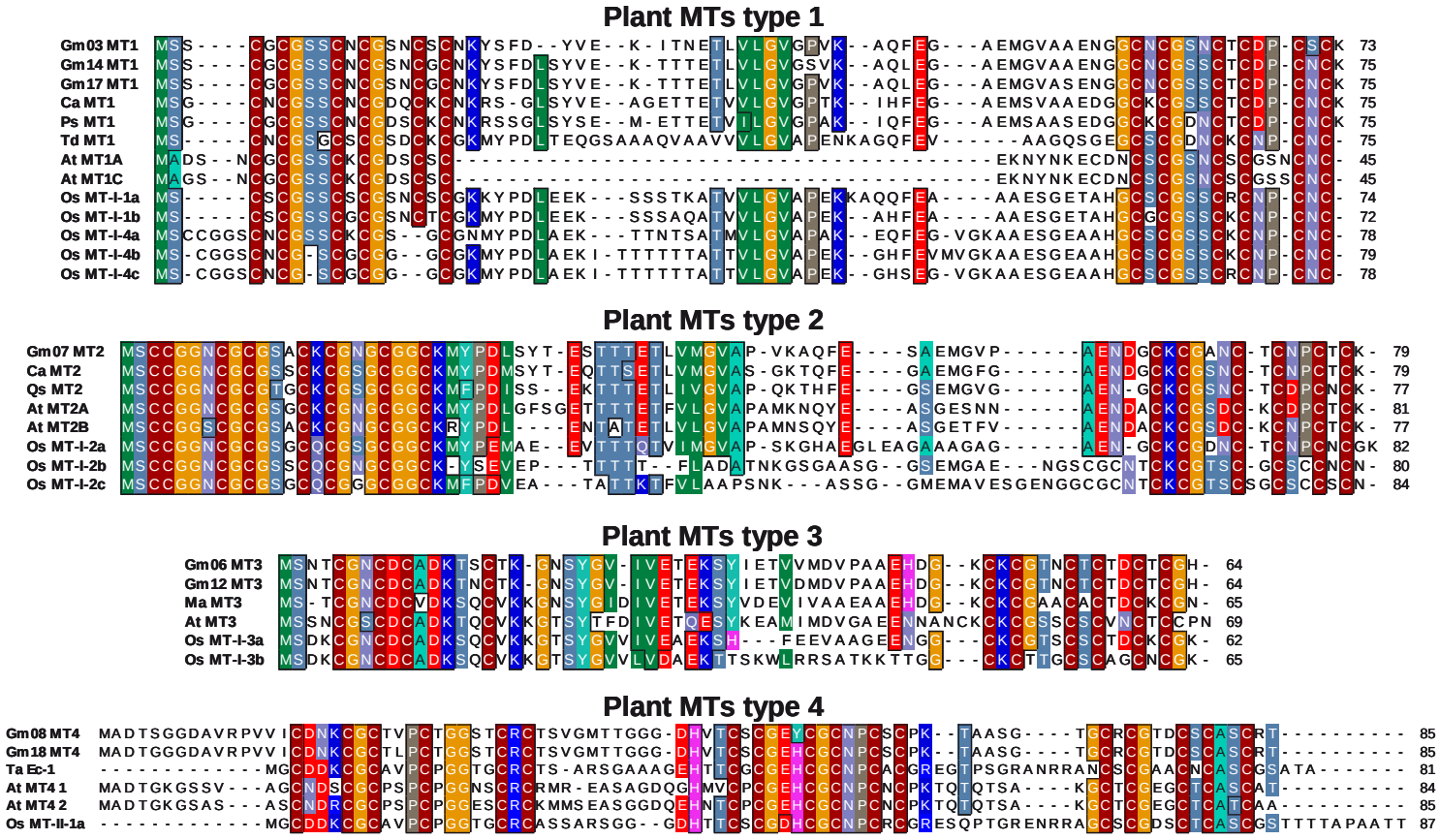

Table S1. Total amount of cadmium extracted by the plants and percentage of the soil total metal taken.

	Available Cd (µg)	Total Cd (µg)	Tissue	Dry weight[a] (g)	Cd extracted[a] (µg)	Percetage taken (from total Cd))
Control	61	349	roots	15.23	15.99	
			leaves	55.34	23.24	
			seeds	10.66	0.85	
			Total plant		**40.08**	**11.4%**
1 ppm	1378	8724	roots	16.75	36.01	
			leaves	60.28	77.76	
			seeds	11.79	6.96	
			Total plant		**120.73**	**1.4%**
1.8 ppm	2992	15703	roots	15.62	37.96	
			leaves	58.35	87.52	
			seeds	11.05	8.28	
			Total plant		**133.77**	**0.9%**

[a] Mean value of all three biological replicates

Table S2. Sequence identity matrix for plant metallothioneins type 1.

	Gm03 MT1	Gm14 MT1	Gm17 MT1	Ca MT1	Ps MT1	Td MT1	At MT1A	At MT1C	Os MT-I-1a	Os MT-I-1b	Os MT-I-4a	Os MT-I-4b	Os MT-I-4c
Gm03 MT1	ID	0.880	0.880	0.697	0.680	0.400	0.315	0.315	0.487	0.473	0.426	0.380	0.385
Gm14 MT1	0.880	ID	0.973	0.736	0.693	0.387	0.294	0.294	0.487	0.486	0.451	0.428	0.445
Gm17 MT1	0.880	0.973	ID	0.736	0.720	0.400	0.294	0.294	0.500	0.500	0.463	0.440	0.457
Ca MT1	0.697	0.736	0.736	ID	0.828	0.425	0.294	0.307	0.474	0.486	0.439	0.440	0.445
Ps MT1	0.680	0.693	0.720	0.828	ID	0.437	0.320	0.333	0.448	0.434	0.414	0.380	0.385
Td MT1	0.400	0.387	0.400	0.425	0.437	ID	0.246	0.246	0.610	0.571	0.505	0.517	0.488
At MT1A	0.315	0.294	0.294	0.294	0.320	0.246	ID	0.955	0.282	0.263	0.259	0.226	0.228
At MT1C	0.315	0.294	0.294	0.307	0.333	0.246	0.955	ID	0.282	0.263	0.259	0.226	0.228
Os MT-I-1a	0.487	0.487	0.500	0.474	0.448	0.610	0.282	0.282	ID	0.851	0.658	0.630	0.638
Os MT-I-1b	0.473	0.486	0.500	0.486	0.434	0.571	0.263	0.263	0.851	ID	0.662	0.670	0.654
Os MT-I-4a	0.426	0.451	0.463	0.439	0.414	0.505	0.259	0.259	0.658	0.662	ID	0.814	0.812
Os MT-I-4b	0.380	0.428	0.440	0.440	0.380	0.517	0.226	0.226	0.630	0.670	0.814	ID	0.949
Os MT-I-4c	0.385	0.445	0.457	0.445	0.385	0.488	0.228	0.228	0.638	0.654	0.812	0.949	ID

Gm: *Glycine max*
Ca: *Cicer arietinum*
Ps: *Pisum sativum*
Td: *Triticum durum*
At: *Arabidopsis thaliana*
Os: *Oryza sativa*

Table S3. Sequence identity matrix for plant metallothioneins type 2.

	Gm07 MT2	Ca MT2	Qs MT2	At MT2A	At MT2B	Os MT-I-2a	Os MT-I-2b	Os MT-I-2c
Gm07 MT2	ID	0.848	0.746	0.703	0.700	0.642	0.447	0.438
Ca MT2	0.848	ID	0.772	0.666	0.662	0.666	0.447	0.438
Qs MT2	0.746	0.772	ID	0.654	0.607	0.682	0.452	0.454
At MT2A	0.703	0.666	0.654	ID	0.802	0.558	0.441	0.444
At MT2B	0.700	0.662	0.607	0.802	ID	0.523	0.428	0.386
Os MT-I-2a	0.642	0.666	0.682	0.558	0.523	ID	0.471	0.417
Os MT-I-2b	0.447	0.447	0.452	0.441	0.428	0.471	ID	0.678
Os MT-I-2c	0.438	0.438	0.454	0.444	0.386	0.417	0.678	ID

Gm*: Glycine max*
Ca: *Cicer arietinum*
Qs: *Quercus suber*
At: *Arabidopsis thaliana*
Os: *Oryza sativa*

Table S4. Sequence identity matrix for plant metallothioneins type 3.

	Gm06 MT3	Gm12 MT3	Ma MT3	At MT3	Os MT-I-3a	Os MT-I-3b
Gm06 MT3	ID	0.968	0.681	0.550	0.575	0.469
Gm12 MT3	0.968	ID	0.681	0.550	0.575	0.469
Ma MT3	0.681	0.681	ID	0.521	0.621	0.500
At MT3	0.550	0.550	0.521	ID	0.521	0.405
Os MT-I-3a	0.575	0.575	0.621	0.521	ID	0.676
Os MT-I-3b	0.469	0.469	0.500	0.405	0.676	ID

Gm: *Glycine max*
Ma: *Musa acuminata*
At: *Arabidopsis thaliana*
Os: *Oryza sativa*

Table S5. Sequence identity matrix for plant metallothioneins type 4.

	Gm08 MT4	Gm18 MT4	Ta Ec-1	At MT4 1	At MT4 2	Os MT-II-1a
Gm08 MT4	ID	0.964	0.400	0.500	0.500	0.382
Gm18 MT4	0.964	ID	0.400	0.522	0.522	0.382
Ta Ec-1	0.400	0.400	ID	0.402	0.391	0.707
At MT4 1	0.500	0.522	0.402	ID	0.835	0.373
At MT4 2	0.500	0.522	0.391	0.835	ID	0.373
Os MT-II-1a	0.382	0.382	0.707	0.373	0.373	ID

Gm: *Glycine max*
Ta: *Triticum aestivum*
At: *Arabidopsis thaliana*
Os: *Oryza sativa*

Capítol 3

Zn(II)- and Cd(II)-binding abilities of plant MT1 and MT2 isoforms with extra Cys residues

CAPÍTOL 3

Zn(II)- and Cd(II)-binding abilities of plant MT1 and MT2 isoforms with extra Cys residues

1. Introduction

Since the first metallothionein (MT) was discovered in horse kidneys in 1957 [1], a lot of work has been done to study this superfamily of Cys-rich low molecular weight metalloproteins that bind heavy metal ions. This peculiar superfamily of proteins lacks secondary and tertiary structure elements in their metal-free forms (apo-MT), from which it becomes evident that metal binding dictates their final steric features. They are involved in metal homeostasis and detoxification, as well as in protection against oxidative stress [2]. These cytosolic metallopeptides exist in most of the living organisms, but with highly diverse amino acid sequences, so that a classification depending on taxonomic criteria is currently used [3]. Family 1 (vertebrate) MTs, and among them mammalian MTs, were the first isolated MTs and have been the most studied ones so far, with their $M(II)_3$-$(SCys)_9$ and $M(II)_4$-$(SCys)_{11}$ clusters being used as a model for metal ion coordination in metal-MT complexes. Contrastingly, the first plant MT (family 15) was not discovered in wheat (*Triticum aestivum*) embryos until a quarter-century later, in 1983 [4]. Although the number of MT sequences identified in plants is increasing day by day, the huge variability in their amino acid sequences, and also if compared to vertebrate MTs, make the available data not sufficient for successfully analysing the relationships between their metal-binding properties and their potential biological functions. This high sequence heterogeneity is the reason why family 15 MTs have been divided into four subfamilies, depending on the number and distribution of their Cys residues [5]. Ec-1, the aforementioned wheat MT, belongs to subfamily MT4, and until nowadays it is both the only plant MT natively isolated and the unique plant MT for which a 3D structure, that of the Zn(II)-Ec-1 complex, has been solved [6]. Concerning MT1, MT2 and MT3 subfamilies, their sequences dramatically diverge from those of subfamily MT4. They present two Cys-rich regions separated by a Cys-free region (the *linker* or *spacer*), whereas MT4 subfamily shows two intercalating Cys-free regions between three Cys-rich regions. Regarding subfamily 1, even if more than 30 MT-like nucleotide sequences have been identified, and their expression patterns

have been analysed, information at the protein level is scarce [*cf*. recent review in 7]. Although MT1 canonical sequence contain six Cys residues both in its N-terminal and C-terminal Cys-rich regions, several variants with one or two extra Cys in the N-term domain are known (Table S1). The divalent metal-binding capacities of five MTs belonging to this subfamily have been determined. Hence, pea (*Pisum sativum*) PsMTA was found to coordinate 5.8 Cd(II) ions when heterogously synthesised in metal-enriched *E. coli* cultures in the form of a GST-fusion protein [8]; 4 Cd(II) ions were found to be bound in wheat (*Triticum durum*) GST-dMT [9]; GST-OsMTI-1b from rice (*Oryza sativa*) coordinated 4.8 Cd(II) and 1.8 Zn(II) ions when reconstituted from its apo-form [10]; chickpea (*Cicer arietinum*) cicMT1 showed to bind up to 5 Zn(II) or Cd(II) ions [11]; and GmMT1 from soybean (*Glycine max*) contained an average 3.8 Zn(II) ions and 8.1 Cd(II) ions per molecule when heterologously synthesised [12]. In contrast to MT1, a considerable amount of data have been reported for the MT2 subfamily. The number of nucleotide sequences belonging to this subfamily in data banks doubles that of MT1s. The archetypal MT2 proteins feature eight Cys residues at their N-term Cys-rich region and six at their C-term domain, but again variations on the number of Cys residues exist (Table S2). Since the N-term Cys residues are highly conserved, this subfamily is further divided into several subtypes according to the arrangement of the Cys residues in the C-terminal domain [13,14]. Reported divalent metal-binding properties of MT2 recombinant plant MTs showed the ability to bind 3.6 Zn(II) ions in the case of watermelon (*Citrullus lanatus*) ClMT2 [15], 3.5 Zn(II) and 5.3-6.5 Cd(II) ions for cork oak (*Quercus suber*) QsMT [16,17], 5 Zn(II) and 5 Cd(II) ions for chickpea (*C. arietinum*) cicMT2 [18], and 4.3 Zn(II) as well as 6.7 Cd(II) ions for soybean (*G. max*) GmMT2 [12].

In this work, we have analysed the divalent metal-binding abilities of one MT1 (HaMT1) and one MT2 (HaMT2) from sunflower (*Helianthus annuus*), whose sequences are here firstly reported. Besides representing the MT1 and MT2 most highly expressed in sunflower, both peptides show the peculiarity of constituting variants of plant MT1 and MT2 canonical sequences, because of their extra Cys residues, which enhances the interest in the study of their metal-binding properties. The characterisation of their Zn(II) and Cd(II) complexes, obtained both by recombinant synthesis in metal-enriched cultures (*in vivo* complexes) and also by Zn/Cd exchange (*in vitro* complexes) has been performed through spectroscopic and spectrometric techniques. The

consequences potentially provoked by the variations in the number of Cys residues from the canonical MT1 and MT2 sequences are also discussed in this work.

2. Experimental Section

2.1. Source of MT cDNA clones and expression vectors construction

To obtain sunflower MT coding sequences, the NCBI EST library database was screened using *blastn* in the Basic Local Alignment Search Tool (BLAST) and the *Arabidopsis thaliana* metallothionein cDNA sequences NM_100633.2 (MT1a) and NM_111773.3 (MT2a) as queries. From all the retrieved *Helianthus annuus* ESTs, clones DY927795 (HaMT1-1), DY927283 (HaMT1-2), DY931085 (HaMT2-1), DY931060 (HaMT2-2) and BQ910832 (HaMT2-3) were purchased from the University of Arizona (The Compositae Genome Project).

The HaMT1-2 and HaMT2-1 cDNAs were subcloned into the pGEX-4T1 vector (GE Healthcare) in order to obtain the pGEX-HaMT1-2 and pGEX-HaMT2-1 expression plasmids, respectively. Flanking *BamH*I/*Xho*I restriction sites were added by PCR amplification using the following oligonucleotides: 5'-CCGGGATCCATGTCTTGCTCAAGTGGAAAGTG-3' as upstream primer and 5'-ATTCTCGAGTCAGCAGTTGCAAGGATCGCACT-3' as downstream primer for *HaMT1-2*; 5'-CACGGATCCATGTCTTGCTGCAGC-3' as upstream primer and 5'-TCTCTCGAGTTAGCAGCTGCAGTTG-3' as downstream primer for *HaMT2-1*. All the PCR reactions consisted of 35-cycle amplifications performed with 1.25 U of GoTaq DNA polymerase (Promega), 0.25 mM dNTPs and 0.20 μM of the required primers at 2 mM $MgCl_2$ (final concentration), in a final volume of 100 μL, under the following cycle conditions: 30 s at 94 ºC (denaturation), 30 s at 55 ºC (hybridisation) and 30 s at 72 ºC (elongation). An initial denaturation step where samples were heated at 94 °C for 5 min ensured the complete target DNA denaturation, and elongation conditions were maintained for 7 min after the 35 cycles. The final products were analysed by agarose gel electrophoresis/GelRed Nucleic Acid Gel Stain (Biotium) staining, and the band with the expected size was excised and subcloned into the pGEX-4T1 vector. All the constructs were confirmed by automated DNA sequencing. To this end, the pGEX-derived constructs were transformed into *E. coli* MATCH I cells, and sequenced using the ABI PRISM

BigDye Terminator v3.1 Cycle Sequencing Kit (Applied Biosystems) in an ABI PRISM 310 Automatic Sequencer (Applied Biosystems).

2.2. Recombinant synthesis and purification of MTs

Firstly, HaMT-GST fusion polypeptides were biosynthesised in 3 mL-cultures of transformed *E. coli* cells (BL21 strain). Expression was induced with isopropyl ß-D-thiogalactopyranoside (IPTG) and were allowed to grow for a further 3 h. Cells were harvested by centrifugation, resuspended in 150 µL PBS buffer and lysed by sonification. The total protein extract was analysed by 15% sodium dodecyl sulfate polyacrilamide gel electrophoresis (SDS-PAGE). Secondly, HaMT-GST fusion polypeptides were biosynthesised in 5 L-cultures of transformed *E. coli* cells (BL21 strain). Expression was induced with IPTG and cultures were supplemented with final concentrations of 300 µM $ZnCl_2$ or 300 µM $CdCl_2$, and were allowed to grow for a further 3 h. Total protein extract was prepared from these cells as previously described [19]. Metal complexes were recovered from the fusion constructs by thrombin cleavage and batch-affinity chromatography using Glutathione-Sepharose 4B (GE Healthcare). After concentration using Centriprep Microcon 3 (Amicon), the metal complexes were finally purified through FPLC in a Superdex 75 column (GE Healthcare) equilibrated with 50 mM Tris-HCl, pH 7.0. Selected fractions were confirmed by ESI-MS (see conditions in next section) and kept at -80 ºC until further use. All procedures were performed using Ar (pure grade 5.6) saturated buffers. Further details on the purification procedure specific for recombinant plant MTs can be found in previous works [17,20]. As a consequence of the cloning procedure, the dipeptide Gly-Ser is added to the N-terminus of the corresponding MT polypeptides. This minor modification of the native form was previously shown not to alter any of the MT metal-binding properties [21].

2.3. Spectroscopic and spectrometric characterisation of the M(II)-HaMT complexes

The S, Zn and Cd content of all the M(II)-MT preparations was analysed by means of inductively coupled plasma atomic emission spectroscopy (ICP-AES) in a Polyscan 61E (Thermo Jarrell Ash) spectrometer, measuring S at 182.040 nm, Zn at 213.856 nm and Cd at 228.802 nm. Samples were treated as previously reported [22], but were alternatively incubated in 1 M HNO_3 at 65 °C for 10 min prior to measurements in

order to eliminate possible traces of acid-labile sulfide ions, as described in [23]. Protein concentrations were calculated from the acidic ICP-AES sulfur measurements, assuming that all S atoms were contributed by the MT peptide.

Molecular mass determinations were performed by electrospray ionisation time-of-flight mass spectrometry (ESI-MS) on a Micro TOF-Q instrument (Bruker) interfaced with a Series 1100 HPLC Agilent pump, equipped with an autosampler, all of them controlled by the Compass Software. Calibration was attained with ESI-L Low Concentration Tuning Mix (Agilent Technologies). Samples containing MT complexes were analysed under the following conditions: 20 μL of protein solution injected through a PEEK (polyether heteroketone) tubing (1.5 m x 0.18 mm i.d.), at 40 $\mu L \cdot min^{-1}$; capillary counter-electrode voltage 5 kV; desolvation temperature 90-110 ºC; dry gas 6 $L \cdot min^{-1}$; spectra collection range 800-2000 m/z. The carrier buffer was a 5:95 mixture of acetonitrile:ammonium acetate/ammonia (15 mM, pH 7.0). For analysis of the sequences of all recombinant MTs, 20 μL of the corresponding Zn-MT samples were injected under the same conditions described before but using a 5:95 mixture of acetonitrile:formic acid pH 2.4 as liquid carrier, which caused the complete demetallation of the peptides.

A Jasco spectropolarimeter (Model J-715) interfaced to a computer (J700 software) was used for CD recording at a constant temperature of 25 ºC maintained by a Peltier PTC-351S apparatus. Electronic absorption measurements were performed on an HP-8453 Diode array UV-visible spectrophotometer. All spectra were recorded with 1 cm capped quartz cuvettes, corrected for the dilution effects and processed using the GRAMS 32 Software.

2.4. Cd(II) titration of Zn(II)-MTs and acidification-reneutralisation of Cd(II)-MTs

For the Zn(II) with Cd(II) replacement studies, 15-20 μM preparations of the Zn(II)-MT complexes were titrated with incremental amounts of $CdCl_2$ (1-9 equiv) at pH 7. CD and UV spectra were recorded immediately after the metal addition and 10 min later, until stable spectra were obtained. For the acidification-reneutralisation studies, 10-20 μM preparations of the Cd(II)-MT complexes were acidified from pH 7 to pH 2 with incremental volumes of diluted HCl solutions, and after that were reneutralised with diluted NaOH. CD, UV and ESI-MS spectra were recorded at selected steps. Oxygen-free conditions were maintained by saturation of all solutions with Ar during all experiments.

3. Results

3.1. In silico *search and sequence analysis of HaMT1 and HaMT2*

The *in silico* genomic screening of the sunflower NCBI EST database retrieved seven sequences, assignable to the four plant MT subfamilies. Two ESTs, named *HaMT1-1* and *HaMT1-2*, coded for MT1 peptides; and three, named *HaMT2-1*, *HaMT2-2* and *HaMT2-3*, for MT2 ones. One EST was identified for the MT3 subfamily and also a single EST was retrieved for the MT4. These cDNAs were named *HaMT3* and *HaMT4*, respectively. The corresponding HaMT3 and HaMT4 peptides have been recently analysed [24].

The HaMT1-1 and HaMT1-2 proteins were classified as plant MT1s despite the respective presence of seven and eight Cys residues at their N-terminal Cys-rich domain, instead of the typical six Cys residues of the MT1 subfamily (Fig. 1A), because they show the conserved CXCGS, CXCG and CXC motifs in their N-terminal region [25] and the CXCG tetrapeptide followed by the CXC and PCXC motifs at their C-terminal domain. Variants with an additional Cys residue located before the first conserved CXCG motif, as it is the case in HaMT1-2 (position 3), are known for several plant MT1s (Table S1). Contrarily, the extra Cys at the end of the N-terminal domain is exclusive of these sunflower MTs, HaMT1-1 and HaMT1-2. Precisely, the presence of two additional Cys residues in MT1s can only be seen for HaMT1-2 and *Huperzia serrata* MT1 (GenBank GO912370; Table S1), but in this case they are distributed one in each Cys-rich domain.

The three amino acid sequences classified as plant MT2s, HaMT2-1, HaMT2-2 and HaMT2-3, (Fig. 1B) feature the CC motif characteristic of this subfamily at position 3-4 and 5-6. Although MT2s typically exhibit six Cys at their C-terminal domains [5], HaMT2-1 features a seventh Cys at this region. The three MT2s analysed here present the highly conserved SCCXGXCGC and CXGC motifs at the end of the N-terminal domainas well as the GVAP tetrapeptide within the spacer region [13]. It is worth pointing out that *Fragaria ananassa* MT2 also shows an additional Cys located in the same region than that of HaMT2-1, and *Ginkgo biloba* MT2 also shows one extra Cys in the C-terminal domain but in this case in a more distant position in relation to the conserved Cys pattern (Table S2). Additionally, other subfamily MT2 variants showing two or three additional Cys in this region also exist (Table S2).

A

```
                    10        20        30        40        50        60        70        80        90
                    ....|....|....|....|....|....|....|....|....|....|....|....|....|....|....|....|...
MT1 Consensus       ----------CXCGS-CXCG---CX--C-------------------------------------------------CXCG--CXC--PCXC-
HaMT1-1             --MS-------CKCGSNCSCGSS-CN--CNSCDV-EKS-------TTTTI----IVDGVAPKMTFAEGS--ETSTVAESGNGCSCGSSCKC-NPCNC-
HaMT1-2             --MSCSSG--KCNCGSSCSCGSS-CN--CNSCNV-EMST------TTTTI----IVDGVAPRMTFAEET--E---VAESGNACKCGSSCKC-DPCNC-
GmMT1               --MSS------CGCGSSCNCGSN-CG--CNKYSF-DLSYV--EK-TTTET----LVLGVGPVKAQLEGA--EMGVASENG-GCNCGSSCTC-DPCNCK
cicMT1              --MSG------CNCGSSCNCGDQ-CK--CNKRS--GLSYV--EAGETTET----VVLGVGPTKIHFEGA--EMSVAAEDG-GCKCGSSCTC-DPCNCK
OsMTI-1b            --MS-------CSCGSSCGCGSN-CT--CGKMYPDLEEK------SSSAQ--ATVVLGVAPEK--AH--FEAAAESGETAHGCGCGSSCKC-NPCNC-
dMT                 --MS-CN------CGSGCSCGSD-CK--CGKMYPDLTEQG-----SAAAQVAAVVVLGVAPENKAGQ--FEVAA--GQSGEGCSCGDNCKC-NPCNC-
PsMTA               --MS--G----CGCGSSCNCGDS-CK--CNKRSS-GLSYS---EMETTET----VILGVGPAKIQFEGA--EMSAASEDG-GCKCGDNCTC-DPCNCK
```

B

```
                    10        20        30        40        50        60        70        80        90       100
                    ....|....|....|....|....|....|....|....|....|....|....|....|....|....|....|....|....|.
MT2 Consensus       -S--CCXGXCGC---CXCG-GCGGC-----------------------GVAP---------------------------CX-C-----------CXC---CXC-
HaMT2-1             MS--CCNGKCGCGSSCSCGSGCNGC---GMYPDVEV--SS--TTVMIVDGVAPKQMFAE----GSEGSFVAE----GGNCNCK-CG---DN-----CKCGNNCSC-
HaMT2-2             MS--CCNGKCGCGSSCSCGSSCKGC---GMYPDIET--ST--TATMIVDGVAPKKMYDD----GSDASFVSE----GGHA-CK-CG---AN-----CKC-DPCNC-
HaMT2-3             MSSSCCGGNCGCGSGCKCGNGCGGC---KMYPEMVSGEST--NNETLILGVAPTETGIET----TGG-VATA----AENEGCK-CN---P------CTC-NPCTCK
GmMT2               MS--CCGGNCGCGSACKCGNGCGGC---KMYPDLSYTEST--TTETLVMGVAPVKAQFE-----SAEMGVP-----AENDGCK-CG---AN-----CTC-NPCTCK
QsMT                MS--CCGGNCGCGTGCKCGSGCGGC---KMFPDIS-SEKT--TTETLIVGVAPQKTHFE-----GSEMGVG-----AEN-GCK-CG---SN-----CTC-DPCNCK
cicMT2              MS--CCGGNCGCGSSCKCGSGCGGC---KMYPDMSYTEQT--TSETLVMGVASGKTQFE-----GAEMGFG-----AENDGCK-CG---SN-----CTC-NPCTCK
ClMT2               MS--CCGGNCGCGSGCKCGSGCGGC---KMFPDMSFSEATA-TIETFVVGFAPHKMSFE-----VAEMG-------AEN-GCK-CG---DN-----CTC-DPCNCK
```

Figure 1. Amino acid sequences of the translated (**A**) MT1 and (**B**) MT2 isoforms identified in sunflower. For comparative purposes, the sequences of *Glycine max* GmMT1 (BQ742738), *Cicer arietinum* cicMT1 (Q39458), *Oryza sativa* OsMTI-1b (BAG87041), *Triticum durum* dMT (AAT99566), *Pisum sativum* PsMTA (P20830), *G. max* GmMT2 (BQ629803), *Quercus suber* QsMT (Q93X22), *C. arietinum* cicMT2 (Q39459) and *Citrullus lanatus* ClMT2 (Q6I674) for which their divalent metal-ion binding abilities have been reported are included. The shaded boxes indicate the cysteine residues and histidines are in bold. The conserved motifs important for the classification of the peptides into the MT1 (MT1 Consensus) or MT2 (MT2 Consensus) plant MT subfamilies are also shown, where X represents any other amino acid. The MTs analysed in this work (HaMT1-2 and HaMT2-1) are in bold.

Overall, HaMT1-1, HaMT1-2 and HaMT2-1 sunflower MTs feature variations in the number of Cys residues when compared to the canonical plant MT1 and MT2 subfamilies, which may affect their metal-binding properties. None of the MT1s and MT2s for which the metal-binding abilities are known up to date show such extra Cys. Conversely, the presence of His as a potential coordinating residue influencing the metal content of the Cd-complexes was demonstrated for QsMT (*Quercus suber* MT2) [17].

3.2. Preparation of the recombinant polypeptides: cloning, synthesis and purity

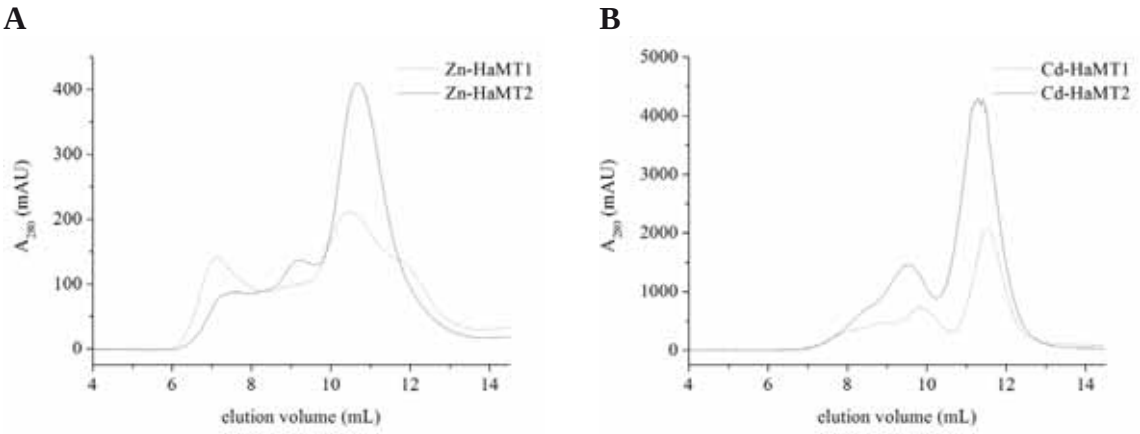

Figure 2. Elution profile from the Superdex75 size exclusion FPLC column (equilibrated with 50 mM Tris-HCl, pH 7.0) of the HaMT preparations after thrombin cleavage of the purified GST-HaMT fusion peptides recombinantly synthesised in (**A**) Zn(II)- and (**B**) Cd(II)-enriched *E. coli* cultures.

Among all the retrieved isoforms, *HaMT1-2* and *HaMT2-1* showed a higher copy number of ESTs in the databank, thus indicating a higher expression level. Consequently, these two most transcribed isoforms were selected to study the metal-binding abilities of their encoded peptides. DNA sequencing confirmed that the recombinant plasmids pGEX-HaMT1 and pGEX-HaMT2 included the expected cDNA sequences, which were cloned in the correct frame after the GST coding portion. It is worth mentioning here that, as a consequence of the GST-fusion construct, the HaMT1 and HaMT2 peptides heterologously synthesised in this work presented the addition of the initial GS dipeptide. Synthesis of the GST-fused polypeptides was first corroborated in small-scale (3 mL) cultures of transformed *E. coli* BL21 cells after induction with IPTG. Subsequently, the Zn(II)- and Cd(II)-HaMT1 and HaMT2 complexes were obtained from large-scale, metal-enriched cultures (5 L) of the recombinant bacteria. In the final purification step, Zn-HaMT1 eluted from the FPLC column in two overlapping peaks, and thus two fraction pools were separated, one comprising from 10.0 mL to 11.0 mL (peak 1) and the other from 11.0 mL to 13.5 mL (peak 2) of the eluted volume (Fig.

2A). The content of both peaks was analysed by ESI-MS at pH 2.4 to determine the molecular mass of the apo-peptides present in the sample. Peak 1 showed the only content of a protein with the molecular mass calculated for HaMT1 (7531.4 Da, Fig. 3A), while in peak 2 this protein was mixed with two additional peptides of 3017.0 ± 0.9 Da and 4529.2 ± 0.6 Da molecular mass (Fig. 3B). Contrarily, Cd-HaMT1 eluted from the FPLC column rendering a unique peak between 10.5 mL and 13.0 mL of the elution

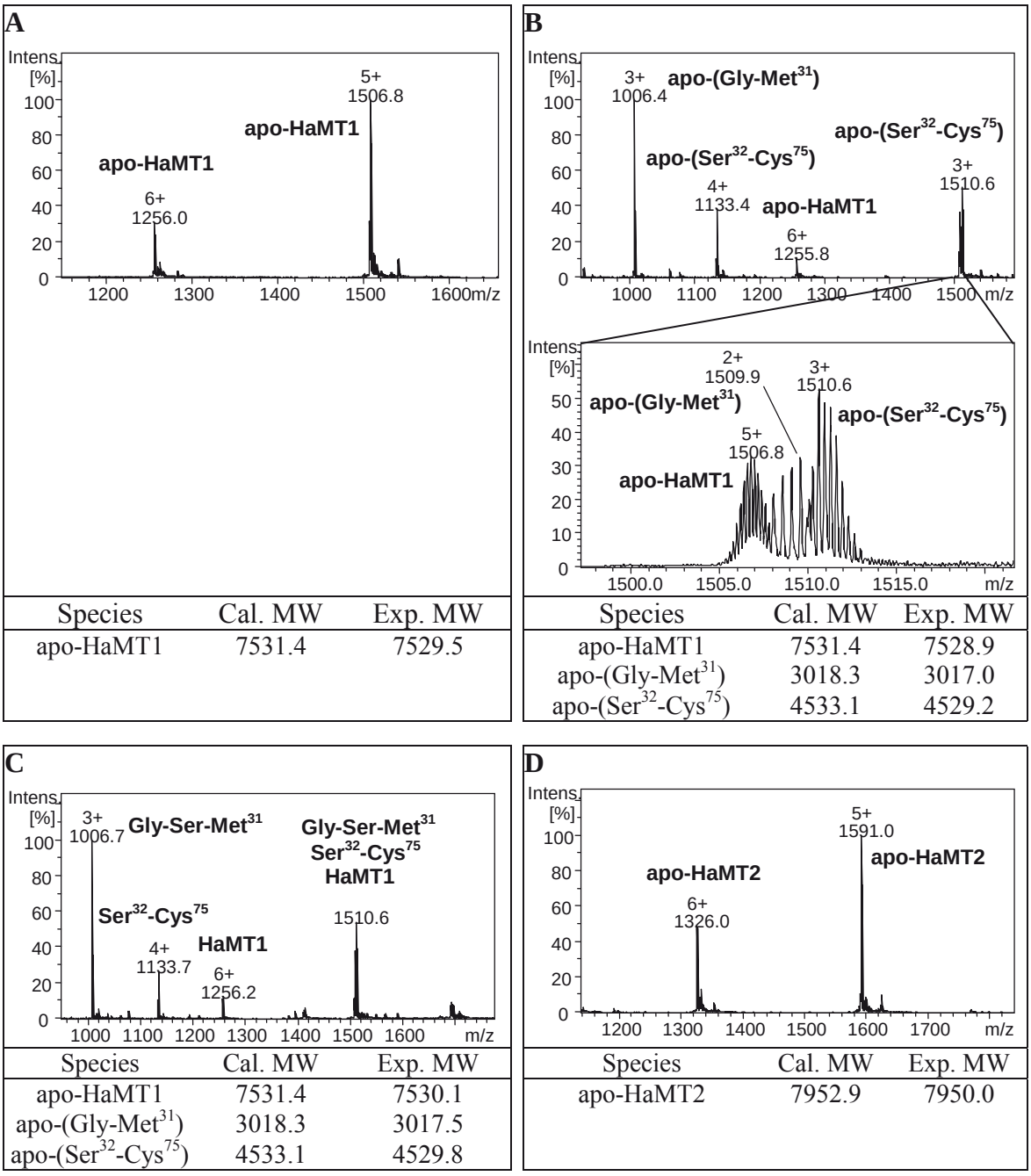

Species	Cal. MW	Exp. MW
apo-HaMT1	7531.4	7529.5

Species	Cal. MW	Exp. MW
apo-HaMT1	7531.4	7528.9
apo-(Gly-Met^{31})	3018.3	3017.0
apo-(Ser^{32}-Cys^{75})	4533.1	4529.2

Species	Cal. MW	Exp. MW
apo-HaMT1	7531.4	7530.1
apo-(Gly-Met^{31})	3018.3	3017.5
apo-(Ser^{32}-Cys^{75})	4533.1	4529.8

Species	Cal. MW	Exp. MW
apo-HaMT2	7952.9	7950.0

Figure 3. ESI-MS spectra recorded at pH 2.4 of (**A**) Zn-HaMT1 peak 1, (**B**) Zn-HaMT1 peak 2, (**C**) Cd-HaMT1 and (**D**) Zn-HaMT2 and Cd-HaMT2. A zoomed view from the 1497 to 1522 m/z spectrum region is shown in (**B**). The error associated with the experimental MW values was always lower than 0.1 %.

volume (Fig. 2B). However, the acid ESI-MS analysis of this peak also revealed the presence of apo-HaMT1 mixed with the two additional peptides detected in the Zn-HaMT1 peak 2 sample (Fig. 3C). These two peptides could be unambiguously assigned to the products of the proteolytic HaMT1 cleavage between the Met31 and Ser32 residues, which would give rise to fragments of 3018.3 Da and 4533.1 Da, respectively. It is worth noting that cleavage at the linker region has also been reported for other recombinantly synthesised plant MT1s, namely the Cd-MT complexes of *P. sativum* [8] and *T. durum* [26]. Conversely, the Zn(II)- and Cd(II)-HaMT2 preparations eluted in one main peak (Fig. 2A and 2B, respectively). Fractions corresponding to the elution volumes from 9.5 mL to 13.0 mL for Zn-HaMT2, and from 10.5 mL to 12.5 mL for Cd-HaMT2 were recovered, from which a single apo-HaMT2 species was invariably detected, exhibiting the expected molecular mass (7952.9 Da, Fig. 3D).

3.3. Characterisation of the M(II)- HaMT1 and HaMT2 recombinant complexes

The main characterisation of the Zn(II)-HaMT1 complexes was performed using the peak 1 preparation, which was devoid of cleaved peptides. A mean value of 4.3 Zn(II) ions per MT was revealed by acid ICP-AES (Table 1), which correlated well with the detection of a major Zn_4-HaMT1 species by ESI-MS, accompanied by an important presence of Zn_3- and Zn_5-HaMT1 species (Table 1, Fig. 4A). Interestingly, the ESI-MS spectra of the HaMT1 (peak 2) preparation revealed that the two proteolytic fragments yielded Zn_1-(Gly-Met^{31}), Zn_2-(Ser^{32}-Cys^{75}) and minor Zn_3-(Ser^{32}-Cys^{75}) species (Fig. S1). Therefore, since the summation of the metal ion content of both moieties does never achieve the Zn_5-HaMT1 stoichiometry, only the assumption of a single cluster involving both the N- and C-terminal Cys-rich domains could account for this complex. However, the Zn_3-HaMT1 and Zn_4-HaMT1 species are compatible with independent Cys-rich Zn-binding domains, although the latter to a lesser extent due to the minor presence of the Zn_3-(Ser^{32}-Cys^{75}) complex. When considering Zn-HaMT2, a 4.4 Zn/MT ratio was determined, which correlated well with the mixture of Zn_4- and Zn_5-HaMT2 species, together with the minor Zn_3-HaMT2 complex detected by ESI-MS (Table 1, Fig. 4B).

Table 1 Analytical characterisation of the recombinant HaMT1 and HaMT2 preparations synthesised in Zn(II)- and Cd(II)-enriched media.

Protein	Zn-MT complexes			Cd-MT complexes		
	Protein concentration[a] (x 10^{-4} M)	Zn/MT content[b]	Zn-MT species[c]	Protein concentration[a] (x 10^{-4} M)	Cd/MT content[b]	Cd-MT species[c]
HaMT1	1.3/1.3	4.6/4.3	**Zn_4** Zn_3, Zn_5	1.1/0.8	5.0/6.1	Cd_6S_8 Cd_7S_7
HaMT2	1.0/0.8	4.5/4.4	**Zn_4** Zn_3, Zn_5	0.4/0.4	6.8/6.3	**Cd_6S_8** Cd_6

[a] Protein concentration calculated from the sulfur content measured by normal/acid ICP-AES, respectively. [b] Metal per MT molar ratio calculated from the total metal and sulfur content measured by normal and acid ICP-AES, respectively. Both Zn and Cd levels were quantified in all samples, but only the metals present at detectable levels are indicated. In the case of Zn-HaMT1, only the values recorded from fraction 1 are indicated. [c] Metal/MT molar ratio calculated from the difference between holo- and apo-protein molecular masses obtained from ESI-MS. Species shown in bold correspond to the major species in the preparations.

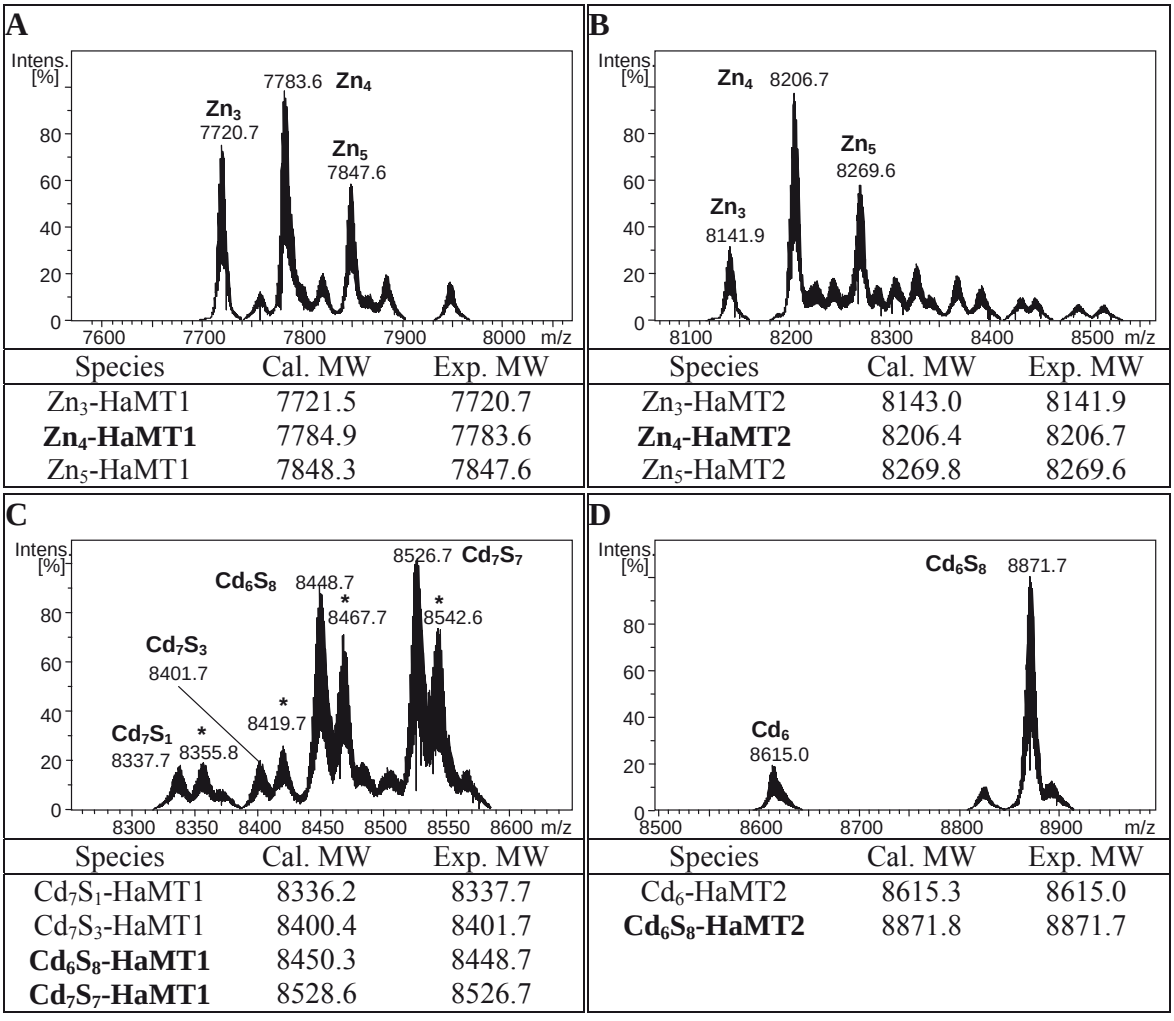

Species	Cal. MW	Exp. MW
Zn_3-HaMT1	7721.5	7720.7
Zn_4-HaMT1	7784.9	7783.6
Zn_5-HaMT1	7848.3	7847.6

Species	Cal. MW	Exp. MW
Zn_3-HaMT2	8143.0	8141.9
Zn_4-HaMT2	8206.4	8206.7
Zn_5-HaMT2	8269.8	8269.6

Species	Cal. MW	Exp. MW
Cd_7S_1-HaMT1	8336.2	8337.7
Cd_7S_3-HaMT1	8400.4	8401.7
Cd_6S_8-HaMT1	8450.3	8448.7
Cd_7S_7-HaMT1	8528.6	8526.7

Species	Cal. MW	Exp. MW
Cd_6-HaMT2	8615.3	8615.0
Cd_6S_8-HaMT2	8871.8	8871.7

Figure 4. Deconvoluted ESI-MS spectra recorded at pH 7.0 for (**A**) Zn-HaMT1 fraction 1, (**B**) Zn-HaMT2, (**C**) Cd-HaMT1 and (**D**) Cd-HaMT2. Species shown in bold correspond to the major species present in the preparations. The asterisk (*) indicates ammonia adducts (+18 Da) of the corresponding metallospecies. The error associated with the experimental MW values was always lower than 0.1 %.

The CD spectra of both Zn-MT preparations showed a low chirality profile (Fig. 5A), lacking the typical exciton coupling band centred at 245 nm of conventional Zn-MTs [21].

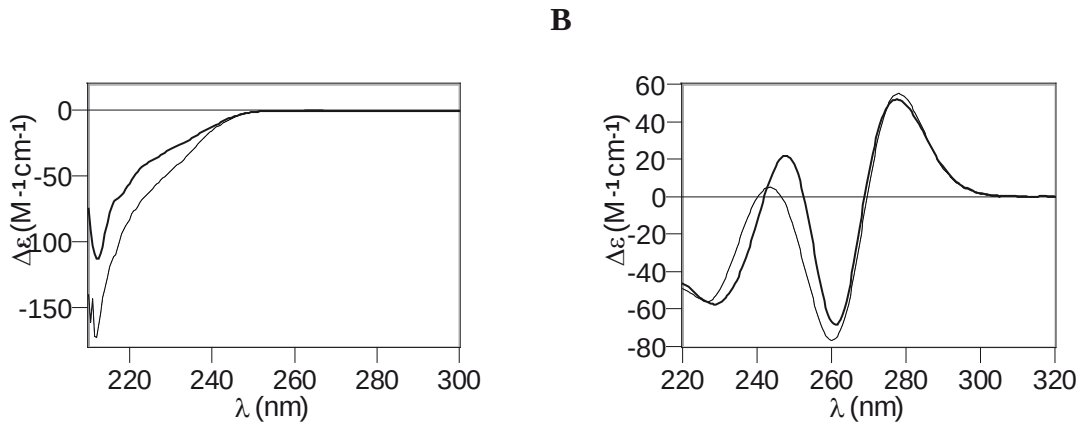

Figure 5. CD spectra corresponding to the recombinant (**A**) Zn(II)- HaMT1 (dotted line) and HaMT2 (solid line) complexes, and (**B**) Cd(II)- HaMT1 (dotted line) and HaMT2 (solid line) complexes.

Synthesis of HaMT1 in Cd(II)-enriched cultures yielded an average 6.1 Cd/HaMT1 ratio, as determined by acid ICP-AES (Table 1), while the differences observed between the conventional and acid ICP-AES measurements suggested the presence of acid-labile sulfide ligands [23]. Indeed, ESI-MS analyses revealed the presence of major Cd_6S_8- and Cd_7S_7-HaMT1 species as well as minor Cd_7S_1- and Cd_7S_3-HaMT1 complexes (Table 1, Fig. 4C). For Cd-HaMT2, the ICP-AES analyses of the recombinantly synthesised Cd(II)-HaMT2 revealed a mean 6.3 Cd/MT content (Table 1), which is in agreement with the major Cd_6S_8-HaMT2 and minor Cd_6-HaMT2 species detected by ESI-MS (Table 1, Fig. 4D). Although the differences between conventional and acid ICP-AES data did not support the existence of sulfide ligands in this case, the intense absorptions at the 270-290 nm range confirmed their presence [23]. Moreover, the CD spectra of both Cd-HaMT1 and Cd-HaMT2 preparations exhibited a 245-250 nm Gaussian band and an exciton coupling band centred at *ca.* 270 nm (Fig. 5B), therefore sharing similar CD fingerprints pointing to comparable protein foldings.

3.4. Zn(II) with Cd(II) replacement studies and acidification-reneutralisation experiments of the Cd(II)-HaMT1 and Cd(II)-HaMT2 biosynthesised complexes

Further information about the Cd(II)-binding properties of HaMT1 and HaMT2 was obtained from the analysis of the Zn/Cd replacement on Zn(II)-loaded MTs,

as well as from the acidification plus subsequent reneutralisation of the recombinant Cd(II)-MT complexes.

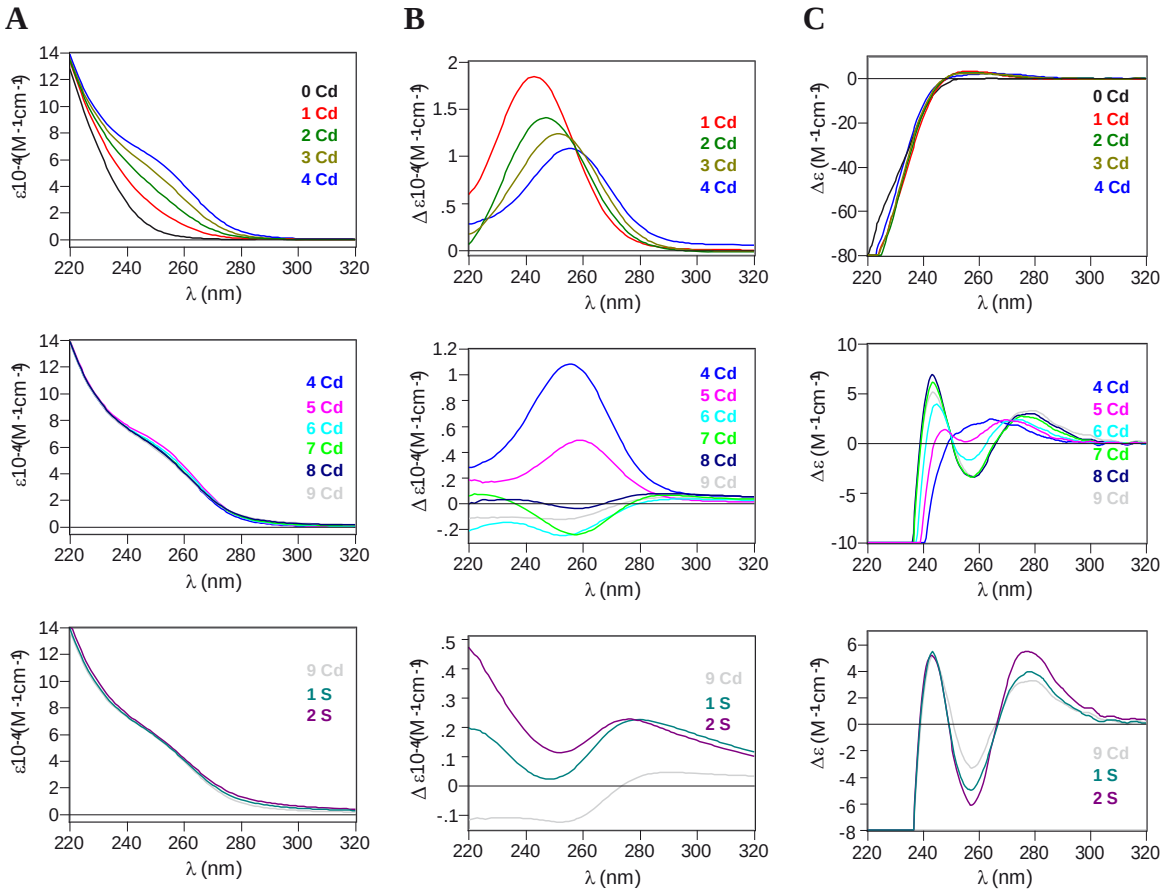

Figure 6. UV (**A**), UV difference (**B**) and CD (**C**) spectra corresponding to the titration of a 15 µM solution of Zn-HaMT1 fraction 1 with Cd(II) at pH 7. The number of Cd(II) equiv in (**B**) indicate the number of the addition which is the responsible for the changes in each absorption spectrum.

The UV data recorded during the titration of Zn-HaMT1 with Cd(II) showed a gradual metal ion replacement up to the 5th Cd(II) equiv added, since the absorptions at *ca.* 250 nm typical of Cd-(SCys) chromophores developped during this stage (Fig. 6A-B). Precisely, it was not until the addition of the 5th Cd(II) equiv that the CD fingerprint started to develop the two bands present in the biosynthesised Cd-HaMT1 preparation (Fig. 7A). Thereafter, the CD spectra evolve through an isodichroic point at *ca.* 250 nm to finally reach the best defined spectrum after 7 Cd(II) equiv added, characterised by an exciton coupling centred at *ca.* 270 nm and a positive Gaussian band at 245 nm (Fig. 6C), therefore suggesting a similar fold to that of recombinant Cd-HaMT1, although with a significant lower chirality (Fig. 7A). At this point, ESI-MS measurements indicated the presence of major Cd_5-HaMT1 and Cd_6-HaMT1 species in solution, together with a minor Cd_4-HaMT1 form (Fig. S2). No significant spectroscopic nor

spectrometric differences were observed after the addition of more Cd(II) ions (Fig. 6, Fig. S2), but significantly the addition of 1 and 2 S^{2-} equiv caused an increase of the intensity of the 280(+) CD absorption band (Fig. 6C), leading to a CD fingerprint with a closer resemblance to that of recombinant Cd-HaMT1 although with much less intensity (Fig. 7A). Similar results were obtained after acidification-reneutralisation of the biosynthesised Cd-HaMT1 complexe, followed by the addition of up to 6 S^{2-} equiv (Fig. 7A). Overall, the data fully confirm the significant presence of sulfide ligands in the biosynthesised Cd-HaMT1 preparations, and indicate that Cd_4-, Cd_5- and Cd_6-HaMT1 species are the most stable ones when Zn(II) is replaced by Cd(II) in HaMT1. Moreover, these data show that 6 Cd(II) ions would be the maximum load that HaMT1 can enclose without the contribution of sulfide ligands.

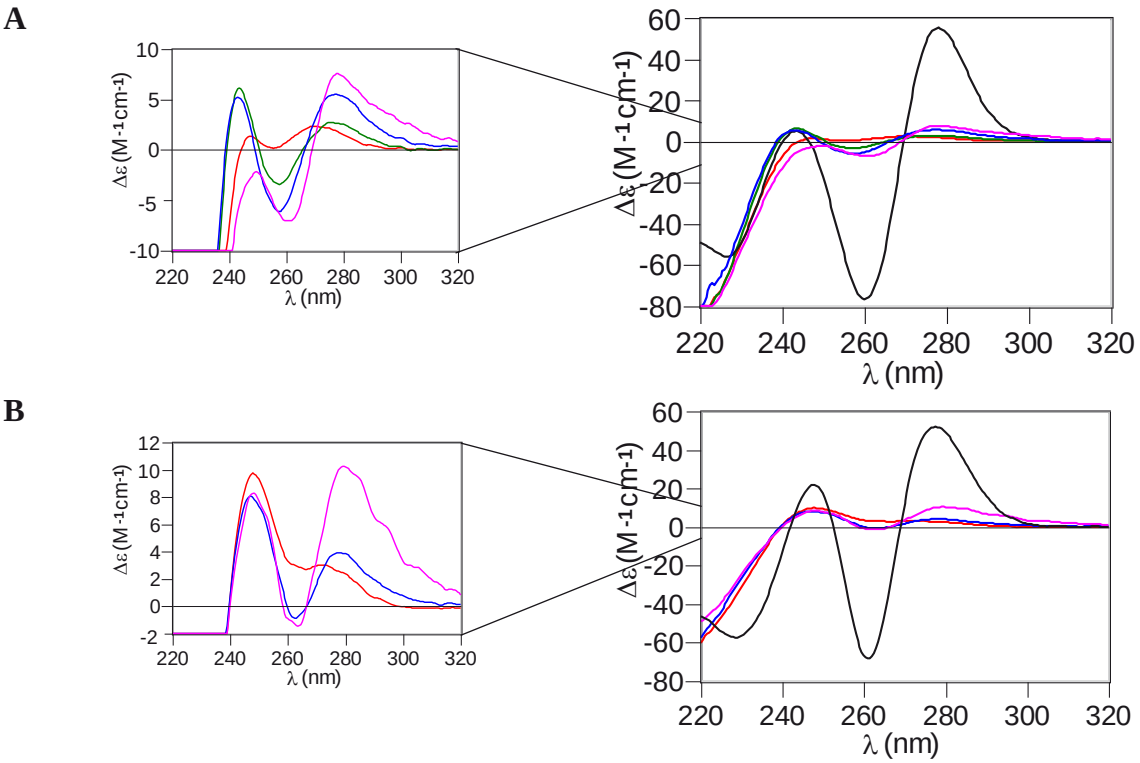

Figure 7. Comparison of the CD spectra of: (**A**) the recombinantly synthesised Cd-HaMT1 (black line), the solution obtained after adding 5 Cd(II) equiv (red line), 7 Cd(II) equiv (green line) and 9 Cd(II) equiv plus 2 S^{2-} equiv (blue line) to Zn-HaMT1 (fraction 1), and the solution recovered after an acidification-reneutralisation process plus the addition of 6 S^{2-} equiv to the initial Cd-HaMT1 recombinant preparation (pink line); (**B**) the recombinantly synthesised Cd-HaMT2 (black line), the solution obtained after adding 6 Cd(II) equiv (red line) and 8 Cd(II) equiv plus 2 S^{2-} equiv (blue line) to Zn-HaMT2, and the solution recovered after an acidification-reneutralisation process plus the addition of 5 S^{2-} equiv to the initial Cd-HaMT2 recombinant preparation (pink line). A zoomed view of each figure has been added for increasing the degree of resolution of the low-intensity CD spectra.

The titration of Zn-HaMT2 with Cd(II) evolved similarly to that of Zn-HaMT1, with UV spectra showing that the replacement of Zn(II) by Cd(II) occurs up to the 6th Cd(II) equiv added (Fig. 8A-B). ESI-MS analyses releaved the presence of a

major Cd_6-HaMT2 species after the addition of the 5th Cd(II) equiv to the Zn-HaMT2 preparation, while minor Cd_4, Cd_5, Cd_5Zn_1 and Cd_7 species were also detected (Fig. S3).

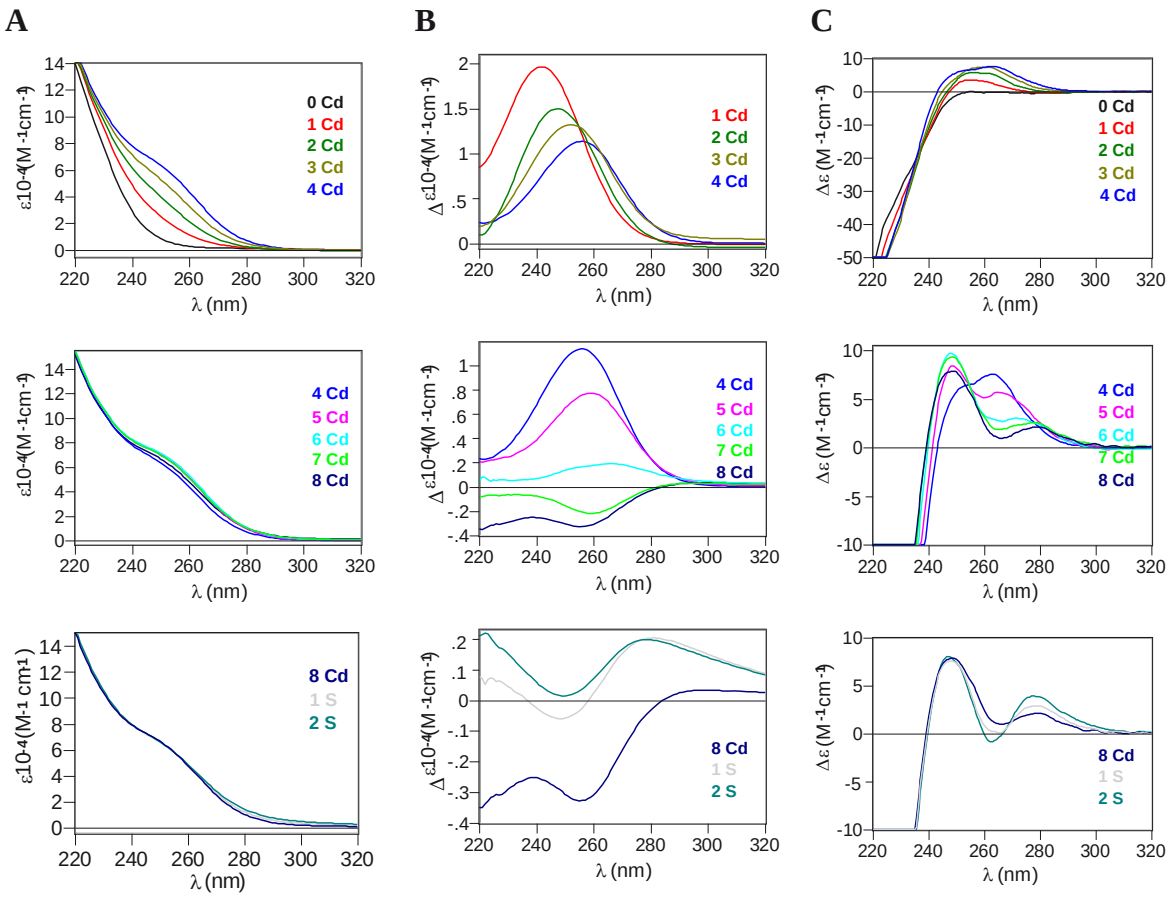

Figure 8. UV (**A**), UV difference (**B**) and CD (**C**) spectra corresponding to the titration of a 15 µM solution of Zn-HaMT2 with Cd(II) at pH 7. The number of Cd(II) equiv in (**B**) indicate the number of the addition which is the responsible for the changes in each absorption spectrum.

From this point onwards, the speciation determined by ESI-MS remained constant, with the only exception of the final disappearance of the Cd_5Zn_1-HaMT2 species (Fig. S3). Thus, these results support the idea that Cd_6-HaMT2 is the main species present when Zn(II) is replaced by Cd(II) in the Zn-HaMT2 preparation. The evolution of the CD fingerprints (Fig. 8C) showed that a typical Cd-MT Gaussian band centred at *ca.* 250 nm was initially formed at the beginning of the titration, which was progressively converted into two bands at *ca.* 250(+) and 280(+) nm through an isodichroic point at *ca.* 255 nm (from 4 to 7 Cd equiv), and finally after the addition of 8 Cd(II) plus 2 S^{2-} equiv the 280(+) nm band was resolved into a 270 nm exciton coupling band, thus resembling the CD fingerprint of recombinant Cd-HaMT2 but with much less intensity (Fig. 7B), analogously to what has been seen for HaMT1. Once more, the need of the presence of S^{2-} ions to reach a similar CD envelope to that obtained from recombinant preparations

confirms the presence of such ligands in the latter case. Concordantly, a weaker but similar CD profile to that of recombinant Cd-HaMT2 was obtained after an acidification-reneutralisation process plus the addition of 5 S^{2-} equiv to the biosynthesised Cd-HaMT2 preparation (Fig. 7B).

4. Discussion

The results presented here report two and three novel plant MT1 and MT2 isoforms, respectively, encoded by the sunflower *Helianthus annuus* genome. None of the two peptides belonging to the MT1 subfamily feature the canonical subfamily Cys content, since they present fourteen and fifteen Cys, instead of twelve (Fig. 1A). Two out of the three MT2 polypeptides contain the standard fourteen Cys in the MT2 subfamily, while one of them also presents one additional Cys at the C-terminal Cys-rich region (Fig. 1B).

The synthesis of HaMT1 in Zn(II)-enriched media yielded major Zn_4-HaMT1 complexes together with substantial Zn_3- and Zn_5-species, affording an average value of 4.3 Zn/MT. These results are only slightly different from those obtained for other plant MT1 isoforms (Table 2). Hence, in the same conditions, soybean GmMT1, a model of the paradigmatic twelve (6+6) Cys pattern of plant MT1s, rendered Zn_4-GmMT1 as the major species, with only a very residual proportion of Zn_3- and Zn_5-GmMT1 complexes [12]. Chickpea cicMT1, containing also twelve Cys plus an additional His residue, showed the Zn_4-MT1 form as nearly the unique species detected by ESI-MS, although a 5^{th} Zn(II) ion was hypothesised to be weakly bound, according to spectroscopic data [11]. Thus, it seems sensible to deduce that the paradigmatic MT1 isoforms yield a canonical Zn_4-MT1 complex, while increasing the number of potential coordinating residues, either Cys (HaMT1) or His (cicMT1) allows a significant presence of Zn_5-MT1, although always coexisting with Zn_4-MT1, which would still remain as the most stable species. It is also interesting to point out that the Gly-Met^{31} and Ser^{32}-Cys^{75} fragments of HaMT1 only bind 1 Zn(II) and 2-3 Zn(II) ions, respectively, thus suggesting that at least the Zn_5-HaMT1 species would be formed of a single cluster involving both the N- and C-terminal Cys-rich domains. Concordantly, it was also hypothesised that the 5^{th} Zn(II) bound to cicMT1 would only be allocated when the peptide folded into a single Zn_5-$(SCys)_{12}$ cluster, while it could only coordinate 4 Zn(II) ions into two separated Zn_2-$(SCys)_6$ clusters [11]. A single Zn_5-$(SCys)_{14}$ cluster

involving both Cys-rich domains was also hypothesised for chickpea Zn_5-cicMT2 [18], containing fourteen Cys. Single joint clusters were also proposed for the Zn_4- and Cu_8-QsMT complexes from cork oak MT2, QsMT [20], containing fourteen Cys as well (Table 2). Thus, considering the observed metal-to-ligand stoichiometries (1:2.4 for Zn_5-$(SCys)_{12}$, 1:3 for Zn_2-Cys_6, and 1:2.8 for Zn_5-$(SCys)_{14}$), it is sensible to assume the existence of the Zn_1-(Gly-Met^{31}) and the Zn_2-(Ser^{32}-Cys^{75}) species, since a Zn_1-$(SCys)_4$ complex could be formed by the HaMT1 N-terminal moiety (containing eight Cys) and a Zn_2-$(SCys)_6$ cluster could be also envisaged for the C-terminal segment (six Cys). Also, even if a Zn_3-$(SCys)_6$ cluster would entail a 1:2 Zn(II)-to-Cys stoichiometry that was not shown by any of the previous examples, such cluster could still be hypothesised for the Zn_3-(Ser^{32}-Cys^{75})-HaMT1 species, since the theoretical maximum binding capacity for an MT containig six Cys is 3 Zn(II) ions if all thiolate groups act as bridging ligands, bearing in mind its assumed tetrahedral coordination geometry. Therefore, in contrast to the hairpin model proposed for the folding of the Zn_5-HaMT1 species, the detected Zn_3-HaMT1 and Zn_4-HaMT1 species are compatible with a dumbbell model, which accounts for independent Cys-rich Zn-binding domains.

HaMT2 binds a mean value of 4.4 Zn/MT, which corresponds to a mixture of Zn_4- and Zn_5-HaMT2 complexes accompanied by a minor Zn_3 species. Almost exact results were reported for soybean Zn-GmMT2 [12], which lacks the Cys63 present in HaMT2. Moreover, the same major Zn_4-MT species was detected for cork oak QsMT [16,17], while for chickpea cicMT2 Zn_5 was the major detected species [18], although both contain fourteen Cys residues. The Zn/MT molar ratio was 3.6 in the case of watermelon MT2, ClMT2 [15] (Table 2). Thus, the extra Cys present in HaMT2 does not seem to increase its Zn(II)-binding abilities compared to GmMT2, QsMT nor cicMT2, whereas data on ClMT2 preparation curiously match those of QsMT, both peptides containing fourteen Cys and one His residues. Therefore, surprisingly, a poorer mean Zn(II) content is observed for His-containing MT2 isoforms compared to His-devoid MT2s.

Cd(II) coordination studies invariably yielded greater metal ion contents compared to Zn(II). Hence, the synthesis of HaMT1 in Cd(II)-enriched cultures afforded sulfide-containing complexes, with Cd_6S_8- and Cd_7S_7-HaMT1 being the major species, and with a concordant mean Cd(II) content of 6.1 Cd/MT. These results are in agreement

with those corresponding to GmMT1, which yielded a mixture of species where Cd_6S_1-GmMT1 was the major complex, together with Cd_5S_6-GmMT1 in second place [12]. Atomic absorption measurements have revealed a 5 Cd/MT ratio for chickpea cicMT1, and 4(±1) and 4.8 Cd(II) for wheat dMT and rice OsMTI-1b undigested GST-fusion proteins, respectively [9,10]. Therefore, it is clear that the incorporation of acid-labile sulfide ions enhances the Cd-binding capacity of plant MTs, as already demonstrated before [16,17,27,28]. For Cd-QsMT complexes from cork oak it was shown that the presence of 2-3 sulfide ions allowed the binding of 1-2 extra Cd(II) ions. Also, the binding of 7 sulfide ions raised the metal content of chickpea cicMT2 from 5 to 9 Cd(II) ions. Therefore, and according to the literature [28], a mean incorporation of 1.5-1.75 S^{2-} per MT would lead to increase the binding capacity of these MTs in one additional Cd(II) ion. Remarkably, the Zn/Cd replacement experiments indicated that the maximum loaded Cd-species for HaMT1 devoid of S^{2-} is Cd_6, therefore becoming the upper limit that cannot be surpassed in the absence of S^{2-} ligands. However, the constant detection of a mixture of the Cd_4, Cd_5 and Cd_6-HaMT1 species during the Zn-HaMT1 titration with Cd(II) lead to conclude that there is an equilibrium between the three Cd(II)-loaded species. Hence, the presence of the Cd_4- and Cd_5-HaMT1 species is in agreement with the 4(±1), 4.8 and 5 Cd/MT ratios found for GST-dMT, GST-OsMTI-1b and cicMT1 [9,10,11], respectively, which contain only twelve Cys residues, while the existence of the Cd_6-HaMT1 species could be only comparable to the 5.8 Cd/MT content found for GST-PsMTA [8], that also contains twelve Cys and for which the presence of sulfide ligands has not been determined (Table 2). Therefore, our results clearly point to an enhanced Cd-binding capacity for HaMT1 probably due to the participation of the extra Cys residues.

HaMT2 has been shown to render an almost unique Cd_6S_8-HaMT2 complex when synthesised in Cd-enriched cultures, only accompanied by very minor sulfide-devoid Cd_6-HaMT2 species. Although the presence of S^{2-} could not be confirmed by the difference between conventional and acid ICP-AES data, it was corroborated by the intense CD absorption than the corresponding preparation exhibited at the 270-290 nm range [23]. Interestingly, the CD fingerprints of Cd-HaMT1 and Cd-HaMT2 were highly similar, with a *ca.* 245 nm Gaussian band and an exciton coupling band centred at *ca.* 270 nm. Moreover, the CD envelope of the reconstituted Cd_9S_7-cicMT2 from chickpea shows completely equivalent signals [27], thus suggesting a similar fold for these three

Table 2 Summary of Zn(II)- and Cd(II)-binding properties of plant MT1 and MT2 proteins.

Protein	Cys	His	Zn/MT content [a]	Recombinant Zn-MT species[b]	Cd/MT content[a]	Recombinant Cd_xS_y-MT species[b]	Reconstituted Cd_xS_y-MT species[c]
HaMT1	14 (8+6)	0	4.3	Zn_4, Zn_3, Zn_5	6.1	Cd_6S_8, Cd_7S_7	Cd_4, Cd_5, Cd_6
GmMT1	12 (6+6)	0	3.8	Zn_4	8.1	Cd_6S_1	---
cicMT1	12 (6+6)	1	5	Zn_4	5	---	---
GST-OSMTI-1b	12 (6+6)	2	1.8	---	4.8	---	---
GST-PsMTA	12 (6+6)	0	---	---	5.8	---	---
GST-dMT	12 (6+6)	0	---	---	4 (±1)	---	---
HaMT2	15 (8+7)	0	4.4	Zn_4, Zn_5	6.3	Cd_6S_8	Cd_6
GmMT2	14 (8+6)	0	4.3	Zn_4, Zn_5	6.7	Cd_6S_1	---
QsMT	14 (8+6)	1	3.5	Zn_4	5.3/6.5	Cd_5/Cd_6S_4	Cd_7S_9
cicMT2	14 (8+6)	0	5	Zn_5	5	---	Cd_5
ClMT2	14 (8+6)	1	3.6	---	---	---	---

[a] Metal per MT molar ratio measured by ICP-AES or F-AAS. The cadmium content for the *GST*-dMT peptide was exceptionally determined by MALDI-TOF-MS.[b] Major M(II)-MT species detected by ESI-MS in the recombinantly obtained preparations. [c] Major Cd(II)-MT species detected by ESI-MS in the solutions obtained either after Zn/Cd replacement plus S^{2-} addition to Zn-MT (HaMT1, HaMT2, QsMT) or after reconstitution of apo-MT with Cd(II) (cicMT2). The data for HaMT1 and HaMT2 (in bold) are from this work, and the data for other MTs are from the literature: GmMT1 and GmMT2 [12], cicMT1 [11], GST-OsMTI-1b [10], GST-PsMTA [8], GST-dMT [9], QsMT [16,17] and cicMT2 [18].

polypeptides. The formation of the Cd_6S_8-HaMT2 complex can be compared to the obtained Cd_6S_1-GmMT2 [12] and Cd_6S_4-QsMT [17] complexes, since these three polypeptides bind 6 Cd(II) ions into sulfide-containing complexes. The main species when Zn is substituted by Cd in Zn-HaMT2 is Cd_6-HaMT2, and 6 Cd(II) is the maximum binding capacity determined for any other plant MT2 isoform in the absence of additional S^{2-} ligands.

5. Conclusions

Five novel plant MTs belonging to the MT1 and MT2 subfamilies have been identified in sunflower (*Helianthus annuus*). The Zn(II)- and Cd(II)-binding properties of HaMT1-2 (HaMT1) and HaMT2-1 (HaMT2), the most likely to be highly expressed *in vivo*, have been extensively studied. Since HaMT1 features fourteen Cys residues, two more than in standard plant MT1 sequences, and HaMT2, with fifteen Cys residues, also contains an extra Cys with respect to the canonical plant MT2 peptides, they are extremely suitable for analysing the effect of extra-coordinating residues in plant MTs. It is worth considering that in both cases the variation in the number of Cys does not drastically modify their M(II)-binding properties, but instead modulates the degree of heterogeneity of the corresponding recombinantly obtained preparations. Hence, the two additional Cys in HaMT1 provoke the almost equimolar presence not only of supermetallated (Zn_5) but also of inframetallatated (Zn_3) complexes in relation to the canonical Zn_4-MT1 species. In the case of Cd(II) the complexity of the obtained sample is notably increased as well. Thus, it seems as if the increased number of Cys in reference to the model pattern of the MT1 subfamily is incompatible with the folding of a unique stable species. Surprisingly, the presence of one additional Cys for the HaMT2 peptide has the contrary effect, reducing the complexity of the recombinantly obtained preparation, as seen for Cd-HaMT2, where the Cd_6S_8 species is almost unique. Comparative results for Zn(II)- and Cd(II)-binding properties also support the idea that the MT2 isoforms are probably associated to Cd(II) metabolism, in contrast to the MT1 peptides, which may be related to functions other than metal detoxification, as also pointed by their low yield of synthesis in metal-supplemented cultures [12]. Additionally, HaMT1 and HaMT2 Zn/Cd substitution experiments have led to the upper Cd(II)-load limit of 6 Cd/MT ever determined for any other plant MT1 and MT2, respectively, in more forced conditions and when sulfide anions are not acting as extra

ligands. These results are probably related to the presence of the extra Cys residues in HaMT1 and HaMT2.

6. References

[1] M. Margoshes, B.L. Vallee, J. Am. Chem. Soc. 79 (1957) 4813-4814.

[2] M. Capdevila, R. Bofill, Ò. Palacios, S. Atrian, Coord. Chem. Rev. 256 (2012) 46– 62.

[3] http://www.bioc.unizh.ch/mtpage/classif.html (accessed July 8th, 2013)

[4] L. Hanley-Bowdoin, B.G. Lane, Eur. J. Biochem. 135 (1983) 9-15.

[5] C. Cobbett, P. Goldsbrough, Annu. Rev. Plant Biol. 53 (2002) 159-182.

[6] E.A. Peroza, R. Schmucki, P. Güntert, E. Freisinger, O. Zerbe, J. Mol. Biol. 387 (2009) 207-218.

[7] O.I. Leszczyszyn, H.T. Imam, C.A. Blindauer, Metallomics 5 (2013) 1146-1169.

[8] A.M. Tommey, J. Shi, W.P. Lindsay, P.E. Urwin, N.J. Robinson, FEBS 292 (1991) 48-52.

[9] K. Bilecen, U.H. Ozturk, A.D. Duru, T. Sutlu, M.V. Petoukhov, D.I. Svergun, M.H. Koch, U.O. Sezerman, I. Cakmak, Z. Sayers, J. Biol. Chem. 280 (2005) 13701-13711.

[10] R.M. Nezhad, A. Shahpiri, A. Mirlohi, Protein J. 32 (2013) 131-137.

[11] O. Schicht, E. Freisinger, Inorg. Chim. Acta 362 (2009) 714-724.

[12] M.A. Pagani, M. Tomas, J. Carrillo, R. Bofill, M. Capdevila, S. Atrian, C.S. Andreo, J. Inorg. Biochem. 117 (2012) 306-315.

[13] J. Guo, L. Xu, Y. Su, H. Wang, S. Gao, J. Xu, Y. Que, Biomed. Res. Int. (2013) doi: 10.1155/2013/904769

[14] H.L. Wong, T. Sakamoto, T. Kawasaki, K. Umemura, K. Shimamoto, Plant Physiol. 135 (2004) 1447-1456.

[15] K. Akashi, N. Nishimura, Y. Ishida, A. Yokota, Biochem. Biophys. Res. Commun. 323 (2004) 72-78.

[16] G. Mir, J. Domènech, G. Huguet, W.J. Guo, P. Goldsbrough, S. Atrian, M. Molinas, J. Exp. Bot. 55 (2004) 2483-2493.

[17] J. Domènech, R. Orihuela, G. Mir, M. Molinas, S. Atrian, M. Capdevila, J. Biol. Inorg. Chem. 12 (2007) 867-882.

[18] X. Wan, E. Freisinger, Metallomics 1 (2009) 489-500.

[19] M. Capdevila, N. Cols, N. Romero-Isart, R. González-Duarte, S. Atrian, P. González-Duarte, Cell. Mol. Life Sci. 53 (1997) 681-688.

[20] J. Domènech, G. Mir, G. Huguet, M. Molinas, M. Capdevila, S. Atrian, Biochimie 88 (2006) 583-593.

[21] N. Cols, N. Romero-Isart, M. Capdevila, B. Oliva, P. Gonzàlez-Duarte, R. Gonzàlez-Duarte, S. Atrian, J. Inorg. Biochem. 68 (1997) 157-166.

[22] J. Bongers, C.D. Walton, D.E. Richardson, J.U. Bell, Anal. Chem. 60 (1988) 2683-2686.

[23] M. Capdevila, J. Domènech, A. Pagani, L. Tío, L. Villarreal, S. Atrian, Angew. Chem. Int. Ed. Engl. 44 (2005) 4618-4622.

[24] M. Tomàs, M.A. Pagani, C.S. Andreo, M. Capdevila, R. Bofill, S. Atrian, J. Biol. Inorg. Chem. (submitted).

[25] N.H. Roosens, R. Leplae, C. Bernard, N. Verbruggen, Planta 222 (2005) 716-729.

[26] P. Kille, D.R. Winge, J.L. Harwood, J. Kay, FEBS Lett. 295 (1991) 171-175.

[27] X. Wan, E. Freisinger, Inorg. Chem. 52 (2013) 785-792.

[28] T. Huber, E. Freisinger, Dalton Trans. 42 (2013) 8878-8889.

Supplementary Material

Table S1

Amino acid sequence alignment for plant MT1s. The UniProtKB or GenBank accession code and the Latin species name is given in each row. The accession code of the MT1 studied in this work is in bold. The shaded boxes indicate the cysteine residues and histidines are in bold.

```
                                  10        20        30        40        50        60        70        80        90       100
                                  ....|....|....|....|....|....|....|....|....|....|....|....|....|....|....|....|....|....|
Q8LGQ8 Allium sativum             --MS-------CSCGSSCNCGSS-CN--CGKMYPDLEEK------STGAQ--ATVVLGVAPEQKVQ---LEAATESGETAHACGCGANCKC-DPCNC---
XM_002892408 Arabidopsis lyrata   --MAGS----NCGCGSSCKCGDS-CS--CEKNYN-------------------------------------------QECDDCSCGSNCSCGSNCNC---
XM_002892362 Arabidopsis thaliana --MAGS----NCGCGSSCKCGDS-CS--CEKNYN-------------------------------------------QECDDCSCGSNCSCGSNCNC---
P43392 Arabidopsis thaliana       --MADS----NCGCGSSCKCGDS-CS--CEKNYN-------------------------------------------KECDNCSCGSNCSCGSNCNC---
Q38803 Arabidopsis thaliana       MGLILTRMILNCGCGSSCKCGDS-CS--CEKNYN-------------------------------------------KECDNCSCGSNCNF---------
Q38804 Arabidopsis thaliana       --MAGS----NCGCGSSCKCGDS-CS--CEKNYN-------------------------------------------KECDNCSCGSNCSCGSSCNC---
A4URF6 Brassica juncea            --MAGS----NCGCGSGCKCGDS-CS--CEKNYN-------------------------------------------TECDNCSCGSNCSCGDSCSC---
ADP37975 Brassica napus           --MAGS----NCGCGSACKCGDS-CS--CEKNYN-------------------------------------------TECDNCSCGSNCSCGDSCSC---
P43402 Brassica napus             --MAGS----NCGCGSGCKCGDS-CS--CEKNYN-------------------------------------------TECDSCSCGSNCSCGDSCSC---
DK501359 Brassica oleracea        --MAGS----NCGCGSACKCGDS-CS--CEKNYN-------------------------------------------TECDNCSCGSNCSCGDNCSC---
Q9M698 Brassica oleracea          --MAGS----NCGCGSGCKCGDS-CS--CEKNYN-------------------------------------------TECDSCSCGSNCSCGDSCGC---
Q508T1 Betula platyphylla         --MSSCGG--NCNCGSDCKCGSG-CK--CGKHA--DLSYS---EKTTTET----IIAGVAPVKINYEGS--EMSSGAEN--GCKCGSNCSC-DPCSCK--
AAY84148 Catharanthus roseus      --MS-------CSCGGSCNCGSG-CS--CGSKKYQDLETS-----ATTTI----IIEGVAPKKMDFEES--EKSFGAEGGHGCKCGSNCNC-DPCNC---
Q39458 Cicer arietinum            --MSG------CNCGSSCNCGDQ-CK--CNKRS--GLSYV--EAGETTET----VVLGVGPTKIHFEGA--EMSVAAEDG-GCKCGSSCTC-DPCNCK--
JG721393 Ephedra distachya        -MSSCGG---NCNCGSNCQCGSS-CN--C--MYP----EL-----TLNLR---SVRMGFVDENIT-------IAG---ENGGCNCGADCQC-DPCNCGK-
O24528 Festuca rubra              --MS-------CSCGSSCGCGSN-CK--CGKMYPDLDEQA-----STTTQ--AVVVVGVAHENKAGQ--FEMAS-----GEGCKCGANCKC-DPCNC---
BQ742738 Glycine max              --MSS------CGCGSSCNCGSN-CG--CNKYSF-DLSYV--EK-TTTET----LVLGVGPVKAQLEGA--EMGVASENG-GCNCGSSCTC-DPCNCK--
GR307619 Grimmia pilifera         --MEGCGNP-NCKCGADCTCAD--CS--CG----------------------------------R-----------TEPDCKCGSDCNC-EDCDCHKS
DY927283 Helianthus annuus        --MSCSSG--KCNCGSSCSCGSS-CN--CNSCNV-EMST------TTTTI----IVDGVAPRMTFAEET--E---VAESGNACKCGSSCKC-DPCNC---
DY927795 Helianthus annuus        --MS-------CKCGSNCSCGSS-CN--CNSCDV-EKS-------TTTTI----IVDGVAPKMTFAEGS--ETSTVAESGNGCSCGSSCKC-NPCNC---
P26571 Hordeum vulgare            --MS-------CSCGSSCGCGSN-CN--CGKMYPDLEEK------SGATMQVTVIVLGVGSAK--VQ--FEEAAEFGEAAHGCSCGANCKC-NPCNC---
GO912370 Huperzia serrata         --MSGCGNA-NCPCGNDCKCGNS-CS--CSS-------------------------EMDIEYVSGVES-------FECDKPGCNCGSNCAC-TSCSCDQ-
Q9ZSC6 Ipomoea batatas            --MSSG-----CKCGSDCKCGSD-CA--CEE-------VT-----TTVT-----IIEGVAPVKLTLEGSS-EK--ATEGGHACKCGSNCTC-DPCNC---
BJ850418 Marchantia polymorpha    --MSGCGNS-GCSCGAACKCASG-NS--CCAK----------------------RSMDDFESSEMRG-------FEGANEGCKCGDKCSC-NPCNCK--
Q9SP23 Medicago sativa            --MSG------CNCGSSCNCGDN-CK--CNSRSS-GLGYL---EGETTET----VILGVGPAKIHFEGA--EMGVAAEDG-GCKCGDSCTC-DPCNCK--
P20238 Mimulus guttatus           --MSSG-----CSCGSGCKCGDN-CS--CSMY--PDMETN-----TTVT-----MIEGVAPLKMYSEGS--EKSFGAEGGNGCKCGSNCKC-DPCNC---
A2ZH20 Oryza sativa               --MS-------CSCGSSCSCGSN-CS--CGKKYPDLEEK------SSSTK--ATVVLGVAPEKKAQQ--FEAAAESGETAHGCSCGSSCRC-NPCNC---
NP_001067063 Oryza sativa         --MS-------CG--GSCNCGSCGCSGGCGKMYPDLAEKI-----TITTT-TTTTVLGVAPEKGQFEG-VGKAAESGEGAHGCSCGSSCKC-NPCNC---
BAG87041 Oryza sativa             --MS-------CSCGSSCGCGSN-CT--CGKMYPDLEEK------SSSAQ--ATVVLGVAPEK--AH--FEAAAESGETAHGCGCGSSCKC-NPCNC---
P0C5B3 Oryza sativa               --MS-------CSCGSSCSCGSN-CS--CGKKYPDLEEK------SSSTK--ATVVLGVAPEKKAQQ--FEAAAESGETAHGCSCGSSCRC-NPCNC---
Q10N03 Oryza sativa               --MS-------CSCGSSCGCGSN-CT--CGKMYPDLEEK------SSSAQ--ATVVLGVAPEK--AH--FEAAAESGETAHGCGCGSSCKC-NPCNC---
Q2QNC3 Oryza sativa               --MS-------CG--GSCNCGSCGCGGGCGKMYPDLAEKI-----TTTTT-TATTVLGVAPEKGHSEG-VGKAAESGEAAHGCSCGSSCRC-NPCNC---
Q2QNE8 Oryza sativa               --MS-------CG--GSCNCGSCGCGGGCGKMYPDLAEKI-----TTTTT-TATTVLGVAPEKGHFEVMVGKAAESGEAAHGCSCGSSCKC-NPCNC---
P20830 Pisum sativum              --MS--G----CGCGSSCNCGDS-CK--CNKRSS-GLSYS---EMETTET----VILGVGPAKIQFEGA--EMSAASEDG-GCKCGDNCTC-DPCNCK--
Q5ZF73 Plantago major             --MSSCGSS-NCSCGSSCKCGSG-CG--CSMYP--DVEKN-----ANQVT----IIEGLAPSKMFSEGV--EESFSAEGGQGCKCGAGCKC-DPCTC---
Q6PML6 Populus trichocarpa        --MS--G----CSCGSDCKCGSG-CK--CGMYP--DLGFS---ENTTTET----IIAGVAPVKMFYERS--EMDFGAEN--GCKCGSNCTC-DPCSCK--
```

```
                                  10        20        30        40        50        60        70        80        90       100
                                  ....|....|....|....|....|....|....|....|....|....|....|....|....|....|....|....|....|....|
Q9LUX2 Pyrus pyrifolia            --MS-CN----CSCGSDCKCGSG-CK--CGMYP--DLSYS---ETTSTETI---IV-GVAPAKMFYEGS--EMNYGAEN--DCKCGSNCSC-TSCGCHK-
AEQ54918 Salvia miltiorrhiza      --MSSG-----CKCGSSCGCGSG-CS--CEM----DVEKS-----TSIA-----MVEGVAPPMMKIEGA--EKSLGAEGGNGCTCGSSCSC-DPCTC---
BM402666 Selaginella lepidophylla --MSSCGSA-NCNCGSNCSCGSG-CK--CGRSFDESTLLM----------REAAGDMSLSSIVSASSGISGESVMSREENGCKCGPNCSC-NDCSCHK-
FE432113 Selaginella moellendorffii --MSSCGSA-NCNCGSNCSCGSG-CK--CGRSFDESTLLM----------REAAGDMSLSSIVSASSGISGESVMSREENGCKCGPNCSC-NDCSCHK-
CN208803 Syntrichia ruralis       --MSGCGNS-KCQCGSSCTCANG-CS--CGG----------------------RTMAVPTFGGLRN---------YNDPDCKCGSTCNC-ADCDCHK-
Q6IV93 Tamarix androssowii        --MSSCGG--SCKCSG-CSCGDS-CN--CRSYG---IEVN-----PSPPT----IIAGVAPVKTVSGKS---SEMNVEG-EGCKCGDGCSC-DPCTC---
AY486003 Thlaspi caerulescens     --MAGS----NCGCGSSCKCGDS-CS--CEMNYN---------------------------------------TECDSCSCGSDCSCGSNCNC---
P43399 Trifolium repens           --MSGCN------CGSSCNCGDS-CK--CNKRSS-GLNYV---EAETTET----VILGVGPAKIQFEDA--EMGVAAEDS-GCKCGSSCTC-DPCNCK--
P43400 Triticum aestivum          --MS-CN------CGSGCSCGSD-CK--CGKMYPDLTEQG-----SAAAQVAAVVVLGVAPENKAGQ--FEVAA--GQSGEGCSCGDNCKC-NPCNC---
AAT99566 Triticum durum           --MS-CN------CGSGCSCGSD-CK--CGKMYPDLTEQG-----SAAAQVAAVVVLGVAPENKAGQ--FEVAA--GQSGEGCSCGDNCKC-NPCNC---
Q41669 Vicia faba                 --MSGCG------CGSSCNCGDS-CK--CNKRSS-GLSYS---EMETKETK-ETVVLGFGPAKIHFDGA--EMSVASKEE-GCKCGDKCTC-DPCNC---
Q41670 Vicia faba                 --MSGCN------CGSSCNCGDS-CK--CNKRSS-GLSYS---EVETKET----VILGVGPAKIQFEGA--EMSFASKEG-GCKCGDNCTC-DPCNCK--
Q6J9F8 Xerophyta humilis          -MAS-CGG--NCGCGPNCKCGSN-CNCGGNKMYPGLAEER-----STSTQ---TNILGVAPQQERRE---GFEAGQRSENGGCKCGPNCNC-NPCNCK--
P30571 Zea mays                   --MS-CS------CGSSCGCGSS-CK--CGKKYPDLEET------STAAQ--PTVVLGVAPEKKAAPEFVEAAAESGEAAHGCSCGSGCKC-DPCNC---
E3W9M4 Ziziphus jujuba            --MS--G----CGCGSSCSCGSG-CK--CGRNP--DLGYS---EKTTTET----IVVGVAPVKIDNDGS--EVSHGTENE-GCGCGSNCKC-DPCTCK--

                                  10        20        30        40        50        60        70        80        90       100
                                  ....|....|....|....|....|....|....|....|....|....|....|....|....|....|....|....|....|....|
Q7XHJ3 Quercus robur              VNSIISRVKYFPILLYSNLKKMSSFGGNCGCGSDCKCGSGCNCNSMNPGLSEKTSTETIITGVAPAKIYSEGSEMSFGAENGGCKCGSNCTCDPCNCK--
```

Table S2

Amino acid sequence alignment for plant MT2s. The UniProtKB or GenBank accession code and the Latin species name is given in each row. The accession code of the MT2 studied in this work is in bold. The shaded boxes indicate the cysteine residues and histidines are in bold.

```
                                    10        20        30        40        50        60        70        80        90       100       110
                                    ....|....|....|....|....|....|....|....|....|....|....|....|....|....|....|....|....|....|....|....|.
D9J388 Acacia auriculiformis        MS--CCGGNCGCGAGCKCGSGCGGC---KMYPDMAEQV---TTTQTLIMGVAPSK-------G-GFVA--AAG----AENGGCK-CG---AN-----CTC-DPCTCK----
P43390 Actinidia deliciosa          MS--CCGGKCGCGSSCSCGSGCGGC---GMYPDLSYSEMT--TTETLIVGVAP-QKTYFE-----GSEMGVA-----AEN-GCK-CG---SD-----CKC-DPCTCK----
DK949736 Adiantum capillus-ve.      MS--CCNGNCGCGANCQCASGCKGCG----RTDSLVLSKEAPLVLSATASVCPSYERALG---------------FGVENISGYLG---SP-----TSC-FPLN------
AAV80430 Allium sativum             MS--CCGGNCGCGSSCKCGNGCGGC---KMYGDVGEERSSM--TTTSILGVAP-QRSFEE------FENEMIA----EGGNACK-CG---SN-----CTC-NPCTCK----
P25860 Arabidopsis thaliana         MS--CCGGNCGCGSGCKCGNGCGGC---KMYPDLGFSGETT-TTETFVLGVAPAMKNQYE-----ASG-ESNN----AENDACK-CG---SD-----CKC-DPCTCK----
Q38805 Arabidopsis thaliana         MS--CCGGSCGCGSACKCGNGCGGC---KRYPDL----ENT-ATETLVLGVAPAMNSQYE-----ASG-ETFV----AENDACK-CG---SD-----CKC-NPCTCK----
Q45W72 Arachis hypogaea             MSS-CCGGNCGCGSGCKCGNGCGGC---KMYPDLSYTESSS-TTESLVMGVAP-AKAQFE-----GAEMGVP-----AENDACK-CG---PN-----CSC-NPCTCK----
Q94I87 Atropa belladonna            MS--CCGGNCGRGSGCKCGNGCGGC---KMYPDMSYTES-T-TTETLVLGVGP-EKTSFD-----AMEFGESL----IAENGCK-CG---SD-----CKC-DPCTCSK---
P69163 Brassica juncea              MS--CCGGNCGCGSGCKCGNGCGGC---KMYPDLGFSGEST-TTETFVFGVAPAMKNQYE-----ASG-EG-V----AENDACK-CG---SD-----CKC-DPCTCK----
P56168 Brassica juncea              MS--CCGGNCGCGSGCKC-VGCGGC---KMYPDLSFSGETT-TTETLVLGVAPAMNSQFE-----ASG-ETFV----AENDACK-CG---SD-----CKC-NPCTCK----
P56170 Brassica juncea              MS--CCGGNCGCGAGCKC-VGCGGC---KMYPDLSFSGETT-TSEALVLGVAPSMNSQYE-----ASG-ETFV----AENDACK-CG---SD-----CKC-NPCTCK----
P56172 Brassica juncea              MS--CCGGNCGCGAGCKC-VGCGGC---KMYPDLSFSGETT-TTETLVLGLAPAMNSQFE-----ASG-ETFV----AENDACK-CG---SD-----CKC-NPCTCK----
P69164 Brassica campestris          MS--CCGGNCGCGSGCKCGNGCGGC---KMYPDLGFSGEST-TTETFVFGVAPAMKNQYE-----ASG-EG-V----AENDACK-CG---SD-----CKC-DPCTCK----
Q9M697 Brassica oleracea            MS--CCGGNCGCGSGCKCGNGCGGC---KMYPDLGFSGELT-TTETFVFGVAPTMKNQHE-----ASG-EG-V----AENDACK-CG---SD-----CKC-DPCTCE----
Q39269 Brassica rapa                MS--CCGGNCGCGSGCKCGNGCGGC---KMYPDLGFSGEST-TTETFVFGVAPAMKNQYE-----ASG-EG-V----AENDRCK-CG---SD-----CKC-DPCTCK----
Q39459 Cicer arietinum              MS--CCGGNCGCGSSCKCGSGCGGC---KMYPDMSYTEQT--TSETLVMGVAS-GKTQFE-----GAEMGFG-----AENDGCK-CG---SN-----CTC-NPCTCK----
Q6I674 Citrullus lanatus            MS--CCGGNCGCGSGCKCGSGCGGC---KMFPDMSFSEATA-TIETFVVGFAP-HKMSFE-----VAEMG-------AEN-GCK-CG---DN-----CTC-DPCNCK----
P43396 Coffea arabica               MS--CCGGNCGCGAGCKCSGGCGGC---KMYPELSYTENT--AAETLILGVAPPKTTYLE-----GAG-EEAA----AENGGCK-CG---PD-----CKC-NPCNCK----
Q19LA2 Colocasia esculenta          MS--CCGGNCGCGSGCQCGNGCGGC---KMFPDFGSDEKIT-TTHTLVLGFAPAKGSVEG-----FEMVAG------AAENDCK-CG---SNC---SCTD---CRCDPCNC
Q9SMG3 Eichhornia crassipes         MS--CCGGNCGCGSGCKCGNGCSGC---KMYPDMEEKT---VTAQTMIMGIAAEK-------G-HFEDFEAAG----SGNEGCK-CG---SN-----CTC-NPCNCK----
Q9ZNT5 Eichhornia crassipes         MS--CCGGNCGCGSGCKCGNGCSGC---KMYPDMEEKT---VTAQTMIMGIAAEK-------G-HFEDFEAAG----SENEGCK-CG---SN-----CTC-NPCNCK----
AFK13199 Elaeis guineensis          MS--CCGGNCGCGSGCKCGTGCGGC---KMFTHMVEER--STTTQTVIMGVAPQKGQ----VE-GFEM--ATG----SENGGCK-CG---SN-----CTC-DPCNCK----
CAA10232 Fagus sylvatica            MS--CCGGNCGCGTGCKCGSGCGGC---KAYPDLSYTEKT--TTETLIVGVAP-QKAHSE-----GSEMGVG-----AENGGCK-CG---SN-----CTC-DPCNCK----
P93134 Fragaria ananassa            MS--CCGGKCGCGAGCKCGSGCNGC---GNYADITEQ-SSA--SETLVMGVVGTQKLNYG----QAEAGVATE----GSCSGCK-CVY---------CTC-DPCTCK----
DR064960 Ginkgo biloba              MS--CCGGNCGCGAGCKCGNGCGGCNM---FPDLTFGEK---TVEAPLFAATASDMGYFEE-MSVAGESGCAK----AGGG-CK-CG---DN-----CTC-DPCNCK----
BQ629803 Glycine max                MS--CCGGNCGCGSACKCGNGCGGC---KMYPDLSYTEST--TTETLVMGVAP-VKAQFE-----SAEMGVP-----AENDGCK-CG---AN-----CTC-NPCTCK----
Q75NI1 Glycine max                  MS--CCGGNCGCGSSCKCGNGCGGC---KMYPDLSYTEST--TTETLVMGVAP-VKAQFE-----SAEMGVP-----AENDGCK-CG---AN-----CTC-NPCTCK----
GR307619 Grimmia pilifera           MEG-CGNPNCKCGADCTCAD-C-SCG--------------------------R----------------------TEPDCK-CG---SD-----CNC-EDCDCHKS--
DY931085 Helianthus annuus          MS--CCNGKCGCGSSCSCGSGCNGC---GMYPDVEV--SS---TTVMIVDGVAPKQMFAE----GSEGSFVAE----GGNCNCK-CG---DN-----CKCGNNCSC-----
DY931060 Helianthus annuus          MS--CCNGKCGCGSSCSCGSSCKGC---GMYPDIET--ST---TATMIVDGVAPKKMYDD----GSDASFVSE----GGHA-CK-CG---AN-----CKC-DPCNC-----
BQ910832 Helianthus annuus          MSSSCCGGNCGCGSGCKCGNGCGGC---KMYPEMVSGEST--NNETLILGVAPTETGIET-----TGG-VATA----AENEGCK-CN---P------CTC-NPCTCK----
AFP93964 Ilex paraguariensis        MS--CCGGNCGCGAGCKCGAGCSGC---KMYPDLSYSEST--TTETLIVGVAP-QKTYFE-----GSEMGVG-----AEN-GCK-CG---DN-----CTC-DPCNCK----
Q9SPE7 Ipomoea batatas              MS--CCGGNCGCGSACKCGGGCGGCG---MFPDVENVKT-----VTLIQGVAPVNNNTFE-----GAEMGAG-----GGDGCK-CGSG-------SCSCGPACNCDPCKC
ABL10085 Limonium bicolor           MS--CCVGSCGCGSDCKCGSGCGGC---KMYADLSYTEAAASTTVSLISGVAP-QRSYHD-----GSEMGVA-----AENDGCK-CG---DN-----CTC-NPCTCK----
AAG44758 Musa acuminata             MS--CSGENCGCGSSCSCGSGCGGC---RKLTDLGEER--SSTSQTMIMGVAPQKGH----FE-ELET--AAG----SENG-CK-CG---SN-----CTC-DPCNCK----
O22319 Musa acuminata               MS--CSGGNCGCGSSCSCGSGCGGC---RMLTDLGEER--SSTSQTMIMGVAPQKGH----FE-ELET--AAG----SDNG-CK-CG---SN-----CTC-DPCNCK----
Q93WW3 Narcissus pseudonarc.        MS--CCGGNCGCGSACKCGSGCGGC---KMYADLAEDR--STATMTLVLGVAPQKGG----IE-GFEM--AEG----AENG-CK-CG---SN-----CTC-DPCNCK----
CAC12823 Nicotiana tabacum          MS--CCGGSCGCGSGCKCGSGCGGC---GMYPDLENTTT-----FTIIEGVAPMKN-----YE-GSAE--KAT----EGGNGCK-CG---AN-----CKC-DPCNC-----
```

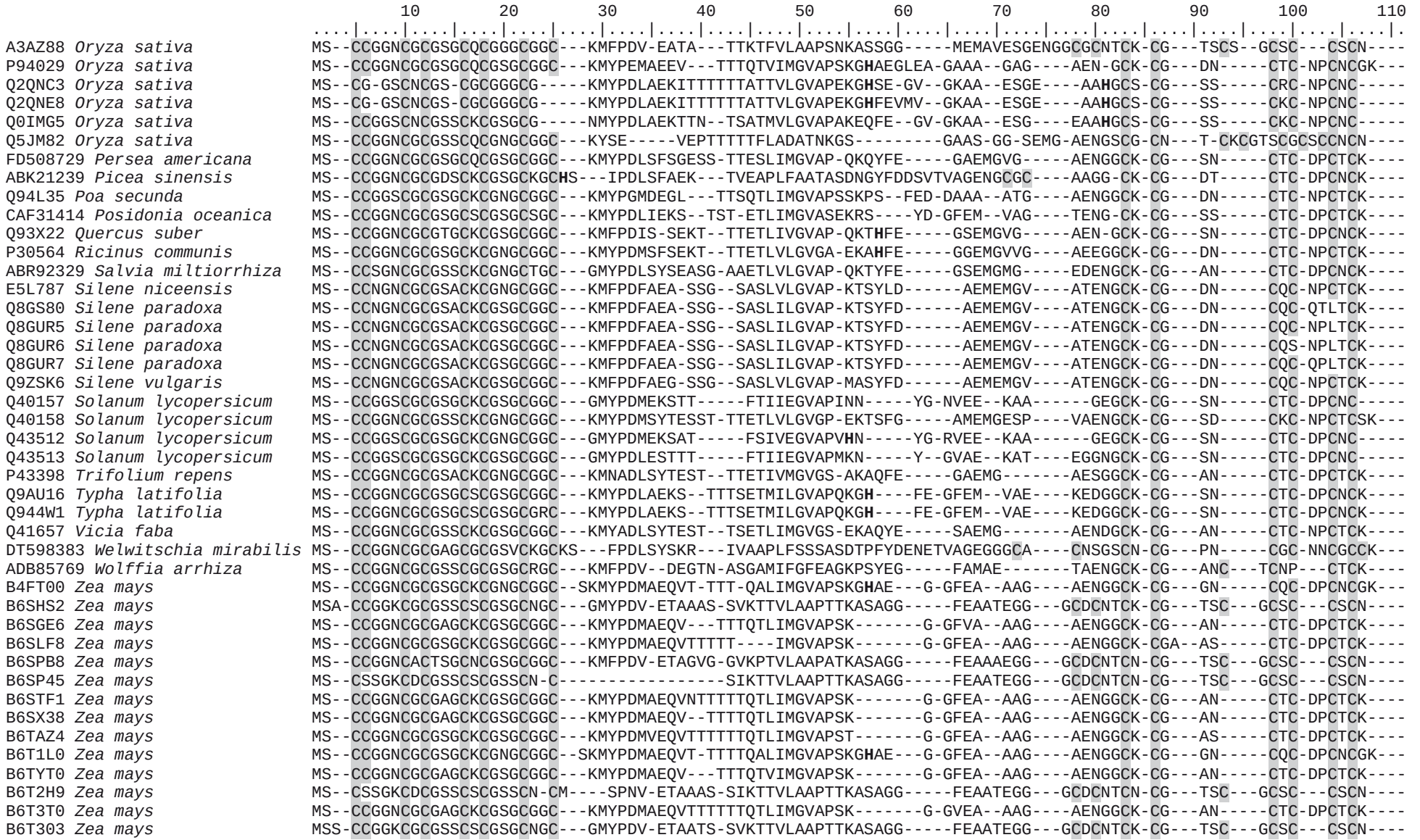
10 20 30 40 50 60 70 80 90 100 110
A3AZ88 Oryza sativa
P94029 Oryza sativa
Q2QNC3 Oryza sativa
Q2QNE8 Oryza sativa
Q0IMG5 Oryza sativa
Q5JM82 Oryza sativa
FD508729 Persea americana
ABK21239 Picea sinensis
Q94L35 Poa secunda
CAF31414 Posidonia oceanica
Q93X22 Quercus suber
P30564 Ricinus communis
ABR92329 Salvia miltiorrhiza
E5L787 Silene niceensis
Q8GS80 Silene paradoxa
Q8GUR5 Silene paradoxa
Q8GUR6 Silene paradoxa
Q8GUR7 Silene paradoxa
Q9ZSK6 Silene vulgaris
Q40157 Solanum lycopersicum
Q40158 Solanum lycopersicum
Q43512 Solanum lycopersicum
Q43513 Solanum lycopersicum
P43398 Trifolium repens
Q9AU16 Typha latifolia
Q944W1 Typha latifolia
Q41657 Vicia faba
DT598383 Welwitschia mirabilis
ADB85769 Wolffia arrhiza
B4FT00 Zea mays
B6SHS2 Zea mays
B6SGE6 Zea mays
B6SLF8 Zea mays
B6SPB8 Zea mays
B6SP45 Zea mays
B6STF1 Zea mays
B6SX38 Zea mays
B6TAZ4 Zea mays
B6T1L0 Zea mays
B6TYT0 Zea mays
B6T2H9 Zea mays
B6T3T0 Zea mays
B6T303 Zea mays

```
                                10        20        30        40        50        60        70        80        90       100       110
                               ....|....|....|....|....|....|....|....|....|....|....|....|....|....|....|....|....|....|....|....|.
B6T953 Zea mays                MA--FGGGNCGCGSGCKCGSGCGGC---KMYPDMVEQVTTTTTTQTLIMGVAPST-------G-GFEA--AAG----AENGGCK-CG---AS-----CTC-DPCTCK----
B6UC14 Zea mays                MS--CSSGKXNCGSSCSCGSSCN-CM----SPDV-ETAAAS-SIKTMVLAAPTTKASAGG-----FEAATEGG---GCDCNTCN-CG---TSC---GCSC---CSCN----
B6U9S4 Zea mays                MS--CCGGNCGCGSGCKCGNGCGGC--SKMYPDMAEQVT-TTTTQALIMGVAPSKGHAE---G-GFEA--AAG----VENGGCK-CG---GN-----CQC-DPCNCGK---

                                10        20        30        40        50        60        70        80        90       100       110
                               ....|....|....|....|....|....|....|....|....|....|....|....|....|....|....|....|....|....|....|....|.
Q43515 Solanum lycopersicum    MSGCGGSCNCGSSCSCGKG-GGCNMYPDL-EKSTTLT----IIEGVAPMNNKGMVEGSIEKATEGGN-GCK-CG--SSCKCDPCNCCSASTIWT----------------
B6TGQ8 Zea mays                MSCCGGNCGCGSGCKCGSGCGGCKMYPDMVEQVTTTTTTQTLIMGVAPST------GGFEAAAGAENGGCK-CG--ASCHLRPLHPASEDDRVQHAXRDDGGSS-------
B6TJN1 Zea mays                MSCCGGNCGCGAGCKCGSGCGGCKMYPDMAEQVTTTT--QTLIMGVAPSK------GGFEAAAGAENGGCKYCGKVKAGGAYTMNTASAVTVRSTIRRLREQTEA------
```

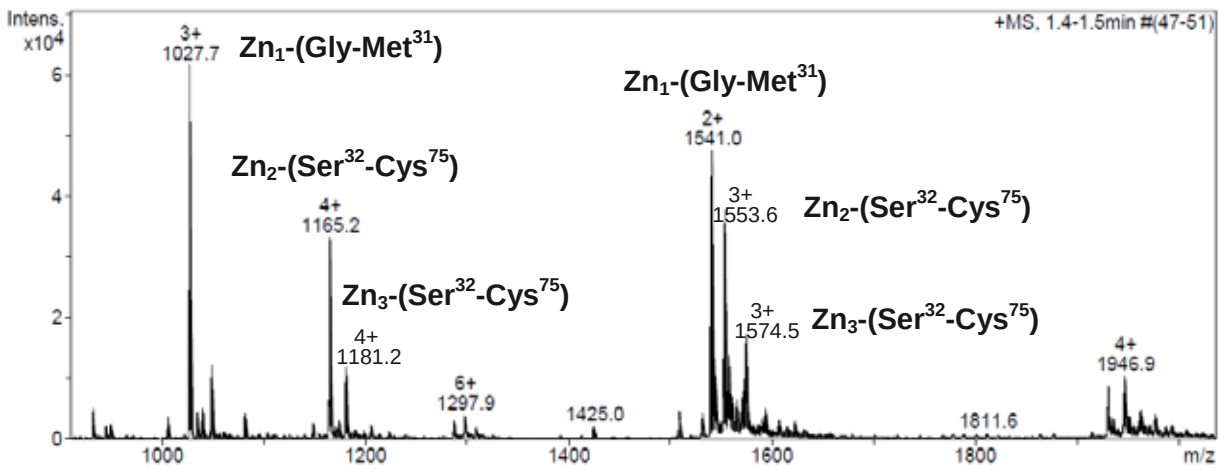

Species	Calculated MW	Experimental MW
Zn_1-(Gly-Met^{31})	3081.4	3080.1
Zn_2-(Ser^{32}-Cys^{75})	4656.4	4657.3
Zn_3-(Ser^{32}-Cys^{75})	4719.7	4720.7

Figure S1. ESI-MS spectrum recorded at pH 7.0 for Zn-HaMT1 fraction 2. The signals at 1297.9 m/z (charge-state 6+) and 1946.9 m/z (charge-state 4+) correspond to the Zn(II)-loaded entire peptide HaMT1 species already assigned in the pure fraction 1. The error associated with the experimental MW values was always lower than 0.1 %.

5 Cd(II) eq added	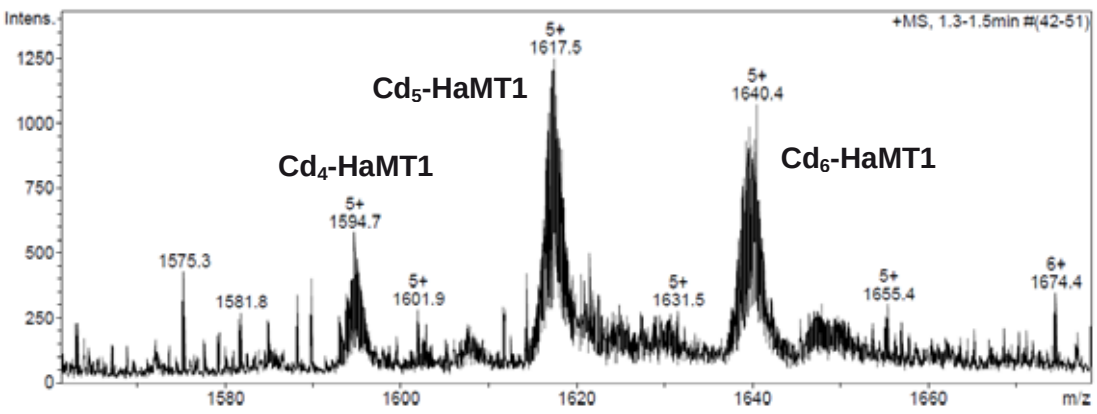
8 Cd(II) eq added	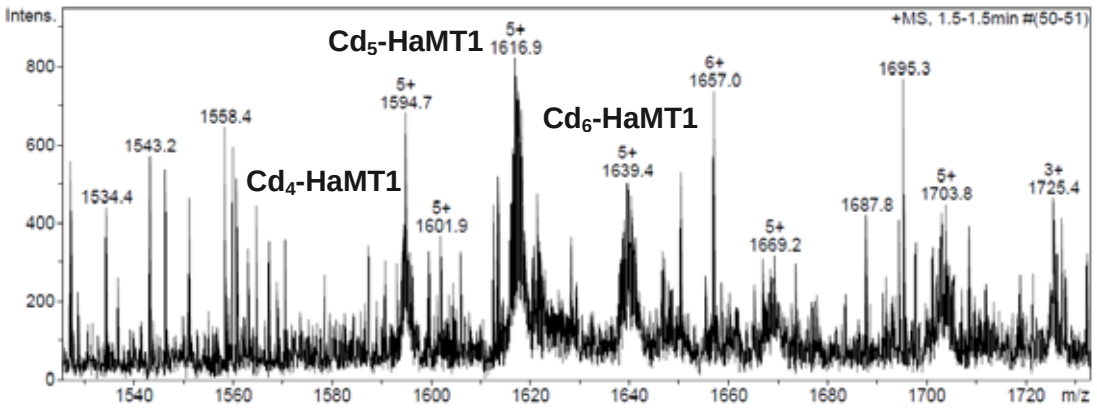
9 Cd(II) eq added	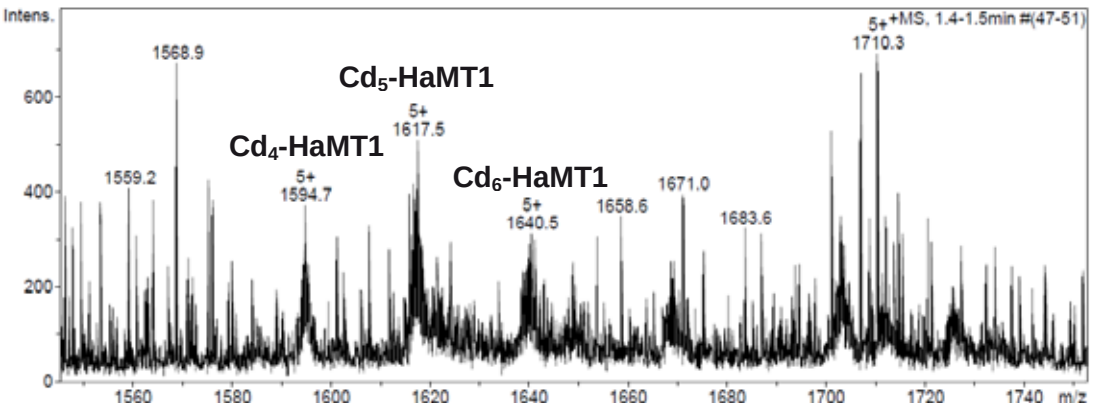

Figure S2. ESI-MS spectra at the +5 charge state recorded at different stages of the titration of Zn-HaMT1 with Cd(II) at pH 7.

5 Cd(II) eq added	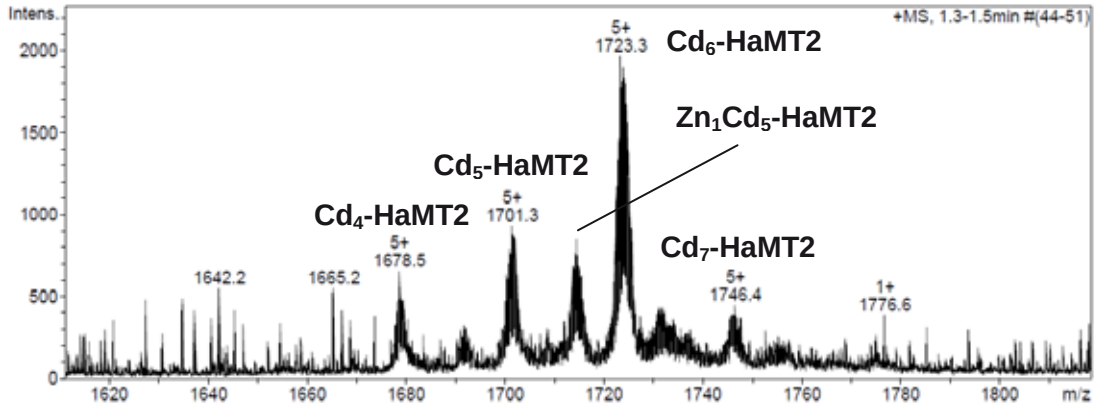
8 Cd(II) eq added	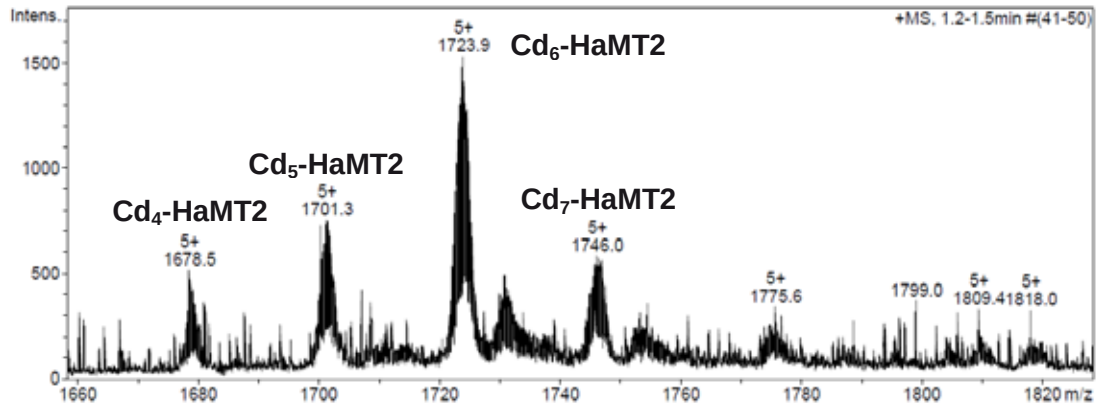

Figure S3. ESI-MS spectra at the +5 charge state recorded at different stages of the titration of Zn-HaMT2 with Cd(II) at pH 7.

Capítol 4

His-containing plant metallothioneins: comparative study of divalent metal-ion binding by plant MT3 and MT4 isoforms

CAPÍTOL 4

His-containing plant metallothioneins: comparative study of divalent metal-ion binding by plant MT3 and MT4 isoforms

1. Introduction

Metallothioneins (MTs) are small, Cys-rich (*ca.* 30% of the amino acid residues) proteins capable of coordinating metal ions such as Zn(II), Cd(II) or Cu(I). Due to the reactivity of the cysteine thiolate groups, MTs show both metal binding and redox activities. Because of these molecular properties [1,2], several different physiological functions have been proposed for MTs, mainly related to metal homeostasis and detoxification processes, as well as to oxidative stress protection. Being widely spread in nature in all eukaryotes and most prokaryotes, MTs are currently classified into fifteen families following taxonomical criteria [3]. Plant MTs, placed in family 15, are further classified into four sub-families based on the patterns of their conserved Cys residues [4]. The p1, p2 and p3 sub-families have two Cys-rich regions, with six Cys at the C-terminal domain and six, eight, and four Cys, respectively, at the N-terminal Cys-rich region; and p4 or pec MTs have three Cys-rich regions containing six, six, and five Cys residues each. Broadly speaking, it could be stated that plant MTs differ from the paradigmatic MT family 1 (mammalian MTs) by exhibiting longer amino acid sequences, even containing some aromatic residues, and a characteristic Cys-free region (or spacer) between their Cys-rich regions [for recent plant MT reviews *cf.* 5,6]. These features give rise to the possibility of considering alternative metal-MT complexes where non-cysteine ligands, such as His, could contribute to metal ion coordination. Interestingly, only three 3D structures for His-containing MTs have been solved so far, and with different results regarding His participation in metal binding. Hence, the His residue does not participate in Cu(I)-binding in yeast Cup1 [7] but, contrarily, His is involved in the Zn(II) coordination of wheat Ec-1 [8] and in Zn(II)- or Cd(II)-binding in *Synechococcus* SmtA [9], to build an $M(II)_4(SCys)_9(NHis)_2$ aggregate. Despite the presence of His being rather unusual in most MT families, at least one representative of each sub-family (p1, p2, p3 or pec) of plant MTs contains one or more His residues.

Type 3 plant MTs (p3 sub-family, MT3 from now on) contain 10 Cys residues within two Cys-rich domains and they are further subdivided into subtypes, since some of them exhibit additional potential metal ligands, either Cys or His residues, in their sequences [10] (*cf*. Table S1). Hence, a few MT3 peptides display additional Cys residues, located at their C-term Cys-rich domains, except for *Noccaea caerulescens* MT3. However, and most significantly, either one or two His residues are also present. If there is only one His, it nearly always constitutes the MT3 C-terminus. If there is a second His, it is located in the spacer region, either central or near the second Cys-rich domain. The only exceptions to this general rule are found in the barley MT3 and in the A2Y1D7 rice MT3 isoform. Very little is known about the plant MT3 metal-binding abilities, thus little information is available on the role of the conserved His occurring in their sequences. Hence, the MT3-A-GST fusion protein from palm oil (*Elaeis guineensis*) was reported to bind 1.7 Zn(II) ions more than the GST tag alone when expressed in Zn-enriched *E. coli* cells [11]. On the contrary, banana (*Musa acuminata*) MT3, sharing high sequence similarity to *E. guineensis* MT3, and which also includes an additional His residue at the same position, was found to coordinate 4.3 Cd(II) and 3.0 Zn(II) ions. Significantly, incubation of *M. acuminata* Zn_3-MT3 complexes with an excess of Zn(II) led to the incorporation of a 4^{th} metal ion, and the study of its His-to-Ala and His-to-Cys mutants revealed that His46 was essential to obtain this Zn_4-MT3 species [10]. Recombinant MT3 from *N. caerulescens*, containing 11 Cys residues, yielded Cd_5- and Zn_4-complexes as major species detected through ESI-MS [12]. And finally, only undermetallated Zn- and Cd-loaded recombinant complexes (metal:MT ratio ranging from 0.00 to 0.81) were recovered for the *H. vulgare* MT3 isoform [13].

In another scenario, type 4 MTs (p4 or pec subfamily, MT4 from now on) have been the most studied among all plant MTs, probably due to their peculiar amino acid sequence and the availability of native material [14]. In particular, Zn-Ec-1 from wheat (*Triticum aestivum*), the paradigmatic type 4 MT, has been shown to bind up to 6 Zn(II) ions [15,16]. Its 3D structure, the only one known for a plant MT, reveals how the three Cys-rich regions are organised into two separate coordinating domains, giving rise to a novel $Zn_2(SCys)_6$ cluster (γ domain) [17], and a Zn_4-β_E domain, which contains the first $Zn(SCys)_2(NHis)_2$ site reported in MTs as well as the typical $Zn_3(SCys)_9$ cluster, also present in mammalian βMT domains [8]. The high affinity that this site shows for Zn(II) over Cd(II) suggests a certain degree of metal specificity [18]. Furthermore, His40, but not

His32, seems to be critical for the correct folding, and hence for the biological function of Ec-1 [19]. Almost all known flowering plant MT4 peptides include two His residues in their central Cys-rich domains, except for *G. max* MT4, for which we previously reported the presence of only one of them [20], and *Camellia japonica* MT4 (JK711196), which lacks the other highly conserved His residue in this sub-family (*cf*. Table S2). With plant type 4 MTs landscape being dominated by Ec-1 from wheat, only a few MT4 peptides from other species have been studied. As for MT3, unexpected poorly loaded Zn- and Cd-MT4 complexes were detected for barley (*Hordeum vulgare*) MT4 (2.6-3.3 Zn/MT and 0.0-0.12 Cd/MT [13]). The same situation was observed for *Sesame indicum* MT4, with only 2 Zn/MT [21]. Finally, the metal-binding capacity of the MT4a and MT4b isoforms from *Arabidopsis thaliana* have been recently reported [5], coinciding with the Zn_6- and Cd_6-species previously established for wheat Ec-1.

To understand further the His contribution to metal coordination in different plant MTs, we report here the Zn(II) and Cd(II) binding properties of type 3 and type 4 MTs from soybean (*Glycine max*) and sunflower (*Helianthus annuus*), either for their wild-type and for some site-directed-mutant forms (Fig. 1). Wild-type MT3 from soybean (GmMT3) contains two His residues, while sunflower MT3 (HaMT3) has only the C-terminal His. The respective C-terminal His-to-Ala mutants H66AGmMT3 and H67AHaMT3 have been constructed in this study for comparative purposes. Sunflower MT4 (HaMT4), equivalent to Ec-1 in terms of Cys and His patterns, and a soybean MT4 isoform (GmMT4), where the second His is naturally substituted by a Tyr, are also analysed. The corresponding Zn- and Cd-complexes of all these MTs have been recombinantly synthesised in metal-enriched *E. coli* cultures. These complexes, together with DEPC-modified forms have been characterised by means of ICP-AES, CD and UV spectroscopies, as well as ESI-TOF mass spectrometry. The information on the role of His in sunflower and soybean MT3 and MT4, the former reported and analysed in this work for the first time, will contribute to a better understanding of the divalent metal ion coordination features of plant MTs.

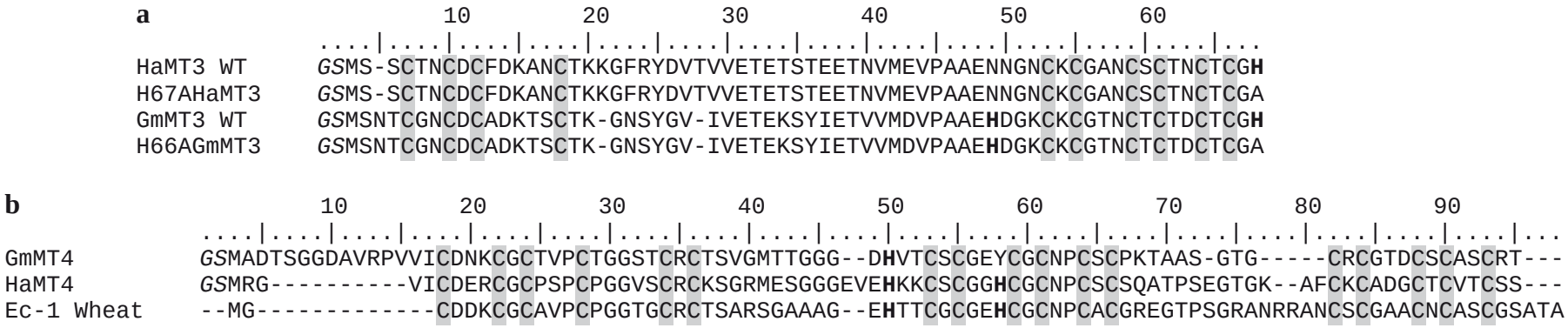

Figure 1 Amino acid sequences of the peptides studied in this work and of Ec-1 from wheat as reference MT4. Clustal alignment of **a** the type 3 MTs HaMT3 (GenBank accession code DY927914), H67AHaMT3, GmMT3 (CA819971.1) and H66AGmMT3, and of **b** the type 4 MTs GmMT4, HaMT4 (BQ975039) and Ec-1 (SwissProt accession code P30569). The shaded boxes indicate the cysteine residues, and histidines are in bold. The plasmid derived Gly-Ser dipeptide is shown in italics

2. Materials and methods

2.1. Source of MT cDNA clones

The GmMT3 and GmMT4 clones were previously obtained as reported [20]. The same strategy was followed to obtain the HaMT3 and HaMT4 cDNA clones. To this end, the NCBI Basic Local Alignment Search Tool (BLAST), namely the nucleotide blastn algorithm, was used to search in the ESTs library database, limiting the results to the *Helianthus annuus* organism. *Arabidopsis thaliana* metallothionein mRNA sequences NM_112401.1 (MT3) and NM_127888.1 (MT4a) were used as queries. Of the retrieved sequences, those showing a higher number of ESTs, indicative of a higher level of expressionfor each type of plant MTs, were selected. The ESTs clones DY927914 (HaMT3) and BQ975039 (HaMT4) were acquired from the University of Arizona (The Compositae Genome Project).

2.2. Expression vectors construction

Construction of the pGEX-GmMT3 and pGEX-GmMT4 expression plasmids was previously reported [20]. Additionally, the coding region of each of the two sunflower cDNAs, *HaMT3* and *HaMT4*, was subcloned into the pGEX-4T1 plasmid (GE Healthcare). Flanking *BamH*I/*Xho*I restriction sites were added by PCR amplification using the following oligonucleotides: 5'ATCGGATCCATGTCTTCCTGTACCAAC-3' as upstream primer and 5'-TATCTCGAGCTAGTGACCACATGTGCA-3' as downstream primer for *HaMT3*; 5'-ATCGGATCCATGAGGGGTGTTATATGTGACGA-3' as upstream primer and 5'-TTGCTCGAGTCAAGAGGAACAAGTGACACAAG-3' as downstream primer for *HaMT4*. For the construction of a cDNA encoding the H66AGmMT3 mutant, the corresponding wild-type sequence was amplified using 5'-GCGGGATCCATGTCGAACACATGCGGC-3' as upstream primer, and 5'-AAACTCGAGTTAAGCGCCACAGGTGCA-3' as downstream primer. The cDNA coding for the H67AHaMT3 peptide was constructed by amplifying the wild-type cDNA using the same upstream primer as for the wild-type cDNA (5'-ATCGGATCCATGTCTTCCTGTACCAAC-3'), but with 5'-TATCTCGAGCTAGGCCCACATGTGCA-3' as downstream primer.

All PCR reactions consisted of 35-cycle amplifications performed with 1.25 U of GoTaq DNA polymerase (Promega), 0.25 mM dNTPs and 0.20 μM of the required primers at 2 mM $MgCl_2$ (final concentration), in a final volume of 100 μL, under the following cycle conditions: 30 s at 94 ºC (denaturation), 30 s at 55 ºC (hybridisation) and 30 s at 72 ºC (elongation). An initial denaturation step, where samples were heated at 94 °C for 5 min, ensured the complete target DNA denaturation, and elongation conditions were maintained for 7 min after the 35 cycles. The final products were analysed by agarose gel electrophoresis/GelRed Nucleic Acid Gel Stain (Biotium) staining; and the band with the expected size was excised and subcloned into the pGEX-4T1 vector. All the cDNAs were confirmed by automated DNA sequencing. To this end, the pGEX-derived constructs were transformed into *E. coli* MATCH I cells, and plasmids recovered from those cells were sequenced using the ABI PRISM BigDye Terminator v3.1 Cycle Sequencing Kit (Applied Biosystems) in an ABI PRISM 310 Automatic Sequencer (Applied Biosystems).

2.3. Recombinant synthesis of MTs

The expression plasmids pGEX-HaMT3, pGEX-HaMT4, pGEX-H67AHaMT3, and pGEX-H66AGmMT3 were individually transformed into the protease defective strain *E. coli* BL21 for the synthesis of the respective GST-MT fusion polypeptides. The recombinant peptides were biosynthesised in 5L-cultures of recombinant *E. coli* BL21 cells. Expression was induced with 100 μM isopropyl ß-D-thiogalactopyranoside (IPTG) and cultures were supplemented with final concentrations of 300 μM $ZnCl_2$ or $CdCl_2$, and were allowed to grow for a further 3 h. Total protein extract was prepared from these cells, as previously described [22]. Metal complexes were recovered from GST fusion constructs by batch-affinity chromatography using Glutathione-Sepharose 4B (GE Healthcare) and thrombin cleavage. After concentration using Centriprep Microcon 3 (Amicon), the metal complexes were finally separated from thrombin through FPLC gel filtration in a Superdex75 column (GE Healthcare) equilibrated with 50 mM Tris-HCl, pH 7.0. Selected fractions were confirmed by 15 % SDS-PAGE and kept at -80 ºC until use. All procedures were performed using Ar (pure grade 5.6) saturated buffers. Further details on the purification procedure specific for recombinant plant MTs can be found in other related works [23,24]. As a consequence of the cloning procedure, the dipeptide Gly-Ser is added to the N-terminus of the

corresponding MT polypeptides. This minor modification of the native form was previously shown not to alter any of the MT metal-binding capacities [25].

2.4. Characterisation of the recombinant metal MT complexes

The S, Zn and Cd content of all M(II)-MT preparations was analysed by means of inductively coupled plasma atomic emission spectroscopy (ICP-AES) in a Polyscan 61E (Thermo Jarrell Ash) spectrometer, measuring S at 182.040 nm, Zn at 213.856 nm and Cd at 228.802 nm. Samples were treated as previously reported [26], but were alternatively incubated in 1 M HNO_3 at 65 °C for 10 min prior to measurements, in order to eliminate possible traces of acid-labile sulphide ions, as otherwise described [27]. Protein concentrations were calculated from the acidic ICP-AES sulphur measurement, assuming that all S atoms were contributed by the MT peptide.

A Jasco spectropolarimeter (Model J-715) interfaced to a computer (J700 software) was used for CD recording at a constant temperature of 25 ºC maintained by a Peltier PTC-351S apparatus. Electronic absorption measurements were performed on an HP-8453 diode array UV-visible spectrophotometer. All spectra were recorded with 1 cm capped quartz cuvettes, corrected for the dilution effects and processed using the GRAMS 32 Software.

Molecular mass determinations were performed by electrospray ionisation time-of-flight mass spectrometry (ESI-MS) on a Micro Q-TOF instrument (Bruker) interfaced with a Series 1100 HPLC Agilent pump, equipped with an autosampler, all of them controlled by the Compass Software. Calibration was attained with ESI-L Low Concentration Tuning Mix (Agilent Technologies). Samples containing MT complexes were analysed under the following conditions: 20 μL of protein solution injected through PEEK (polyether heteroketone) tubing (1.5 m x 0.18 mm i.d.) at 40 $\mu L \cdot min^{-1}$; capillary counter-electrode voltage 5 kV; desolvation temperature 90-110 ºC; dry gas 6 $L \cdot min^{-1}$; spectra collection range 800-2000 m/z. The carrier buffer was a 5:95 mixture of acetonitrile:ammonium acetate/ammonia (15 mM, pH 7.0). For analysis of all apo-MTs, 20 μL of the corresponding Zn-MT samples were injected under the same conditions described above, but using a 5:95 mixture of acetonitrile:formic acid pH 2.4 as liquid carrier, which caused the complete demetallation of the peptides.

2.5. In vitro *Zn(II) and Cd(II) binding studies*

Incubation of the Zn-MT samples with excess Zn(II) was carried out by adding five Zn(II) equivalents ($ZnCl_2$) to 15-20 μM solutions of the recombinantly obtained Zn-MT preparations. The mixtures were incubated overnight on ice in Tris-HCl 50 mM pH 7.0. Subsequently, CD and ESI-MS spectra were recorded at pH 7.0. For the Zn(II) with Cd(II) replacement studies, 15-20 μM preparations of the Zn(II)-MT complexes were titrated with incremental amounts of $CdCl_2$ (1-8 equiv) at pH 7. CD and UV spectra were recorded immediately after metal addition, and 10 min later, until stable spectra were obtained. All solutions were saturated with Ar to maintain oxygen-free conditions, and all the spectra were corrected for dilution effects.

2.6. Analysis of the histidine residues involved in metal ion coordination

Two strategies were used to ascertain whether the His residues of the analysed polypeptides contributed to divalent metal ion coordination. On the one hand, modification of the Zn(II)- and Cd(II)-loaded peptides with diethyl pyrocarbonate (DEPC) was followed by ESI-MS at pH 7.0 (conditions described above). A fresh DEPC solution in absolute ethanol (DEPC:ethanol 1:100) was allowed to react with a *ca.* 100 μM solution of the tested metal-MT complex in 50 mM Tris-HCl buffer pH 7.0. ESI-MS spectra were recorded at 5- and 24-min reaction times, and molar excess of DEPC was used to ensure the completeness of the modification. The resulting DEPC:polypeptide ratios used were 7:1 for GmMT3, 5:1 for H66AGmMT3, 5:1 for HaMT3, 7:1 for H67AHaMT3, 7:1 for HaMT4 and 5:1 for GmMT4. Half of the values of these DEPC ratios were also assayed in order to obtain more information on the patterns of modification. On the other hand, 10-20 μM preparations of the Cd(II)-MT complexes were acidified from pH 7 to pH 2 with incremental volumes of diluted HCl solutions, and subsequently re-neutralised to pH 7 with diluted NaOH. CD and UV spectra were recorded at each step, and all results were corrected for dilution effects. Oxygen-free conditions were maintained by saturation of all solutions with Ar during the experiments.

3. Results

3.1. Identification of the MT genes in sunflower

The *in silico* analysis of the whole soybean MT system has been recently reported by our group [20]. As regards the sunflower MT system, seven ESTs assignable to the four plant MT types were identified after an *in silico* NCBI EST database screening. One MT3-type EST was retrieved, which coded for a protein containing the canonical 4- and 6-Cys domains separated by a spacer region of 35 residues long. A single EST also was identified for the MT4 type, encoding a protein containing 17 Cys and 2 His, and matching the typical distribution pattern for this sub-family. These cDNAs were named *HaMT3* and *HaMT4* and the corresponding proteins, HaMT3 and HaMT4, respectively (*cf*. Fig. 1). The deduced soybean and sunflower MT3 and MT4 polypeptide sequences showed variability in their His content. Soybean MT3 (GmMT3) featured one His located in the spacer region, near the second Cys-rich domain, and a second His in the C-terminal position; whereas sunflower HaMT3 only contained the C-term His. Thus, these MTs represent some of the alternative Cys/His distribution patterns within the MT3 sub-family (*cf*. Table S1). As already stated before, HaMT4 showed the two conserved MT4 His residues at the Cys-rich central domain, so that the characteristic Cys and His distribution for the MT4 subfamily appeared untouched. On the other hand, soybean MT4 (GmMT4) showed a His-to-Tyr natural substitution for the second His in type 4 plant MTs (*cf*. Table S2).

3.2. Identity, purity and integrity of the recombinant polypeptides

DNA sequencing confirmed that the pGEX constructs for HaMT3, HaMT4, H67AHaMT3, and H66AGmMT3 synthesis included no artifactual nucleotide substitutions, and that the respective cDNAs were cloned in the correct frame after the GST coding sequence. The DNA constructs for GmMT3 and GmMT4 had been previously validated [20]. Recombinant syntheses yielded MT peptides in which their identity, purity and integrity were confirmed by the ESI-MS spectra of the respective apo-forms, obtained by acidification at pH 2.4 of the corresponding Zn-MT complexes. Hence, in each synthesis, a unique polypeptide of the expected molecular mass (including N-terminal Gly-Ser residues derived from the GST-fusion construct) was detected: 7114.9 ± 0.2 Da for HaMT3 (calculated average mass 7115.8 Da), 7048.9 ± 0.1 Da for

H67AHaMT3 (calculated 7049.8 Da); 6877.7 ± 0.5 Da for GmMT3 (calculated 6878.7 Da); 6811.6 ± 0.5 Da for H66AGmMT3 (calculated 6812.6 Da); 8451.5 ± 0.3 Da for GmMT4 (calculated 8452.5 Da); and 8265 ± 2 Da for HaMT4 (calculated 8265 Da) (*cf.* sequences in Fig. 1).

3.3. Zn(II)-binding properties of the recombinant MT3 polypeptides

Table 1

Analytical characterisation of the recombinant HaMT3, H67AHaMT3, GmMT3, H66AGmMT3, HaMT4 and GmMT4 preparations synthesised in Zn(II)-enriched media

Protein	His content	Protein concentration of Zn-MT preparations[a] (x 10^{-4} M)	Zn/MT content[b]	Zn-MT species[c]
HaMT3	1	2.2/2.1	3.6/3.5	**Zn_3**, **Zn_4**, Zn_2
H67AHaMT3	0	2.2/2.4	3.2/2.9	**Zn_3**, Zn_2, Zn_4
GmMT3	2	2.1/2.0	2.9/3.0	**Zn_3**, Zn_2, Zn_4
H66AGmMT3	1	0.2/0.2	3.0/3.1	**Zn_3**, Zn_2, Zn_4
HaMT4	2	1.7/2.0	6.7/6.0	Zn_6
GmMT4	1	1.1/1.2	5.8/5.6	Zn_5, Zn_6

[a] Protein concentration calculated from the sulfur content in normal/acid ICP-AES measurements, respectively. [b] Metal per MT molar ratio calculated from the zinc and sulfur content measured by normal or acid ICP-AES, respectively. [c] Zn-MT species present in the preparations calculated from the difference between holo- and apoprotein molecular masses obtained from ESI-MS. Major species are shown in bold

The recombinant syntheses of the four MT3 isoforms were first performed in Zn(II)-enriched *E. coli* cultures: wild-type MT3 from soybean (GmMT3), containing two His residues, sunflower MT3 (HaMT3), with only one C-term His, and the respective C-terminal His-to-Ala mutants H66AGmMT3 (keeping only the His of the spacer region), and H67AHaMT3 (devoid of His). The recovered Zn-MT3 complexes showed Zn(II)-to-MT3 stoichiometries concordant with their Cys content (10 residues), and comparable to those reported before for the GmMT3 isoform [20] (Table 1). In particular, HaMT3 yielded a mixture of major Zn_3- and Zn_4-HaMT3 species (Fig. 2a, upper panel), which correlated well with the mean *ca.* 3.5 Zn(II)/MT obtained from ICP-AES results (Table 1). In contrast, for H67AHaMT3, GmMT3 and H66AGmMT3, the major species detected was invariably Zn_3-MT3 (Fig. 2b-d, respectively), in agreement with the approximately 3 Zn(II)/MT measured by ICP-AES in all these cases. Significantly, the comparison between HaMT3 and its mutant form H67AHaMT3 reveals that the His/Ala substitution drastically reduces the presence of the Zn_4-species (Fig. 2a and 2b, upper panels, respectively), thus strongly suggesting the participation of His67 in Zn(II) binding, at least

a

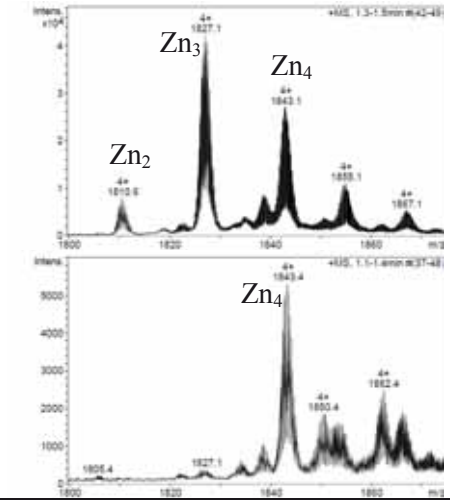

Species	Cal. MW	Exp. MW
Zn_2-HaMT3	7242.6	7239.4
Zn_3-HaMT3	7306.0	7304.4
Zn_4-HaMT3	7369.3	7368.4

b

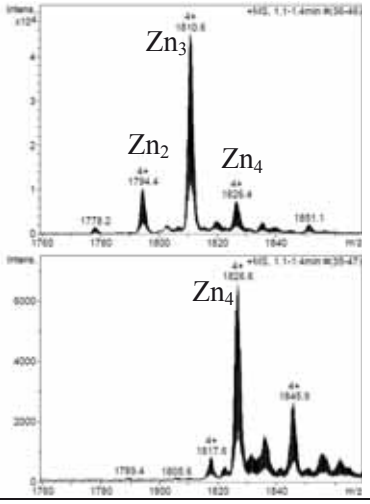

Species	Cal. MW	Exp. MW
Zn_2-H67AHaMT3	7176.5	7173.6
Zn_3-H67AHaMT3	7239.9	7238.4
Zn_4-H67AHaMT3	7303.3	7301.6

c

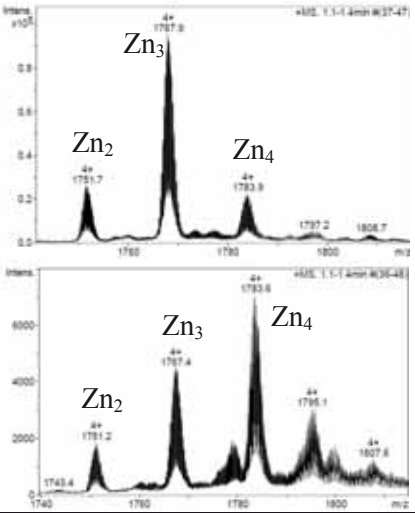

Species	Cal. MW	Exp. MW
Zn_2-GmMT3	7005.4	7002.0
Zn_3-GmMT3	7068.8	7067.6
Zn_4-GmMT3	7132.2	7131.6

d

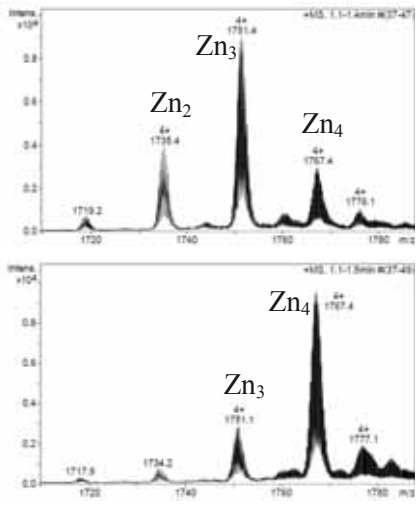

Species	Cal. MW	Exp. MW
Zn_2-H66AGmMT3	6939.3	6937.6
Zn_3-H66AGmMT3	7002.7	7001.6
Zn_4-H66AGmMT3	7066.1	7065.1

Figure 2 Representative charge states for the ESI-MS spectra recorded at pH 7.0 of recombinant **a** Zn-HaMT3, **b** Zn-H67AHaMT3, **c** Zn-GmMT3 and **d** Zn-H66AGmMT3 before (above) and after (below) the incubation with an excess of Zn(II) (5 equiv, over-night incubation on ice). The error associated with the experimental MW values was always lower than 0.1 %. Major species in the recombinantly synthesised preparations (above) are shown in bold

in the subset of the Zn_4-complexes present in the sample. Contrarily, at this point, no relevant differences are observed between GmMT3 and H66AGmMT3 (Fig. 2c and 2d, respectively). In order to detect other possible differences in Zn(II) coordination between GmMT3 and HaMT3, all the recovered preparations were Zn-saturated by incubation with

an excess of this metal ion (addition of 5 Zn(II) ions per mol of recombinant MT). Surprisingly, all cases (including H67AHaMT3) rendered the corresponding Zn_4-MT3 complexes as the major species (lower panels in Fig. 2 a-d), although clear differences appeared for secondary peaks, which could not be unambiguously attributed. However, it is worth noting that these minor, overmetallated peaks were less important in the His-to-Ala mutants. Unfortunately, the CD spectra of all these preparations exhibited non-informative fingerprints, devoid of clear absorption maxima at the expected wavelengths – *i.e. ca.* 240 nm- (Fig. 3), which furthermore remained unaltered after exposure to the additional 5 Zn(II) equiv (data not shown). Bearing in mind the canonical Zn_3-$(SCys)_9$ and Zn_4-$(SCys)_{11}$ clusters formed by the mammalian MTs, one could expect that the lack of an 11^{th} ligand would lead to a major Zn_3-species, as is also the case for the *M. acuminata* H46A MT3 mutant [10], bearing 10 Cys, and no His residues. However, this is not the case for H67AHaMT3, as our results under excess Zn(II) conditions have clearly demonstrated.

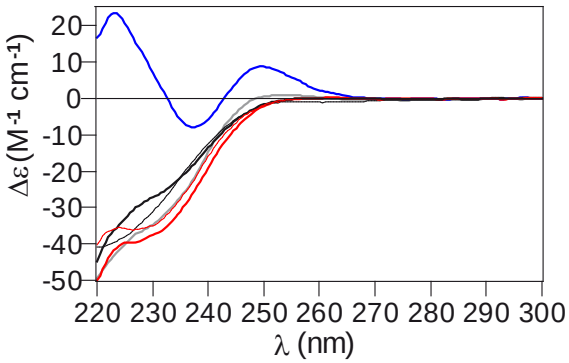

Figure 3 CD spectra corresponding to recombinant Zn-HaMT3 (red solid line), Zn-H67AHaMT3 (red dashed line), Zn-GmMT3 (black solid line), Zn-H66AGmMT3 (black dashed line), Zn-HaMT4 (blue line) and Zn-GmMT4 (grey line)

3.4. Zn(II)-binding properties of the recombinant MT4 polypeptides

Sunflower MT4 (HaMT4), with a Cys/His pattern identical to Ec-1, and a soybean MT4 (GmMT4), where the second His is naturally substituted by a Tyr, were also synthesised in Zn(II)-supplemented bacterial cultures. A unique Zn_6-HaMT4 species was recovered, while conversely, GmMT4 yielded an equimolar mixture of Zn_5- and Zn_6-GmMT4 complexes (Fig. 4a, Table 1), thus reproducing the stoichiometry and speciation reported before [20]. This mixture evolved to an almost unique Zn_6-GmMT4 species only after incubation with a Zn(II) excess (Fig. 4b). The Zn_6-HaMT4 species remained invariable after the addition of an excess of Zn(II) and, exceptionally, when compared to

the rest of the Zn-MT preparations analysed here, its CD spectrum (Fig. 3) showed the typical exciton coupling at *ca.* 245 nm normally associated with the $Zn(SCys)_4$ chromophores [25]. The strict conservation of the His and Cys pattern in Ec-1 and HaMT4 (Fig. 1), and the fact that a unique Zn_6 species was also recovered after recombinant synthesis of Ec-1 in Zn(II)-enriched media [8,17], strongly supports similar architectures for both Zn(II)-MT4 complexes. Hence, two separate Zn_2-γ and Zn_4-β_E domains, containing a $Zn_2(SCys)_6$ cluster in the former, and both a $Zn(SCys)_2(NHis)_2$ site and a $Zn_3(SCys)_9$ cluster in the latter, could be present in Zn-HaMT4. Furthermore, it has been reported that both the single and double His-to-Ala mutants of Ec-1 rendered a mixture of Zn_5 and Zn_6 species when synthesised in Zn(II)-enriched cultures [19], thus our results for Zn-GmMT4 fit perfectly well within this scenario, since GmMT4 features a H40Y mutation with respect to Ec-1 (numbering refers to Ec-1 sequence; see Fig. 1). Besides, the forced Zn_6-GmMT4 complexes presented the same non-informative CD spectrum as the initial Zn_5- and Zn_6-GmMT4 mixture (data not shown). It is worth noting that recent studies on *A. thaliana* MT4a and MT4b, also encompassing 17 Cys and 2 His residues, coincidently showed the formation of major Zn_6- and Cd_6-species when exposed to Zn(II) or Cd(II), respectively [5]. Therefore, similar metal-binding features are envisaged for all the MT4-type proteins that include 2 His in their sequence (*i.e*. Ec-1, *A. thaliana* MT4a and MT4b, and HaMT4), in contrast with GmMT4, encompassing a unique His.

a

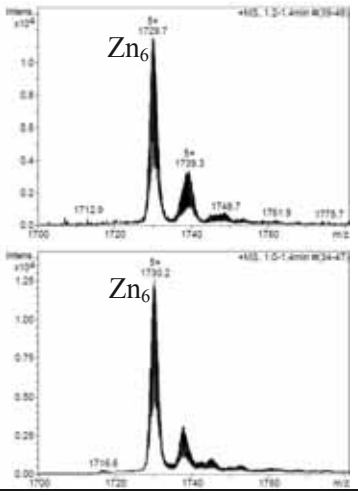

Species	Cal. MW	Exp. MW
Zn_6-HaMT4	8645.7	8645.0

b

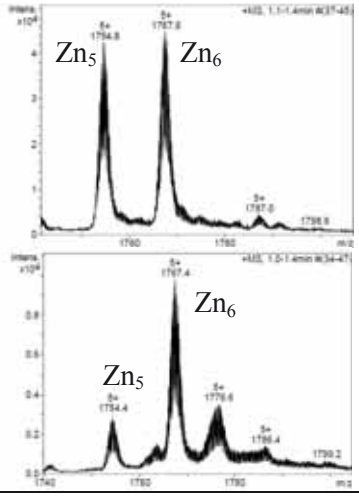

Species	Cal. MW	Exp. MW
Zn_5-GmMT4	8769.4	8769.0
Zn_6-GmMT4	8832.8	8833.0

Figure 4 Representative charge states for the ESI-MS spectra recorded at pH 7.0 of recombinant **a** Zn-HaMT4 and **b** Zn-GmMT4 before (above) and after (below) the incubation with an excess of Zn(II) (5 equiv, over-night incubation on ice). The error associated with the experimental MW values was always lower than 0.1 %

3.5. Cd(II)-binding properties of the recombinant MT3 and MT4 polypeptides

When HaMT3 or H67AHaMT3 were synthesised in Cd(II)-enriched *E. coli* cultures, a unique Cd_4 species was invariably detected by ESI-MS (Table 2, Fig. 5a,b). Furthermore, the differences observed between the conventional and acid ICP-AES measurements of both preparations (Table 2), as well as their characteristic CD spectra (see below), clearly suggested the presence of some Cd-complexes containing S^{2-} ligands [27], although these species could not be detected by ESI-MS. Cd_4-GmMT3 was also the most abundant species for the *G. max* MT, although here Cd_5 and Cd_6S_1 minor species were also detected (Fig. 5c). Cd-H66AGmMT3 yielded the most heterogeneous sample, including a mixture of species ranging from Cd_4 to Cd_6S_1, with Cd_5S_3 and Cd_6S_1 being the major complexes (Fig. 5d). These results, together with the low amount of protein rendered by the recombinant syntheses, suggested a low stability of the Cd-GmMT3 complexes.

Table 2

Analytical characterisation of the recombinant HaMT3, H67AHaMT3, GmMT3, H66AGmMT3, HaMT4 and GmMT4 preparations synthesised in Cd(II)-enriched media

Protein	His content	Protein concentration of Cd-complexes[a] (x 10^{-4} M)	Cd/MT content[b]	Cd-MT species[c]
HaMT3	1	1.8/1.1	2.7/4.5	Cd_4
H67AHaMT3	0	1.1/0.8	3.9/3.1	Cd_4
GmMT3	2	0.3/0.3	5.2/6.2	**Cd_4** Cd_5, Cd_6S_1
H66AGmMT3	1	0.6/0.5	3.4/4.0	**Cd_5S_3, Cd_6S_1** Cd_4, Cd_5, Cd_5S_1
HaMT4	2	1.7/1.5	4.3/7.5	**Cd_6** Cd_8S_1
GmMT4	1	1.9/1.3	5.9/7.7	**Cd_6** Cd_8S_1

[a] Protein concentration calculated from the sulfur content in normal/acid ICP-AES measurements, respectively. [b] Metal per MT molar ratio calculated from the cadmium and sulfur content measured by normal or acid ICP-AES, respectively. [c] Cd-MT species present in the preparations calculated from the difference between holo- and apoprotein molecular masses obtained from ESI-MS. Major species are shown in bold

a

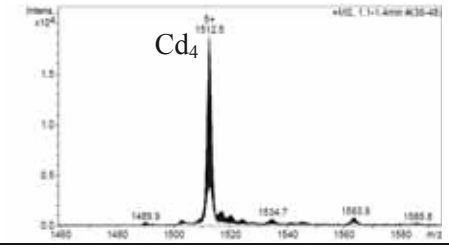

Species	Cal. MW	Exp. MW
Cd_4-HaMT3	7557.4	7557.5

b

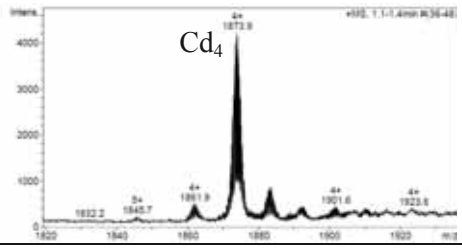

Species	Cal. MW	Exp. MW
Cd_4-H67AHaMT3	7491.3	7491.6

c

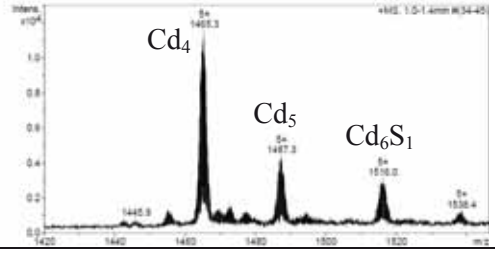

Species	Cal. MW	Exp. MW
Cd_4-GmMT3	7320.2	7320.5
Cd_5-GmMT3	7430.6	7431.5
Cd_6S_1-GmMT3	7575.1	7575.0

d

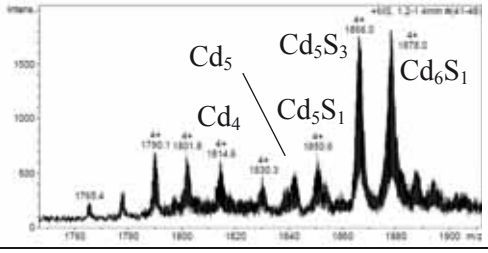

Species	Cal. MW	Exp. MW
Cd_4-H66AGmMT3	7254.2	7254.4
Cd_5-H66AGmMT3	7364.6	7363.8
Cd_5S_1H66AGmMT3	7398.7	7398.4
Cd_5S_3H66AGmMT3	7466.8	7460.0
Cd_6S_1H66AGmMT3	7509.0	7508.0

Figure 5 Representative charge states for the ESI-MS spectra recorded at pH 7.0 of recombinant **a** Cd-HaMT3, **b** Cd-H67AHaMT3, **c** Cd-GmMT3 and **d** Cd-H66AGmMT3. The error associated with the experimental MW values was always lower than 0.1 %. Major species are shown in bold

The CD spectra of all the Cd-MT3 preparations (Fig. 6a,b) exhibited two types of absorptions: those typical of the $Cd(SCys)_4$ chromophores of the Cd-MT complexes centred at *ca.* 250 nm [25] and those in the 275-300 nm range, which are related to the presence of S^{2-} ligands as a third component of the Cd-MT species [27]. Although the complex speciation found for both Cd-GmMT3 preparations (ESI-MS spectra; Fig. 5c,d) precluded any assignment of the CD spectra in relation to the participation of the C-term His in Cd(II)-binding (Fig. 6a), the patent difference between the ESI-MS spectra suggested a participation of His66 in Cd(II) coordination. More significant differences were detected when comparing the CD spectra of the Cd_4-HaMT3 and Cd_4-H67AHaMT3 complexes (Fig. 6b). While Cd_4-HaMT3 showed a clear exciton coupling centred at 250 nm, this absorption was far less intense and slightly red-shifted in Cd_4-H67AHaMT3, and the absorption maxima at 280(+) nm of the latter was also red-shifted towards that of the former – at 275 nm. These variations supported the participation of HaMT3 His67 in Cd(II)-binding, despite the apparent similarity of the speciation of both samples shown by ESI-MS (*cf.* Fig. 5a,b). To further ascertain this point, Cd_4-HaMT3 preparations were

acidified from pH 7 to pH 2, with the rationale that Cd(II) is released from NHis binding sites at a 4-5 pH range owing to His protonation [28], while the lower pKa of the cysteine thiolates still allows the existence of CdSCys bonds. Hence, for Cd_4-HaMT3, the initial exciton coupling CD band centred at 250 nm decreased its intensity when lowering the pH from 4.9 to 4.0 (Fig. 6b and Fig. S1), thus generating a CD fingerprint close to that of Cd-H67AHaMT3. In other words, the CD spectra of the preparations of Cd-HaMT3 devoid of His, or when this residue is no longer able to bind Cd(II) because of a solution with a pH lower than the His pKa (*i.e.* His-to-Ala mutant and Cd-HaMT3 at pH 4.0, respectively), similarly exhibited a poorly resolved exciton coupling band at *ca.* 255 nm and a positive band at 280 nm. On the other hand, the spectra of Cd-HaMT3 at higher pH, when His is not supposed to be protonated, showed the intense and well-defined exciton coupling band at 250 nm, as well as an intense 275(+) nm band.

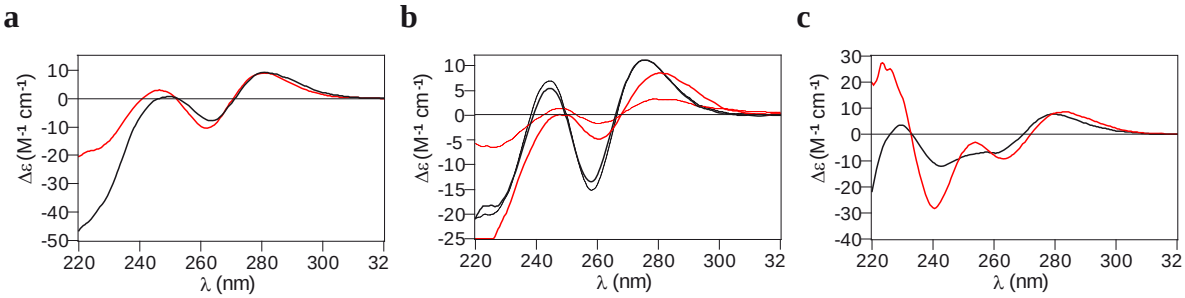

Figure 6 Comparison of the CD spectra of recombinantly synthesised: **a** Cd-GmMT3 (black line) and Cd-H66AGmMT3 (red line) at pH 7.0; **b** Cd-HaMT3 at pH 7.0 (black solid line), Cd-H67AHaMT3 at pH 7.0 (red solid line), Cd-HaMT3 at pH 4.9 (black dashed line) and Cd-HaMT3 at pH 4.0 (red dashed line); **c** Cd-GmMT4 (black line) and Cd-HaMT4 (red line)

As regards the type 4 MTs, Cd_6 was the major species detected for both GmMT4 and HaMT4, together with a minor Cd_8S_1 form (Fig. 7). Thus, the Cd-GmMT4 recombinant synthesis fully reproduced the previously reported results [20]. Unlike the CD spectra obtained for the Zn(II)-MT complexes, those of the Cd(II) preparations were complex but more informative. Hence, the CD fingerprints of the Cd-HaMT4 and Cd-GmMT4 samples were comparable (Fig. 6c). In this sense, it is interesting to point out that the CD spectrum reported for the recombinantly obtained Cd_6-Ec-1 features a different CD envelope, because it only exhibits a positive Gaussian band centred at 255 nm corresponding to its $Cd(SCys)_4$ chromophores [29]. Contrarily, both Cd-HaMT4 and Cd-GmMT4 CD spectra show comparable absorptions at almost the same wavelengths (although more intense for Cd-HaMT4, and thus compatible with a better folded complex). The clear and coincident absorbance at *ca.* 280 nm exhibited by both Cd-

HaMT4 and Cd-GmMT4 samples are a clear indication of the presence of sulphide ligands in both recombinant preparations [27].

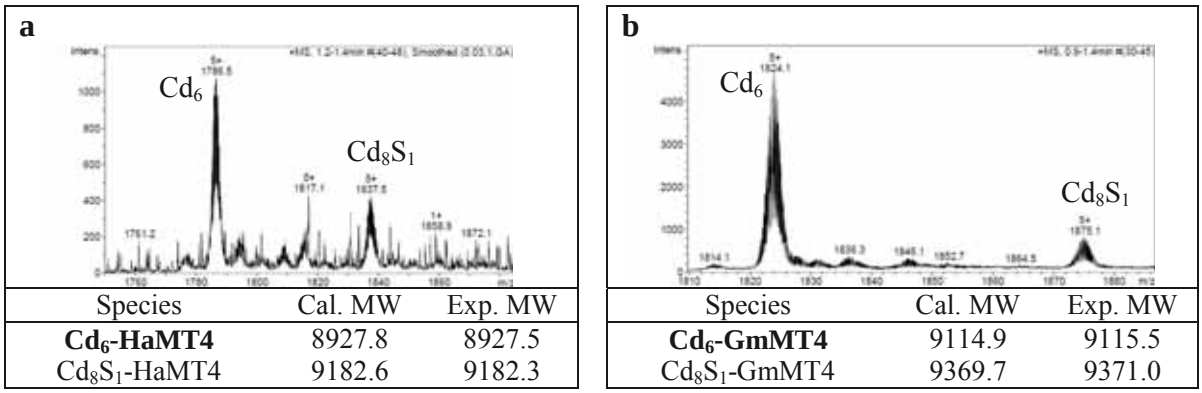

Species	Cal. MW	Exp. MW
Cd_6-HaMT4	8927.8	8927.5
Cd_8S_1-HaMT4	9182.6	9182.3

Species	Cal. MW	Exp. MW
Cd_6-GmMT4	9114.9	9115.5
Cd_8S_1-GmMT4	9369.7	9371.0

Figure 7 Representative charge states for the ESI-MS spectra recorded at pH 7.0 of recombinant **a** Cd-HaMT4 and **b** Cd-GmMT4. The error associated with the experimental MW values was always lower than 0.1 %. Major species are shown in bold

3.6. Histidine modification analysis

Diethyl pyrocarbonate (DEPC) is known to covalently modify the free (*i.e.* non-metal coordinated) histidine residues of proteins with a high efficiency [30,31,32,33]. In order to evaluate the number of histidines bound to metal ions in the metal-MT complexes studied in this work, the corresponding Zn- and Cd-MT preparations were incubated with DEPC, and the DEPC-modified derivatives were determined by ESI-MS. As previously reported for other Zn(II)- and Cd(II)-MT complexes, the free terminal α-NH_2 groups also react with DEPC [34], and therefore, when analysing the resulting ESI-MS spectra, at least this carboxyethyl (CEt) species (molecular mass increment of 72.1 Da) should be detected, and further CEt adducts would reflect the reaction of the non-protected (*i.e.* metal ion unbound) His residues within the metal-MT complexes present in the preparations. Two times of incubation and two DEPC:protein ratios were tested for each experiment. At the longest time of incubation (24 min), the number and amount of DEPC-modified species detected was comparable for the two doses of DEPC reactant assayed, and thus only the results at the longest time and higher dose conditions are here presented.

Zn-HaMT3 yielded two peaks corresponding to the one- and two-carboxyethylated derivatives (Fig. 8a), while only a mono-carboxyethylated Zn_4 species was identified for the His67Ala mutant (Fig. 8b). Hence, it can be assumed that the two-carboxyethylated Zn_4-HaMT3 species origins from the reaction of His67 with DEPC, thus

a

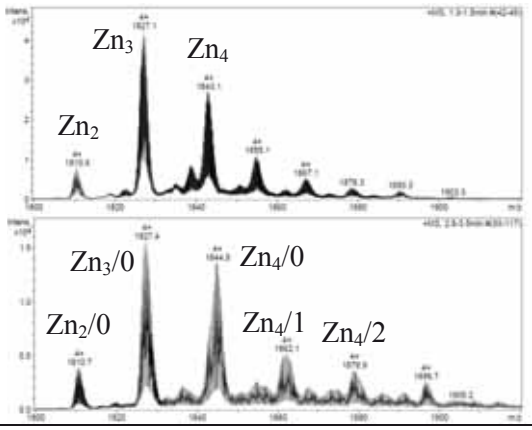

Species	Cal. MW	Exp. MW
Zn_3-HaMT3	7306.0	7304.4
Zn_4-HaMT3	7369.3	7368.4
Zn_4-HaMT3(CEt)	7444.4	7441.1
Zn_4-HaMT3(CEt)$_2$	7513.4	7511.6

b

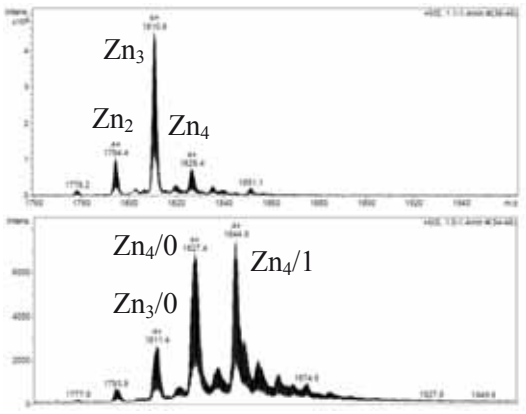

Species	Cal. MW	Exp. MW
Zn_2-H67AHaMT3	7176.5	7173.6
Zn_3-H67AHaMT3	7239.9	7238.4
Zn_4-H67AHaMT3	7303.3	7301.6
Zn_4-H67A(CEt)	7375.3	7374.4

c

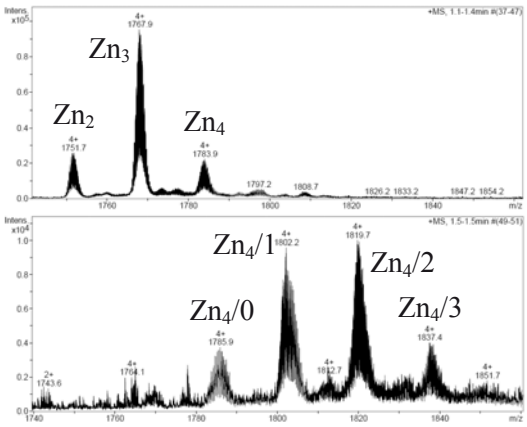

Species	Cal. MW	Exp. MW
Zn_2-GmMT3	7005.4	7002.0
Zn_3-GmMT3	7068.8	7067.6
Zn_4-GmMT3	7132.2	7131.6
Zn_4-GmMT3(CEt)	7204.2	7203.6
Zn_4-GmMT3(CEt)$_2$	7276.3	7273.6
Zn_4-GmMT3(CEt)$_3$	7348.3	7348.8

d

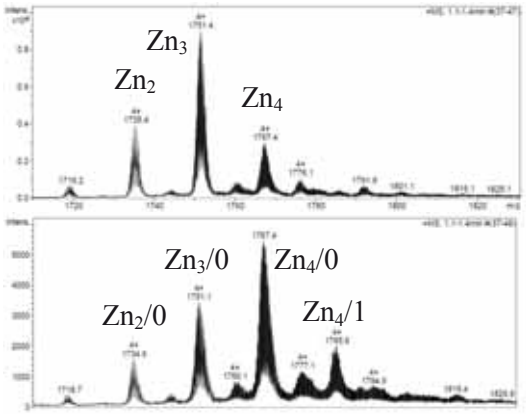

Species	Cal. MW	Exp. MW
Zn_2-H66AGmMT3	6939.3	6937.6
Zn_3-H66AGmMT3	7002.7	7001.6
Zn_4-H66AGmMT3	7066.1	7065.1
Zn_4-H66A(CEt)	7138.2	7137.6

Figure 8 Representative charge states for the ESI-MS spectra recorded at pH 7.0 for **a** Zn-HaMT3, **b** Zn-H67AHaMT3, **c** Zn-GmMT3 and **d** Zn-H66AGmMT3 before (above) and after (below) incubation with DEPC. The DEPC-modified peptide includes a carboxyethyl (CEt) group. The numbers in the spectra below indicate the number of CEt groups bound. The error associated with the experimental MW values was always lower than 0.1 %

showing that this residue is unbound for some of the complexes present in the solution. It can be also concluded that two sub-populations of complexes mainly coexist in the Zn-HaMT3 preparation as regards His participation in Zn(II)-binding: one where His67 was DEPC-protected (*i.e.* involved in metal ion coordination), and another where this His is free. For Zn-GmMT3, two main peaks corresponding to the one- and two-carboxyethylated derivatives were detected, while only a small signal matched the

molecular mass of the three-carboxyethylated species (Fig. 8c). Conversely, in the mutant, only one position (presumably its N-terminus) is strongly modified by DEPC (Fig. 8d), and therefore the remaining His (His47) could not be carboxyethylated. These results are in agreement with the existence of one subpopulation of Zn-GmMT3 complexes where both His are involved in Zn(II)-binding, and a subset of complexes where one His is free and the other participates in the metal cluster. Thus, it is suitable to conclude that in GmMT3, His47 would almost always contribute to Zn(II)-binding, while the C-term His66 would only participate in the subset of complexes where both His are coordinating Zn(II). Finally, the three-carboxyethylated species mentioned above would be representative of very minor Zn_4-GmMT3 complexes, where neither His47 nor His66 would be involved in Zn(II) coordination. Some observations regarding the results of the DEPC treatment are not easy to interpret, but they are in agreement with those observed in a parallel study with the *C. elegans* MT isoforms [34]. They mainly refer to the different DEPC-reactivity exhibited by several complexes of a same MT, or the apparent redistribution of species, even in the absence of DEPC modification. These phenomena could be due to different protein folding, which would condition the availability of reactant to amino acid side chains, or to a DEPC effect on weak metal-MT bonds, leading to cluster rearrangements.

With respect to Cd-HaMT3, the results on the Cd_4-HaMT3 (Fig. 9a) and Cd_4-H67AHaMT3 (Fig. 9b) complexes mainly indicate a mono-carboxyethylated derivative, which is attributable to the N-term residue modification, and we can therefore conclude that His67 participates in Cd(II)-binding in the wild type complexes. For Cd-GmMT3, the results were more complex, since a mixture of modified and unmodified species was detected by ESI-MS. For the wild-type protein, one- and two-carboxyethylated derivatives were identified for each one of the initial complexes (Cd_4-, Cd_5- and Cd_6S_1-GmMT3) (Fig. 9c), thus suggesting that one of the GmMT3 His would be always DEPC-protected, while the other would only be protected in a part of the complexes. The three-carboxyethylated species is of less importance than in the corresponding experiment with Zn-GmMT3, so that these data suggest a greater involvement of His in the Cd(II)- than in the Zn(II)-clusters, which can be related to physiological conditions where plant type 3 MTs are induced (discussed below) and/or may be in accordance with the greater bulkiness of Cd(II) ions. Moreover, the presence of two-carboxyethylated Cd_4 and Cd_6S_1 species in the mixture of the DEPC-incubated solution of the Cd-H66AGmMT3 preparation (Fig. 9d)

allows us to propose that His66 is most certainly the His residue involved in Cd(II)-binding in Cd_4- and Cd_6S_1-GmMT3. This means that the terminal histidine residue is involved in Cd-coordination in both MT3 studied.

a

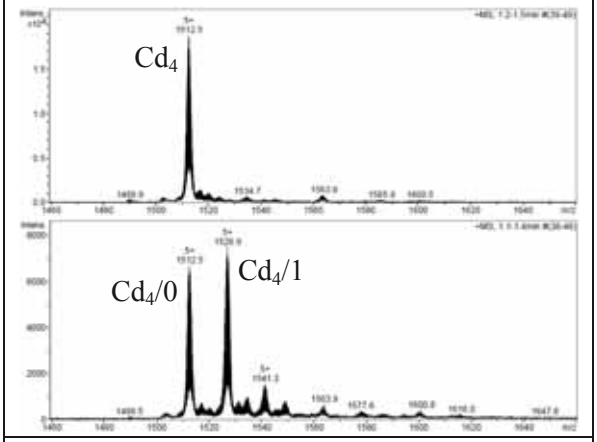

Species	Cal. MW	Exp. MW
Cd_4-HaMT3	7557.4	7557.5
Cd_4-HaMT3(CEt)	7629.5	7629.5

b

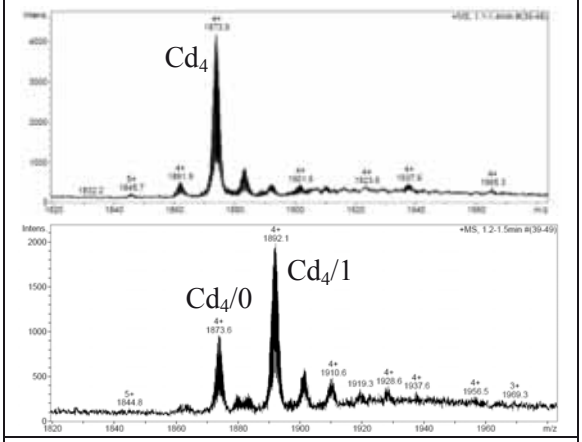

Species	Cal. MW	Exp. MW
Cd_4-H67AHaMT3	7491.3	7491.6
Cd_4-H67A(CEt)	7563.4	7562.4

c

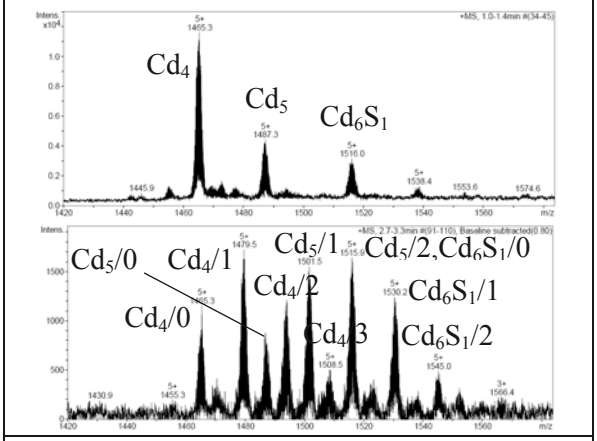

Species	Cal. MW	Exp. MW
Cd_4-GmMT3	7320.2	7320.5
Cd_4-GmMT3(CEt)	7392.3	7392.5
Cd_4-GmMT3(CEt)$_2$	7464.4	7464.5
Cd_4-GmMT3(CEt)$_3$	7536.4	7537.3
Cd_5-GmMT3	7430.6	7431.5
Cd_5-GmMT3(CEt)	7502.7	7502.5
Cd_5-GmMT3(CEt)$_2$	7574.8	7575.0
Cd_6S_1-GmMT3	7575.1	7575.0
Cd_6S_1-Gm3(CEt)	7647.2	7648.0
Cd_6S_1-Gm3(CEt)$_2$	7719.2	7720.0

d

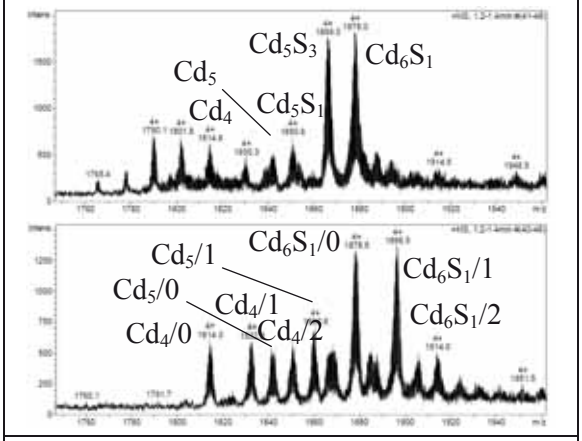

Species	Cal. MW	Exp. MW
Cd_4-H66AGmMT3	7254.2	7254.4
Cd_4-H66A(CEt)	7326.2	7327.2
Cd_4-H66A(CEt)$_2$	7398.3	7398.4
Cd_5-H66AGmMT3	7364.6	7365.2
Cd_5-H66A(CEt)	7436.6	7438.4
Cd_5S_1-H66A	7398.7	7398.4
Cd_5S_3-H66A	7466.8	7460.0
Cd_6S_1-H66A	7509.0	7508.0
Cd_6S_1-H66A(CEt)	7581.1	7581.2
Cd_6S_1-H66A(CEt)$_2$	7653.2	7652.0

Figure 9 Representative charge states for the ESI-MS spectra recorded at pH 7.0 for **a** Cd-HaMT3, **b** Cd-H67AHaMT3, **c** Cd-GmMT3 and **d** Cd-H66AGmMT3 before (above) and after (below) incubation with DEPC. The DEPC-modified peptide includes a carboxyethyl (CEt) group. The numbers in the spectra below indicate the number of CEt groups bound. The error associated with the experimental MW values was always lower than 0.1 %

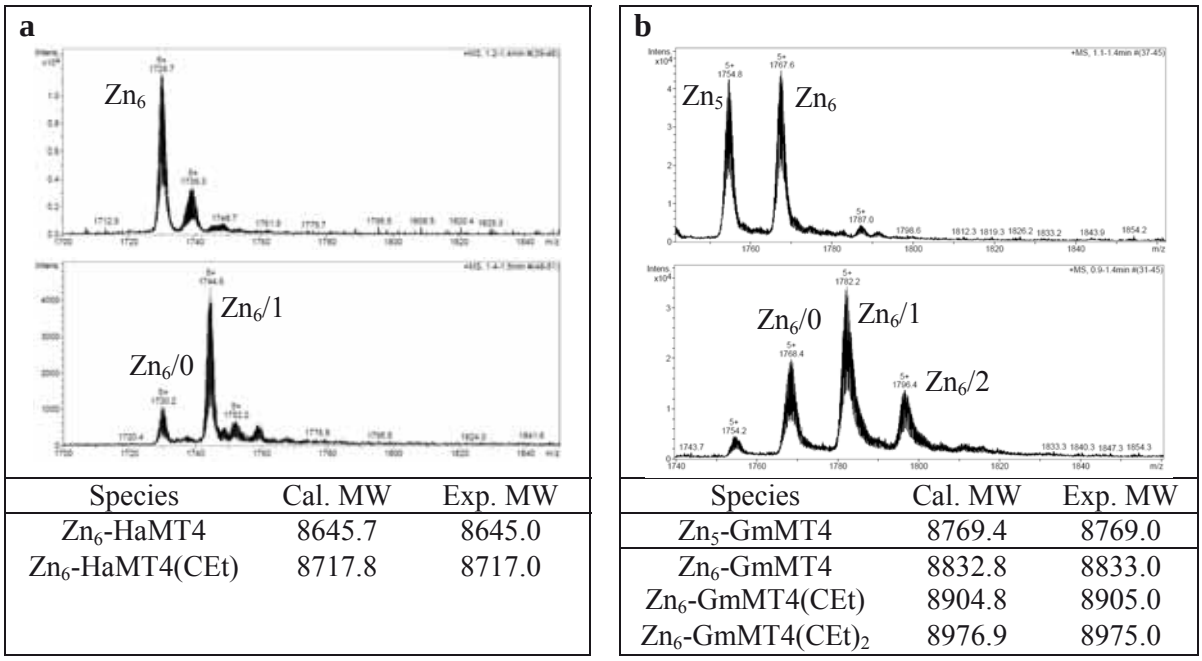

Species	Cal. MW	Exp. MW
Zn_6-HaMT4	8645.7	8645.0
Zn_6-HaMT4(CEt)	8717.8	8717.0

Species	Cal. MW	Exp. MW
Zn_5-GmMT4	8769.4	8769.0
Zn_6-GmMT4	8832.8	8833.0
Zn_6-GmMT4(CEt)	8904.8	8905.0
Zn_6-GmMT4(CEt)$_2$	8976.9	8975.0

Figure 10 Representative charge states for the ESI-MS spectra recorded at pH 7.0 for **a** Zn-HaMT4, **b** Zn-GmMT4 before (above) and after (below) incubation with DEPC. The DEPC-modified peptide includes a carboxyethyl (CEt) group. The numbers in the spectra below indicate the number of CEt groups bound. The error associated with the experimental MW values was always lower than 0.1 %

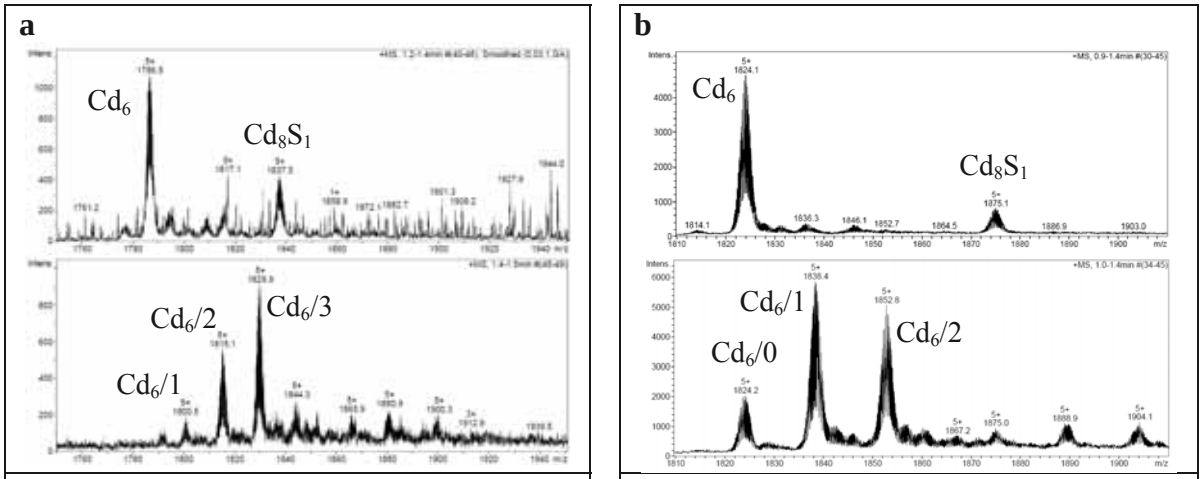

Species	Cal. MW	Exp. MW
Cd_6-HaMT4	8927.8	8927.5
Cd_6-HaMT4(CEt)	8999.8	8997.5
Cd_6-HaMT4(CEt)$_2$	9071.9	9070.5
Cd_6-HaMT4(CEt)$_3$	9144.0	9144.5

Species	Cal. MW	Exp. MW
Cd_6-GmMT4	9114.9	9115.5
Cd_6-GmMT4(CEt)	9186.9	9188.0
Cd_6-GmMT4(CEt)$_2$	9259.0	9258.0

Figure 11 Representative charge states for the ESI-MS spectra recorded at pH 7.0 for **a** Cd-HaMT4, **b** Cd-GmMT4 before (above) and after (below) incubation with DEPC. The DEPC-modified peptide includes a carboxyethyl (CEt) group. The numbers in the spectra below indicate the number of CEt groups bound. The error associated with the experimental MW values was always lower than 0.1 %

The results of the DEPC-reactivity experiments performed with the Zn- and Cd-complexes of the sunflower and soybean MT4 isoforms offered a more straightforward

interpretation. Hence, a mono-carboxyethylated derivative is detected for Zn-HaMT4 (Fig. 10a), leading to the conclusion that both His residues contribute to Zn(II)-binding in this complex. Conversely, for Zn-GmMT4, the mono-carboxyethylated derivative is assignable to the product of the reaction with the N-terminal amino group, while the two-carboxyethylated derivative (Fig. 10b) suggests that the unique His present in this polypeptide is mainly not involved in metal ion coordination, since it is accessible to DEPC. Finally, by analogy with the results obtained with Zn-HaMT4 and Zn-GmMT4, it is reasonable to conclude that none of the His residues existing in their sequences are involved in Cd(II) coordination (Fig. 11).

These results enable most of the roles of His residues in divalent metal ion coordination envisaged in the previous sections of this work to be confirmed. Zn-HaMT3 was the exception, where the experiments with DEPC (Fig. 8a) were not completely conclusive, since the amount of DEPC-modified species detected was unexpectedly low. However, the observed differences in stoichiometry for the recombinant wild-type and the His-to-Ala mutant Zn(II)-complexes (Table 1), together with the fact that the Zn/Cd replacement is isostructural for HaMT3 (Fig. S2 and Fig. S3), fully support the previous hypothesis of His67 participating in metal-binding in both Zn(II)- and Cd(II)-complexes.

4. Discussion and Conclusions

It can be concluded from the comprehensive interpretation of all the results presented in this work, that both soybean GmMT3 and sunflower HaMT3 feature similar divalent metal ion binding capacities, while substantial differences between soybean GmMT4 and sunflower HaMT4 have been detected. Focusing on His-metal coordination, it should be noted in advance that its occurrence does not always involve the totality of the complexes present in a preparation, but it rather defines a subset of His-contributed Zn- or Cd-species. Two clear examples of His coordination seem to arise from our data: the participation in Zn-binding of both His residues in HaMT4, and the involvement of C_{term} His in the coordination of Cd(II) in both MT3 isoforms studied. It is also patently evident that His would not contribute to Cd-binding in soybean and sunflower MT4. A comprehensive table (Table 3) summarises the most significant results contributed by this work and the main experimental data that support them.

Table 3

Summary of the Zn- and Cd-binding features of the plant MT3 and MT4 proteins analysed in this work.

Zn-MT complex	Zn/MT content[a]	Major Zn-MT species[b]	Major Zn-MT species after Zn(II) addition[b]	CD data[c]	DEPC-modified His[d]	Zn-binding His	His location scheme	Conclusions
HaMT3	3.5	Zn_3, Zn_4	Zn_4	n.i.	0/1	1/0	————H	C_{term} His binds Zn(II)
H67AHaMT3	2.9	Zn_3	Zn_4	n.i.	0	0	————	negative control
GmMT3	3.0	Zn_3	Zn_4	n.i.	0/1	2/1	———H——H	central His binds Zn(II)
H66AGmMT3	3.1	Zn_3	Zn_4	n.i.	0	1	———H———	central His binds Zn(II)
HaMT4	6.0	Zn_6	Zn_6	Zn(SCys)	0	2	———H—H—	both His bind Zn(II)
GmMT4	5.6	Zn_5, Zn_6	Zn_6	n.i.	1	0	———H———	His does not bind Zn(II)

Cd-MT complex	Cd/MT content[a]	Major Cd-MT species[b]	S^{2-} presence in Cd-complexes	CD data[e]	DEPC-modified His[d]	Cd-binding His	His location scheme	Conclusions
HaMT3	4.5	Cd_4	+	His	0	1	————H	C_{term} His binds Cd(II)
H67AHaMT3	3.1	Cd_4	+/-	---	0	0	————	negative control
GmMT3	6.2	Cd_4	+	His	1	1	———H——H	C_{term} His binds Cd(II)
H66AGmMT3	4.0	Cd_5S_3,Cd_6S_1	+	---	1	1	———H———	His does not bind Cd(II)
HaMT4	7.7	Cd_6	+	n.i.	2	0	———H—H—	None of the His bind Cd(II)
GmMT4	7.5	Cd_6	+	n.i.	1	0	———H———	His does not bind Cd(II)

[a] Metal per MT molar ratio calculated from the metal and sulfur content measured by acid ICP-AES. [b] Major M(II)-MT species present in the preparations calculated from the difference between holo- and apoprotein molecular masses obtained from ESI-MS. [c] Zn(SCys) means that the typical fingerprint attributed to this chromophore is clearly detected; n.i. stands for non-informative data. [d] This figure corresponds to the number of DEPC-modified residues minus 1, assuming that the N-term peptide residue is always modified. [e] Evidences coming from the analysis of the CD spectra on recombinant preparations and acidified samples; n.i. stands for non-informative data. 'His' means that the effect of His binding to Cd(II) has been observed.

Regarding the type 3 MTs studied in this work, the results show that both GmMT3 and HaMT3 render major Zn_3- and Cd_4-complexes. GmMT3 encompasses two His residues, in positions 47 and 66, the latter being its C-terminus. Our results suggest that GmMT3 His47 is almost invariably involved in Zn(II)-binding, as it has also been hypothesised for the homologous His in the banana MT3 isoform [10], in which the amino acid sequence is comparable to that of GmMT3 in terms of His47 presence (numbering referring to the GmMT3 protein) and Cys distribution. Otherwise, His66 seems to participate in Zn(II)-coordination, although not in all the Zn(II)-GmMT3 complexes, so that this would establish an equilibrium of species in the preparation. On the other hand, GmMT3 His66, but not His47, seems to participate in Cd(II) coordination, which could be related with the coordinative requirements imposed by the bulkier Cd(II) ions and/or the natural physiological conditions when the peptide performs its function, as discussed below. The former hypothesis is supported by the observation that the minor presence of S^{2-}-containing complexes in the Cd-GmMT3 preparation becomes a major predominance for the corresponding H66A mutant, where sulphide ligands may compensate for the absent His66 additional ligand. In fact, the existence of different subsets of species where an His residue may or may not participate in metal-binding has been previously reported for the type 2 MT from cork oak [24], which contains an His within the spacer region that was proposed to participate in Cd(II)-binding in the S^{2-}-devoid preparations, but not in the S^{2-}-containing ones. Regarding HaMT3, the hypothesis of the participation of its unique His67 in both Zn(II)- and Cd(II)-binding is also supported by our results. Again, this C-term His is only involved in a subpopulation of the Zn_4-HaMT3 complexes, while it would be constant for the Cd_4-HaMT3 complexes. In conclusion, our findings point towards a significant involvement of GmMT3 and HaMT3 terminal histidines in Cd(II) coordination. A plausible explanation for this can be related to the natural expression pattern of MT3s and the physiological events in which they are needed. Plant type 3 MT genes are highly expressed in leaves and fruits [5], and many of them, including soybean and sunflower (our unpublished results), are particularly induced during senescence. Leaf senescence is a highly controlled oxidative process that involves degradation of the cellular and sub-cellular structures, and the mobilisation of nutrients from older senescing organs into developing parts of the plant [35]. Breakdown of vacuoles releases both stored mineral nutrients and toxicants, in relation to which it has been hypothesised that plant MTs may play a part in reallocating essential minerals. Here we propose that type 3 MTs – and not types 1 and 2- may instead have a role in scavenging and immobilising toxic

cadmium, preventing its transport to new vegetative tissues or seeds. In fact, the involvement of terminal histidines –a semi-conserved residue among MT3s, and absent in type 1 and 2 plant MTs- in Cd-coordination makes these complexes more resistant to oxidative attack and metal release than a cadmium cluster entirely coordinated by thiolates, since the Cys_3His sites are less nucleophilic and thus less vulnerable to oxidation than the Cys_4 ones, as was extensively discussed by Blindauer [36]. Moreover, although it is thought that the ligand variation from Cys to His would increase selectivity towards zinc instead of cadmium, it has to be stressed that the Cys_3His site that must be present in Cd-MT3 complexes would have a similar affinity for either metal, in accordance with Pearson´s HSAB principle [37]. M(II)-MT3 CD spectra also point towards the preference of these MTs for Cd(II) and the importance of a Cys_3His site, since (i) Zn-MT3 spectra exhibited non-informative fingerprints devoid of clear absorption maxima, (ii) Cd-MT3 CD spectra showed the typical Cd-MT absorption bands centred at *ca.* 250 nm, and (iii) acidic treatment of Cd-HaMT3 down to a pH below His pKa clearly decreased the overall intensity of the spectrum.

Turning to the Zn(II)-binding abilities of type 4 MTs, HaMT4 binds 6 Zn(II) ions, probably sharing the architecture fully determined for Zn_6-Ec-1 [8,17] (*i.e.* a two-domain structure with a $Zn_2(SCys)_6$ cluster at the N-term part and a $Zn_3(SCys)_9$ aggregate plus a single $Zn(SCys)_2(NHis)_2$ site within the C-term moiety). On the other hand, the presence of a Tyr in position 54 of GmMT4 gives rise to an equimolar mixture of Zn_5 and Zn_6 species, coincidently with the results for the replacement of either one or both His in the Ec-1 protein [19]. In contrast, spectroscopic and spectrometric data led to the conclusion that both GmMT4 and HaMT4 bind 6 Cd(II) ions with no participation of their His residues, as has already been proposed for wheat Cd_6-Ec-1 [5]. Significantly, for both cases, minor Cd_8S_1-MT4 complexes could be clearly detected in the recombinant preparations, this also highlighting their similar Cd(II) coordination abilities. Although the 3D structures of the corresponding metal complexes are needed in order to corroborate these architectures, differential Zn(II)-binding preferences are undoubtedly shown for HaMT4 and GmMT4 as a consequence of the variability in the His content, thus envisaging putative differences for the proposed physiological role of zinc seed source for the development of the future plant [14]. A major metabolic event in the germinating seed is the hydrolysis of reserve proteins to provide the growing seedling with the necessary nutrients before photosynthesis is established, a reason why there is an intense proteolytic

activity [38]. It has been shown very recently that proteolytic cleavage is much more efficient than oxidation in promoting zinc deliverance from wheat Ec-1. Moreover, it was proposed that the exact position of the cleavage site can also be determinant [39]. Hence, in GmMT4, the substitution of His54 for Tyr can either add a new protease cleavage site or facilitate proteolysis. Many seed proteases, as for instance C2 from soybean, show little or no preference for specific amino acids forming the peptide bond to be cleaved. Instead, its specificity stems from the three-dimensional structure of the native proteins, where peptide bonds in a very flexible surface loop would be readily accessible to proteolytic attack [40]. The comparison of the Zn-GmMT4 and Zn-HaMT4 CD spectra clearly suggests a less structured Zn-complex for GmMT4, which would be more prone to proteolytic attack, thus enhancing zinc transfer to requiring enzymes. On the other hand, the less structured Zn-GmMT4 complex does not jeopardise the ability of soybean seeds to store zinc, as this plant has another type of MT4 (Glyma18g32760), also highly expressed in seeds, with the classical 17:2 Cys and His content to rely on.

Overall, the results emphasise the importance of His residues in plant MTs, especially among type 3 and type 4 isoforms, where His patterns are considerably conserved. The picture presented hers for the MT4 isoforms supports the already described idea of the Cys_2His_2 mononuclear site being critical for their Zn(II)-binding properties [18,19], which does not preclude the existence of the natural variability of His presence. For the MT3 isoforms, the involvement of their His residues in divalent metal ion binding and the way how it would condition their putative biological properties might be understood in two different ways. On the one hand, we show that the C_{term} His in HaMT3 slightly enhances its Zn(II)-binding capacity, maybe in relation to improved Zn-mediated functions (*i.e.* Zn homeostasis, redox homeostasis). On the other hand, although also participating in metal ion coordination, neither the His of the linker of Zn-GmMT3 nor the His at the C_{term} of both Cd(II)-MT3 complexes substantially modified their respective metal-binding capacities, so that the hypothesis of conferring an improved resistance towards oxidation should be analysed. Non-Cys residues have been shown to exert a profound effect on the metal binding properties of MTs, the most clear example being the pulmonate snail MTs [41]. The complete sequential identity of Cys residues and a high degree of conserved positions for other amino acids shared between the strict Cd- and Cu-MT snail isoforms illustrates how the second shell of interactions forced by the side-chains of non-chelating amino acids can impose a completely different metal-specific

character on to the coordination chemistry of an MT peptide. A less drastic effect, although significant for its reactivity, is seen when a histidine residue of *H. pomatia* HpCuMT is mutated to alanine [42]. It was shown that the presence of His in this peptide decreases the Cu-binding performance of the isoform, thus probably facilitating the transfer of the metal to biomolecules that require copper. The presence of His residues also has deep consequences on reactivity by providing local order through weak interactions, thus reducing conformational flexibility, as seen in SmtA [43]. We can therefore envisage that His residues of soybean and sunflower MT3 and MT4 may have those and/or other effects on their properties, and therefore more subtle *in vitro* experiments are needed to shed light on metal preferences and reactivities of these particular proteins, as well as insightful *in vivo* and/or *in planta* research to unveil the elusive biological function/s of these and other plant MTs.

5. References

[1] Capdevila M, Atrian S (2011) J Biol Inorg Chem 16: 977-989.

[2] Capdevila M, Bofill R, Palacios O, Atrian S (2012) Coord Chem Rev 256: 46-62.

[3] http://www.bioc.unizh.ch/mtpage/classif.html (accessed June 5th, 2013).

[4] Cobbett C, Goldsbrough P (2002) Annu Rev Plant Biol 53: 159-182.

[5] Leszczyszyn OI, Imam HT, Blindauer CA (2013) Metallomics 5:1146-1169.

[6] Freisinger E (2011) J Biol Inorg Chem 16: 1035-1045.

[7] Calderone V, Dolderer B, Hartmann HJ, Echner H, Luchinat C, Del Bianco C, Mangani S, Weser U (2005) Proc Natl Acad Sci USA 102: 51-56.

[8] Peroza EA, Schmucki R, Güntert P, Freisinger E, Zerbe O (2009) J Mol Biol 387: 207-218.

[9] Blindauer CA, Harrison MD, Parkinson JA, Robinson AK, Cavet JS, Robinson NJ, Sadler PJ (2001) Proc Natl Acad Sci USA 98: 9593-9598.

[10] Freisinger E (2007) Inorg Chim Acta 360: 369-380.

[11] Abdullah SNA, Cheah SC, Murphy DJ (2002) Plant Physiol Biochem 40: 255-263.

[12] Rubio Fernandez L, Vandenbussche G, Roosens N, Govaerts C, Goormaghtigh E, Verbruggen N (2012) Biochim Biophys Acta 1824: 1016-1023.

[13] Hegelund JN, Schiller M, Kichey T, Hansen TH, Pedas P, Husted S, Schjoerring JK (2012) Plant Physiol 159: 1125-1137.

[14] Hanley-Bowdoin L, Lane BG (1983) Eur J Biochem 135: 9-15.

[15] Peroza EA, Freisinger E (2007) J Biol Inorg Chem 12: 377-391.

[16] Leszczyszyn OI, Schmid R., Blindauer CA (2007) Proteins: Struct Funct Bioinf 68: 922-935.

[17] Loebus J, Peroza EA, Blüthgen N, Fox T, Meyer-Klaucke W, Zerbe O, Freisinger E (2011) J Biol Inorg Chem 16(5): 683-694.

[18] Blindauer CA (2013) J Inorg Biochem 121: 145-155.

[19] Leszczyszyn OI, White CR, Blindauer CA (2010) Mol Biosyst 6(9): 1592-1603.

[20] Pagani MA, Tomas M, Carrillo J, Bofill R, Capdevila M, Atrian S, Andreo CS (2012) J Inorg Biochem 117: 306-315.

[21] Chyan CL, Lee TT, Liu CP, Yang YC, Tzen JT, Chou WM (2005) Biosci Biotechnol Biochem 69: 2319-2325.

[22] Capdevila M, Cols N, Romero-Isart N, Gonzàlez-Duarte R, Atrian S, Gonzàlez-Duarte P, (1997) Cell Mol Life Sci 53: 681-688.

[23] Domènech J, Mir G, Huguet G, Molinas M, Capdevila M, Atrian S, (2006) Biochimie 88: 583-593.

[24] Domènech J, Orihuela R, Mir G, Molinas M, Atrian S, Capdevila M, (2007) J Biol Inorg Chem 12: 867-882.

[25] Cols N, Romero-Isart N, Capdevila M, Oliva B, Gonzàlez-Duarte P, Gonzàlez-Duarte R, Atrian S (1997) J Inorg Biochem 68: 157-166.

[26] Bongers J, Walton CD, Richardson DE, Bell JU (1988) Anal Chem 60: 2683-2686.

[27] Capdevila M, Domènech J, Pagani A, Tío L, Villarreal L, Atrian S (2005) Angew Chem Int Ed Engl 44: 4618-4622.

[28] Leszczyszyn OI, Schmid R, Blindauer CA (2007) Proteins 68: 922-935.

[29] Peroza EA, Freisinger E (2007) J Biol Inorg Chem 12: 377-391.

[30] Miles EW (1977) Methods Enzymol 47: 431-442.

[31] Li C, Rosenberg RC (1993) J Inorg Biochem 51: 727-735.

[32] Qin K, Yang Y, Mastrangelo P, Westaway D (2002) J Biol Chem 277: 1981-1990.

[33] Binolfi A, Lamberto GR, Duran R, Quintanar L, Bertoncini CW, Souza JM, Cerveñansky C, Zweckstetter M, Griesinger C, Fernández CO (2008) J Am Chem Soc 130: 11801-11812.

[34] Bofill R, Orihuela R, Romagosa M, Domènech J, Atrian S, Capdevila M (2009) FEBS J 276: 7040-7056.

[35] Prochazkova D, Sairam RK, Srivastava GC, Singh DV (2001) Plant Science 161: 765–771.

[36] Blindauer CA (2008) J Inorg Biochem 102: 507-521.

[37] Pearson RG (1963) J Am Chem Soc 85: 3533-3543.

[38] Muntz K, Belozersky MA, Dunaevsky YE, Schlereth A, Tiedemann J (2001) J Exp Bot 52: 1741–1752.

[39] Peroza EA, dos Santos Cabral A, Wanz X, Freisinger E (2013) Metallomics 5: 1204-1214.

[40] Seo S, Tan-Wilson A, Wilson KA (2001) Biochim Biophys Acta 1545: 192–206.

[41] Palacios O, Pagani A, Perez-Rafael S, Egg M, Höckner M, Brandstätter A, Capdevila M, Atrian S, Dallinger R (2011) BMC Biology 9: 4.

[42] Perez-Rafael S, Pagani A, Palacios O, Dallinger R, Capdevila M, Atrian S (2013) ZAAC 639: 1356-1360.

[43] Blindauer CA, Razi MT, Campopiano DJ, Sadler PJ (2007) J Biol Inorg Chem 12: 393-405.

Supplementary Material

Table S1

Amino acid sequence alignment for type 3 plant MTs. GmMT3 and HaMT3 are the peptides studied in this work. The UniProtKB or GenBank accession code and the Latin species name is given in each row. The shaded boxes indicate the cysteine residues, and histidines are in bold

```
                                                  10        20        30        40        50        60        70
                                                  ....|....|....|....|....|....|....|....|....|....|....|....|
CA819971 GmMT3                                    MSNTCGNCDCADKTSCTK-GNSYGV-IVETEKSYIETVVMDVPA--AEHDG-KCKCGTNCTCTDCTCGH-
DY927914 HaMT3                                    MS-SCTNCDCFDKANCTKKGFRYDVTVVETETSTEETNVMEVPA--AENNG-NCKCGANCSCTNCTCGH-
P43389 Actinidia deliciosa                        MSDKCGNCDCADSSQCVKKGNSID--IVETDKSYIEDVVMGVPA--AESGG-KCKCGTSCPCVNCTCD--
XP_002885083 Arabidopsis lyrata                   MSSNCGSCDCADKTQCVKKGTSYTFDIVKTQESYKEAMIMDVGAEENDAN-CKCKCGSTCSCVNCTCCPN
O22433 Arabidopsis thaliana                       MSSNCGSCDCADKTQCVKKGTSYTFDIVETQESYKEAMIMDVGAEENNAN-CKCKCGSSCSCVNCTCCPN
Q84RC4 Arachis hypogaea                           MSNTCGNCDCADKTQCVK-GNKYGVDIVETEKRMVETVVMEVPA--GENDG-KCKCGANCSCTNCTCGH-
Q852U3 Brassica juncea                            MS-SCGNCDCADKTQCVKKGTSYTLDIVETQESYKEAMIMEVNG--AEENGCQCKCGSSCSCVNCTCCPN
J7G5T6 Brassica napus                             MS-SCGNCDCADKTQCVKKGTSYTFDIVETKESYKEAMIMDVNG--AEENGCQCKCGSSCSCVNCTCCPN
G8FMJ0 Carica papaya                              MSDTCGNCDCADKTQCVKKGSSYTADIIETEKS-IMTVVMDAPA--AENDG-KCKCGPSCSCTNCTCGH-
Q96386 Carica papaya                              MSDTCGNCDCADKTQCVKKGSSYTADIIETEKS-IMTVVMDAPA--AENDG-KCKCGPSCSCTNCTCGH-
Q9STC4 Elaeis guineensis                          MS-TCGNCDCADKSQCVKKGNSYGIEIIETEKSNFNNVI-DAPAA-AEHEG-NCKCGASCACVDCKCGQ-
I1SN86 Hevea brasiliensis                         MSSTCGNCDCADKSQCVKKGSSYTADIVETEKSFVSTVVMEVPA--TEPDG-KCRCGAGCTCTNCTCGH-
AFK12211 Hordeum vulgare                          MADKCGNCDCADKTQCVKKGDSYGIVMVDTEKSHLEVHET------AENDD-KCKCGTSCTCTNCTCGH-
D6BQM9 Jatropha curcas                            MSSTCGNCDCADKSQCVKKGSSYTADIVETEKSFVSTIVMDVPAG-AENDG-KCKCGPSCTCVDCGCGH-
I3S039 Lotus japonicus                            MSSSCGNCDCADKSQCGK-GNSYGLNIVETQTSYVETVAMDVSA--AEHDG-NCKCGASCTCVNCTCGH-
D2CGP2 Malus domestica                            MSGKCDNCDCADSTQCVKKGNSYDLVIVETENRSMDTVFVDAPA--AEHDG-KCKCGTGCSCVSCTCGH-
O24059 Malus domestica                            MSGKCDNCDCADSTQCVKKGNSYDLVIVETENRSMDTVFVDAPA--AEHDG-KCKCGTGCSCVSCTCGH-
G7LCX2 Medicago truncatula                        MSSSCGNCDCADKSQCGK-GNNYGMTIVETQKSFVETVVMDAPA--VEHD---CKCGSNCTCTNCTCGH-
Q40256 Musa acuminata                             MS-TCGNCDCVDKSQCVKKGNSYGIDIVETEKSYVDEVIVAAEA--AEHDG-KCKCGAACACTDCKCGN-
AAS99234 Noccaea caerulescens                     MSDKCGSCDCCDKTQCVTKSTSYTLDMVETQESYKEAMNMDVGA---EENGCKCMCGSTCSCVNGTCSPN
A3FPF9 Nelumbo nucifera                           MS-TCGNCDCADKSQCVKKGNGYTIEIIETEKSFYKNTVSEVPA--AEHDG-KCKCGSSCTCVDCTCGGH
A2WLS0 Oryza sativa                               MSDKCGNCDCADKSQCVKKGTSYGVVIVEAEKSHFEEV---AAG--EENGG--CKCGTSCSCTDCKCGK-
A2Y1D7 Oryza sativa                               MSDKCGHCDCADKSQCVKKGTSYGVVIVDAEKSHFEMA--EEVGY-EENDG-KCKCTTGCSCAGCNCGK-
A3B0Y1 Oryza sativa                               MSDKCGNCDCADKSQCVKKGTSYGVVIVDAEKSHFEMA--EEVGY-EENDG-KCKCTTGCSCAGCNCGK-
Q40854 Picea glauca                               MSSDCGNCDCADKSQCTKKGFQIDG-IVETSYEMGHGG--DVSL---END---CKCGPNCQCGTCTCHT-
Q564J8 Populus alba x Populus glandulosa          MSSTCDNCDCADKTQCVKKGSSYTAGIVETEKSYVSTGAMEVPA--TENDG-KCKCGANCTCTTCTCGH-
A9PHS5 Populus trichocarpa                        MSSTCDNCDCADKTQCVKKGSSYTADIVETEKSHVYTGVMEVPA--TENDG-KCKCGANCTCTTCTCGH-
A9PI97 Populus trichocarpa                        MSSTCDTCDCADKTQCVKKGSSYTAGIVETEKNYVSSVVMEVPA--AENDG-KCNCGTGCTCTTCTCGH-
B9N1H1 Populus trichocarpa                        MSSTCDNCDCADKTQCVKKGSSYTAGIVETEKNYVSSVVMEVPA--AENDG-KCNCGTGCTCTTCTCGH-
A9PIV0 Populus trichocarpa x Populus deltoides    MSSTCDNCDCADKTQCVKKGSSYTADIVETEKSHVSTGVMEVPA--TENDG-KCKCGANCTCTTCTCGH-
Q6PML1 Populus trichocarpa x Populus deltoides    MSSTCDTCDCADKTQCVKKGSSYTAGIVETEKNYVSAVVMEVPA--DENDG-KCNCGTGCTCTTCTCGH-
Q6PML2 Populus trichocarpa x Populus deltoides    MSSTCDNCDCADKTQCVKKGSSYTADIVETEKSHVYTGVMEVPA--TENDG-KCKCGANCTCTTCTCGH-
O48951 Prunus avium                               MSSKCSNCDCSDSSQCTKKGYSFDLVIVETENRSMDTVIMDAPA--AENGG-NCKCGPSCACVDCKC---
J7G035 Pyrus x bretschneideri                     MSGKCDNCDCADSSQCTKKGKSYDLVIVETENRSMDTVVVDAPA--AENDG-KCKCGTVCLCVNCTCGH-
O82046 Ribes nigrum                               MS-SCGNCDCADKTNCPKKGNSYGFDIIETQKSYDDVVVMDVQA--AENDG-KCKCGPSCSCVGCSCGH-
B9SIK2 Ricinus communis                           MSSTCGNCDCADKSQCVKKGSSYTADIVETEKSFVSTIIMDVPA--AEHDG-KCKCGASCTCVTCTCGH-
B9T0E5 Ricinus communis                           MSSTCGNCDCADKSQCVKKGSSYTADVVETEKSSVSTIVMEVPA--AEHDG-KCKCGASCTCVNCTCGH-
Q9M4H3 Vitis vinifera                             MS-TCGNCDCADKSQCVKKGNSYGIDIVETEKSYVATVVMEVPA--AQHEG-SCKCGDSCACIDCTCGQ-
```

Table S2

Amino acid sequence alignment for type 4 plant MTs. GmMT4 and HaMT4 are the peptides studied in this work. The UniProtKB or GenBank accession code and the Latin species name is given in each row. The shaded boxes indicate the cysteine residues, and histidines are in bold

```
                                  10        20        30        40        50        60        70        80        90        100       110
                                  ....|....|....|....|....|....|....|....|....|....|....|....|....|....|....|....|....|....|....|....|....
GmMT4                             MADTSGGDAVRPVVICDNKCGCTVPCTGGSTCRCTSVGMTTGGGD-------HVTCSCGEYCGCNPCSCPKTAAS-GTG-----CRCGTDCSCASCRT----------
BQ975039 HaMT4                    ----MRG------VICDERCGCPSPCPGGVSCRCK----SGRMES-GGGEVEHKKCSCGGHCGCNPCSCSQATP--SEGTGKAFCKCADGCTCVTCSS----------
P93746 Arabidopsis thaliana       MADTGKGSS-V--AGCNDSCGCPSPCPGGNSCRC-RMREASAGDQ------GHMVCPCGEHCGCNPCNCPKTQT--QTS-AKG-CTCGEGCTCASCAT----------
Q42377 Arabidopsis thaliana       MADTGKGSA-S--ASCNDRCGCPSPCPGGESCRCKMMSEASGGDQ------EHNTCPCGEHCGCNPCNCPKTQT--QTS-AKG-CTCGEGCTCATCAA----------
D7LEQ9 Arabidopsis lyrata         MADTGKGSS-S--ASCNDRCGCPSPCPGGESCRCKMMSEASGGDQ------EHNTCPCGEHCGCNPCNCPKTQT--QTS-TKG-CTCGEGCTCATCAA----------
Q0Q0Q8 Arachis hypogaea           MADKAMKGGAR----CNDRCGCSIPCPGDSTCRCASGSEGGGETQ-------HLTCPCGEHCECNPCTCPKTFAA-GAG-----CKCGPGCSCASCRRA----------
Q0Q0Q9 Arachis hypogaea           MADTAMKGGTR----CNDRCGCSVPCPGDSTCRCASGNEGGGGTQ-------HLTCPCGEHCECNPCTCPKTVAA-GAG-----CKCGPGCTCASCRRA----------
J7G1D0 Brassica napus             MADIGKGTS-V--AGCNDRCGCPSPCPGGESCRC-RMSAASGGDQ------EHNMCPCGEHCGCNPCTCSKTQT--SAKGGKAFCTCGEGCTCASCAA----------
M4C8R2 Brassica rapa              MADIGKGTS-V--AGCNSRCGCPSPCPGGESCRC-RMSAASGGDQ------EHNMCPCGEHCGCNPCTCAKTQT--SAKVGKAFCTCGEGCTCATCAA----------
JK711196 Camellia japonica        MTDVM-GSSGV----CDDKCGCPSPCPGSSSCRCDSIIGTEGGDDTSM---EDKRCPCGEHCGCNPCTCPKTVT---AAAAAG-CKCAEGCTCVTCAYPFRSSSYYSTPFYHYY
R0G0J5 Capsella rubella           MADTGKGSSGA--TSCNDRCGCPSPCPGGESCRC-RMSEASGGDQ------EHITCPCGDHCGCNPCTCPKTRT--QTT-AKG-CTCGEGCTCATCAA----------
O22378 Glycine max                MADTSGGDAVRPVVICDNKCGCTVPCTGGSTCRCTSVGMTTGGGN-------HVTCSCGEHCGCNPCSCPKTAAS-GTG-----CRCGTDCSCASCRT----------
Q84L51 Hordeum vulgare            -------------MGCDDKCGCAVPCPGGTGCRCTS-ARSGA---------EHTTCACGEHCGCNPCACGREGTPSGRENRRSNCSCGAACNCASCGSTA----------
I1QVK0 Oryza glaberrima           -------------MGCDDKCGCAVPCPGGTGCRCASSARSGG--G------DHTTCSCGDHCGCNPCRCGRESQPTGRENRRAGCSCGDSCTCASCGSTTTAPAATT-------
A2Z9V1 Oryza sativa               -------------MGCDDKCGCAVPCPGGTGCRCASSARSGG--G------DHTTCSCGDHCGCNPCRCGRESQPTGRENRRAGCSCGDSCTCASCGSTTTAPAATT-------
A3C6Y9 Oryza sativa               -------------MGCDDKCGCAVPCPGGTGCRCASSARSGG--G------DHTTCSCGDHCGCNPCRCGRESQPTGRENRRAGCSCGDSCTCASCGSTTTAPAATT-------
Q109B0 Oryza sativa               -------------MGCDDKCGCAVPCPGGTGCRCASSARSGG--G------DHTTCSCGDHCGCNPCRCGRESQPTGRENRRAGCSCGDSCTCASCGSTTTAPAATT-------
Q9ZTM1 Petunia hybrida            MAD-LRGSS----AICDERCGCPSPCPGGVACRCA----SGGAATAGGGDMEHKKCPCGEHCGCNPCTCPKSEGT-TAGSGKAHCKCGPGCTCVQCAS----------
B9MZ02 Populus trichocarpa        MAD-TRGGT----VGCNDGCGCPVPCAGGTSC--------GGEGA------GHNKCSCGEHCGCNPCTCPRSVV--TTGVGKAYCKCGADCACPTCSS----------
M5VN72 Prunus persica             MADTTTGGGIK--ASCNDSCGCPNPCPGGVTCRCTNTAEATSGGG------DHMTCSCGEHCGCNPCTCAKSVV--STKTGKAYCKCGEGCACVSCAA----------
B9S4K8 Ricinus communis           MAD-TRGGS----IACNDRCGCPVPCPGGTACRCRISQAAGGAGD------AHSKCSCGEHCGCNPCTCPKGLE--TVGVGRASCKCGPGCTCATCAS----------
Q9FUJ8 Sesamum indicum            MAD-MRGSG----VVCDDRCGCPSPCPGGIACRCS----TGGGDD---TTTEHKQCTCGEHCGCNPCTCSKSE---IRGTGKAFCRCGTGCTCPTCAA----------
K4B484 Solanum lycopersicum       MAD-VRGSS----GTCNERCGCPCPCPGGTSCRCA----SSDAN------MEHKRCSCGEHCGCNPCTCSKSEGT-TAAAGKSNCKCGPGCACPTCAA----------
C5WTK2 Sorghum bicolor            -------------MGCDDKCGCAVPCPGGKDCRCTSGSGAGGQ-R------EHTTCGCGEHCECSPCTCGRATMPSGRQNRKANCSCGPACNCASCASAS----------
P30569 Triticum aestivum          -------------MGCDDKCGCAVPCPGGTGCRCTS-ARSGAAAG------EHTTCGCGEHCGCNPCACGREGTPSGRANRRANCSCGAACNCASCGSATA----------
P30570 Triticum aestivum          -------------MGCNDKCGCAVPCPGGTGCRCTS-ARSDAAAG------EHTTCGCGEHCGCNPCACGREGTPSGRANRRANCSCGAACNCASCGSTTA----------
M7YY35 Triticum urartu            -------------MGCNDKCGCAVPCPGGTSCRCTS-ARSDAAAG------EHTTCGCGEHCGCNPCACGREGTPSGRANRRANCSCGAACNCASCGSTTA----------
B6SIN8 Zea mays                   -------------MGCDDKCGCAVPCPGGKDCRCTSGS--GGQ-R------EHTTCGCGEHCECSPCTCGRATMPSGRENRRANCSCGASCNCASCASA----------
P43401 Zea mays                   -------------MGCDDKCGCAVPCPGGKDCRCTSGS--GGQ-R------EHTTCGCGEHCECSPCTCGRATMPSGRENRRANCSCGASCNCASCASA----------
```

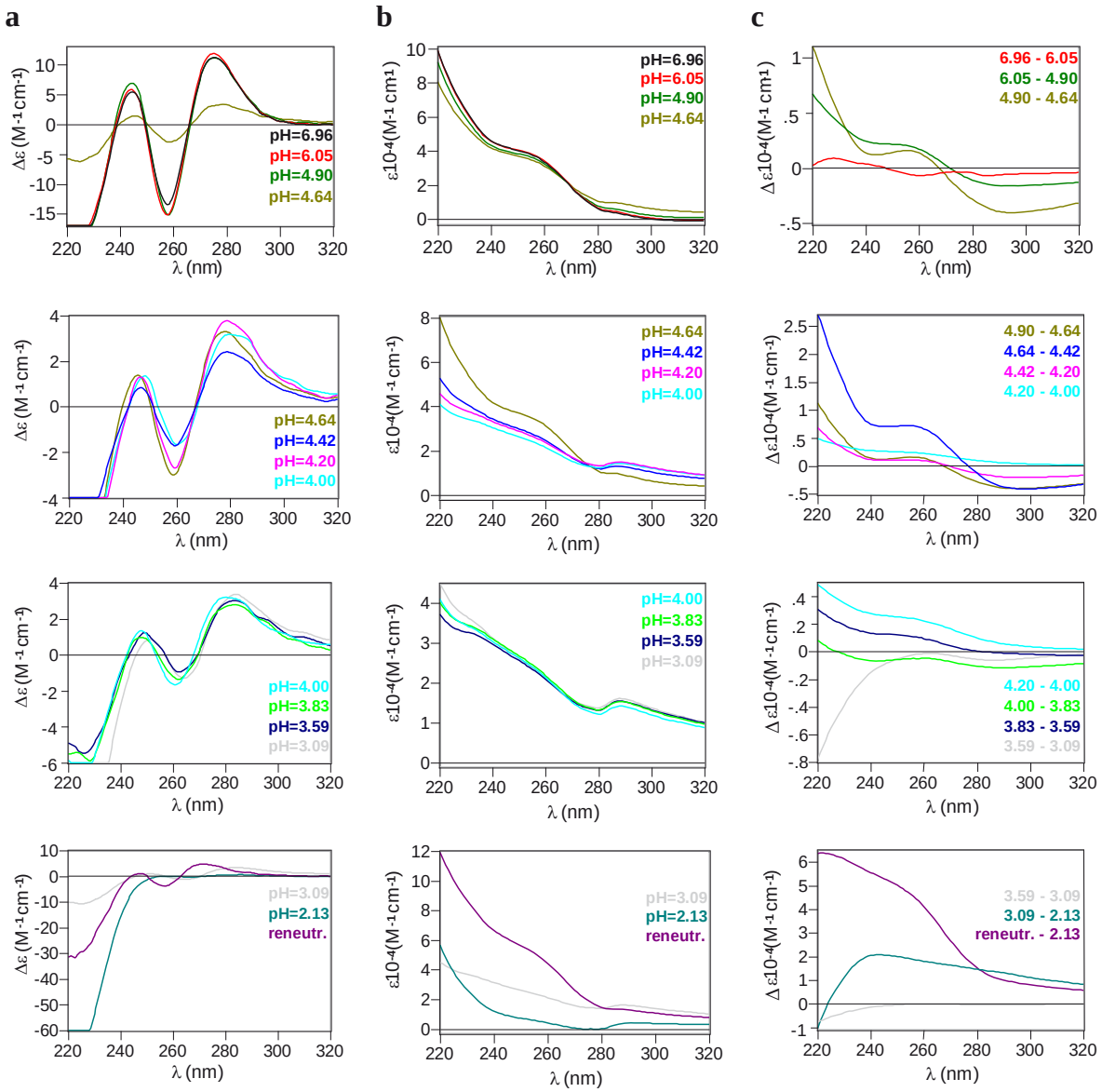

Fig. S1 a CD, **b** UV and **c** UV difference spectra corresponding to the acidification of a 20 μM solution of recombinant Cd-HaMT3

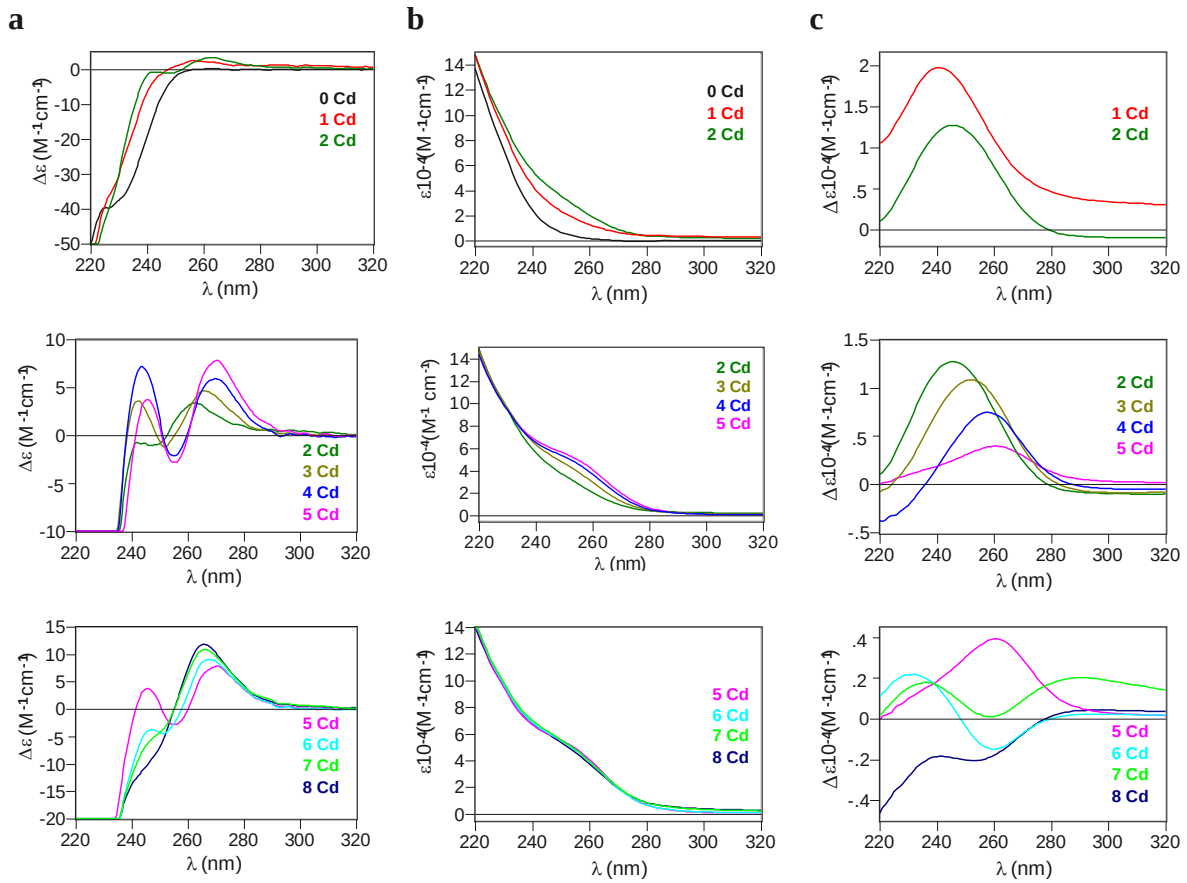

Fig. S2 a CD, **b** UV and **c** UV difference spectra corresponding to the titration of a 15 µM solution of recombinant Zn-HaMT3 with Cd(II) at pH 7. The number of Cd equiv in **c** indicate the number of the addition which is the responsible for the changes in each absorption spectrum

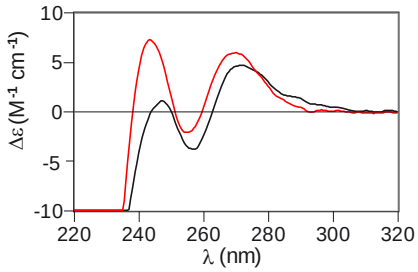

Fig. S3 CD spectra corresponding to an acidified and reneutralised Cd-HaMT3 preparation (black) and to Zn-HaMT3 after the addition of four Cd(II) equivalents at pH 7 (red)

Capítol 5

Comparative analysis of the soybean metallothionein system under radical and oxidative stress

CAPÍTOL 5

Comparative analysis of the soybean metallothionein system under radical and oxidative stress

1. Introduction

Reactive oxygen species (ROS) are constantly produced *in vivo* as a consequence of the aerobic environment where life takes place. The activation of molecular oxygen to toxic forms such as superoxide anion radical, hydrogen peroxide or hydroxyl radical comes from the stepwise reduction of O_2, which also occurs in living organisms. Although they are involved in physiological processes (*e.g.* cell signalling, regulation of gene expression), these species can react with nucleic acids, lipids or proteins, thus causing cellular damage. This is the reason why organisms have developed a plethora of antioxidant systems in order to avoid and repair the negative effects that ROS can exert on them, among which metallothioneins (MTs) – ubiquitous Cys-rich low molecular weight metalloproteins capable of coordinating heavy metal ions – have been proposed to play a protective/regulatory role during oxidative stress episodes [1]. Indeed, many investigations point towards a direct relationship between MTs and ROS. The synthesis induction of these peptides in response to the presence of oxidants [2,3] or their ability to scavenge hydroxyl or superoxide radicals [4,5] as well as hydrogen peroxide [6] has been made patent. However, indirect and thus more complex mechanisms through which MTs are related to antioxidant functions are also proposed. For instance, since these peptides are metal transporters, they may be related to antioxidant enzymes which require the binding of metal ions in their active sites [7]. Additionally, the oxidation of Zn(II)-loaded MTs gives rise to the Zn(II) release in a process that could be controlled by the gluthatione (GSH)/gluthatione disulfide (GSSG) pair, thus establishing a cycle which would involve Zn(II) ions and redox metabolisms [8]. However, not only oxidative species but also reductive ones, such as hydrogen atoms and solvated electrons, have been found to cause deleterious effects in cells [9,10,11].In this context, a tandem radical damage involving polypeptides and lipid compartments has been evidenced under free radical stress for sulfur-containing proteins [12]. The characteristic high Cys content of MTs (*ca.* 30% of their amino acidic

residues) makes them a very interesting protein system to be studied in the context of tandem protein-lipid damage [13]. In fact, the connection between MT reactivity and membrane lipid transformations can contribute to the puzzling context of radical stress occurring to biomolecules and its role in biological signalling.

As regards plant MTs, some investigations have also pointed towards their potential ROS scavenging activity [*cf.* 14], as well as their capacity to intercept reductive reactive species, being involved in the aforementioned tandem protein/lipid damage [15,16]. Unlike the mammalian isoforms, plant MT amino acidic sequences present a few aromatic residues and a long Cys-free region (up to 40 residues), which probably make them more prone to react with radical and/or oxidative species. Plant MTs are subdivided into the p1, p2, p3 and p4 subfamilies depending on the number and distribution of their Cys residues [17]. p1, p2 and p3 show two Cys-rich domains separated by one Cys-free region (also called *linker* or *spacer*), and they contain six Cys in their C-terminal Cys-rich region. Their Cys content diverges at the N-terminal Cys-rich domain, exhibiting six, eight and four Cys residues for the p1, p2 and p3 subfamilies, respectively. Contrastingly, p4 subfamily presents three Cys-rich regions which contain six, six and five Cys residues, separated by two Cys-free regions which are considerably shorter than those of subfamilies p1-3.

Despite all data reported before, the heterogeneity of the protein sequences in the MT superfamily and the wide range of redox related biological functions in which they were proposed to be involved, point to the need of carrying out more intensive research in this field. Hence, in this work we present a comparative study of each one of the four MTs from soybean (*Glycine max*) plant under free radical and oxidative stress. To this purpose, the four soybean *MT* genes (*GmMT1*, *GmMT2*, *GmMT3* and *GmMT4*) expression was examined after H_2O_2 exposure. The capacity of each of the soybean MTs (GmMT1-4) to protect against H_2O_2 as well as against a ROS generator was also tested by yeast complementation assays. Furthermore, the four peptides were recombinantly synthesised in *E. coli* Zn(II)-enriched cultures. Two strategies were followed for the latter objective: first, the eventual Zn(II) release from Zn(II)-GmMTs upon H_2O_2 exposure was monitored, and second, the damage on a model cell membrane that the attack of $HO^{\bullet}$, H-atoms or solvated electrons on each of the Zn(II)-GmMT complexes

can cause was measured. Overall, the results provide new insights into the plant MT family in relation to their potential redox homeostasis functions.

2. Experimental Section

2.1. Quantitative real time polymerase chain reaction (qPCR)

21 day-old soybean plants were exposed to 10 mM H_2O_2 for 24h, after which the leaves and roots were collected separately, frozen in liquid nitrogen and stored at – 80 ºC until use. Three biological replicates were analysed. Total RNA was isolated with TRIZOL® Reagent (Invitrogen) following the manufacturer's protocol and treated with DNase I (Fermentas). The cDNA was synthesised using an oligo(dT_{18}) primer from 1 μg of total RNA with the reverse transcriptase RevertAid™ (Fermentas) and RNaseOUT™ Recombinant RNase Inhibitor (Invitrogen). Quantitative real time PCR reactions were performed in a 20-μl reaction volume with 0.5 μM gene-specific primers, 2 μl of 1/100 diluted cDNA as a template, and SYBR Green I (Invitrogen) as detection reagent. Soybean actin 11 (Glyma02g10170) was used as a reference gene. The amplicon lengths were 158 bp for GmMT1, 182 bp for GmMT2, 59 bp for GmMT3, 105 bp for GmMT4 and 94 bp for actin 11. The reactions were performed in an MX3000P QPCR System (Stratagene) in triplicate (technical replicates). PCR conditions were: 94 °C for 5 min, followed by 45 cycles of 94 °C for 15 s, 55 °C for 30 s and 72 °C for 15 s. After final annealing (72 °C, 5 min), a melt curve analysis was made by increasing the temperature from 65 °C to 95 °C at 0.5 °C intervals to check on the specificity of the assays, with all real time PCR reactions passing this quality control. The SYBR® Green I fluorescent signal was determined for each cycle at the end of the extension step. The fold-change in gene expression was calculated using the comparative Ct method ($2^{-\Delta\Delta Ct}$) [18].

2.2. Yeast functional complementation assays

The cDNAs coding for GmMT1, GmMT2, GmMT3 and GmMT4 were excised from the corresponfing pGEX recombinant plasmids [19] by digestion with *Bam*HI/*Xho*I (Fermentas) and ligated into the same sites of the yeast vector p424-GPD [20]. Vector p424 and the constructs p424-GmMT1-4 were introduced into DTY4 *Saccharomyces cerevisiae* cells using the lithium acetate procedure [21]. Transformed cells were selected by their capacity to grow in synthetic complete medium (SC) without

Trp (p424 vector selection marker) and Ura (DTY4 strain selection marker) (SC-Trp-Ura medium).

For the hydrogen peroxide and paraquat tolerance tests, transformed DTY4 cells and parental DTY3 cells were used. DTY4 cells were initially grown in selective SC-Trp-Ura medium and DTY3 cells in SC medium, both at 30 ºC and 250 rpm until reaching an OD_{600} of 0.5. Three 10-fold dilutions were performed, and 3 µL of each dilution were spotted on SC-Trp plates and on SC-Trp supplemented with increasing concentrations of hydrogen peroxide or paraquat. Plates were incubated for 3 days at 30 ºC and photographed after that period. DTY4 cells transformed with the p424 vector were used as a negative control. DTY3 cells were grown in SC medium and used as a positive control.

2.3. Preparation and characterisation of the recombinant Zn(II)-GmMT complexes

The recombinant peptides were biosynthesised in 5L-cultures of *E. coli* BL21 cells supplemented with final concentrations of 300 µM $ZnCl_2$. Clones containing each of the pGEX-GmMT-1, -2, -3 and -4 expression plasmids were constructed as previously reported [19]. Expression was induced with 100 µM isopropyl ß-D-thiogalactopyranoside (IPTG) and cultures were allowed to grow for further 3 h. Total protein extracts were prepared from these cells as previously described [22]. Metal complexes were recovered from GST fusion constructs by batch-affinity chromatography using Glutathione-Sepharose 4B (GE Healthcare) and thrombin cleavage. After concentration using Centriprep Microcon 3 (Amicon), the metal complexes were finally separated from thrombin through FPLC gel filtration in a Superdex75 column (GE Healthcare) equilibrated with 50 mM Tris-HCl, pH 7.0. Selected fractions were kept at -80 ºC until further use.

The S and Zn content of all M(II)-MT preparations was analysed by means of inductively coupled plasma atomic emission spectroscopy (ICP-AES) in a Polyscan 61E (Thermo Jarrell Ash) spectrometer, measuring S at 182.040 nm and Zn at 213.856 nm. Samples were treated as previously reported [23], but were alternatively incubated in 1 M HNO_3 at 65 °C for 10 min prior to measurements in order to eliminate possible traces of acid-labile sulfide ions, as otherwise described [24]. Protein concentrations were calculated from the acidic ICP-AES sulfur measurement, assuming that all S atoms were contributed by the MT peptide.

Molecular mass determinations were performed by electrospray ionisation time-of-flight mass spectrometry (ESI-MS) on a Micro Tof-Q instrument (Bruker) interfaced with a Series 1100 HPLC Agilent pump, equipped with an autosampler, all of them controlled by the Compass Software. Calibration was attained with ESI-L Low Concentration Tuning Mix (Agilent Technologies). Samples containing MT complexes were analysed under the following conditions: 20 µL of protein solution injected through a PEEK (polyether heteroketone) tubing (1.5 m x 0.18 mm i.d.), at 40 $\mu L \cdot min^{-1}$; capillary counter-electrode voltage 5 kV; desolvation temperature 90-110 ºC; dry gas 6 $L \cdot min^{-1}$; spectra collection range 800-2000 m/z. The carrier buffer was a 5:95 mixture of acetonitrile:ammonium acetate/ammonia (15 mM, pH 7.0). For analysis of the sequences of all recombinant MTs, 20 µL of the corresponding Zn-MT samples were injected under the same conditions described before but using a 5:95 mixture of acetonitrile:formic acid pH 2.4 as liquid carrier, which caused the complete demetallation of the peptides.

2.4. Colorimetric monitoring of the Zn(II) release upon H_2O_2 exposure

Hydrogen peroxide (1:10 Cys:H_2O_2 molar ratio) was added to each of the solutions containing *ca.* 15 µM of the recombinantly obtained Zn(II)-GmMT complexes and 1 mM Zincon (2-carboxy-2'-hydroxy-5'-sulfoformazylbenzene, purchased from Sigma-Aldrich) in 50 mM Tris-HCl, pH 7. The metal-to-protein ratios deduced by acid ICP-AES for each of the analysed Zn(II)-GmMT complexes were: $Zn_{3.8}$-GmMT1, $Zn_{4.3}$-GmMT2, $Zn_{3.3}$-GmMT3 and $Zn_{5.6}$-GmMT4. Formation of the Zn(II)-Zincon complex was followed by monitoring the changes in Zincon absorbance at 620 nm during 400 min at 21 ºC. Measurements were performed on an HP-8453 Diode array UV-visible spectrophotometer with 1 cm capped quartz cuvettes. Since formation of the dye-metal complexes is pH- and concentration-dependent [25,26,27], the Beer-Lambert's law behaviour was verified under the conditions used here, thus obtaining an ε_{620} for Zn(II)-Zincon of 20371 M^{-1} cm^{-1}. Zincon was used in excess to ensure the quantitative formation of the Zn(II)-Zincon complex, and the lack of reaction between Zincon and Zn-GmMTs or Zincon and H_2O_2 was confirmed since absorbance at 620 nm remained constant in those two cases.

The absorbance data were converted to the percentage of released Zn(II) ions using the ε_{620} value of the Zn(II)-Zincon complex after substraction of the blank (*i.e.* 0 µM Zn) absorbance and the Zn/MT ratio obtained by acid ICP-AES. Kinetics of Zn(II) release

were fitted by nonlinear least squares into a first order model (single exponential function) according to the expression $A(t)= A(max) [1-e^{(-k \cdot t)}]$, where *t* is time (expressed in min), A(t) is the absorbance at 620 nm of the Zn(II)-Zincon complex, and A(max) is the maximum absorbance at 620 nm achieved at the end of reaction (t=400 min).

2.5. Radiolytic production of free radicals

In order to mimic the conditions of an endogenous radical damage, γ-radiolysis can be used to obtain free radicals. When diluted aqueous solutions are irradiated by γ-rays, practically all the energy absorbed is deposited in water molecules and the chemical changes in solutes are brought about indirectly by the primary water reactive species that are three short lived species, hydrated electron (e_{aq}^-), hydroxyl radicals ($HO^\bullet$) and hydrogen atoms ($H^\bullet$), as shown in Equation (1). The values in parentheses represent the radiation chemical yields (*G*) in units of μmol J^{-1}. Continuous radiolysis was performed by using a ^{60}Co-Gammacell at a dose rate of 4.3 J kg^{-1} min^{-1} (or Gy min^{-1}).

$$H_2O \rightarrow e_{aq}^-(0.27), HO^\bullet(0.28), H^\bullet(0.062) \qquad (1)$$

The radical stress on Zn-MT was stimulated by using two sets of experimental procedures in oxygen-free atmosphere, *i.e.*, when the three reactive species (in different proportions) react with Zn-MT (*Method A*) or when the hydroxyl radicals are scavenged by *t*BuOH (*Method B*).

Method A1: N_2O-saturated Zn-MT aqueous solutions. Under these conditions, e_{aq}^- are efficiently transformed into $HO^\bullet$ radicals by the ~0.02 M of N_2O [Eq. (2)], affording a $G(HO^\bullet)$=0.55 μmol J^{-1}, *i.e.*, $HO^\bullet$ and $H^\bullet$ radicals accounted for 90% and 10%, respectively, of the reactive species.

$$e_{aq}^- + N_2O + H_2O \rightarrow HO^\bullet + N_2 + HO^- \qquad (2)$$

Method A2: Oxygen-free (Ar-flushed) solutions containing 30 μmol Zn-MT. Under these conditions, both e_{aq}^- and $HO^\bullet$ radicals accounted for 45% of the reactive species, whereas $H^\bullet$ for 10%.

Method B1: N_2O-saturated aqueous solutions containing 0.2 M *t*BuOH and Zn-MTs. In the presence of *t*BuOH, hydroxyl radicals are efficiently scavenged [Eq.(3)], whereas hydrogen atoms react only slowly with the alcohol [Eq.(4)] In N_2O-saturated solutions (~0.02 M), e_{aq}^- are efficiently transformed into $HO^\bullet$ radicals [Eq. (2)], which are subsequently scavenged by *t*-BuOH [Eq.(3)]. Thus under these conditions, $H^\bullet$ is the only the reactive species present in the system

$$HO^\bullet + t\text{BuOH} \rightarrow (CH_3)_2C(OH)CH_2^\bullet + H_2O \qquad (3)$$

$$H^\bullet + t\text{BuOH} \rightarrow (CH_3)_2C(OH)CH_2^\bullet + H_2 \qquad (4)$$

Method B2: Oxygen-free (Ar-flushed) aqueous solutions containing 0.2 M *t*BuOH and 30 μmol Zn-MT. This experimental condition allows to investigate the reactivity of only reductive species (e_{aq}^- and $H^\bullet$) and their consequences on protein structure. In the presence of *t*-BuOH, $HO^\bullet$ are efficiently scavenged [Eq.(3)], thereby limiting the eventual observations of undesired polypeptide modifications resulting from the latter species. Thus, under these experimental conditions e_{aq}^- and $H^\bullet$ accounted for about 80% and 20% of the reactive species, respectively.

2.6. γ-radiolysis of the Zn(II)-GmMT complexes and analysis of the induced structural modifications

To overcome the radical scavenging activity and the spectroscopic masking effect of the Tris-HCl buffer in radical species attack and Raman spectroscopy, respectively, approximately 1 mL of each of the recombinantly obtained Zn-GmMT preparations containing up to 1 mg of metal-protein complex were previously dialysed. The solutions were subjected to 2 h of dialysis against 200 mL of 5 mM Tris-HCl pH 7.2 followed by two cycles of 2 h dialysis against distilled water by using 6.3 mm-radius dialysis membranes (Medicel International). Dialysed samples were liophilised on a Modulo 4K Freeze Dryer equipped with a RV8 Rotary Vane Pump (Edwards) and kept at -20 ºC until further use. The resulting solid precipitates were redissolved in distilled water in order to obtain 150 μM solutions of each of the Zn(II)-GmMT complexes that were irradiated (see *2.5. Radiolytic production of free radicals*). For the analysis of the modifications induced by γ-irradiation, approximately 0.6 mg for Zn-GmMT3 and 0.5 mg for Zn-GmMT1, Zn-GmMT2 or Zn-GmMT4 of the irradiated and subsequently

lyophilised samples were dissolved in 200 µL of distilled water. 60 µL of each of the obtained solutions were analysed by ESI-MS at pH 7.0 and pH 2.4 (conditions described above). Raman spectra were obtained on lyophilised samples, before and after irradiation of the aqueous solutions, with a Bruker IFS 66 spectrometer equipped with a FRA-106 Raman module and a cooled Ge-diode detector. The excitation source was a Nd3+-YAG laser (1064 nm), the spectral resolution was 4 cm^{-1} and the total number of scans for each spectrum were 6000. The laser power on the sample was about 100 mW.

2.7. γ-radiolysis of biomimetic Zn(II)-GmMT-lipid systems: tandem damage

Biomimetic models can be very useful to address lipid-protein damage, in order to extrapolate the results to the more complex situations present *in vivo*. For simulating the biological membrane environments and the organization of a lipid bilayer in aqueous environment, liposomes are very useful. In particular, monolamellar vesicles, formed by the extrusion methodology and made of phospholipid–containing unsaturated fatty acid moiety (oleic acid), were used as model membranes. In detail, 1.7 mM suspensions of POPC (1-palmitoyl-2-oleoyl-phosphatidylcholine) liposomes containing large unilamellar vesicles (LUVET) to which 30 µM Zn(II)-GmMT aqueous solutions were added, were γ-irradiated (see *2.5. Radiolytic production of free radicals*). 100 µL-aliquots of the protein-lipid suspension were withdrawn at different irradiation times for lipid isolation, following the procedure describe elsewhere [28]. After trans-esterification of the phospholipids to the corresponding fatty acid methyl esters (FAME), the methyl oleate/methyl elaidate ratios were obtained by gas chromatographic (GC) analysis. Based on the palmitic moiety of POPC, serving as an internal standard, *trans* isomers were quantified and no side-reactions occured. A Varian CP-3800 gas chromatograph equipped with a flame ionisation detector and a Rtx-2330 column (90% biscyanopropyl-10% phenylcyanopropyl polysiloxane capillary column; 60 m, 0.25 mm i. d., 0.20 µm film thickness) was used. Temperature started from 160 °C held for 25 min, followed by an increase of 10 °C/min up to 250 °C. The method included a constant pressure mode at 29 psi. *Cis* and *trans* FAME, that is methyl oleate and elaidate, were identified by comparison with the retention times of commercially available samples. In all experiments, the geometrical isomerisation of the lipid chains of the POPC vesicles occurred. Control experiments in the absence of Zn-GmMTs confirmed that *trans*-isomer formation under these conditions is less than 0.2% after exposure to 500 Gy.

3. Results

3.1. GmMT *gene expression in response to H_2O_2*

Hydrogen peroxide is a primary ROS which can directly lead to oxidative damage or, indirectly, give rise to secondary ROS such as the more damaging hydroxil radical. The inducibility or repression of a gene transcription by external stimulants is a well-established method to hypothesise about the possible biological function of MTs. Hence, in order to examine whether the transcription of these *MT*s responds to H_2O_2, soybean plants were treated with 10 mM H_2O_2 during 24h and the expression level of each of the *GmMT*s in leaves and roots was analysed by quantitative real time PCR (Fig. 1).

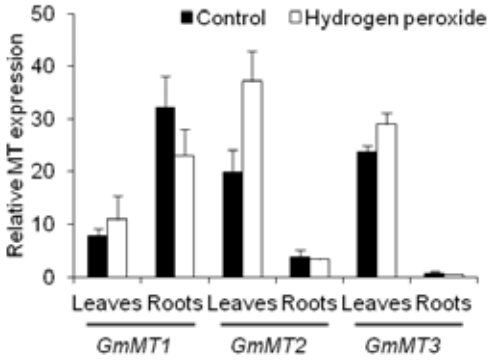

Figure 1. Real time PCR analysis of soybean metallothionein expression in roots and leaves of plants treated with 10 mM H_2O_2 for 24h (Hydrogen peroxide) *vs.* untreated plants (Control). Relative expression refers to the levels of transcript when compared to actin, in percentage. Means were generated from three independent measurements, and bars indicate standard deviations.

The basal expression of each *GmMT* gene was previously evaluated [19] showing that, following the generally assumed expression patterns for each of the plant MT types [17], *GmMT1*, *GmMT2* and *GmMT3* were expressed in leaves, seeds and roots, while *GmMT4* was only expressed in seeds. Thus, considering the basal expression of each gene in the tested tissues (control treatment), the results showed that in leaves *GmMT2* and *GmMT3* expression was enhanced, whereas no significant differences have been seen for *GmMT1*. Concerning expression in roots, no differences have been detected for any of the *MT* genes. Although tested, mRNA levels were not detectable for *GmMT4* in any of the assayed tissues.

3.2. GmMTs *overexpression in MT-null yeast cells supplemented with H_2O_2 or paraquat*

Yeast complementation studies are also commonly performed to determine the *in vivo* function of MTs in more complex eukaryotic organisms, such as plants. Baker's yeast *Saccharomyces cerevisiae* expresses two MTs, CUP1 and CRS5, both involved in copper tolerance [29,30,31]. DTY3 *S. cerevisiae* strain possesses a single copy of CUP1 ($cup1^{S}crs5^{\Delta}$), while DTY4 lacks these endogenous MTs ($cup1^{\Delta}crs5^{\Delta}$). In order to test the role of soybean plant MTs in conferring oxidative stress tolerance to an MT-defective yeast, DTY3 and DTY4 *S. cerevisiae* cells were transformed to constitutively express each one of the individual studied GmMTs, and their subsequent growth in solid medium containing H_2O_2 or paraquat at different concentrations was analysed. Paraquat is known to induce the production of superoxide anions in living organisms, thus giving rise to H_2O_2 after the action of superoxide dismutases, and therefore also yielding $HO^{\bullet}$ [32].

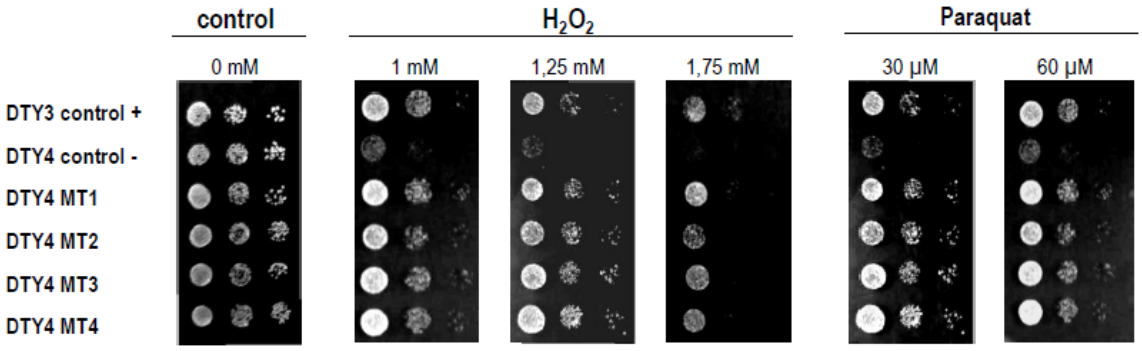

Figure 2. Growth of yeast cells in solid media supplemented with H_2O_2, paraquat or none (control). *Saccharomyces cerevisiae* DTY4 cells (lacking endogenous MTs; $cup1^{\Delta}crs5^{\Delta}$) were transformed to constitutively express one of the GmMTs (DTY4 MT1, DTY4 MT2, DTY4 MT3 and DTY4 MT4). DTY3 (containing a single copy of cup1; $cup1^{S}crs5^{\Delta}$) and DTY4 cells transformed with the empty p424 vector are the positive (DTY3 control +) and negative (DTY4 control –) controls for the experiment, respectively.

As shown in Fig. 2, both H_2O_2 and paraquat inhibited the growth of DTY4 cells containing the empty p424 plasmid at every dose tested, whereas the same cells carrying the p424-GmMT1, -GmMT2, -GmMT3 or –GmMT4 construction were able to grow at a similar rate to parental DTY3-p424 cells, thus showing the capacity of each of these soybean MTs to confer oxidative-stress protection in a comparable level to the one that CUP1 exerts in the same conditions (DTY3 control +). Moreover, no clear differences in growth and hence in protection against oxidative stress could be detected between the four GmMTs in this experiment.

3.3. Metal release from the Zn(II)-GmMT complexes upon H_2O_2 exposure

Hydrogen peroxide is able to oxidise the cysteine thiolate groups of MT peptides and provoke a subsequent metal ion release [6,33]. In order to compare the vulnerability to oxidation of the four different MT types present in soybean, the recombinantly synthesised Zn(II)- GmMT1, GmMT2, GmMT3 or GmMT4 complexes were exposed to H_2O_2 in a 1:10 Cys:H_2O_2 ratio and in the presence of an excess of Zincon, a commercially available colorimetric reagent for the quantification of Zn(II) ions, at pH 7. Zincon was confirmed not to compete for Zn(II) bound to the protein in the absence of H_2O_2, and the extinction coefficient at 620 nm for the Zn(II)-Zincon complex was determined in the experimental conditions employed. Hence, the H_2O_2-derived time-dependent displacement of Zn(II) from the four Zn-GmMTs was followed by monitoring the binding reaction of Zincon to free Zn(II) ions at 620 nm by UV-vis spectroscopy. The experimental data points as well as the calculated curves are depicted for each Zn-GmMT complex in Fig. 3.

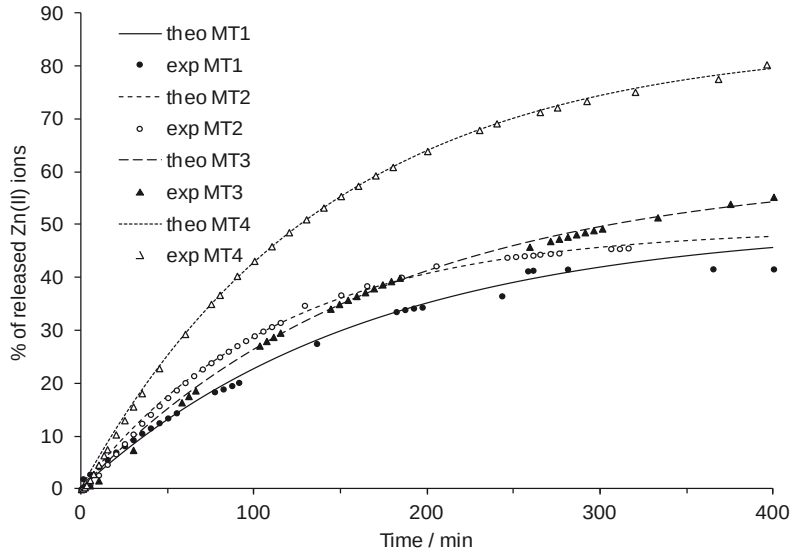

Figure 3. Representation of the experimental points (exp MT1, exp MT2, exp MT3 and exp MT4) and the calculated curves (theo MT1, theo MT2, theo MT3 and theo MT4) for the Zn(II) release process when each Zn(II)-GmMT complex reacted with H_2O_2 (1:10 Cys:H_2O_2 molar ratio) in 50 mM Tris-HCl, pH 7, at 21 ºC in the presence of 1 mM Zincon (see Experimental Section for further details).

The results showed that, although all the four GmMTs give rise to Zn(II) release caused by oxidation of the MT thiolate groups, a different percentages of released Zn(II) ions were achieved at the same time exposure. GmMT1, -2 and -3 released 40-50% of the initially bound metal, while nearly 80% of the total Zn(II) ions was displaced for GmMT4. Thus, GmMT4 shows the fastest reaction kinetics. In addition, by comparing the

kinetics of the GmMT1, -2 and -3 isoforms, slight differences could be detected, although the percentages of displaced Zn(II) ions were comparable for the three peptides at every time tested. In fact, GmMT1 and GmMT2 reached a plateau after ~250 min (with *ca.* 40% of initial Zn(II) released), whereas GmMT3 did not reach it even after 400 min.

3.4. Zn(II)-GmMT complexes under free radical attack: formation of trans*-unsaturated lipids in model membranes and protein modifications*

In the context of free-radical damage, the fate of radical species derived from protein damage has been subject of many investigations. A tandem radical damage involving aqueous and lipid domains was evidenced by using sulfur-containing proteins in the presence of unsaturated membrane phospholipids [12]. It was shown that the damage starts from a specific radical attack towards sulfur moieties of proteins, leading to the release of diffusible sulfur-centered radicals $RS^{\bullet}$ (*i.e.* $CH_3S^{\bullet}$ from Met residue or $HS^{\bullet}/S^{\bullet-}$ from Cys) able to migrate from the aqueous phase to the membrane bilayer. At this site, these radicals react with the naturally occurring *cis* double bonds of the phospholipid fatty acids, causing their transformation to the corresponding *trans* isomers (Fig. S1), which damages the cell membrane by varying its viscosity and permeability [34]. In fact, since the *trans* lipid geometry resembles that of saturated lipids, the geometrical isomerisation can be considered equivalent to a decrease in the number of unsaturations in the membrane, thus causing an impairment of its functions.

Thus, in order to investigate the secondary damage that free radical stress on the Zn(II)-GmMT complexes can cause in cell membranes, Zn(II)-GmMT solutions were added to a suspension of POPC liposomes, saturated with an appropriate gas, and γ-irradiated. Aliquots of the suspensions were withdrawn at different irradiation times for lipid isolation and determination of the *cis*/*trans* isomeric ratio. In addition, the degradation of the metal complexes was followed by mass spectrometry and Raman spectroscopy.

3.4.1. Effect of 90 % $HO^{\bullet}$ and 10% $H^{\bullet}$ species on Zn(II)-GmMTs complexes

Figure 4 shows the irradiation-dose profiles for the *trans*-isomer formation in N_2O-saturated conditions (Method A1) for the Zn-GmMT2, Zn-GmMT3 and Zn-

GmMT4 preparations. This condition has been already used before as a model of oxidative damages occurring *in vivo* [35].

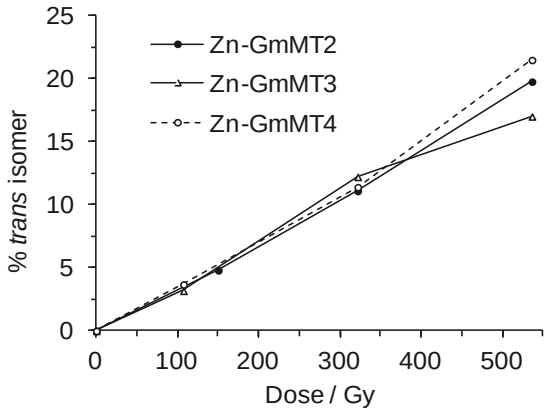

Figure 4. Dose dependence of the formation of elaidate (*trans* isomer) residues from γ-irradiation of POPC vesicles (1.7 mM) containing Zn-GmMTs aggregates (30 μM) in N_2O-saturated aqueous solutions.

The results showed that all the three Zn(II)-GmMT complexes under the attack of mainly $HO^{\bullet}$ radical species were able to cause the *trans*-isomerisation of the naturally occurring fatty acid in a dose-dependent manner, giving rise to almost the same isomerisation yield. Very small differences in the *trans*-isomer formation percentage between the isoforms were detected only at the highest dose (*ca.* 500 Gy) where the metal complexes have completely lost their secondary structure elements. It is worth noting that the highest isomerisation (*ca.* 22%) was caused by Zn-GmMT4, containing 2 Met and 17 Cys residues, whereas the lowest value (*ca.* 17%) was obtained by using Zn-GmMT3, containing an equal number of Met and only 10 Cys, and the intermediate isomerisation value was achieved with Zn-GmMT2, with 4 Met and 14 Cys. This behaviour suggests a more relevant role of the Cys-metal clusters in the tandem protein-lipid damage than the other sulfur-containing residue (Met) able to form isomerising sulfur-centred radicals under mainly oxidative radical stress conditions.

ESI-MS analyses allowed to establish that the attack of $HO^{\bullet}$ and $H^{\bullet}$ radical species on Zn(II)-GmMTs gives rise to small variations of their mass compatible with desulfurisation of some sulfur-containing residues. Figure 5 shows the ESI-MS spectra at pH 2.4 of the four Zn(II)-GmMT preparations before and after mainly oxidative radical attack. The species with a lower molecular mass than the corresponding apo-forms detected for the Zn-GmMT2, Zn-GmMT3 and Zn-GmMT4 preparations (ΔMW= -33.0 Da, -34.2 Da and -37.8 Da, respectively) derive from the lost of $CH_3S^{\bullet}$ from Met and/or

$HS^{\bullet}/S^{\bullet-}$ from Cys and their subsequent reactions. The huge variety of species that could be formed because of the combination of all reactions taking place in the presence of $HO^{\bullet}$ and $H^{\bullet}$ makes extremely difficult univocal assignments. Interestingly, no signals of the less heavy species attributable to desulfurisation processes were detected for the Zn-GmMT1 preparation.

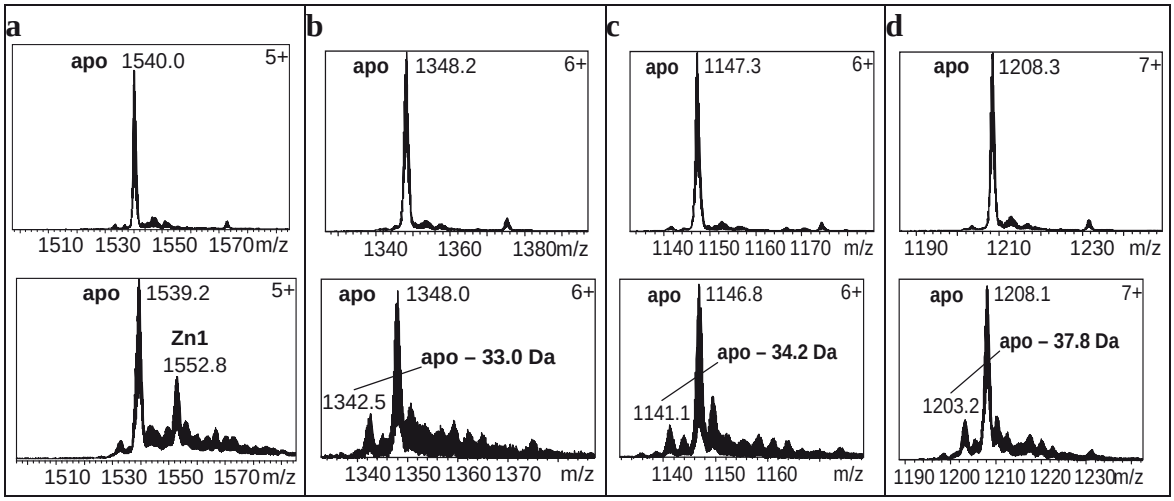

Figure 5. Representative charge states for the ESI-MS spectra at pH 2.4 of (**a**) Zn-GmMT1, (**b**) Zn-GmMT2, (**c**) Zn-GmMT3 and (**d**) Zn-GmMT4 aggregates before (above) and after (below) the γ-irradiation in N_2O-saturated aqueous solutions at 300 Gy. For all spectra, the y axis corresponds to intensity percentage, from 0 to 100. The calculated and experimental molecular masses of the observed species are collected in Table S1.

Regarding the ESI-MS spectra at neutral pH recorded before and after irradiation, they showed that a slight demetalation proceeds for Zn-GmMT2, Zn-GmMT3 and Zn-GmMT4, while this process was more complete for Zn-GmMT1, since the completely demetalated apo-form became the major species (Fig. 6). In addition to these modifications, some species containing the addition of either oxygen atoms (probably because of the methionine sulfoxide formation) or hydroxyl groups (i.e. to the ring of aromatic amino acids) were also detected for all the preparations (Fig. S2-S5).

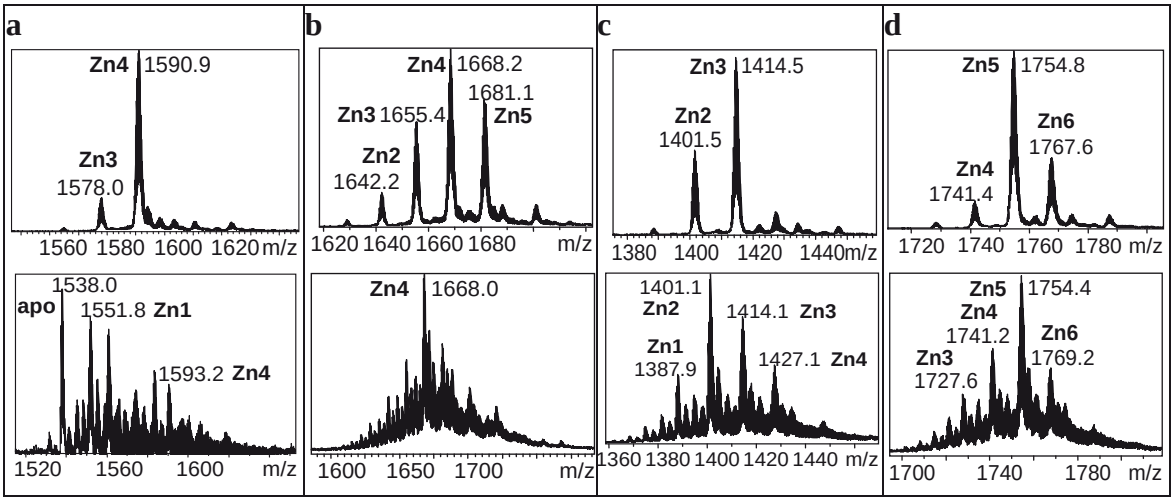

Figure 6. Representative charge states for the ESI-MS spectra at pH 7.0 of (**a**) Zn-GmMT1, (**b**) Zn-GmMT2, (**c**) Zn-GmMT3 and (**d**) Zn-GmMT4 aggregates before (above) and after (below) the γ-irradiation in N_2O-saturated aqueous solutions at 300 Gy. For all spectra, the +5 charge state is shown and the y axis corresponds to intensity percentage, from 0 to 100. Only the most abundant species are annotated for clarity. The calculated and experimental molecular masses of the observed species are collected in Table S1 and Figs. S2-S5.

To obtain further information on protein modifications on $HO^{\bullet}$ and $H^{\bullet}$ and the microenvironment of some amino acidic residues, the Raman spectra of Zn-GmMT2 irradiated at different doses were recorded. From a qualitative examination of the spectra many differences were evident, in particular in the bands due to metal clusters and Tyr (Fig. 7). Among the amino acid residues present in Zn-GmMT2, Cys resulted to be among the most sensitive residues towards radical attack. This conclusion was drawn out from the analysis of the several bands attributable to the metal-thiolate bonds (νZn-S) visible at low wavenumbers (< 500 cm^{-1}). The free radical attack caused a significant spectral modifications of some metal-S stretching bands (280-350 cm^{-1}) at both doses, suggesting a partial rearrangement and deconstruction of tetrahedral metal clusters (Fig. 7). In addition, a slight intensity decrease in the bands in the 410-440 cm^{-1} region was visible at the highest dose, indicating a slight decrease in the number of metal-S_b-metal bonds (by bridging Cys). Conversely, a small intensity increase in the S-S stretching bands (520-500 cm^{-1} region) was observed. Also Met resulted to be sensitive to the free radical attack, as indicated by the intensity decrease of the 726 cm^{-1} band, due to the νC-S of Met residues (Fig. 7). The appearance of a weak band at 1050 cm^{-1}, attributable to the νS=O vibration, was also indicative of the formation of a small amount of methionine sulfoxide (MetS=O). Thus, with respect to the Met radical damage, the radical attack on these residues can take place both by $HO^{\bullet}$ radicals, leading to oxidation

products and by $H^{\bullet}$ atoms, giving rise to generation of thiyl radicals ($CH_3S^{\bullet}$) and the conversion of Met into α-amino butyric acid (Aba).

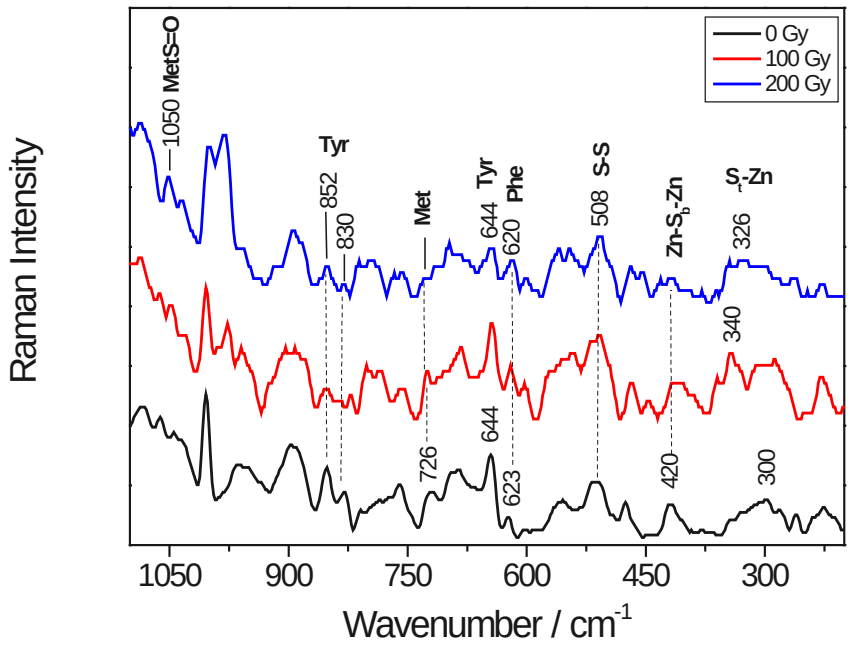

Figure 7. Raman spectra in the 1100-200 cm^{-1} region for the Zn-GmMT2 aggregates before (black) and after the γ-irradiation of an N_2O-saturated aqueous solution containing Zn-GmMT2 (150 μM) at 100 Gy (red) and 200 Gy (blue).

GmMT2 contains 2 Tyr and 1 Phe residues that give rise to many Raman bands due to aromatic ring vibrations. Exposure of the protein to radical stress led to changes in the bands due to aromatic side chains of these residues, suggesting the occurrence of radical-induced modifications on them. In fact, some Tyr bands strongly decreased (i.e. the 850 a and 644 cm^{-1} bands) and the I_{852}/I_{830} ratio, marker of the state of the hydrogen bonding involving the HO^- group of Tyr, increased when the sample was undergone to the free radical attack (Fig. 7). This indicates that some Tyr are located in a more hydrophilic environment and/or are less bound to negative acceptors such as COO^- of aspartic and glutamic acid residues. In addition, the intensity ratio between the ~620 and ~ 645 cm^{-1} bands due to Phe and Tyr residues, respectively, significantly increased. Since the I_{620}/I_{640} ratio has been connected to the Phe/Tyr content ratio in some proteins, this change could be indicative of a radical-induced modification of some Try residues into Phe residues.

3.4.1. Effect of reducing species (20% $H^{\bullet}$ and 80% e^-_{aq}) on Zn(II)-GmMT2 complexes

Fig. 8 presents the irradiation-dose profile for the *trans*-isomer formation in oxygen-free *t*-BuOH containing conditions for the Zn-GmMT2 preparation, thus showing that the attack of 20% $H^{\bullet}$ and 80% e^-_{aq} (*i.e.*, reductive radical stress conditions, Method B2) on these complexes caused the *trans*-isomerisation of the naturally occurring oleic acid in a dose-dependent manner.

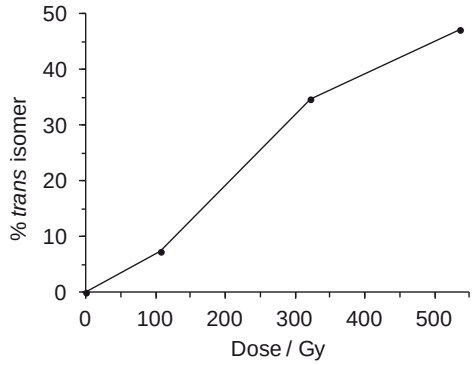

Figure 8. Dose dependence of the formation of elaidate (*trans* isomer) residues from γ irradiation of POPC vesicles (1.7 mM) containing Zn-GmMT2 aggregates (30 μM) in Ar-flushed solutions containing 0.2 M *t*-BuOH.

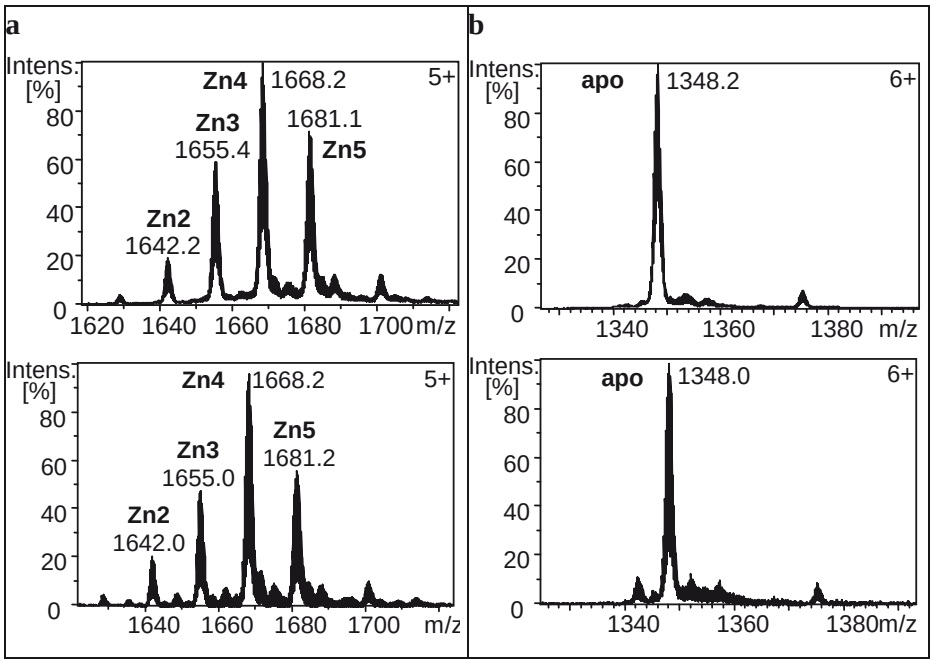

Figure 9. Representative charge states for the ESI-MS spectra at (**a**) pH 7.0 and (**b**) pH 2.4 before (above) and after (below) the γ-irradiation of Ar-flushed aqueous solutions containing Zn-GmMT2 aggregates (150 μM) and 0.2 M *t*-BuOH at 100 Gy. The calculated and experimental molecular masses of the observed species are collected in Table S1.

ESI-MS measurements showed that the Zn(II) ions remained bound to Zn-GmMT2 (Fig. 9a) and the protein backbone also remained invariable after the radical species exposure (Fig. 9b). On the other hand, Raman spectra before and after irradiation showed the formation of disulfide bridges (510 cm^{-1}) and some changes in the thiolate ligands that bind the Zn(II) ions (375, 328 and 300 cm^{-1}). Furthermore, acidic amino acids (*i.e.* Asp and Glu) participated in metal-binding through their carboxylate groups (1400 cm^{-1} and 1366 cm^{-1}) after the exposure of the Zn(II)-GmMT2 complex to the 20% $H^{\bullet}$ and 80% e^{-}_{aq} mixture (Fig. 10).

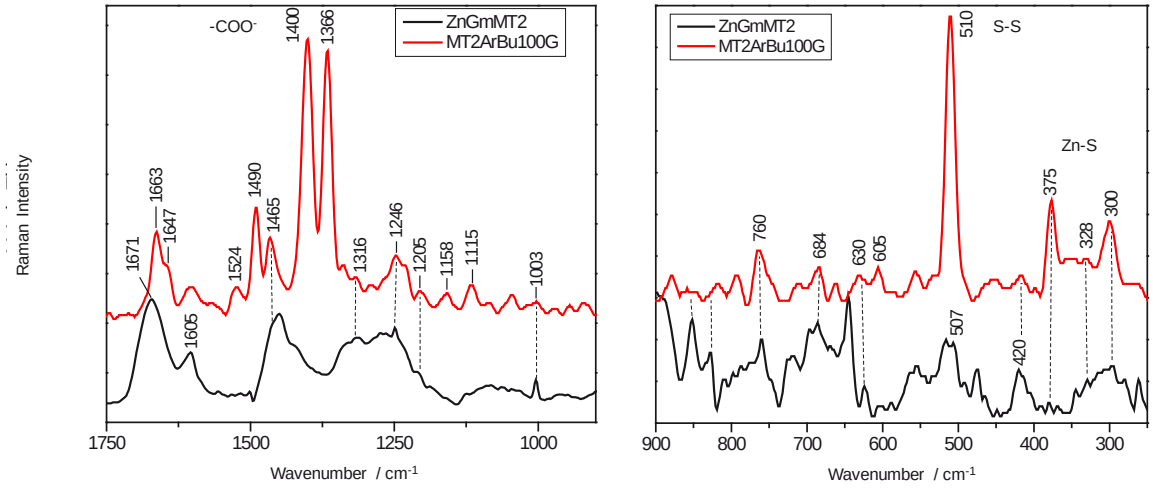

Figure 10. Raman spectra in the 1750-875 cm^{-1} (left) and 900-250 cm^{-1} (right) regions for the Zn-GmMT2 aggregates before (black) and after (red) the γ-irradiation of an Ar-flushed aqueous solution containing Zn-GmMT2 (150 μM) and 0.2 M *t*-BuOH at 100 Gy.

3.4.3. Additional experiments with POPC-LUVET

Additional irradiation experiments on solutions containing Zn(II)-GmMT2 complexes and POPC vesicles under oxygen-free conditions (*i.e.* accounting for a e_{aq}^{-}:$HO^{\bullet}$:$H^{\bullet}$ 45:45:10 proportion, Method A2) gave rise to a dose-effect profile equivalent to that obtained for the e_{aq}^{-}:$H^{\bullet}$ 80:20 (Fig. 8). Moreover, γ-irradiation under N_2O-saturated solutions containing *t*-BuOH (*i.e.*100% $H^{\bullet}$, Method B1) was also performed for the Zn-GmMT2-4 complexes at the 500 Gy dose. The results showed a percentage of *trans*-isomer formation of 56, 51 and 56% for the Zn-GmMT2, Zn-GmMT3 and Zn-GmMT4 complexes, respectively. Altogether, these results showthat the *trans*-isomerisation is always higher when *t*-BuOH is present in solution, *i.e.*, when hydroxil radicals are

scavenged; and that the presence or absence of solvated electrons as reactive species does not significantly affect the *trans*-isomerisation percentage in the case of the Zn-GmMT2 complexes.

4. Discussion

A high percentage of metallothionein residues are Cys, which confer them a potential activity in redox processes. With this idea in mind, it seems reasonable to expect differential redox properties for MTs exhibiting different Cys contents, which is the scenario drawn by the four different soybean MT isoforms studied in this work (Fig. 11). In fact, their involvement in oxidative processes has already been hypothesised when analysing their metal-binding abilities [19, and other unpublished works in our group], but the need of a more detailed comparative study of their behaviour when being exposed to radical and/or oxidising agents was made patent.

```
           10        20        30        40        50        60        70        80
   ....|....|....|....|....|....|....|....|....|....|....|....|....|....|....|....|
p1 MSSCGCGSSCNCGSNCGCNKYSFDLSYVEKTTTETLVLGVGPVKAQLEGAEMGVASENGGCNCGSSCTCDPCNCK

p2 MSCCGGNCGCGSACKCGNGCGGCKMYPDLSYTESTTTETLVMGVAPVKAQFESAEMGVPAENDGCKCGANCTCNPCTCK

p3 MSNTCGNCDCADKTSCTKGNSYGVIVETEKSYIETVVMDVPAAEHDGKCKCGTNCTCTDCTCGH

p4 MADTSGGDAVRPVVICDNKCGCTVPCTGGSTCRCTSVGMTTGGGDHVTCSCGEYCGCNPCSCPKTAASGTGCRCGTDCSCASCRT
```

Figure 11. Amino acid sequences of the peptides studied in this work. p1 refers to the soybean MT isoform belonging to subfamily p1 of plant MTs, GmMT1, and p2-p4 analogously refer to GmMT2, GmMT3 and GmMT4. The shaded boxes indicate the cysteine residues, aromatic amino acids are in bold and methionines are underlined.

In this work we have shown that the transcription of the type 2 MT gene from soybean, *GmMT2*, is clearly enhanced in leaves when the plant is exposed to 10 mM hydrogen peroxide for 24h. Furthermore, the accumulation of the *GmMT3* transcript is also slightly enhanced in leaves under these conditions, while none of the other analysed genes and tissues are affected (Fig. 1). An increase in gene expression for MT types 1-3 from napus (*Brassica rapa*) seedlings treated in similar conditions was reported, although these levels were detected to be either higher or lower depending on the duration of the H_2O_2 exposure, with a non-linear relationship dependence [36]. Indeed, a 24h-treatment – again strictly under the same conditions- showed to restablish the levels of the MT3 transcript in buckwheat (*Fagopyrum esculentum*), which were also enhanced in leaves at

earlier times [37]. The fact that the gene expression patterns are non-linearly time-dependent is noteworthy, since the lack of accumulation of transcripts in a specific tissue after the exposure to an oxidising agent for a fixed period of time does not lead to conclude their lack of involvement in redox homeostasis. For instance, for GmMT1, for which no variation in gene expression was detected after hydrogen peroxide treatment in this work, the amount of *GmMT1* transcript increased after drought stress in root nodules infected with rhizobia *Bradyrhizobium japonicum*, a N_2 fixing bacteria [38]. However, transcript up-regulation was completely reversed after rehydration, thus showing that transient accumulation could protect the plant against drought induced alterations, such as oxidative stress. Moreover, its transient down-regulation in roots was already demonstrated when the plant was exposed to Cd(II) based on the hypothesis that, since GmMT1 is a ROS scavenger, the down-regulation of its expression might favour the ROS signalling that would finally reduce the damage in other tissues [19]. Besides, our results on yeast complementation assays point towards a protective role against oxidative stress for the four GmMTs, irrespective of the isoform under study and of the toxic agent added, since overexpression of each of the soybean MTs in MT-null *S. cerevisiae* cells confers resistance to both H_2O_2 and paraquat (Fig. 2). Reported results on a comparable experiment showed the ability of the MT3 from *F. esculentum* to improve the growth of yeast cells when they were exposed to up to 3 mM H_2O_2 [37], concentration that falls within the tolerated range for our GmMT-containing cells here analysed.

Turning to the results on the recombinantly obtained Zn(II)-GmMT complexes, it is worth to point out that the release of Zn(II) ions from MTs, which would make the metal available for proteins with Zn-binding sites with lower affinities than MTs, was proposed to occur under oxidative stress conditions [8]. At this point, the comparison of the capabilities in liberating the Zn(II) ions in response to the attack of an oxidising agent for each of the Zn-GmMT complexes appears to be informative. We have determined that GmMT4 is the most prone to Zn(II) removal as a consequence of H_2O_2 exposure. It shows the highest final amount of released metal, when values are corrected for the initially bound Zn(II), and the process is also faster than for any other soybean isoform. Looking at the percentages of released Zn (*ca.* 80% for GmMT4 and 40-50% for GmMT1-3) and at the kinetics for each of the processes, the four soybean isoforms can be organised into two groups: GmMT4, on the one hand, and GmMT1-3, on the other hand. Analogous groups were observed in a similar experiment where representants of each of

the plant MT subfamilies, thus containing the same number of Cys residues within their sequences as our GmMT isoforms, were exposed to the GSH/GSSG redox couple [39]. However, trends were inverted in that case, since MTs belonging to subfamilies 1-3 displaced up to 80% of the initially bound Zn(II) ions, whereas the analysed MT4 liberated only 40% of it (as it also happened for human MT2 used for comparison). Many considerations could be taken into account to explain these divergent results, although probably the main reason could be related to the differences in structure between the Zn-complexes of the tested MT4 isoforms in all experiments. Hence, the canonical MT4 from wheat (*Triticum aestivum*), Ec-1, for which the existence of a Zn-$(NHis)_2(SCys)_2$ site [40] and its role in Zn(II) storage [41] are known, was used for the analysis of the metal release in the presence of GSH/GSSG. However, the here studied GmMT4 from soybean lacks one of the conserved His residues in the family, thus probably not folding in an optimally structured Zn-complex, as our previous results on metal-binding suggested (unpublished work). Therefore, the more pronounced vulnerability to lose Zn that GmMT4 shows over Ec-1 could be related to its lower Zn-binding ability, consequently pointing towards a biological function other than acting as a Zn(II) storage protein. Moreover, among other considerations such as the intrinsic different reactivities of each of the Zn-MT complexes, the resistance of the GmMT1-3 to lose their metal ions when compared to other types 1-3 plant MTs reported in the literature [39] (up to 50% for the former, up to 80% for the latter) could be explained by the competing reactions of H_2O_2 with Met and the oxidation of thiols beyond the level of disulfide groups, which would not take place with GSSG acting as the only oxidising agent [8]. Hence, the higher level of metal loss that GmMT4 exhibited over GmMT1-3 could also be explained by the occurrence of alternative reactions in the Zn-GmMT1-3 complexes, since the long Cys-free stretches in these three peptides are probably more exposed to H_2O_2 than their Cys thiolates.

Regarding γ-irradiation experiments of the Zn-GmMT complexes, the exposure of the Zn-GmMT2-4 complexes to mainly $HO^{\bullet}$ has also showed to cause the *trans*-isomerisation in model cell membranes (Fig. 4). ESI-MS spectra of each of these apo-GmMT isoforms have confirmed the presence of desulfurised products (*i.e.* species that have lost the sulfur-centered radicals) after irradiation (Fig. 5). These data are remarkably different for the Zn-GmMT1, for which no signals of the desulfurisation process have been detected. Unfortunately, a low sample availability precluded us to determine the level of *trans*-isomerisation that these complexes caused, which would be of

interest in order to confirm this different behaviour. Moreover, similar patterns of modification have been detected by ESI-MS at pH 7.0 for Zn-GmMT2-4, whereas differences also arise for Zn-GmMT1 (Fig. 6). All the Zn-GmMT preparations partially lose metal ions upon $HO^{\bullet}$ exposure, as it happened in front of H_2O_2, thus showing that the oxidation of Cys thiolates to disulfides is again taking place. Oxidation at the level of Met residues and/or aromatic amino acids also occurs for all cases (Fig. S2-S5). However, the dematalation of the Zn-GmMT1 complexes is significantly more intense, since apo-GmMT1 becomes the major species after the $HO^{\bullet}$ attack. Hence, after $HO^{\bullet}$ exposure, Zn-GmMT2-4 complexes are less vulnerable than Zn-GmMT1 to metal ion release. Moreover, the protein backbone is nearly unaltered for the latter, while desulfurisation occurs for GmMT2-4 (Fig. 5), which can cause cellular damage. Taking all data in consideration, the lack of formation of desulfurised species together with the higher reactivity of the Cys thiolates of Zn-GmMT1 complexes point towards a major role of this Zn-MT in protecting the cell against $HO^{\bullet}$ attack. Also, the capacity of the Zn-GmMT2 complexes to generate the sulfur-centered radicals that cause damage in a model cell membrane upon exposure to reductive radical stress has been confirmed (Fig. 8), as it was expected based on the high degree of homology between the MT2 from *Quercus suber*, QsMT, and GmMT2 amino acidic sequences (Fig. S6). Indeed, previously reported data on Zn-QsMT showed that these complexes also respond to the 20% $H^{\bullet}$ and 80% e_{aq}^{-} attack by increasing the percentage of *trans* isomer fatty acid (an isomerisation which damages the cell membrane) in a dose-dependent manner [16]. This effect is comparable for both Zn-MT2 complexes at the 100 Gy dose, while Zn-GmMT2 shows a higher percentage of *trans* isomer formation from this dose on, reaching a 50% at the approximately 500 Gy dose instead of the 30% that was determined for Zn-QsMT. The reason for this differential effect is probably the existence of an additional Met residue in position 42 of GmMT2 sequence, which is absent in QsMT. Moreover, the Zn-GmMT2 modification associated with reductive stress has been determined to consist in a partial oxidation of the Cys residues as well as the participation of ligands other than Cys in Zn(II)-binding (Fig. 10), which were unbound before the free radicals attack. These effects were also detected for the Zn-QsMT complexes [15], while the differences between the sequences of both peptides (Fig. S6) seem to be determinant for explaining the last modification. Thus, His50 in QsMT but acidic amino acids (*i.e.* Asp and Glu) in GmMT2 have been shown to bind Zn(II) ions after radical exposure.

In conclusion, the expression of *GmMT2* is enhanced in leaves as a consequence of the exposure of the plant to a 24h-treatment with hydrogen peroxide. However, the lack of response of the *GmMT1*, *GmMT3* and *GmMT4* genes does not preclude the involvement of them in redox homeostasis. Indeed, all soybean MTs studied here react with radical and oxidative species, thus conferring them a protective role against these stressors. Furthermore, all the Zn-GmMT complexes release metal ions when being exposed to hydrogen peroxide or hydroxil radicals, with Zn-GmMT4 being the most sensitive to H_2O_2 attack and Zn-GmMT1 to $HO^{\bullet}$ exposure for this effect. Given the fact that $HO^{\bullet}$ is the most reactive species among all biologically relevant ROS and that it is a secondary ROS, generated from the primary ones $^{-\bullet}O_2$ and H_2O_2, it is sensible to conclude that Zn-GmMT1 complexes display a higher ROS scavenging activity than the Zn-GmMT2-4 complexes. Additionally, radical stress on Zn-GmMT2-4 complexes might cause cellular damage.

5. References

[1] M. Capdevila, R. Bofill, Ò. Palacios, S. Atrian, Coord. Chem. Rev. 256 (2012) 46-62.

[2] T. Dalton, R.D. Palmiter, G.K. Andrews, Nucleic Acids Res. 22 (1994) 5016-5023.

[3] S. Zeitoun-Ghandour, O.I. Leszczyszyn, C.A: Blindauer, F.M. Geier, J.G. Bundy, S.R. Stürzenbaum, Mol. BioSyst. 7 (2011) 2397-2406.

[4] P.J. Thornalley, M. Vasák, Biochim. Biophys. Acta 827 (1985) 36-44.

[5] J. Abel, N. de Ruiter, Toxicol. Lett. 47 (1989) 191-196.

[6] A.R. Quesada, R.W. Byrnes, S.O. Krezoski, D.H. Petering, Arch. Biochem. Biophys. 334 (1996) 241-250.

[7] Y.J. Kang, Exp. Biol. Med. 231 (2006) 1459-1467.

[8] W. Maret, B.L. Vallee, Proc. Natl. Acad. Sci. USA 95 (1998) 3478-3482.

[9] B. Lipinski, Br. J. Nutr. 87 (2002) 93-94.

[10] N.S. Rajasekaran, P. Connell, E.S. Christians, L.J. Yan, R.P. Taylor, A. Orosz, et al., Cell 130 (2007) 427-439.

[11] X. Zhang, X. Min, C. Li, I.J. Benjamin, B. Qian, X. Zhang, et al., Hyperthension 55 (2010) 1412-1417.

[12] C. Chatgilialoglu, C. Ferreri, A. Torreggiani, A.M. Salzano, G. Renzone, A. Scaloni, J. Proteomics 74 (2011) 2264-2273.

[13] A. Torreggiani, C. Chatgilialoglu, C. Ferreri, M. Melchiorre, S. Atrian, M. Capdevila, J. Proteomics 92 (2013) 204-215.

[14] V.H. Hassinen, A.I. Tervahauta, H. Schat, S.O. Kärenlampi, Plant Biology 13 (2011) 225-232.

[15] A. Torreggiani, J. Domènech, A. Tinti, J. Raman Spectrosc. 40 (2009) 1687-1693.

[16] A. Torreggiani, J. Domènech, R. Orihuela, C. Ferreri, S. Atrian, M. Capdevila, C. Chatgilialoglu, Chem. Eur. J. 15 (2009) 6015-6024.

[17] C. Cobbett, P. Goldsbrough, Annu. Rev. Plant Biol. 53 (2002) 159-182.

[18] K.J. Livak, T.D. Schmittgen TD, Methods 25 (2001) 402–408.

[19] M.A. Pagani, M. Tomas, J. Carrillo, R. Bofill, M. Capdevila, S. Atrian, C.S. Andreo, J. Inorg. Biochem. 117 (2012) 306-315.

[20] D. Mumberg, R. Müller, M. Funk, Gene 156 (1995) 119-122.

[21] T. Stearns, H. Ma, D. Botstein, Methods Enzymol. 185 (1991) 280-297.

[22] M. Capdevila, N. Cols, N. Romero-Isart, R. Gonzàlez-Duarte, S. Atrian, P. Gonzàlez-Duarte, Cell. Mol. Life Sci. 53 (1997) 681-688.

[23] J. Bongers, C.D. Walton, D.E. Richardson, J.U. Bell, Anal. Chem. 60 (1988) 2683-2686.

[24] M. Capdevila, J. Domènech, A. Pagani, L. Tío, L. Villarreal, S. Atrian, Angew. Chem. Int. Ed. Engl. 44 (2005) 4618-4622.

[25] C.F. Shaw, J.E. Laib, M.M. Sabas, D.H. Petering, Inorg. Chem. 29 (1990) 403-408.

[26] C.E. Säbel, J.M. Neureuther, S. Siemann, Anal. Biochem. 397 (2010) 218-226.

[27] J. Vuković, M.A. Avidad, L.F. Capitán-Vallvey, Talanta 94 (2012) 123-132.

[28] B. Mihaljević, I. Tartaro, C. Ferreri, C. Chatgilialoglu, Org. Biomol. Chem. 9 (2011) 3541-3548.

[29] A. Brenes-Pomales, G. Lindegren, C.C: Lindegren, Nature 176 (1955) 841-842.

[30] T.R: Butt, E.J. Sternberg, J.A. Gorman, P. Clark, D. Hamer, M. Rosenberg, S.T. Croke, Proc. Natl. Acad. Sci. USA 81 (1984) 3332-3336.

[31] V.C: Culotta, W.R. Howard, X.F. Liu, J. Biol. Chem. 269 (1994) 25295-25302.

[32] J.A.F. Vicente, F. Peixoto, M.L. Lopes, V.M.C. Madeira, J. Biochem. Mol. Toxicol. 15 (2001) 322-330.

[33] S. Zeitoun-Ghandour, O.I. Leszczyszyn, C.A. Blindauer, F.M. Geier, J.G. Bundy, S.R. Stürzenbaum, Mol. Biosyst. 7 (2011) 2397-2406.

[34] T.L. Roberts, D.A. Wood, R.A. Riemersma, P.J. Gallagher, F.C. Lampe, Lancet 345 (1995) 278-282.

[35] A. Torreggiani, S. Barata-Vallejo, C. Chatgilialoglu, Anal. Bioanal. Chem. 401 (2011) 1231-1239.

[36] Y.O. Ahn, S.H. Kim, J. Lee, H. Kim, H.S. Lee, S.S. Kwak, Mol. Biol. Rep. 39 (2012) 2059-2067.

[37] J.T. Samardzić, D.B. Nikolić, G.S. Timotijević, Z.S. Jovanović, M. Đ. Milisavljević, V.R. Maksimović, J. Plant Physiol. 167 (2010) 1407-1411.

[38] M. Clement, A. Lambert, D. Herouart, E. Boncompagni, Gene 426 (2008) 15-22.

[39] E.A. Peroza, A. dos Santos Cabral, X. Wan, E. Freisinger, Metallomics 5 (2013) 1204-1214.

[40] E.A. Peroza, R. Schmucki, P. Güntert, E. Freisinger, O. Zerbe, J. Mol. Biol. 387 (2009) 207-218.

[41] L. Hanley-Bowdoin, B.G. Lane, Eur. J. Biochem. 135 (1983) 9-15.

SUPPORTING INFORMATION

Table S1. Calculated and experimental molecular masses for the apo- and Zn-GmMT species detected by ESI-MS in this work.

MT	ESI-MS		
	Species	**Calc. MW (Da)**	**Exp. MW (Da)**
GmMT1	apo	7696.6	7693.0
	Zn_1	7760.0	7759.0
	Zn_3	7886.7	7885.2
	Zn_4	7950.1	7949.8
GmMT2	apo	8085.2	8082.6
	Zn_2	8212.0	8205.5
	Zn_3	8275.3	8271.0
	Zn_4	8338.7	8336.0
	Zn_5	8402.1	8400.8
GmMT3	apo	6878.7	6879.9
	Zn_2	7005.4	7003.2
	Zn_3	7068.8	7067.5
GmMT4	apo	8452.5	8450.4
	Zn_4	8706.0	8703.5
	Zn_5	8769.4	8769.8
	Zn_6	8832.8	8832.9

a **b**

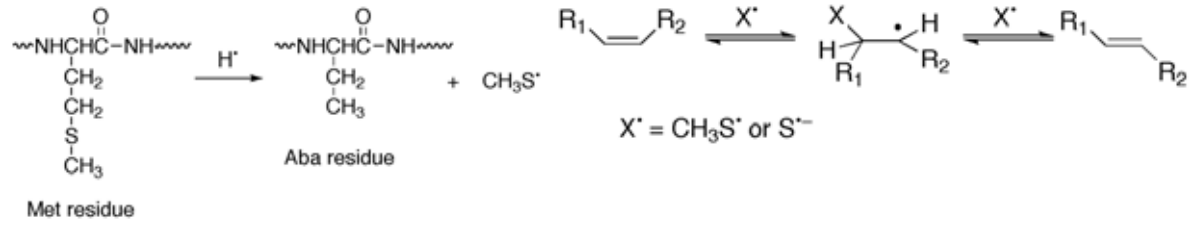

Figure S1. (**a**) Proposed mechanism for the formation of the diffusible isomerising thiyl radicals from Met under reductive radical attack and (**b**) scheme for the transformation of the double bond of a *cis*-fatty acid into its corresponding *trans*-isomer by the catalytic addition-elimination mechanism.

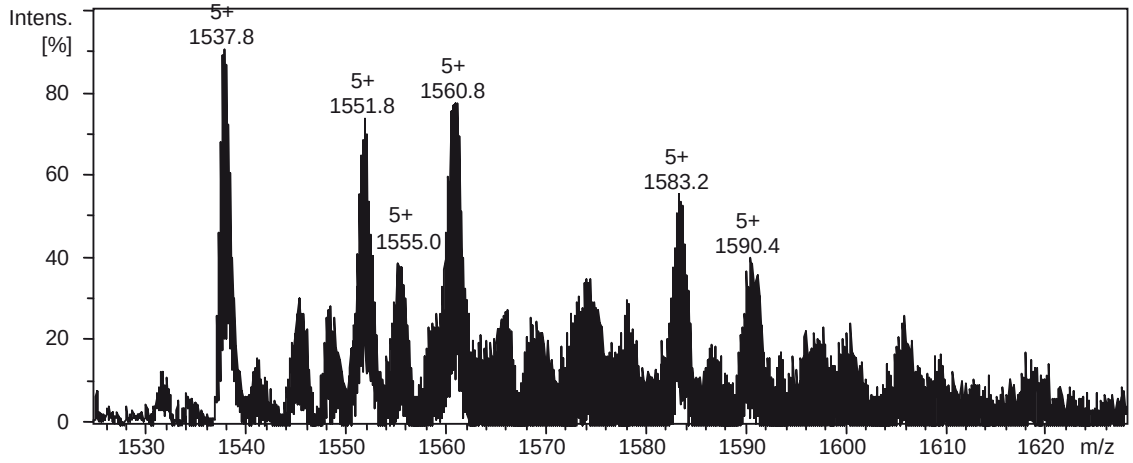

Species		m/z value	Cal. MW (Da)	Exp. MW (Da)
apo-GmMT1	-12H	1537.8	7684.6	7684.0
Zn_1-GmMT1	-4H	1551.8	7756.0	7759.0
	-4H +1O	1555.0	7772.0	7770.0
	-4H +3O	1560.8	7804.0	7799.0
Zn_4-GmMT1	-3H	1590.4	7947.1	7947.0

Figure S2. Representative charge-state for the ESI-MS spectra at pH 7.0 of the Zn-GmMT1 preparation after the γ-irradiation in N_2O-saturated aqueous solutions at 300 Gy. Calculated and experimental molecular masses corresponding to oxidised species have been attached for facilitating the interpretation of the experimental data: these species could combine a weight loss due to the oxidation of the non-coordinating Cys residues (-*x*H), a weight gain because of the extra O atoms coming from sulfoxidation reactions (+*y*O) and/or a weight gain due to the extra O and H atoms coming from hydroxilation reactions (+*z*OH, which accounts for +*z*H +*z*O in the global assignment).

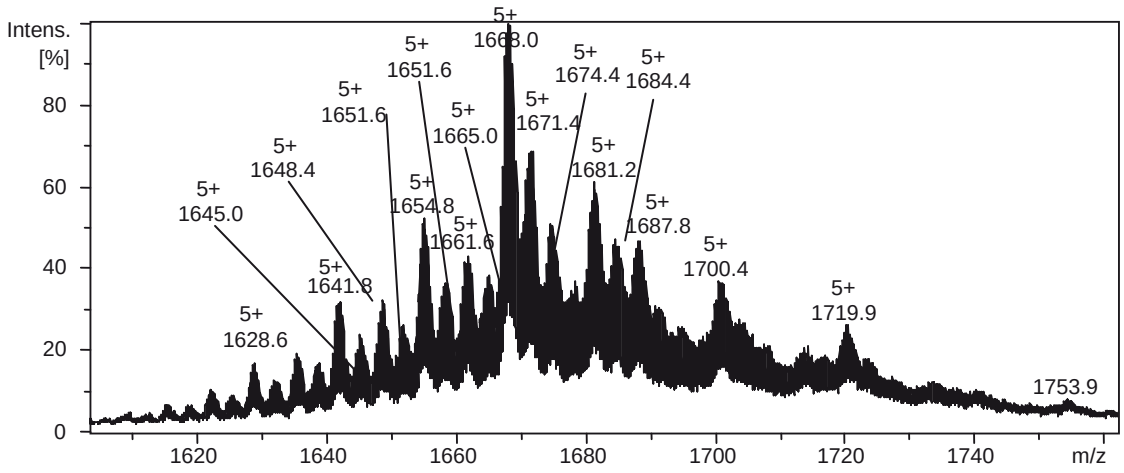

Species		m/z value	Cal. MW (Da)	Exp. MW (Da)
Zn_1-GmMT2	-10H	1628.6	8138.6	8138.0
Zn_2-GmMT2	-8H	1641.8	8204.0	8204.0
	-8H +1O	1645.0	8220.0	8220.0
	-8H +2O	1648.4	8236.0	8237.0
	-8H +3O	1651.6	8252.0	8253.0
Zn_3-GmMT2	-6H	1654.8	8269.3	8269.0
	-4H +1O	1658.4	8287.3	8287.0
	-4H +2O	1661.6	8303.3	8303.0
	-4H +3O	1665.0	8319.3	8320.0
Zn_4-GmMT2	-3H	1668.0	8335.7	8335.0
	-3H +1O	1671.4	8351.7	8352.0
	-3H +2O	1674.4	8367.7	8367.0
Zn_5-GmMT2	-H	1681.2	8401.1	8401.0
	-H +1O	1684.4	8417.1	8417.0
	+2O	1687.8	8434.1	8434.0

Figure S3. Representative charge-state for the ESI-MS spectra at pH 7.0 of the Zn-GmMT2 preparation after the γ-irradiation in N_2O-saturated aqueous solutions at 300 Gy. Calculated and experimental molecular masses corresponding to oxidised species have been attached for facilitating the interpretation of the experimental data: these species could combine a weight loss due to the oxidation of the non-coordinating Cys residues (-*x*H), a weight gain because of the extra O atoms coming from sulfoxidation reactions (+*y*O) and/or a weight gain due to the extra O and H atoms coming from hydroxilation reactions (+*z*OH, which accounts for +*z*H +*z*O in the global assignment).

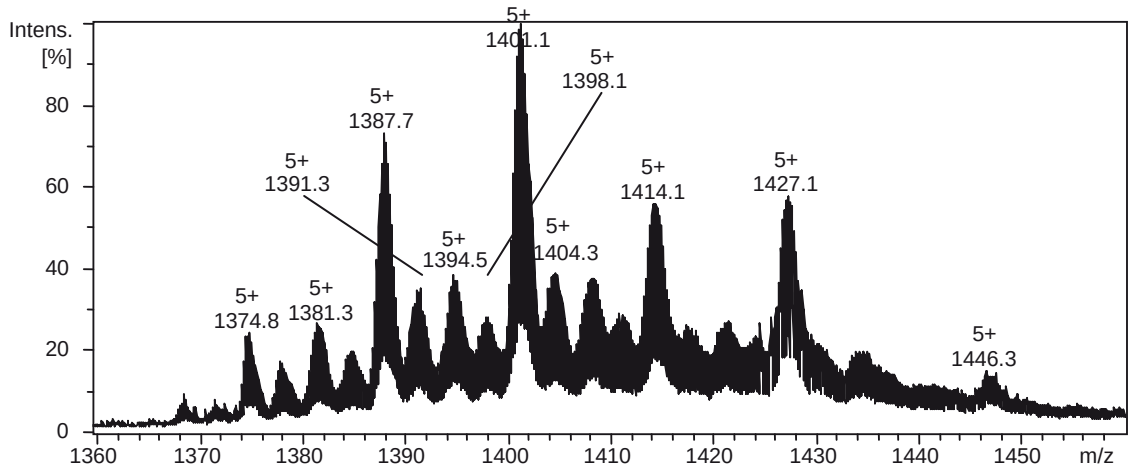

Species		m/z value	Cal. MW (Da)	Exp. MW (Da)
apo-GmMT3	-10H	1374.7	6868.7	6868.5
	-10H +2O	1381.3	6900.7	6901.5
Zn_1-GmMT3	-7H	1387.9	6935.0	6934.5
	-7H +1O	1391.3	6951.0	6951.5
	-7H +2O	1394.5	6967.0	6967.5
	-7H +3O	1398.1	6983.0	6985.5
Zn_2-GmMT3	-5H	1401.1	7000.4	7000.5
	-5H +1O	1404.3	7016.4	7016.5
Zn_3-GmMT3	-3H	1414.1	7065.8	7065.5
Zn_4-GmMT3	-2H	1427.1	7130.2	7130.5

Figure S4. Representative charge-state for the ESI-MS spectra at pH 7.0 of the Zn-GmMT3 preparation after the γ-irradiation in N_2O-saturated aqueous solutions at 300 Gy. Calculated and experimental molecular masses corresponding to oxidised species have been attached for facilitating the interpretation of the experimental data: these species could combine a weight loss due to the oxidation of the non-coordinating Cys residues (-*x*H), a weight gain because of the extra O atoms coming from sulfoxidation reactions (+*y*O) and/or a weight gain due to the extra O and H atoms coming from hydroxilation reactions (+*z*OH, which accounts for +*z*H +*z*O in the global assignment).

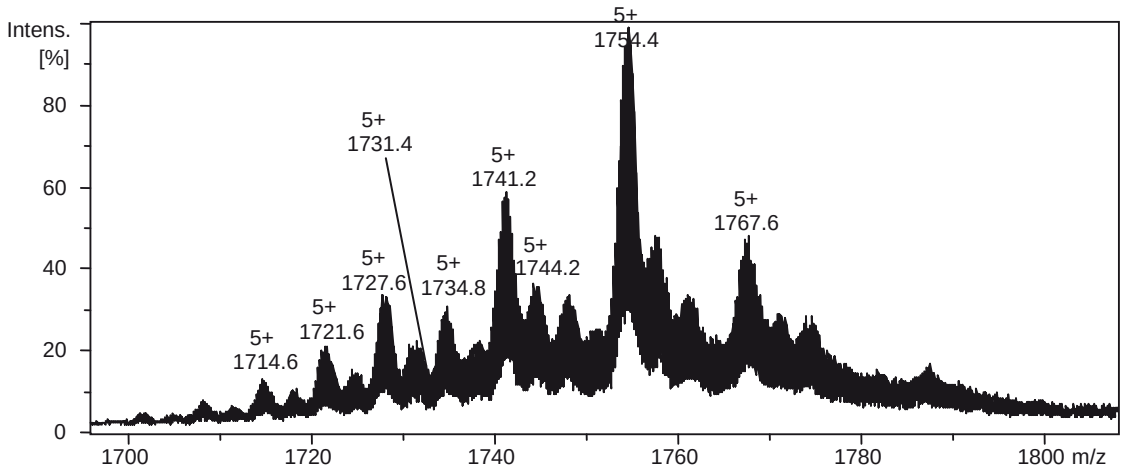

Species		m/z value	Cal. MW (Da)	Exp. MW (Da)
Zn_2-GmMT4	-11H	1714.6	8568.3	8568.0
	-9H +2O	1721.6	8602.3	8603.0
Zn_3-GmMT4	-9H	1727.6	8633.6	8633.0
	-7H +1O	1731.4	8651.6	8652.0
	-7H +2O	1734.8	8667.6	8669.0
Zn_4-GmMT4	-5H	1741.2	8701.0	8701.0
	-5H +1O	1744.2	8717.0	8716.0
Zn_5-GmMT4	-2H	1754.4	8767.4	8767.0
Zn_6-GmMT6	----------	1427.1	8832.8	8833.0

Figure S5. Representative charge-state for the ESI-MS spectra at pH 7.0 of the Zn-GmMT4 preparation after the γ-irradiation in N_2O-saturated aqueous solutions at 300 Gy. Calculated and experimental molecular masses corresponding to oxidised species have been attached for facilitating the interpretation of the experimental data: these species could combine a weight loss due to the oxidation of the non-coordinating Cys residues (-*x*H), a weight gain because of the extra O atoms coming from sulfoxidation reactions (+*y*O) and/or a weight gain due to the extra O and H atoms coming from hydroxilation reactions (+zOH, which accounts for +zH +zO in the global assignment).

```
                10        20        30        40        50        60        70
        ....|....|....|....|....|....|....|....|....|....|....|....|....|....|....|....
QsMT    MSCCGGNCGCGTGCKCGSGCGGCKMFPDIS-SEKTTTETLIVGVAPQKTHFEGSEMGVGAEN-GCKCGSNCTCDPCNCK
GmMT2   MSCCGGNCGCGSACKCGNGCGGCKMYPDLSYTESTTTETLVMGVAPVKAQFESAEMGVPAENDGCKCGANCTCNPCTCK
        ***********:.****.*******:**:* :*.******::**** *::**.:**** *** *****:****:**.**
```

Figure S6. ClustalW alignment for the amino acidic sequences of the type 2 plant MT from *Quercus suber*, QsMT, *versus* the type 2 plant MT from *Glycine max*, GmMT2. The shaded boxes indicate the Cys residues, aromatic amino acids are in bold and Met are underlined. The asterisk (*) indicates positions which have a single, fully conserved residue, the colon (:) indicates conservation between groups of strongly similar properties and the period (.) indicates conservation between groups of weakly similar properties.

5. RESUM I DISCUSSIÓ

5. RESUM I DISCUSSIÓ

En aquest treball s'han estudiat tres sistemes MT que es composen de diferents isoformes, tot tractant de respondre a l'objectiu comú d'ampliar el coneixement sobre la relació estructura-funció de les MT. Els resultats obtinguts s'agrupen en tres blocs, d'acord amb els objectius proposats en aquesta Tesi Doctoral. Concretament, d'una banda s'han analitzat les preferències metàl·liques de les dues isoformes de MT presents en l'eriçó de mar (*Strongylocentrotus purpuratus*), un organisme model en biologia del desenvolupament. Els resultats d'aquest estudi (**Capítol 1**) es discutiran en l'apartat **5.1**. D'altra banda, s'ha aprofundit en l'estudi de propietats coordinants envers metalls divalents de les quatre isoformes de MT que sintetitzen les plantes, les quals s'han estudiat en soja (*Glycine max*) i gira-sol (*Helianthus annuus*), i la discussió dels resultats obtinguts en aquest estudi (**Capítols 2**, **3** i **4**) es recollirà en l'apartat **5.2**. En aquests dos blocs de la discussió s'analitzarà també el significat que els resultats obtinguts puguen tindre en relació a la possible funció d'aquestes MT. Addicionalment, s'ha fet un estudi comparatiu del possible paper com a antioxidants i/o captadors de radicals lliures de les quatre MT presents en la planta de soja (**Capítol 5**), els resultats del qual es discutiran en l'apartat **5.3**.

Al llarg de tot el treball ens hem servit dels recursos en Bioinformàtica per a la cerca de noves MT, així com de les eines bàsiques en Biologia Molecular i Enginyeria Genètica per a la construcció dels plasmidis que ens han permés la síntesi de les proteïnes recombinants en bacteris *E. coli*. En aquest sentit, cal destacar l'ús del sistema d'expressió i purificació basat en la síntesi de les proteïnes de fusió glutatió-*S*-transferasa-MT (GST-MT), exitosament emprada en el nostre laboratori des que es posà a punt fa ja 17 anys,[89,90] i que permet l'obtenció dels complexos metall-MT desitjats amb una elevada puresa i quantitat. Per altra banda, ha sigut a través de tècniques espectroscòpiques i espectromètriques habituals (UV-Vis, DC, ICP-AES, ESI-MS) que hem caracteritzat els complexos que aquestes MT formen en presència de Zn(II), Cd(II) o Cu(I).

[89] M. Capdevila, N. Cols, N. Romero-Isart, R. Gonzàlez-Duarte, S. Atrian, P. Gonzàlez-Duarte, Cell Mol. Life Sci. 53 (1997) 681-688.
[90] N. Cols, N. Romero-Isart, M. Capdevila, B. Oliva, P. Gonzàlez-Duarte, R. Gonzàlez-Duarte, S. Atrian, J. Inorg. Biochem. 68 (1997) 157-166.

5.1. El sistema MT de *Strongylocentrotus purpuratus*

Un dels aspectes considerats en aquesta Tesi ha estat l'estudi del sistema MT de l'equinoderm *S. purpuratus*. En treballs anteriors al que ara es presenta, en aquest organisme s'han descrit set gens *MT*, d'entre els quals s'ha vist que tres s'expressen de manera constitutiva: *SpMTA*, que codifica per a la proteïna SpMTA, i el parell *SpMTB*$_1$-*SpMTB*$_2$, on ambdós codifiquen per a la mateixa proteïna SpMTB. També se sap que aquests gens *SpMTA*, d'una banda, i *SpMTB*$_1$-*SpMTB*$_2$, de l'altra, presenten patrons d'expressió diferencials.[66,91,92] Així, amb la consideració que el fet que un organisme que presenta diverses isoformes de MT amb patrons d'expressió gènica diferencials pot respondre al fet que aquestes MT desenvolupen funcions diferents en aquest organisme, ens plantejàrem estudiar les habilitats coordinants envers Zn(II), Cd(II) i Cu(I) de les dues MT que sintetitza l'eriçó de mar, SpMTA i SpMTB.[93] Aquests dos pèptids de 64 i 66 aminoàcids, respectivament, que contenen vint residus Cys, mostren un 85% d'identitat de seqüència. A més, el coneixement previ de l'estructura 3D del complex Cd_7-SpMTA, amb els dos dominis α (N-terminal) i β (C-terminal) que contenen els clústers Cd_4-$(SCys)_{11}$ i Cd_3-$(SCys)_9$, respectivament, ens serví de guia per a delimitar els extrems dels fragments que inclourien els dominis equivalents en SpMTB. És així com també hem fet un estudi comparatiu de les preferències metàl·liques de cadascun dels dominis per separat, havent sintetitzat els fragments αSpMTA i αSpMTB, que mostren un 86% d'identitat de seqüència, així com els βSpMTA i βSpMTB, també amb un 86% d'identitat de seqüència (Figura 13).

```
                10        20        30          40        50        60
       ....|....|....|....|....|....|....|....  |....|....|....|....|....|...
SpMTA  GSMPDVKCVCCKEGKECACFGQDCCKTGECCKDGTCC-G  ICTNAACK-CANGCKCGSGCSCTEGNCAC 64
SpMTB  GSMPDVKCVCCKEGNECACKGQDCCTTGECCKGGTCCTG  KCSNAACKTCADGCKCGSGCSCTEGNCPC 66
       ──────────────────────────────────────  ──────────────────────────────
                    domini alfa                          domini beta
```

Figura 13. Alineament de les seqüències aminoacídiques de les dues isoformes de MT de *S. purpuratus*. El dipèptid GS N-terminal és conseqüència del sistema d'expressió emprat per a la síntesi de les proteïnes recombinants i s'ha demostrat que no modifica les propietats coordinants de les MT resultants.

En el nostre treball mostrem que les dues MT de *S. purpuratus* enllacen 7 ions Zn(II), que es reparteixen entre els complexos Zn_4-αSpMT i Zn_3-βSpMT. Tanmateix, hem

[91] P. Harlow, E. Watkins, R.D. Thornton, M. Nemer, Mol. Cell Biol. 9 (1989) 5445-5455.
[92] M. Nemer, R.D. Thornton, E.W. Stuebing, P. Harlow, J. Biol. Chem. 266 (1991) 6586-6593.
[93] M. Tomas, J. Domènech, M. Capdevila, R. Bofill, S. Atrian, FEBS Open Bio 3 (2013) 89-100.

trobat diferències en el comportament d'aquestes MT davant el Zn(II), donat que els complexos Zn_7-SpMTB incorporen lligands sulfur àcid-làbils, probablement en els agregats Zn_3-βSpMTB. Per a Zn_7-SpMTA, en canvi, no hi ha indicis que aquests lligands hi siguen presents. Seguint els criteris de classificació de les MT proposat pel grup d'investigació en què s'ha dut a terme aquesta Tesi,[6] la presència de lligands sulfur àcid-làbils en els complexos metall-MT que formen les MT recombinants obtingudes en cultius d'*E. coli* rics en Zn(II) o Cd(II) denota una baixa habilitat d'aquestes MT per a enllaçar aquests metalls. Les diferències més importants en relació a l'enllaç a metalls divalents, però, les hem trobades davant el Cd(II). Si bé ja es coneixia que SpMTA forma les espècies Cd_7-SpMTA, Cd_4-αSpMTA i Cd_3-βSpMTA, i les nostres dades coincideixen amb aquestes, cal destacar la presència de l'espècie Cd_3Zn_1-βSpMTA quan aquest pèptid recombinant se sintetitza en medis rics en Cd(II). La presència d'ions Zn(II) en les preparacions Cd-MT, al contrari que la presència de sulfurs, indica una major preferència per a coordinar metalls divalents en comparació amb els monovalents. A més, l'espècie majoritària que SpMTB forma en les mateixes condicions en què hem estudiat SpMTA és Cd_8-SpMTB. Per a aquesta isoforma, Cd_7-SpMTB és minoritària i es detecta juntament amb Cd_7S_2-SpMTB. El domini αSpMTB presenta les mateixes habilitats de coordinació enfront de Cd(II) que αSpMTA, anàlogament al que passava en presència de Zn(II). βSpMTB, per contra, incorpora lligands sulfur àcid-làbils i forma l'espècie majoritària Cd_3S_2, en lloc de l'espècie Cd_3 que trobem per a βSpMTA. És per tot això que les nostres dades suggereixen una millor habilitat per a la coordinació de Zn(II) i Cd(II) de SpMTA en comparació amb SpMTB, la qual vindria principalment determinada pels seus fragments β.

Pel que fa a les habilitats coordinants envers metalls monovalents, ambdues isoformes formen majoritàriament complexos d'estequiometria Cu_4Zn_x-MT o Cu_8Zn_y-MT. Tanmateix, mentre que SpMTA tan sols forma espècies homometàl·liques de Cu(I) en les condicions més forçades d'exposició al metall (*i.e.* síntesi heteròloga en medis rics en coure a baixa oxigenació), per a SpMTB les obtenim ja en condicions més suaus que suposen una menor concentració de Cu(I) disponible per a la MT en l'interior cel·lular (*i.e.* síntesi heteròloga en medis rics en coure a oxigenació normal). La formació d'espècies homometàl·liques de Cu(I), en contraposició a les heterometàl·liques Cu,Zn-MT, quan una MT se sintetitza en medis enriquits en coure, s'ha relacionat amb una elevada habilitat d'aquesta MT per a enllaçar aquest metall.6 Addicionalment, els nostres

resultats han demostrat que el domini α de SpMTB presenta millors habilitats per a la coordinació de Cu(I) que αSpMTA, fet que contrasta amb el comportament anàleg que ambdós fragments mostren davant el Zn(II) o el Cd(II), mentre que la comparació dels fragments β ha posat de manifest la major capacitat de coordinació de Cu(I) que presenta βSpMTB en comparació amb βSpMTA. Per tant, s'ha demostrat que SpMTB presenta millors habilitats de coordinació de Cu(I) que SpMTA, segurament a causa de la influència conjunta d'ambdós dominis α i β, a diferència del que s'ha vist per a la coordinació de metalls divalents, en què era tan sols el domini β el responsable de la major habilitat coordinant de SpMTA.

Una anàlisi global dels nostres resultats en el sistema MT de l'eriçó de mar, juntament amb les dades de la bibliografia que han demostrat que els nivells d'expressió de *SpMTB* són menors que els de *SpMTA* en condicions de baixa concentració de Zn(II), però que aquests augmenten fins a nivells comparables entre ambdós transcrits sota elevades concentracions de Zn(II) o Cd(II),[66] suggereixen la implicació de cadascuna de les dues isoformes en funcions d'homeòstasi de metalls diferenciades. Així, és raonable proposar un paper en el manteniment dels nivells de Zn(II) per a SpMTA, mentre que SpMTB només intervindria en situacions d'estrés per metalls divalents. En la bibliografia trobem altres casos de sistemes MT en animals que presenten sistemes MT polimòrfics amb diferents preferències metàl·liques per a cadascuna de les isoformes, les quals han estat relacionades amb una diferent especialització pel que fa a les seues funcions biològiques, bàsicament el manteniment dels nivells de metalls essencials, d'una banda, i la resposta davant les situacions d'estrés per metalls, de l'altra. És el cas, per exemple, de CeMT-1 i CeMT-2 del nemàtode *Caenorhabditis elegans*, per a les quals es proposa que CeMT-2 participaria en la destoxicació de Cd(II) mentre que ambdues isoformes intervindrien en l'homeòstasi de Zn(II).[35,36,37] Les dues isoformes de MT identificades en amfioxos del gènere *Branchiostoma*, BfMT1 i BfMT2, són un altre exemple. Per a aquestes es proposa que BfMT1 tindria un paper més important en el manteniment dels nivells de metalls essencials, mentre que BfMT2 participaria en els processos de destoxicació de cadmi.[94] Els estudis amb les isoformes de MT dels cargols *Helix pomatia*[95] i *Cantareus aspersus*[96] mostren un escenari molt similar. Els sistemes MT

[94] M. Guirola, S. Pérez-Rafael, M. Capdevila, Ò. Palacios, S. Atrian, PLoS One 7 (2012) e43299.
[95] O. Palacios, A. Pagani, S. Pérez-Rafael, M. Egg, M. Höckner, A. Brandstätter, M. Capdevila, S. Atrian, R. Dallinger, BMC Biol. 9 (2011) 4-24.

d'aquests cargols presenten cadascun tres isoformes, una específica de Cu(I), una altra de Cd(II) i una darrera isoforma que no mostra especificitat metàl·lica. Així, de nou trobem una isoforma que participaria en l'homeòstasi de metalls essencials, en aquest cas del coure, i una altra probablement especialitzada en la protecció davant la intoxicació per cadmi. La funció de les isoformes que no mostren especificitats metàl·liques seria menys important, tal i com s'esdevé del fet que no s'ha detectat la presència d'isoformes equivalents en altres espècies de cargol, així com de la detecció d'una molt baixa proporció de la mateixa en *C. aspersus*. Recentment s'ha descrit també una situació similar per a les MT1 i MT2 de mamífer, les quals han estat històricament considerades com a equivalents des del punt de vista de la seua funció, i fins i tot referides com a MT1/MT2 sense més diferenciació.[97] Per a aquestes, tot i la completa conservació dels patrons de Cys i el seu elevat percentatge d'identitat, s'ha proposat un paper òptim de MT1 en processos de destoxicació de Cd(II), mentre que MT2 exerciria millor la seua funció en el manteniment dels nivells de zinc.

5.2. Els sistemes MT de *Glycine max* i *Helianthus annuus*

La variabilitat en les seqüències de les MT de planta és encara superior que la present en les MT d'animals, convertint-les en un grup de MT fins i tot encara més interessant per al seu estudi. Les diferències de seqüència entre aquestes afecta tant el nombre com la distribució de les seues Cys, i per tant és raonable esperar que afectaran les seues habilitats coordinants i funcions. Tenint en compte aquest escenari, en els treballs que versen sobre la família de les MT de planta hem tractat d'obtindre més informació sobre representants de les quatre subfamílies en què aquesta família es divideix.[68] A més, hem pretés aprofundir en l'impacte que té la variabilitat en el contingut d'aminoàcids potencialment coordinants en les propietats de les MT de planta, centrant-nos en les variants que ens ha oferit l'estudi del sistema MT de soja i de gira-sol.

[96] M. Höckner, K. Stefanon, A. de Vaufleury, F. Monteiro, S. Pérez-Rafael, Ò. Palacios, M. Capdevila, S. Atrian, R. Dallinger, Biometals 24 (2011) 1079-1092.
[97] E. Artells, Ò. Palacios, M. Capdevila, S. Atrian, Metallomics 5 (2013) 1397-1410.

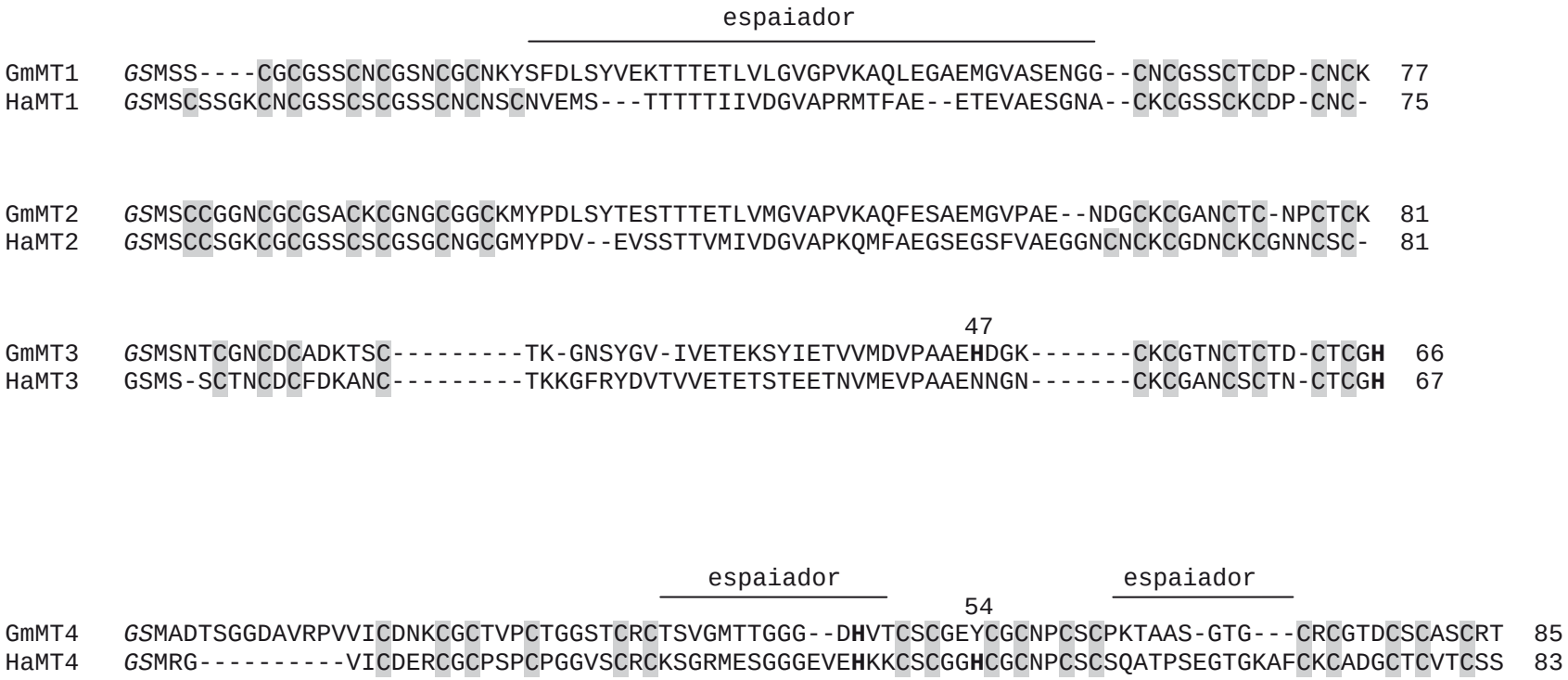

Figura 14. Alineament de les seqüències aminoacídiques de GmMT1 *vs.* HaMT1, GmMT2 *vs* HaMT2, GmMT3 *vs* HaMT3 i GmMT4 *vs* HaMT4 de *G. max* i *H. annuus*. El dipèptid GS N-terminal és conseqüència del sistema d'expressió emprat per a la síntesi de les proteïnes recombinants i s'ha demostrat que no modifica les propietats coordinants de les MT resultants.

Els estudis de les MT en les plantes de soja i gira-sol s'iniciaren a partir de la col·laboració amb un grup del Centro de Estudios Fotosintéticos y Bioquímicos del Consejo Nacional de Investigaciones Científicas y Técnicas d'Argentina, on ambdues representen conreus de gran importància agro-econòmica. En un primer treball presentat en aquesta Tesi s'ha demostrat que la planta de soja acumula ions Cd(II) en els seus teixits, fet que té relació amb els efectes tòxics que aquest metall pot causar en humans, donat l'ús de les llavors de soja en alimentació.[98] Així, hem dut a terme l'estudi de les MT de la planta de soja com a possibles determinants moleculars de l'acumulació d'aquest metall en la planta. Primerament s'han descrit els nou gens de MT que presenta la planta de soja (*G. max*), els quals s'han classificat en les quatre subfamílies en què es divideix la família de les MT de planta, segons el nombre i la distribució de les seues Cys.[68] D'entre aquests gens s'ha seleccionat un representant de cada subfamília, els productes proteics dels quals s'han anomenat GmMT1, GmMT2, GmMT3 i GmMT4, les seqüències dels quals es mostren en la Figura 14. Així, GmMT1 és el producte de *Gm17 MT1*, que codifica per a un pèptid de 75 aminoàcids que conté 12 Cys distribuïdes en dos clústers de 6 situats en els extrems N- i C-terminal, amb una regió lliure de Cys (o espaiador) de 40 residus, i que es classifica per tant com a pertanyent a la subfamília p1 de planta (d'ara endavant MT1); GmMT2 és el producte de *Gm07 MT2*, que codifica per a un pèptid de 79 aminoàcids amb una distribució de 8+6 Cys i un espaiador de 40 residus, pertanyent per tant a la subfamília p2 (d'ara endavant MT2); GmMT3 és el producte de *Gm06 MT3*, que codifica per a un pèptid de 64 aminoàcids amb una distribució de 4+6 Cys i un espaiador de 38 residus, corresponent a la subfamília p3 (d'ara endavant MT3); i GmMT4 és el producte de *Gm08 MT4*, que codifica per a una proteïna de 85 aminoàcids i tres regions riques en Cys, distribuïdes successivament en regions amb 6, 6 i 5 Cys separades entre si per un espaiador, i que s'ha classificat com a pertanyent a la subfamília p4 o pec (d'ara endavant MT4), tot i que només presenta una de les dues His altament conservades en la regió central rica en Cys d'aquesta subfamília.

La planta de gira-sol és també molt important en alimentació. Els resultats presentats en aquest treball de Tesi mostren la identificació de representants de les MT pertanyents a les quatre subfamílies de MT de planta en el gira-sol (*H. annuus*). En aquesta planta s'han trobat set EST (de l'anglés *Expressed Sequence Tag*), d'entre els

[98]M.A. Pagani, M. Tomas, J. Carrillo, R. Bofill, M. Capdevila, S. Atrian, C.S. Andreo, J. Inorg. Biochem. 117 (2012) 306-315.

quals s'ha seleccionat un representant de cadascuna de les quatre isoformes de MT de planta per a l'estudi de les seues habilitats coordinants. Els seus productes proteics s'han anomenat HaMT1, HaMT2, HaMT3 i HaMT4, les seqüències dels quals es mostren en la Figura 14. HaMT1 és el producte de *HaMT1-2*, que codifica per a un pèptid de 73 aminoàcids que conté 14 Cys distribuïdes segons el patró 8+6 en els fragments N- i C-terminal rics en Cys, respectivament, i que s'ha classificat com a pertanyent a les MT1. Tot i que HaMT1 no segueix el patró característic de distribució 6+6 de les Cys de les MT1 típiques, sí que presenta la seqüència consens que conté els motius CXCGS (on X≠Cys) seguit de CXCG i CXC en la seua regió N-terminal, característica de les MT1.[70] A més, presenta també el fragment CKCG seguit dels motius CXC i PCXC en la regió C-terminal.[99] HaMT2 és el producte proteic de *HaMT2-1*, que codifica per a un pèptid de 79 aminoàcids que conté 15 Cys distribuïdes en un esquema 7+6 en els fragments N- i C-terminals, i s'ha classificat com a pertanyent a les MT2. De nou, tot i que aquest pèptid no respon al contingut i distribució de Cys estàndard per a les MT2, el fet que presenta el doblet CC dins del fragment conservat SCCXGKCGC així com el tetrapèptid CXGC en la regió N-terminal, juntament amb la presència també del pèptid GVAP en l'espaiador, fa que l'hàgem classificat com a pertanyent a aquesta subfamília.[71] HaMT3 és el producte proteic de *HaMT3*, l'única EST que s'ha identificat que codifica per a un pèptid que presenta les 10 Cys típiques de les MT3 de planta, distribuïdes segons l'esquema 4+6 entre les regions N- i C-terminal. Aquest pèptid conté 65 aminoàcids i l'espaiador en comprén 35. HaMT4 és el producte proteic de *HaMT4*, que és també l'única EST que s'ha identificat en *H. annuus* que codifica per a un pèptid de 81 aminoàcids que presenta les 17 Cys i 2 His característiques de les MT4 de planta.

Els nostres estudis en els sistemes MT de les plantes de soja i gira-sol han permés mostrar les propietats d'enllaç a Zn(II) i Cd(II) de cadascuna de les MT seleccionades descrites abans. Així, GmMT1 i HaMT1, amb 12 Cys i 14 Cys, respectivament (Figura 14), formen majoritàriament els complexos Zn_4-MT1 quan s'obtenen per síntesi heteròloga en cultius *d'E. coli* enriquits en Zn(II). Aquests resultats coincideixen amb els descrits per a cicMT1 del cigró (*Cicer arietinum*), que conté les 12 Cys típiques de les MT1.[76] A més, s'ha vist que HaMT1 té una lleugera major capacitat coordinant d'ions Zn(II) que GmMT1, ja que forma també els complexos Zn_5-HaMT1. Per

[99] N.N. Alexandrov, V.V. Brover, S. Freidin, M.E. Troukhan, T.V. Tatarinova, H. Zhang, T.J. Swaller, Y.P. Lu, J. Bouck, R.B. Flavell, K.A. Feldmann, Plant. Mol. Biol. 69 (2009) 179-194.

a aquests s'ha proposat que HaMT1 es plega segons l'anomenat model en forma de pinça, el qual suposa la interacció dels dominis N- i C-terminal a través de la formació d'un únic clúster que permet l'enllaç d'un ió Zn(II) addicional. Aquest clúster ha estat prèviament proposat per als complexos Zn_5-cicMT1 que MT1 de cigró també és capaç de formar.[76] Els resultats en presència de Cd(II) mostren, d'una banda, que Cd_6S_1 és l'espècie majoritària que detectem per ESI-MS quan GmMT1 es biosintetitza en medis enriquits en aquest metall i que HaMT1 dóna lloc a una mescla de Cd_6S_8 i Cd_7S_7. Així, no trobem diferències significatives en relació a les capacitats de coordinació de Cd(II) d'ambdós pèptids en aquestes condicions. A més, les preparacions d'ambdues MT1 incorporen anions sulfur àcid-làbils que augmenten la seua capacitat coordinant, com s'ha descrit també per a QsMT d'alzina surera (*Quercus suber*)[52] i cicMT2 de cigró.[81,82] D'altra banda, però, s'ha vist que quan els ions Cd(II) s'intercanvien per Zn(II) en experiments en què partim del complex Zn-HaMT1, les espècies més estables són Cd_4-, Cd_5- i Cd_6-HaMT1. Així, la formació dels complexos Cd_4- i Cd_5-MT1 són resultats comparables a la mitjana de 4(±1), 4.8 i 5 Cd per proteïna que enllacen dMT del blat (*Triticum durum*),[100] OsMTI-1b de l'arròs (*Oryza sativa*)[101] o cicMT1.[81] La formació del complex Cd_6-HaMT1, en canvi, tan sols és comparable a la mitjana de 5.8 Cd/MT que s'ha determinat per a PsMTA de pèsol (*Pisum* sativum)[102] en experiments amb la proteïna de fusió GST-MT en els quals no s'ha determinat la presència o absència de lligands sulfur. Per tant, probablement es pot justificar la presència d'aquest complex en solució per les dues Cys de més que HaMT1 conté en comparació amb les MT1 típiques.

Pel que fa a GmMT2 i HaMT2, que contenen 14 Cys i 15 Cys, respectivament (Figura 14), s'ha determinat que enllacen una mitjana de 4.3-4.4 Zn/MT, on l'espècie majoritària és Zn_4-MT2, però el complex Zn_5-MT2 es forma també en gran proporció. Aquests resultats coincideixen amb els descrits per a QsMT,[52] una MT2 de planta, i també són comparables amb els obtinguts per a HaMT1 de gira-sol. Per a cicMT2 del cigró, en canvi, s'ha vist que forma majoritàriament els complexos Zn_5-MT2.[81] La síntesi de GmMT2 i HaMT2 en medis rics en Cd(II) ha donat lloc a resultats comparables per a ambdues MT2, igual com hem vist per a les corresponents MT1 d'aquestes plantes. Així,

[100] K. Bilecen, U.H. Ozturk, A.D. Duru, T. Sutlu, M.V. Petoukhov, D.I. Svergun, M.H. Koch, U.O. Sezerman, I. Cakmak, Z. Sayers, J. Biol. Chem. 280 (2005) 13701-13711.
[101] R.M. Nezhad, A. Shahpiri, A. Mirlohi, Protein J. 32 (2013) 131-137.
[102] A.M. Tommey, J. Shi, W.P. Lindsay, P.E. Urwin, N.J. Robinson, FEBS 292 (1991) 48-52.

GmMT2 i HaMT2 enllacen un valor mitjà de 6.7 i 6.3 ions Cd(II) per MT, respectivament, i les espècies majoritàries que detectem per ESI-MS són Cd_6S_1-GmMT2 i Cd_6S_8-HaMT2. Tanmateix, de nou de manera anàloga a allò que hem vist per a Cd-HaMT1, el complex més estable que s'ha determinat en experiments en què s'han addicionat Cd(II) i S^{2-} a solucions de Zn-HaMT2 ha sigut Cd_6-HaMT2, el qual presenta el major contingut en Cd(II) detectat mai per a cap altra MT2 de planta. La formació d'aquest complex s'explica tant a través de la participació de la Cys de més que conté HaMT2 en comparació amb les MT2 típiques, com a través de la formació d'un únic clúster Cd_6-$(SCys)_{14/15}$ que suposaria la interacció dels dos dominis rics en Cys. D'altra banda, cal destacar que les especiacions de les preparacions de Cd-GmMT1 i Cd-GmMT2 han mostrat ser similars (espècie Cd_6S_1 majoritària), tot i la diferència en el contingut en Cys entre aquestes MT (12 per a GmMT1 *vs* 14 per a GmMT2).

Una de les conclusions més importants que hem extret de l'estudi de les propietats d'enllaç a metalls divalents en aquestes MT1 i MT2 és l'augment de la capacitat coordinant envers Cd(II) en HaMT1 i HaMT2, que hem relacionat amb la presència dels residus Cys de més respecte de les MT1 i MT2 típiques. Un alineament de totes les seqüències aminoacídiques de MT1 de planta, d'una banda, i de MT2, de l'altra, permet observar la presència d'aquests residus extra en algunes d'aquestes seqüències. Aquests resultats permeten especular sobre un possible efecte similiar en les variants d'aquestes subfamílies de MT de planta amb nombre i distribució de Cys alineables. Per exemple MT2 de *Fragaria ananassa* (UniProtKB P93134), per a la qual no es disposa de cap dada en relació a la seua capacitat coordinant o possible funció biològica, presenta 15 Cys alineables a les de HaMT2. D'altra banda, l'anàlisi de la resposta a la intoxicació per cadmi en la planta de soja ha demostrat que *GmMT1* i *GmMT2* també s'indueixen en condicions d'excés del metall, tot i que aquestes dues MT no són les principals involucrades en els mecanismes de defensa a aquesta situació d'estrés.[98] Cal destacar, a més, la complexitat de la mostra obtinguda en sintetitzar HaMT1 en medis rics en Cd(II), la qual denota la manca de l'existència d'una espècie clarament més estable que la resta. Per a HaMT2, per contra, Cd_6S_8-HaMT2 és el complex que es forma quasi únicament en la biosíntesi en *E. coli*, i aquests resultats s'han relacionat amb el fet que les MT2 estarien més optimitzades per a participar en funcions destoxicadores de cadmi més que les MT1. Per últim, la proposta de plegament segons el model en pinça per als complexos Zn_5-HaMT1 i Cd_6-HaMT2 posa de manifest la importància de l'espaiador en aquestes MT,

donat que permet la interacció dels seus fragments N- i C-terminal i així la incorporació d'un ió metàl·lic addicional. L'existència d'aquesta regió lliure de Cys que connecta ambdós extrems s'ha proposat com a determinant per a l'estabilitat de les MT.[72] Tanmateix, en la bibliografia només trobem un treball en què l'efecte de l'espaiador en la funció d'una MT de planta es pose de manifest. Així, és en un estudi anterior del mateix grup de recerca on s'ha dut a terme aquesta Tesi Doctoral que s'ha demostrat que l'espaiador de QsMT de l'alzina surera és determinant per a la funció destoxicadora de coure d'aquesta MT2.[75]

Un altre tema de debat científic important i actual en relació a les MT de planta és l'efecte potencial de la presència de residus His en les característiques químiques dels clústers metàl·lics que formen i, per extensió, en la funció biològica que aquestes MT puguen desenvolupar. Un alineament de totes les seqüències aminoacídiques de MT3 de planta permet observar la presència d'aquests residus en gran part d'aquestes. Les GmMT3 i HaMT3 aquí estudiades, que contenen 10 residus Cys i dues i una His, respectivament (Figura 14), no són una excepció.[103] L'estudi de capacitats coordinants en aquests dos pèptids ha demostrat que aquestes MT enllacen una mitjana de 3.0 i 3.5 Zn/MT, respectivament, quan se sintetitzen en medis rics en aquest metall. La diferència entre aquests valors, juntament amb la detecció per ESI-MS d'una espècie Zn_3 majoritària per a GmMT3, i una mescla de Zn_3 i Zn_4 per a HaMT3, ens feren plantejar la possibilitat de la participació de les His en la coordinació metàl·lica com a causa del diferent comportament envers Zn(II) d'aquestes dues MT3. En aquest sentit, els estudis d'habilitats coordinants envers metalls divalents d'aquests dos pèptids i dels mutants H66AGmMT3 i H67AHaMT3, així com la quantificació del nombre de residus His lliures en cadascun dels complexos Zn(II)-MT a través de la modificació química d'aquests amb el reactiu pirocarbonat de dietil (DEPC), han permés suggerir la participació en la coordinació de Zn(II) d'His47 en GmMT3 i His67 en HaMT3. Pel que fa a la coordinació de Cd(II), si bé tant GmMT3 com HaMT3 formen majoritàriament el complex Cd_4-MT3, l'anàlisi de la participació de les His en aquests complexos ha permés concloure que les His terminals d'ambdós pèptids participen en l'enllaç a aquest metall, mentre que His47 de GmMT3 no hi participa, a diferència del que hem vist en presència de Zn(II). La participació de les His de MT3 en la coordinació metàl·lica només s'havia proposat per a MT3 de la banana,[77]

[103] M. Tomàs, M.A. Pagani, C.S. Andreo, M. Capdevila, R. Bofill, S. Atrian, J. Biol. Inorg. Chem. (sotmés).

amb una His en la regió de l'espaiador propera al domini ric en Cys C-terminal, i per tant en una posició equivalent a la d'His47 de GmMT3.

En resum, els resultats obtinguts amb les MT3 de soja i gira-sol han permés demostrar que la participació d'His67 de HaMT3 en l'enllaç a Zn(II) augmenta la capacitat de coordinació de Zn(II), fet que podria relacionar-se amb una millora en les funcions relacionades amb aquest metall. Per contra, la participació d'His47 en els complexos Zn-GmMT3 o de les His C-terminals en qualsevol dels dos complexos Cd-MT3 no modifiquen la seua capacitat coordinant. En aquests casos, s'ha proposat que l'efecte de la introducció d'un lligand NHis, que necessàriament participa en un lloc de coordinació $(SCys)_3(NHis)$, podria relacionar-se amb una major resistència a l'oxidació,[33] la qual és particularment important en els processos bioquímics que tenen lloc durant la senescència de les fulles de la planta, en què alguns resultats preliminars suggereixen que GmMT3 i HaMT3 hi participen. Cal aclarir que la participació dels residus His en aquests llocs de coordinació no suposarien cap canvi en les afinitats per al Cd(II) en comparació amb els llocs de coordinació $(SCys)_4$.[30] En aquest sentit, cal destacar que en el nostre treball es mostra que GmMT3 és la MT de soja que estaria més involucrada en la protecció contra la intoxicació per cadmi d'entre les quatre MT que hem estudiat en aquesta planta.[98] D'entre les quatre isoformes, GmMT3 i GmMT4 han mostrat les millors habilitats per a enllaçar metalls divalents, Zn(II) i Cd(II). D'entre GmMT3 i GmMT4, s'ha postulat que GmMT3 tindria un paper més important en la funció destoxicadora de cadmi donada la gran inducció de *GmMT3* en les fulles quan la planta s'exposa a elevades concentracions del metall, juntament amb la demostració que en aquestes condicions d'estrés per metalls hi ha una important acumulació de cadmi en aquest mateix teixit.

Respecte les isoformes GmMT4 i HaMT4, la presència de la mutació natural His54Tyr en GmMT4, juntament amb les dues His altament conservades en la subfamília en HaMT4, ens posà de nou en la qüestió del paper de les His en aquestes dues isoformes.[103] Així, HaMT4, amb una seqüència alineable a la MT4 paradigmàtica, Ec-1 de blat, ha demostrat enllaçar 6 ions Zn(II) en un complex en què participen ambdues His, probablement a través d'una estructuració anàloga a la que s'ha descrit per a Ec-1, amb un clúster Zn_2-$(SCys)_6$,[25] un lloc mononuclear Zn-$(SCys)_2(NHis)_2$ i un clúster Zn_3-$(SCys)_9$.[24] GmMT4, en canvi, dóna lloc a una mescla equimolar Zn_5-, Zn_6-GmMT4 quan se sintetitza en medis rics en Zn(II), probablement a causa que la substitució His/Tyr la incapacita per a formar el lloc mononuclear $(SCys)_2(NHis)_2$, el qual suposa una afinitat per al Zn(II)

major que per al Cd(II).[30] Aquests resultats són comparables als obtinguts en el cas de mutants simples His/Ala de Ec-1, els quals presentaven una única His romanent.[104] D'altra banda, la incubació de la solució contenint la mescla Zn_5-, Zn_6-GmMT4 amb un excés de Zn(II) ha donat lloc a la formació de l'espècie única Zn_6-GmMT4. Així doncs, la participació de les His en l'enllaç metàl·lic en Zn-HaMT4 ha suposat una millor habilitat per a la coordinació de Zn(II) per a HaMT4 en comparació amb GmMT4, coincidint amb la hipòtesi descrita en la bibliografia segons la qual la presència del lloc de coordinació mononuclear $(SCys)_2(NHis)_2$ en les MT4 és determinant per a enllaçar aquest metall de manera òptima.[30,104] Pel que fa al Cd(II), ambdós pèptids GmMT4 i HaMT4 han donat lloc a complexos Cd-MT4 en què cap de les His participa en la coordinació metàl·lica, probablement formant un clúster Cd_4-$(SCys)_{11}$, igual com el descrit per a Ec-1 de blat.[36] Les diferències en les propietats d'enllaç envers Zn(II) entre GmMT4 i HaMT4 s'han relacionat amb possibles funcions biològiques diferents per a aquestes dues MT4. Així, s'ha suggerit que HaMT4 podria tindre una funció probablement equivalent a la de Ec-1 en el blat com a reservori de zinc per al desenvolupament de la planta,[32] mentre que GmMT4 funcionaria millor en els processos de transferència del metall.

5.3. Estudi comparatiu de les habilitats de les quatre isoformes de MT de soja com a antioxidants i/o captadors de radicals lliures

La possible funció de les MT com a reguladores i protectores envers oxidants i radicals lliures es pot veure també afectada per la diferent reactivitat davant d'aquests agents que poden presentar les diverses isoformes de MT que sintetitza un organisme. Les diferències en l'estructura primària que trobem entre MT de planta pertanyents a subfamílies diferents, igual com hem suggerit per a les reaccions d'incorporació de metalls, podrien suposar diferències en aquestes reaccions. És així com, en un estudi fet en paral·lel al de la determinació de la inducció dels gens *MT* quan la planta de soja és exposada a un excés de cadmi,[98] s'ha demostrat que l'expressió de *GmMT2* i *GmMT3* s'indueix en les fulles després d'un tractament de 24h amb peròxid d'hidrogen. La mesura puntual del manteniment dels nivells d'expressió de *GmMT1* i *GmMT4*, però, no demostra que aquestes MT no participen en processos d'homeòstasi redox. Addicionalment, la

[104] O.I. Leszczyszyn, C.R. White, C.A. Blindauer, Mol. Biosyst. 6 (2010) 1592-1603.

sobreexpressió de cadascuna de les quatre isoformes de MT estudiades en la soja ha conferit resistència a peròxid d'hidrogen i paraquat a cèl·lules del llevat *Saccharomyces cerevisiae* deficients en les MT pròpies, demostrant per tant la seua capacitat per a intervindre en processos d'estrés oxidatiu. Així, aquests resultats marcaren els indicis per abordar el darrer objectiu perseguit en aquesta Tesi Doctoral, que ha estat determinar la diferent capacitat protectora que cadascuna de les MT de la soja presenta durant processos d'estrés radicalari i/o oxidatiu.

Una de les informacions obtingudes en aquest estudi ha estat la determinació de les cinètiques d'alliberament del metall dels complexos Zn-GmMT a causa de l'exposició a peròxid d'hidrogen. Aquest procés s'ha demostrat que ocorre en condicions d'estrés oxidatiu,[57] i en un estudi comparatiu com el que aquí es presenta ens informa sobre la vulnerabilitat de les Cys de cadascuna de les MT a ser oxidades en presència d'aquest agent. Així, els nostres resultats han demostrat que els grups tiolat cisteínics en les MT de soja que contenen els espaiadors més llargs (*i.e.* GmMT1, GmMT2 i GmMT3) són més resistents a l'oxidació causada per l'exposició a peròxid d'hidrogen que els de GmMT4, amb dues regions lliures de Cys més curtes. L'espaiador torna així a aparéixer possiblement com un element estructural que condiciona l'activitat biològica de les MT de planta, tal i com hem vist també en aquesta Tesi en referència a funcions relacionades amb l'homeòstasi i destoxicació de metalls. A més, en un treball similar amb representants de les quatre MT de planta exposades a disulfur de glutatió (GSSG) s'han proposat també aquests dos grups: MT1, MT2, MT3, d'una banda, i MT4, de l'altra.[105] En aquest darrer cas s'han obtingut tendències oposades en els percentatges de Zn(II) alliberat i en les cinètiques determinades per a cadascun dels processos, i s'ha proposat que el fet clau que ho justifica és que la MT4 analitzada en l'estudi que se cita és Ec-1, amb el patró típic de 17 Cys i 2 His, i en canvi és GmMT4 en el nostre estudi, amb la mutació His54Tyr, que probablement disminueix l'avidesa per al Zn(II) d'aquesta MT, com ja s'ha discutit abans. Així, la major facilitat per a perdre el Zn(II) que GmMT4 presenta en comparació amb Ec-1 podria relacionar-se amb la seua menor habilitat per a la coordinació d'aquest metall, la qual està probablement lligada a funcions de transferència de zinc, com s'ha proposat en l'apartat 5.2.

[105] E.A. Peroza, A. dos Santos Cabral, X. Wan, E. Freisinger, Metallomics 5 (2013) 1204-1214.

Un altre resultat interessant obtingut en aquest estudi ha sigut la determinació que l'exposició de les preparacions de Zn-GmMT1, Zn-GmMT2, Zn-GmMT3 i Zn-GmMT4 a radiacions γ en condicions en què es produeixen principalment radicals hidroxil (90% $HO^{\bullet}$ i 10% $H^{\bullet}$) mostra comportaments diferents per a Zn-GmMT1 en comparació amb la resta de MT de soja. Així, s'ha demostrat que l'atac dels radicals hidroxil suposa l'oxidació de les Cys i per tant la pèrdua del metall, així com l'oxidació de les Met i els residus aromàtics en tots els casos, però que aquests efectes són més dràstics per als complexos Zn-GmMT1, els quals arriben a demetal·lar-se completament. Conseqüentment, Zn-GmMT1 tindrà un major efecte protector del dany que els radicals hidroxil poden causar sobre altres biomolècules. A més, s'ha vist també que aquestes reaccions podrien causar dany cel·lular com a conseqüència dels processos de desulfurització dels residus Met i Cys, els quals acaben en la isomerització *cis-trans* dels àcids grassos que trobem de manera natural en les membranes cel·lulars. Aquest dany s'ha determinat també per a d'altres MT,[58] en concret per exemple per a QsMT de l'alzina surera. Aquest efecte perjudicial que és conseqüència de l'exposició a espècies radicalàries s'ha detectat que ocorre per a les preparacions de Zn-GmMT2, Zn-GmMT3 i Zn-GmMT4, però no per a Zn-GmMT1. Per tant, en les nostres condicions d'estudi, les quals permeten la comparació entre les quatre MT de soja, s'ha conclòs que Zn-GmMT1 és el complex que ha mostrat les millors propietats per a actuar com a captador d'espècies reactives d'oxigen, donat que els complexos Zn-GmMT1 són els més sensibles a l'atac dels radicals hidroxil i que aquestes reaccions no causen dany cel·lular.

6. CONCLUSIONS/CONCLUSIONS

6. CONCLUSIONS/CONCLUSIONS

A partir dels resultats presentats i discutits en aquesta Tesi Doctoral podem extraure les següents conclusions:

1. Les dues isoformes de MT de l'equinoderm *Strongylocentrotus purpuratus*, SpMTA i SpMTB, presenten diferents propietats per a l'enllaç de metalls mono- i divalents. SpMTA mostra millors habilitats per a coordinar Zn(II) i Cd(II) que SpMTB, fet que ve principalment determinat pels fragments β de cadascun dels pèptids. SpMTB, en canvi, mostra millors habilitats per a coordinar Cu(I) que SpMTA, sense que la influència d'un dels dos fragments, α o β, predomine sobre la de l'altre. Aquestes preferències metàl·liques poden estar relacionades amb una diferenciació funcional en l'organisme, de manera que SpMTA podria ocupar-se del manteniment dels nivells de metalls essencials i SpMTB de la protecció enfront de situacions d'estrés per metalls.

2. Els sistemes MT de la soja (*Glycine max*) i el gira-sol (*Helianthus annuus*) contenen representants de les quatre subfamílies de MT de planta. Les MT1 i MT2 de soja presenten els patrons de Cys característics de les respectives subfamílies, mentre que entre les MT1 i MT2 de gira-sol hi ha variants amb major nombre d'aquests residus. Les MT3 d'ambdós organismes presenten els patrons de Cys característics de la subfamília però diferent contingut en residus His. Les MT4 de soja i gira-sol presenten els patrons de Cys i His típics de la subfamília, a excepció d'una seqüència de soja que conté la mutació His54Tyr, un fet rar en aquesta subfamília.

3. Tant les MT1 (GmMT1, HaMT1) com les MT2 (GmMT2, HaMT2) estudiades mostren habilitats de coordinació de Zn(II) comparables entre si, així com entre isoformes de la mateixa planta. Tots els complexos Cd-MT1 i Cd-MT2 estudiats incorporen lligands sulfur àcid-làbils que n'augmenten la capacitat coordinant. La capacitat de coordinació de Cd(II) de HaMT1 és major que la de GmMT1 i la més elevada mai determinada per a una MT1 de planta quan aquests complexos no incorporen lligands sulfur. Anàlogament, la capacitat de coordinació de Cd(II) de HaMT2 és també superior a la de GmMT2, i alhora la major mai observada per a una MT2 de planta en absència de lligands sulfur. Aquest augment de capacitat coordinant envers Cd(II) és probablement conseqüència del seu major contingut en Cys respecte de les MT1 i MT2 típiques.

4. La capacitat de coordinació de Zn(II) de la MT3 de gira-sol, HaMT3, és lleugerament major que la de soja, GmMT3, probablement a causa que la His C-terminal que ambdues MT3 contenen només participa en l'enllaç al Zn(II) en HaMT3. D'altra banda, His47 de GmMT3 participa en l'enllaç al Zn(II) sense augmentar la seva capacitat coordinant. Pel que fa al Cd(II), ambdues MT3 mostren capacitats de coordinació anàlogues, i encara que les seues His C-terminals participen en l'enllaç al Cd(II), no modifiquen la seua capacitat coordinant. La participació dels residus His C-terminals podria estar relacionada amb una major resistència a l'alliberament del Cd(II) en condicions d'estrés oxidatiu respecte de les MT3 que no presenten residus His C-terminals, i per tant amb un paper en la protecció de la planta enfront dels efectes tòxics del Cd(II).

5. La capacitat de coordinació de Zn(II) de MT4 de gira-sol, HaMT4, és lleugerament major que la de soja, GmMT4, a causa de la mutació His54Tyr en GmMT4, la qual no permet la formació del lloc de coordinació Zn-$(SCys)_2(NHis)_2$ que molt probablement està present en Zn-HaMT4. En canvi, ambós pèptids presenten capacitats de coordinació de Cd(II) anàlogues i les seues His no participen en l'enllaç al Cd(II).

6. Els complexos de Zn(II) de les quatre isoformes de MT de soja estudiades reaccionen amb espècies oxidants i radicalàries. Les MT de soja que contenen els espaiadors més llargs (GmMT1, GmMT2 i GmMT3) són les més resistents a l'alliberament del metall provocat per l'exposició a peròxid d'hidrogen. D'altra banda, Zn-GmMT1 és el complex que probablement protegiria millor davant l'atac d'espècies reactives d'oxigen *in vivo*, mentre que l'estrés radicalari sobre els complexos Zn-GmMT2, Zn-GmMT3 i Zn-GmMT4 podria causar dany cel·lular.

6. CONCLUSIONS/CONCLUSIONS

From the results presented and discussed in this PhD Thesis we can conclude the following:

1. Both MT isoforms present in the echinoderm *Strongylocentrotus purpuratus*, SpMTA and SpMTB, exhibit different mono- and divalent metal-binding properties. SpMTA shows better Zn(II)- and Cd(II)-binding abilities than SpMTB, and this is predominantly determined by the β fragment of each peptide. Contrarily, SpMTB shows better Cu(I)-binding abilities than SpMTA, and this is not affected by any of the fragments, α or β. These metal preferences may be related to a functional differentiation in the organism, so that SpMTA could perform housekeeping Zn(II) homeostasis, while SpMTB could protect in metal stress emergency events.

2. Soybean (*Glycine max*) and sunflower (*Helianthus annuus*) MT systems contain representatives from the four plant MT subfamilies. Soybean MT1 and MT2 show the characteristic Cys-patterns in the respective subfamilies, while variants with extra Cys residues exist for sunflower MT1 and MT2 sequences. Both MT3 peptides present the standard Cys patterns for the subfamily but different His content. Soybean and sunflower MT4 show the typical Cys and His patterns for the subfamily, except for one sequence from soybean showing the His54Tyr mutation, which is not common for this subfamily.

3. Both MT1 (GmMT1, HaMT1) and MT2 (GmMT2, HaMT2) here studied show similar Zn(II)-binding abilities when comparing between different plants and also between different isoforms from the same plant. All the studied Cd-MT1 and Cd-MT2 complexes incorporate acid-labile sulfide ligands, which enhance their metal-binding capacities. The Cd(II)-binding capacity is higher for HaMT1 than for GmMT1 and represents the highest capacity ever reported for a plant MT1 when these complexes do not incorporate sulfide ligands. Analogously, the Cd(II)-binding capacity is higher for HaMT2 than for GmMT2, and the highest ever measured for a plant MT2 in the absence of sulfide ligands. This Cd(II)-binding capacity increase is probably caused by their higher Cys content when compared to standard MT1 and MT2 peptides.

4. Sunflower MT3, HaMT3, shows a higher Zn(II)-binding capacity than soybean MT3, GmMT3, probably because the C-terminal His residue that both MT3 show only participates in Zn(II) binding in the case of Zn-HaMT3. On the other hand, GmMT3 His47 participates in Zn(II)-binding without increasing its metal-binding capacity. Regarding Cd(II)-coordination, both MT3 show analogous metal-binding capacities and both C-terminal His residues participate in Cd(II)-binding without modifying their metal-binding capacities. The participation of the C-terminal His residues may be related to an improved resistance against Cd(II) release in oxidative stress conditions when compared to MT3 peptides that do not contain these residues. This fact could be related to a potential role in protecting the plant from the deleterious effects of Cd(II) in oxidative stress conditions.

5. Sunflower MT4, HaMT4, shows a slighlty higher Zn(II)-binding capacity than soybean MT4, GmMT4, due to the GmMT4 His54Tyr mutation, which abolishes the formation of the Zn-$(SCys)_2(NHis)_2$ site that is otherwise probably present in Zn-HaMT4. Contrastingly, both peptides show analogous Cd(II)-binding capacities and their His residues do no participate in Cd(II)-coordination.

6. The Zn(II)-complexes from the four soybean MT isoforms here analyzed react with oxidative and radical species. Soybean MT with longer spacers (GmMT1, GmMT2 and GmMT3) are the most resistant against the metal release caused by hydrogen peroxide exposure. On the other hand, the Zn-GmMT1 complex would better protect against an *in vivo* reactive oxygen species (ROS) attack than the Zn-GmMT2, Zn-GmMT3 or Zn-GmMT4 species, while the radical stress on the latter complexes could provoke cellular damage.

7. REFERÈNCIES

7. REFERÈNCIES

1. M. Margoshes, B.L. Vallee, J. Am. Chem. Soc. 79 (1957) 4813-1814.
2. M. Capdevila, R. Bofill, O. Palacios, S. Atrian, Coord. Chem. Rev. 256 (2012) 46-62.
3. J.H.R. Kägi, Y. Kojima, Experientia Supplementum Metallothionein II, vol. 52, Birkhäuser Verlag, Basel, 1987.
4. http://www.bioc.unizh.ch/mtpage/classif.html, 2013 (accés 25.11.13)
5. M. Valls, R. Bofill, R. González-Duarte, P. González-Duarte, M. Capdevila, S. Atrian, J. Biol. Chem. 276 (2001) 32835-32843.
6. R. Bofill, M. Capdevila, S. Atrian, Metallomics 1 (2009) 229-234.
7. C.A. Blindauer, O.I. Leszczyszyn, Nat. Prod. Rep. 27 (2010) 720-741.
8. G. Digilio, C. Bracco, L. Vergani, M. Botta, D. Osella, A. Viarengo, J. Biol. Inorg. Chem. 14 (2009) 167-178.
9. B.A. Messerle, A. Schäffer, M. Vašák, J.H. Kägi, K. Wüthrich, J. Mol. Biol. 214 (1990) 765-779.
10. K. Zangger, G. Oz, J.D. Otvos, I.M. Armitage, Protein Sci. 8 (1999) 2630-2638.
11. G. Oz, K. Zangger, I.M. Armitage, Biochemistry 40 (2001) 11433-11441.
12. W. Braun, M. Vašák, A.H. Robbins, C.D. Stout, G. Wagner, J.H. Kägi, K. Wüthrich, Proc. Natl. Acad. Sci. USA 89 (1992) 10124-10128.
13. P. Schultze, E. Wörgötter, W. Braun, G. Wagner, M. Vašák, J.H. Kägi, K. Wüthrich, J. Mol. Biol. 203 (1988) 251-268.
14. A. Arseniev, P. Schultze, E. Wörgötter, W. Braun, G. Wagner, M. Vašák, J.H. Kägi, K. Wüthrich, J. Mol. Biol. 201 (1988) 637-657.
15. R. Riek, B. Prêcheur, Y. Wang, E.A. Mackay, G. Wider, P. Güntert, A. Liu, J.H. Kägi, K. Wüthrich, J. Mol. Biol. 291 (1999) 417-428.
16. C. Capasso, V. Carginale, O. Crescenzi, D. Di Maro, E. Parisi, R. Spadaccini, P.A. Temussi, Structure 11 (2003) 435-443.
17. S.S. Narula, M. Brouwer, Y. Hua, I.M. Armitage, Biochemistry 34 (1995) 620-631.

18. A. Muñoz, F.H. Försterling, C.F. Shaw 3rd, D.H. Petering, J. Biol. Inorg. Chem. 7 (2002) 713-724.

19. C.W. Peterson, S.S. Narula, I.M. Armitage, FEBS Lett. 379 (1996) 85-93.

20. I. Bertini, H.J. Hartmann, T. Klein, G. Liu, C. Luchinat, U. Weser, Eur. J. Biochem. 267 (2000) 1008-1018.

21. V. Calderone, B. Dolderer, H.J. Hartmann, H. Echner, C. Luchinat, C. Del Bianco, S. Mangani, U. Weser, Proc. Natl. Acad. Sci. USA 102 (2005) 51-56.

22. C.A. Blindauer, M.D. Harrison, J.A. Parkinson, A.K. Robinson, J.S. Cavet, N.J. Robinson, P.J. Sadler, Proc. Natl. Acad. Sci. USA 98 (2001) 9593-9598.

23. P.A. Cobine, R.T. McKay, K. Zangger, C.T. Dameron, I.M. Armitage, Eur. J. Biochem. 271 (2004) 4213-4221.

24. E.A. Peroza, R. Schmucki, P. Güntert, E. Freisinger, O. Zerbe, J. Mol. Biol. 387 (2009) 207-218.

25. J. Loebus, E.A. Peroza, N. Blüthgen, T. Fox, W. Meyer-Klaucke, O. Zerbe, E. Freisinger, J. Biol. Inorg. Chem. 16 (2011) 683-694.

26. K. Tarasava, S. Johannsen, E. Freisinger, Molecules 18 (2013) 14414-14429.

27. M. Vašák, A. Galdes, H. Allen, O. Hill, J.H.R. Kägi, I. Bremner, B.W. Young, Biochemistry 19 (1980) 416-425.

28. A. Presta, A.R. Green, A. Zelazowski, M.J. Stillman, Eur. J. Biochem. 227 (1995) 226-240.

29. N. Romero-Isart, M. Vašák, J. Inorg. Biochem. 88 (2002) 388-396.

30. C.A. Blindauer, J. Inorg. Biochem. 121 (2013) 145-155.

31. O.I. Leszczyszyn, C.R. White, C.A. Blindauer, Mol. Biosyst. 6 (2010) 1592-1603.

32. O.I. Leszczyszyn, H.T. Imam, C.A. Blindauer, Metallomics 5 (2013) 1146-1169.

33. C.A. Blindauer, J. Inorg. Biochem. 102 (2008) 507-521.

34. C.A. Blindauer, M.T. Razi, D.J. Campopiano, P.J. Sadler, J. Biol. Inorg. Chem. 12 (2007) 393-405.

35. R. Bofill, R. Orihuela, M. Romagosa, J. Domènech, S. Atrian, M. Capdevila, FEBS J. 276 (2009) 7040-7069.

36. S. Zeitoun-Ghandour, J.M. Charnock, M.E. Hodson, O.I. Leszczyszyn, C.A. Blindauer, S.R. Stürzenbaum, FEBS J. 277 (2010) 2531-2542.

37. O.I. Leszczyszyn, S. Zeitoun-Ghandour, S.R: Stürzenbaum, C.A: Blindauer, Chem. Commun. 47 (2011) 448-450.

38. H. Akashi, T. Gojobori, Proc. Natl. Acad. Sci. USA 99 (2002) 3695-3700.

39. A. Murasugui, C. Wada, Y.J. Hayashi, J. Biochem. 93 (1983) 661-664.

40. C.T. Dameron, R.N. Reese, R.K. Mehra, A.R. Kortan, P.J. Carroll, M.L. Steigerwald, L.E. Brus, D.R. Winge, Nature 338 (1989) 596-597.

41. D. Winge, C.T. Dameron, R.K. Mehra (1992), dins: J.H.R. Kägi, Y. Kojima (Eds.), Metallothionein II, 52 (1992) 257-270.

42. M. Capdevila, J. Domènech, A. Pagani, L. Tío, L. Villarreal, S. Atrian, Angew. Chem. Int. Ed. 44 (2005) 4618-4622.

43. O. Palacios, S. Atrian, M. Capdevila, J. Biol. Inorg. Chem. 16 (2011) 991-1009.

44. R. Orihuela, F. Monteiro, A. Pagani, M. Capdevila, S. Atrian, Chem. Eur. 16 (2010) 12363-12372.

45. M. Capdevila, S. Atrian, J. Biol. Inorg. Chem. 16 (2011) 977-989.

46. C.D. Klaassen, J. Liu, S. Chouhuri, Annu. Rev. Pharmacol. Toxicol 39 (1999) 267-294.

47. P.J. Thornalley, M. Vašák, Biochim. Biophys. Acta 827 (1985) 36-44.

48. J. Abel, N. de Ruiter, Toxicol. Lett. 47 (1989) 191-196.

49. A.R. Quesada, R.W. Byrnes, S.O. Krezoski, D.H. Petering, Arch. Biochem. Biophys. 334 (1996) 241-250.

50. S. Zeitoun-Ghandour, O.I. Leszczyszyn, C.A. Blindauer, F.M. Geier, J.G. Bundy, S.R. Stürzenbaum, Mol. Biosyst. 7 (2011) 2397-2406.

51. T. Dalton, R.D. Palmiter, G.K. Andrews, Nucleic Acids Res. 22 (1994) 5016-5023.

52. G. Mir, J. Domènech, G. Huguet, G. Woei-Jiun, P. Goldsbrough, S. Atrian, M. Molinas, J. Exp. Bot. 55 (2004) 2483-2493.

53. H.L. Wong, T. Sakamoto, T. Kawasaki, K. Umemura, K. Shimamoto, Plant Physiol. 135 (2004) 1447-1456.

54. V.H. Hassinen, A.I. Tervahauta, H. Schat, S.O. Kärenlampi, Plant Biol. 13 (2011) 225-232.

55. Y.J. Kang, Exp. Biol. Med. 231 (2006) 1459-1467.

56. W. Maret, J. Biol. Inorg. Chem. 16 (2011) 1079-1086.

57. W. Maret, B.L. Vallee, Proc. Natl. Acad. Sci. USA 95 (1998) 3478-3482.

58. A. Torreggiani, C. Chatgilialoglu, C. Ferreri, M. Melchiorre, S. Atrian, M. Capdevila, J. Proteomics 92 (2013) 204-215.

59. B. Lipinski, Br. J. Nutr. 87 (2002) 93-94.

60. N.S. Rajasekaran, P. Connell, E.S. Christians, L.J. Yan, R.P. Taylor, A. Orosz, et al., Cell 130 (2007) 427-439.

61. X. Zhang, X. Min, C. Li, I.J. Benjamin, B. Qian, X. Zhang, et al., Hyperthension 55 (2010) 1412-1417.

62. http://www.uniprot.org/, 2013 (accés 13-Gener-2014).

63. L. Vergani, Met. Ions Life Sci. 5 (2009) 199-237.

64. R. Scudiero, C. Capasso, V. Carginale, M. Riggio, A. Capasso, M. Ciaramella, S. Filosa, E. Parisi, Cell. Mol. Life Sci. 53 (1997) 472-477.

65. G. Bai, E.W. Stuebing, H.R. Parker, P. Harlow, M. Nemer, Mol. Cell Biol. 13 (1993) 993-1001.

66. D.G. Wilkinson, M. Nemer, Mol. Cell Biol. 7 (1987) 48-58.

67. L. Hanley-Bowdoin, B.G. Lane, Eur. J. Biochem. 135 (1983) 9-15.

68. C. Cobbett, P. Goldsbrough Annu. Rev. Plant Biol. 53 (2002) 159-182.

69. E. Freisinger, Met. Ions Life Sci. 5 (2009) 107-153.

70. N.H. Roosens, R. Leplae, C. Bernard, N. Verbruggen, Planta 222 (2005) 716-729.

71. J. Guo, L. Xu, Y. Su, H. Wang, S. Gao, J. Xu, Y. Que, Biomed. Res. Int. (2013) doi: 0.1155/2013/904769

72. E. Freisinger, J. Biol. Inorg. Chem. 16 (2011) 1035-1045.

73. E.A. Peroza, E. Freisinger, J. Biol. Inorg. Chem. 12 (2007) 377-391.

74. X. Wan, E. Freisinger, Metallomics 1 (2009) 489-500.

75. J. Domènech, G. Mir, G. Huguet, M. Capdevila, M. Molinas, S. Atrian, Biochimie 88 (2006) 583-593.

76. O. Schicht, E. Freisinger, Inorg. Chim. Acta 362 (2009) 714-724.

77. E. Freisinger, Inorg. Chim. Acta 360 (2007) 369-380.

78. A. Torreggiani, J. Domènech, A. Tinti, J. Raman Spectrosc. 40 (2009) 1687-1693.

79. L. Tío, L. Villarreal, S. Atrian, M. Capdevila, M. Exp. Biol. Med. 231 (2006) 1522-1527.

80. A. Pagani, L. Villarreal, M. Capdevila, S. Atrian, Mol. Microbiol. 63 (2007) 256-269.

81. X. Wan, E. Freisinger, Inorg. Chem. 52 (2013) 785-792.

82. T. Huber, E. Freisinger, Dalton Trans. 42 (2013) 8878-8889.

83. Y.O. Ahn, S.H. Kim, J. Lee, H. Kim, H.S. Lee, S.S. Kwak, Mol. Biol. Rep. 39 (2012) 2059-2067.

84. D.B. Nikolić, J.T. Samardžić, A.M. Bratić, I.P. Radin, S.P. Gavrilović, T. Rausch, V.R. Maksimović, J. Agric. Food Chem. 58 (2010) 3488-3494.

85. A. Brenes-Pomales, G. Lindegren, C.C: Lindegren, Nature 176 (1955) 841-842.

86. T.R: Butt, E.J. Sternberg, J.A. Gorman, P. Clark, D. Hamer, M. Rosenberg, S.T. Croke, Proc. Natl. Acad. Sci. USA 81 (1984) 3332-3336.

87. V.C: Culotta, W.R. Howard, X.F. Liu, J. Biol. Chem. 269 (1994) 25295-25302.

88. W.J. Guo, M. Meetam, P. Goldsbrough, Plant Physiol. 146 (2008) 1697-1706.

89. M. Capdevila, N. Cols, N. Romero-Isart, R. Gonzàlez-Duarte, S. Atrian, P. Gonzàlez-Duarte, Cell Mol. Life Sci. 53 (1997) 681-688.

90. N. Cols, N. Romero-Isart, M. Capdevila, B. Oliva, P. Gonzàlez-Duarte, R. Gonzàlez-Duarte, S. Atrian, J. Inorg. Biochem. 68 (1997) 157-166.

91. P. Harlow, E. Watkins, R.D. Thornton, M. Nemer, Mol. Cell Biol. 9 (1989) 5445-5455.

92. M. Nemer, R.D. Thornton, E.W. Stuebing, P. Harlow, J. Biol. Chem. 266 (1991) 6586-6593.

93. M. Tomas, J. Domènech, M. Capdevila, R. Bofill, S. Atrian, FEBS Open Bio 3 (2013) 89-100.

94. M. Guirola, S. Pérez-Rafael, M. Capdevila, Ò. Palacios, S. Atrian, PLoS One 7 (2012) e43299.

95. O. Palacios, A. Pagani, S. Pérez-Rafael, M. Egg, M. Höckner, A. Brandstätter, M. Capdevila, S. Atrian, R. Dallinger, BMC Biol. 9 (2011) 4-24.

96. M. Höckner, K. Stefanon, A. de Vaufleury, F. Monteiro, S. Pérez-Rafael, Ò. Palacios, M. Capdevila, S. Atrian, R. Dallinger, Biometals 24 (2011) 1079-1092.

97. E. Artells, Ò. Palacios, M. Capdevila, S. Atrian, Metallomics 5 (2013) 1397-1410.

98. M.A. Pagani, M. Tomas, J. Carrillo, R. Bofill, M. Capdevila, S. Atrian, C.S. Andreo, J. Inorg. Biochem. 117 (2012) 306-315.

99. N.N. Alexandrov, V.V. Brover, S. Freidin, M.E. Troukhan, T.V. Tatarinova, H. Zhang, T.J. Swaller, Y.P. Lu, J. Bouck, R.B. Flavell, K.A. Feldmann, Plant. Mol. Biol. 69 (2009) 179-194.

100. K. Bilecen, U.H. Ozturk, A.D. Duru, T. Sutlu, M.V. Petoukhov, D.I. Svergun, M.H. Koch, U.O. Sezerman, I. Cakmak, Z. Sayers, J. Biol. Chem. 280 (2005) 13701-13711.

101. R.M. Nezhad, A. Shahpiri, A. Mirlohi, Protein J. 32 (2013) 131-137.

102. A.M. Tommey, J. Shi, W.P. Lindsay, P.E. Urwin, N.J. Robinson, FEBS 292 (1991) 48-52.

103. M. Tomàs, M.A. Pagani, C.S. Andreo, M. Capdevila, R. Bofill, S. Atrian, J. Biol. Inorg. Chem. (sotmés).

104. O.I. Leszczyszyn, C.R. White, C.A. Blindauer, Mol. Biosyst. 6 (2010) 1592-1603.

105. E.A. Peroza, A. dos Santos Cabral, X. Wan, E. Freisinger, Metallomics 5 (2013) 1204-1214.

8. ANNEX

8. ANNEX

Els resultats d'aquesta Tesi Doctoral han donat lloc a articles publicats, enviats o que es troben en fase avançada de redacció, per als quals a continuació es detalla l'aportació personal de l'autora de la present Tesi, en cada cas:

1. The sea urchin metallothionein system: comparative evaluation of the SpMTA and SpMTB metal-binding preferences

Autors: M. Tomas, J. Domènech, M. Capdevila, R. Bofill, S. Atrian

Publicat en: FEBS Open Bio 3 (2013) 89-100

Aquest treball s'ha realitzat conjuntament amb autors del Departament de Genètica de la Universitat de Barcelona i del Departament de Química de la Universitat Autònoma de Barcelona. Per al desenvolupament del mateix, l'autora de la present Tesi Doctoral ha treballat en el Departament de Genètica en la construcció dels plasmidis recombinants de SpMTB, αSpMTB i βSpMTB, així com en la síntesi i purificació dels complexos d'aquests pèptids amb Zn(II), Cd(II) i Cu(I). També ha realitzat la caracterització espectroscòpica i espectromètrica d'aquests complexos en el Departament de Química, així com els experiments d'intercanvi Zn/Cd i Zn/Cu amb aquests mateixos complexos. Addicionalment, ha participat en l'elaboració del text i ha confeccionat les Figures 2, 4, 8 i 10 de la publicació.

2. The response of the different soybean metallothionein isoforms to cadmium intoxication

Autors: M.A. Pagani, M. Tomas, J. Carrillo, R. Bofill, M. Capdevila, S. Atrian, C.S. Andreo

Publicat en: J. Inorg. Biochem. 117 (2012) 306-315

Aquest treball s'ha realitzat amb autors del Departament de Genètica de la Universitat de Barcelona, del Departament de Química de la Universitat Autònoma de Barcelona i del Centro de Estudios Fotosintéticos y Bioquímicos del Consejo Nacional de Investigaciones Científicas y Técnicas (CEFOBI-CONICET, Argentina). L'aportació

personal de l'autora d'aquesta Tesi Doctoral a aquest treball ha estat la síntesi i purificació dels complexos de GmMT1, GmMT2, GmMT3 i GmMT4 amb Zn(II) i Cd(II) i la seua caracterització analítica. Addicionalment, ha participat en l'elaboració de l'apartat 3.4 del text i ha confeccionat les Figures 5, 6 i la Taula 2 de la publicació.

3. Zn(II)- and Cd(II)-binding abilities of plant MT1 and MT2 isoforms with extra Cys residues

Autors: M. Tomàs, M.A. Pagani, C.S. Andreo, M. Capdevila, S. Atrian, R. Bofill

Manuscrit en preparació

Aquest treball s'ha realitzat amb autors del Departament de Genètica de la Universitat de Barcelona, del Departament de Química de la Universitat Autònoma de Barcelona i del Centro de Estudios Fotosintéticos y Bioquímicos del Consejo Nacional de Investigaciones Científicas y Técnicas (CEFOBI-CONICET, Argentina). A partir de la identificació *in silico* de les MT presents en la planta de gira-sol pel grup del CEFOBI-CONICET, l'autora d'aquesta Tesi Doctoral ha participat en la classificació de les MT en els diversos tipus de MT de planta i ha construït els plasmidis recombinants d'HaMT1 i HaMT2. A continuació ha sintetitzat i purificat els complexos d'aquests pèptids amb Zn(II) i Cd(II) i els ha caracteritzat a través de les tècniques espectroscòpiques i espectromètriques habituals, així com dels experiments d'intercanvi Zn/Cd i d'acidificació-reneutralització. Finalment ha elaborat el text, figures i taules del manuscrit.

4. His-containing plant metallothioneins: comparative study of divalent metal-ion binding by plant MT3 and MT4 isoforms

Autors: M. Tomàs, M.A. Pagani, C.S. Andreo, M. Capdevila, R. Bofill, S. Atrian

Enviat a: J. Biol. Inorg. Chem. (Gener 2014)

Aquest treball s'ha realitzat amb autors del Departament de Genètica de la Universitat de Barcelona, del Departament de Química de la Universitat Autònoma de Barcelona i del Centro de Estudios Fotosintéticos y Bioquímicos del Consejo Nacional de Investigaciones Científicas y Técnicas (CEFOBI-CONICET, Argentina). Per a

l'elaboració d'aquest treball, les MT de soja i gira-sol aquí estudiades foren identificades i classificades en els diversos tipus de MT de planta pel grup del CEFOBI-CONICET. També obtingueren els plasmidis recombinants de les MT de soja, GmMT3 i GmMT4. A continuació, l'autora d'aquesta Tesi Doctoral ha construït els plasmidis recombinants d'HaMT3 i HaMT4, així com els mutants H66AGmMT3 i H67AHaMT3. També ha sintetitzat i purificat els complexos d'aquests pèptids amb Zn(II) i Cd(II) i els ha caracteritzat. Finalment, ha elaborat el text, figures i taules del manuscrit.

5. Comparative analysis of the soybean metallothionein system under radical and oxidative stress

Manuscrit en preparació

Aquest treball començà a elaborar-se gràcies a la col·laboració amb el grup de la Dra. M.A. Pagani del Centro de Estudios Fotosintéticos y Bioquímicos del Consejo Nacional de Investigaciones Científicas y Técnicas (CEFOBI-CONICET, Argentina), el qual primerament ha fet la identificació *in silico* i la classificació dels quatre representants de cada tipus de MT de planta en la soja. Així mateix, també ha obtingut els plasmidis recombinants d'aquestes MT i ha realitzat els experiments de reacció en cadena de la polimerasa quantitativa (qPCR) i de complementació en llevat que donaren lloc als indicis que era interessant estudiar les capacitats antioxidants i antiradicalàries del sistema MT de la soja. L'autora de la present Tesi Doctoral ha fet una estada de tres setmanes en aquest laboratori de l'Argentina, on ha participat en els experiments de qPCR. A més ha participat en la síntesi i purificació dels quatre complexos Zn-MT duta a terme en el Departament de Genètica de la Universitat de Barcelona, i n'ha fet la caracterització analítica i mesura dels processos d'alliberament de Zn(II) en el Departament de Química de la Universitat Autònoma de Barcelona. Els experiments en què s'han produït radicals lliures a través de la radiòlisi γ de solucions aquoses i les mesures per espectroscòpia Raman s'han desenvolupat en el BioFreeRadicals Group al Consiglio Nazionale delle Ricerche-Istituto per la Sintesi Organica e la Fotoreattività (Itàlia), durant una estada de tres mesos de l'autora d'aquesta Tesi Doctoral. Finalment, l'autora de la Tesi ha elaborat el text, figures i taules del manuscrit.